The synthesis, structural characterization and *in vitro* anticancer activity of novel ferrocenyl bioconjugates

by

Andy Garry Harry B.Sc. (Hons)

A thesis presented for the degree of Doctor of Philosophy

at

Dublin City University

Under the supervision of Dr Peter T. M. Kenny

Ollscoil Chathair Bhaile Atha Cliath

School of Chemical Sciences

March 2013

Declaration

I hereby certify that this material, which I now submit for assessment on the programme of study leading to the award of Ph.D is entirely my own work, that I have exercised reasonable care to ensure that the work is original, and does not to the best of my knowledge breach any law of copyright, and has not been taken from the work of others and to the extent that such work has been cited and acknowledged within the text of my work.

Signed: _____

Andy Garry Harry

ID No.: _53952011_____

Date: _____

Acknowledgements

I would like to thank Dr. Peter T. M. Kenny for giving me the opportunity to conduct research under his supervision and for being supportive and patient during my four years in the lab. I would also like to thank: Health Research Board, Grant Reference Number HRA/09/86 for funding this research. Dr. Norma O'Donovan, Naomi Walsh and James Murphy for conducting the biological studies. Dr. Dilip K. Rai in Teagasc, for obtaining the tandem MS spectra. To all the technical and academic staff for their help, especially John McLoughlin, Brendan Tweat, Damien McGuirk and Ambrose May. A special thank you to all the Peter Kenny Research Group members, past and present especially Dr. Will, Rachel, Dr. Alan and Dr. Aine and James. Special thanks to my fellow postgraduates especially Rohit, Mukund, Declan (aka ma man), Tom, Sarah C. Eoin and Sarah K big thanks to you all.

Last but not list to family especial my mum (Chief) for all her support. To my dad (KWANGA), thank you for all your sacrifices. To my uncle Tommy and aunt Natty thank you for always being there. To my brothers Alvis and Adam thank you and last but not my sister Cathy for all the cigarettes you sent me. Could not have done without Madison that blend from Zimbabwe. Ambuya Norris tazopedza.

Finally thank you GOD

Abstract

A series of 1-alkyl-1'-*N*-*para*, *N*-*meta* and *N*-*ortho*-(ferrocenyl) benzoyl dipeptide esters and *N*-{*para*-(ferrocenyl) ethynyl benzoyl}, *N*-{6-(ferrocenyl) ethynyl-2-naphthoyl} and *N*-{5-(ferrocenyl) ethynyl-2-furanoyl} amino acid and dipeptide esters were prepared. The novel ferrocenyl based bioconjugates were prepared by coupling 1-alkyl-1'-*N*-*para*, *N*-*meta* and *N*-*ortho*-(ferrocenyl) benzoic acid and *N*-{*para*-(ferrocenyl) ethynyl benzoyl}, *N*-{6-(ferrocenyl) ethynyl-2-naphthoyl} and *N*-{5-(ferrocenyl) ethynyl-2-furanoyl} benzoic acid to α-amino acid ethyl esters and dipeptide ethyl esters using the conventional *N*-(3-dimethylaminopropyl)-*N*'-ethylcarbodiimidehydrochloride (EDC), 1-hydroxybenzotriazole (HOBt) protocol. The new classes of compounds were characterized by a combination of ^{1}H NMR, ^{13}C NMR, DEPT-135 and ^{1}H-^{13}C COSY (HMQC) spectroscopy, electrospray ionization mass spectrometry (ESI-MS). Biological evaluation of the 1-alkyl-1'-*N*-*para*, *N*-*meta* and *N*-*ortho*-(ferrocenyl) benzoyl dipeptide esters were carried out in the H1299 non-small cell lung cancer (NSCLC) cells.

The most active derivatives of the 1-alkyl-1'-*N*-*para*, *N*-*meta* and *N*-*ortho*-(ferrocenyl) benzoyl dipeptide esters are the 1-methyl-1'-*N*-{*para*-(ferrocenyl) benzoyl} glycine glycine ethyl ester with an IC_{50} value of 2.8 ± 1.23 μM, the 1-ethyl-1'–*N*-{*para*-(ferrocenyl) benzoyl} glycine glycine ethyl ester with an IC_{50} value of 3.5 ± 0.82 μM and the 1-methyl-1'-*N*-{*meta*-(ferrocenyl) benzoyl} glycine glycine ethyl ester with an IC_{50} of 2.6 ± 0.62 μM and these derivatives are more cytotoxic *in vitro* than the clinically employed anti-cancer drug carboplatin. In addition, these compounds display improved bioactivity in comparison to the corresponding most active benzoyl analogues which were the *N*-{meta-(ferrocenyl) benzoyl} glycine L-alanine ethyl ester and *N*-{para-(ferrocenyl) benzoyl} glycine L-alanine ethyl ester which displayed IC_{50} values of 4.0 μM and 6.6 μM respectively

The biological evaluation of *N*-{*para*-(ferrocenyl) ethynyl benzoyl}, *N*-{6-(ferrocenyl) ethynyl-2-naphthoyl} and *N*-{5-(ferrocenyl) ethynyl-2-furanoyl} amino acid and dipeptide esters were also carried out in the H1299 non-small cell lung cancer (NSCLC) cells. The most active derivatives of the *N*-{*para*-(ferrocenyl) ethynyl benzoyl}, *N*-{6-(ferrocenyl) ethynyl-2-naphthoyl} and *N*-{5-(ferrocenyl) ethynyl-2-

furanoyl} amino acid and dipeptide esters are the *N*-{*para*-(ferrocenyl) ethynyl benzoyl} glycine L-alanine ethyl ester with an IC_{50} value of 3.8 ± 1.92 μM and the *N*-{6-(ferrocenyl) ethynyl-2-naphthoyl} sarcosine L-alanine ethyl ester with an IC_{50} value of 3.2 ± 2.64 μM. These compounds are more active than carboplatin with an IC_{50} value of 10 ± 1.60 μM but are less effective than cisplatin with an IC_{50} value of 1.5 ± 0.10 μM which are clinically employed anti-cancer drugs. However, the presence of the ethynyl moiety had a negative effect of anti-proliferative effect compared to analogous compounds prepared previously lacking the ethynyl group. For example for *N*-{6-(ferrocenyl) ethynyl-2-naphthoyl} γ-aminobutyric acid ethyl ester the IC_{50} value is 7.2 ± 1.51 μM whereas for *N*-(6-ferrocenyl-2-naphthoyl) γ-aminobutyric acid ethyl ester the IC_{50} value was 0.62 ± 0.03 μM

Table of contents

Chapter 4: Synthesis and structural characterisation of *N*-{*para*-(ferrocenyl) -ethynyl benzoyl}, *N*-{6-(ferrocenyl) ethynyl-2-naphthoyl} and *N*-{5-(ferrocenyl)-ethynyl-2-furanoyl} amino acids and dipeptide esters

Chapter 1

1.1 Cancer

Cancer is a set of diseases in which the affected cells display the following abnormalities: (i) uncontrolled growth and division beyond what is normal, (ii) invasion and destruction of neighbouring cells and (iii) metastasis may occur, that is the spreading of the disease to other locations.[1] The biochemistry of cancer is enormously complex, but one cause that has been generally accepted is that reactive oxygen species, (ROS) play many important roles, in carcinogenesis and the progression of tumour. Examples of these reactive oxygen species produced in cells of living organisms include: (i) superoxide anion radical (O_2^-), (ii) hydrogen peroxide (H_2O_2) and (iii) hydroxyl radical (·OH).[2] Typically these ROS are generated during continuous exposure to irradiation by X-ray or gamma rays, are present as pollutants in the atmosphere or are by-products of mitochondria-catalyzed electron transport reactions.[2] In biological systems, these reactive oxygen species are well known to play a dual role, they can either be harmful or beneficial to living systems.[2] The beneficial effects of ROS involve physiological roles in the cellular response to noxia, as for example in defence against infectious agents and in the function of a number of cellular signalling systems. In living organisms, normally the harmful effects of the ROS are regulated by the detoxifying action of a variety of cell protective enzymes such as superoxide dismutase, catalase and heme oxidase. However, high accumulation of ROS can be catastrophic to cells because they trigger chemical chain reactions such as lipid peroxidation, or they can cause the oxidation of DNA which causes DNA mutations which may result in the development of cancer. In many cancer cells it has been observed that there is an elevated concentration of ROS and a strongly reduced activity of the ROS regulating enzymes compared to normal cells.[2]

The most frequent types of cancer which cause the most deaths include lung, stomach, liver, colon and breast cancer. According to reports from the World Health Organization (WHO), cancer accounts for 7.9 million deaths and around 13 % for all deaths in 2007.[3] Lung cancer is the most common cancer in the world and approximately 1.35 million new cases of lung cancer occur worldwide every year.[3]

Lung cancer is divided into two major types based on histological appearance: small cell lung cancer (SCLC) and non-small cell lung cancer (NSCLC). Approximately 20% of all lung cancers are SCLC, which is a very aggressive form of cancer due to early metastasis.[4] Chemotherapy is the most common treatment for SCLC because of early metastatic spread. However, even with treatment, long-term survival remains poor. The remaining 80% of all lung cancers are NSCLC, which comprise of adenocarcinomas, squamous cell and large cell carcinomas.[4] Surgery is generally regarded as the best treatment option for NSCLC. However, 75% of NSCLC tumours are inoperable at the time of diagnosis.[5] A further 20% of patients with locally advanced disease receive radiotherapy. In these cases, chemotherapy following standard treatment has been shown to help patients live longer.[6]

Consequently, the research within this project is focussed on the synthesis 1-alkyl-1'-*N*-*para*, *N*-*meta* and *N*-*ortho*-(ferrocenyl) benzoyl dipeptide esters and *N*-{*para*-(ferrocenyl) ethynyl benzoyl}, *N*-{6-(ferrocenyl) ethynyl-2-naphthoyl} and *N*-{5-(ferrocenyl) ethynyl-2-furanoyl} amino acid and dipeptide esters and their biological evaluation as potential chemotherapeutic agents for the treatment of non-small cell lung cancer (NSCLC).

1.1.2 Cancer treatment

Cancer can be treated by surgery, immuno therapy, radiation therapy and chemotherapy or a combination of them depending on the location and stage of the disease.[7] Chemotherapy is the treatment of cancer using drugs. Traditionally, the drugs that have been used in cancer chemotherapy have been predominantly organic compounds which have been synthesized or have been isolated from natural sources. These conventional chemotherapeutic drugs elicit cancer cell death by interfering with the cell replication process. This can be accomplished by disrupting the function of DNA, either by acting directly on DNA (alkylating agents) or by inhibiting the enzymes involved in DNA synthesis using antimetabolites.[8] Alternatively, chemotherapeutic may act by interfering with the mechanics of cell division for example, by binding to microtubules.[8]

Dacarbazine **1** (figure 1.1) is an alkylating agent prodrug, currently used in the treatment of metastatic melanoma cancer.[8] Dacarbazine undergoes activation via cytochrome P450 in the liver to form a reactive compound, methyltriazenoimidazole carboxamide (MTIC) **2** (figure 1.1).[9] This reactive compound spontaneously degrades to form diazomethane, a potent alkylating agent. Alkylating agents in cancer treatment are highly electrophilic compounds that attach alkyl groups to DNA by reacting at the nucleophilic sites present in the DNA bases.[10] The main nucleophilic sites are the N-1 and N-3 of adenine, N-3 of cytosine and in particular, the N-7 of guanine. Thus, alkylation prevents DNA replication and RNA transcription which results in cell death of affected cells.

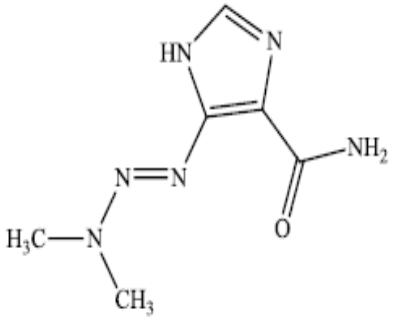

1

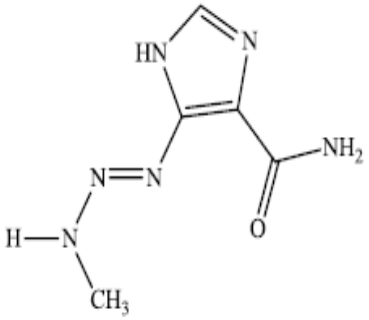

2

Figure 1.1: Structure of dacarbazine **(1)** and its active form MTIC **(2).**

Antimetabolite drugs were among the first effective chemotherapeutic agents discovered and are currently still being used in cancer treatment.[11] Generally, antimetabolites induce cell death during the S phase of cell growth when incorporated into RNA and DNA. Gemcitabine **3** (figure 1.2) is a pyrimidine antimetabolite which has shown good clinical activity in pancreatic, breast, ovarian, non small cell lung, and bladder cancer.[12] Gemcitabine, is a fluorinated analogue of the naturally occurring DNA building block 2-deoxycytidine **4** (figure 1.2). The mode of action of gemcitabine occurs as a result of intracellular conversion of the prodrug into two active metabolites, gemcitabine diphosphate and gemcitabine triphosphate.[13] Gemcitabine diphosphate inhibits the enzyme responsible for catalyzing the synthesis of deoxynucleoside triphosphates required for DNA synthesis, and gemcitabine

triphosphate competes with endogenous deoxynucleoside triphosphates required in the synthesis of DNA.[13] Thus, the gemcitabine diphosphate induced reduction of the intracellular concentrations of deoxynucleoside triphosphates results in increased incorporation of gemcitabine triphosphate into DNA and, consequently, resulting in inhibition of DNA synthesis.

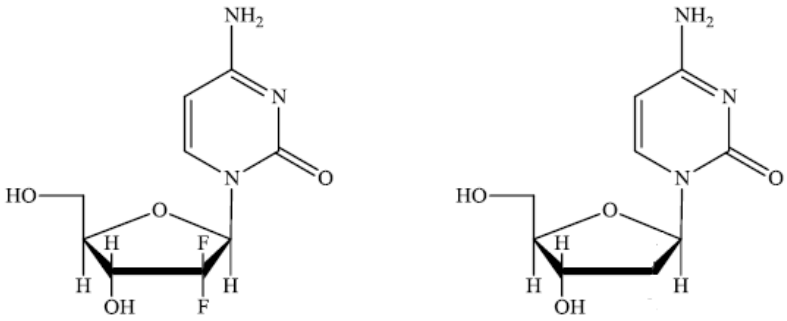

3 **4**

Figure 1.2: Structure of gemcitabine **3** and 2-deoxycytidine **4.**

Etopside **5** (figure 1.3) is a semi-synthetic derivative of the naturally occurring podophyllotoxin, and exerts its anticancer activity by inhibiting the DNA-topoisomerase II enzyme.[8] The DNA topoisomerase II enzyme is essential for the separation of entangled daughter strands during replication.[14] Failure to separate these strands as a result of inhibition of the enzyme leads to cell death

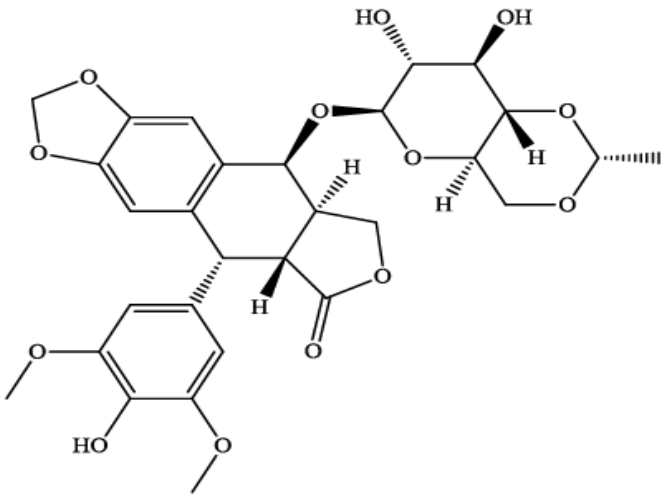

5

Figure 1.3: Structure of etopside **5**.

Antimicrotubule agents prevent cell mitosis by interfering with the formation of the mitotic spindle required for cell division.[10] The main cellular target of these compounds is the structural protein tubulin. During mitosis, tubulin undergoes polymerisation to form the mitotic spindle. The vinca alkaloids (figure 1.4), vinblastine (**6)** and vincristine (**7)** bind to tubulin and prevent polymerisation from occurring thus resulting in cell death. These compounds are frequently used in combination therapies for the treatment of lung cancer and melanoma.[10]

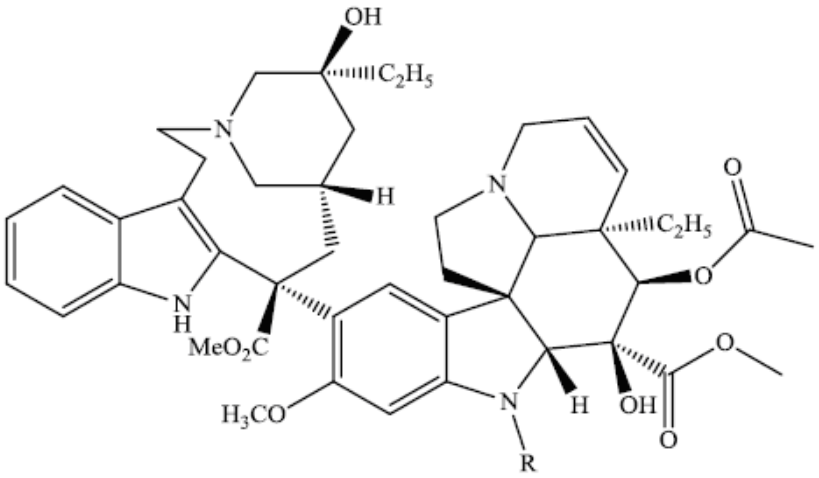

6, R= CH_3; **7,** R = CHO

Figure 1.4: Structures of vinblastine (**6)** and vincristine (**7).**

The selectivity of these drugs are based primarily on the fact that cancer cells divide more rapidly than normal cells.[10] Unfortunately, there are also cells in the bone marrow, digestive tract and hair follicles that divide rapidly under normal circumstances. Most cytotoxic agents also act on these cells and for this reason myelosuppression (decreased production of blood cells), mucositis (inflammation of lining of the digestive tract) and hair loss are all common side effects.

The appearance of cancer cells resistant is also a serious problem in cancer chemotherapy. There are two main types of cancer resistance.[15] Intrinsic drug resistance is present at the time of diagnosis in tumours that fail to respond to first-line chemotherapy. In contrast, acquired drug resistance occurs in tumours that can often be highly responsive to initial treatment, but display strong resistance to the original

treatment upon tumour reocurrence.[15] In such cases, the tumour becomes resistant to previously used drugs. A large number of metal containing compounds with antitumour properties have been reported in the literature, some of which are in clinical use and others still being evaluated as potential anticancer agents.[18]

1.1.3 Bioorganometallic chemistry

The discovery of cisplatin a coordination metal complex by Rosenberg in 1965 marked the genesis of bioorganometallic chemistry due to the success of cisplatin against various types of cancer.[16] Despite the success of cisplatin as a clinical anticancer drug over the past decades, side effects accompany its use in the treatment of cancer, for instance it causes the formation of lung adenomas, also repeating cancer cell lines develop resistance during long term therapy. As a result of the drawbacks associated with the administration of cisplatin, this has prompted the search for alternative anticancer drugs which are non toxic whilst retaining therapeutic efficacy. To date, bioorganometallic chemistry is a rapidly growing area of science that is being conducted at the interface between organometallic chemistry and biology and it has provided significant structural and molecular recognition advancement in the exploration of new innovative solutions to the emerging existing problems encountered in biomedical applications. Metallocenes in the recent years has come to play a pre-eminent part in research in a wide range of biological application.[17] Amongst the numerous examples, ferrocene has in recent years gained increasing interest as the building block in the development of a number of promising ferrocene based biomedical therapeutic agents. The biomedical application of ferrocene based prodrugs is currently an active field of research with many reports showing its activity *in vivo* and *in vitro* as a potential therapeutic in cancer, malaria and fungal infection treatments.[18] Taking this into consideration the stability of ferrocenyl groups in aerobic media and its vast potential for derivatization and its favourable electrochemical properties have made it an excellent candidate in the synthesis of anticancer therapeutics the ultimate goal of this research.[19]

1.2 Examples of biomedical application of organometallic compounds

1.2.1 Anticancer therapeutics

1.2.1.1 Platinum complexes as anticancer agents

Cisplatin **8** (figure 1.5) was the first potent and effective metal-based complex used in cancer treatment.[16] It was discovered serendipitously by Rosenberg *et* al. in 1965 and it was later approved for clinical use in 1978. By 1983 cisplatin was the US's biggest selling antitumor drug

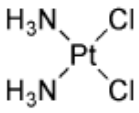

8

Figure 1.5: Structure of cisplatin **8.**

Its importance as a chemotherapeutic agent is largely derived from its ability to confer complete remission in patients with advance testicular cancer and it also is effective against ovarian, bladder and neck cancers.

Despite its success, the clinical use of cisplatin coincides with marked toxic effects due to its lack of selectivity to tumour tissues and as a result, this has lead to severe side effects such as neurotoxicity, nephrotoxicity and in addition there is a propensity for tumours to develop resistance during long term therapy.[20] As a result the toxic effects of cisplatin limit the dose and frequency with which the drug can be administered to patients.[20] However, the effectiveness of cisplatin against a wide range of human tumours has spawned the preparation and evaluation of new organometallic complexes as potential anticancer therapeutics. Three other metal-based complexes of platinum are now used in cancer treatment namely carboplatin **9**, oxaliplatin **10** and nedaplatin **11** (figure 1.6) and they all appear to have similar modes of action.[21]

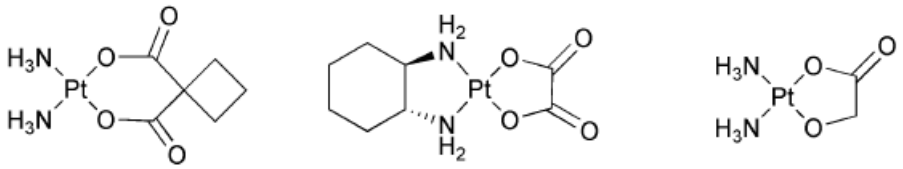

9 **10** **11**

Figure 1.6: Structures of carboplatin **9**, oxaliplatin **10** and nedaplatin **11.**

Carboplatin was the first second generation analogue of cisplatin to be synthesized, which showed less toxic side effects associated with its administration compared to cisplatin and also it was effective against a wide range of tumours, whilst oxaliplatin is the only platinum based complex that displays activity against colorectal cancer.[21]

The *in vivo* anticancer activity of cisplatin and its analogues is due to the replacement of the chloride ligands by neutral water ligands to give reactive positively charged species (scheme 1.1).[10] This process is facilitated within the cell by the relatively low cellular concentration of chloride ions.[10] The platinum atom of these positively charged species binds strongly to DNA, forming covalent bonds with the N-7 positions of guanine bases in DNA of infected cancer cells thus, preventing replication and/or transcription, thereby halting cancer cell proliferation (scheme 1.1).[22]

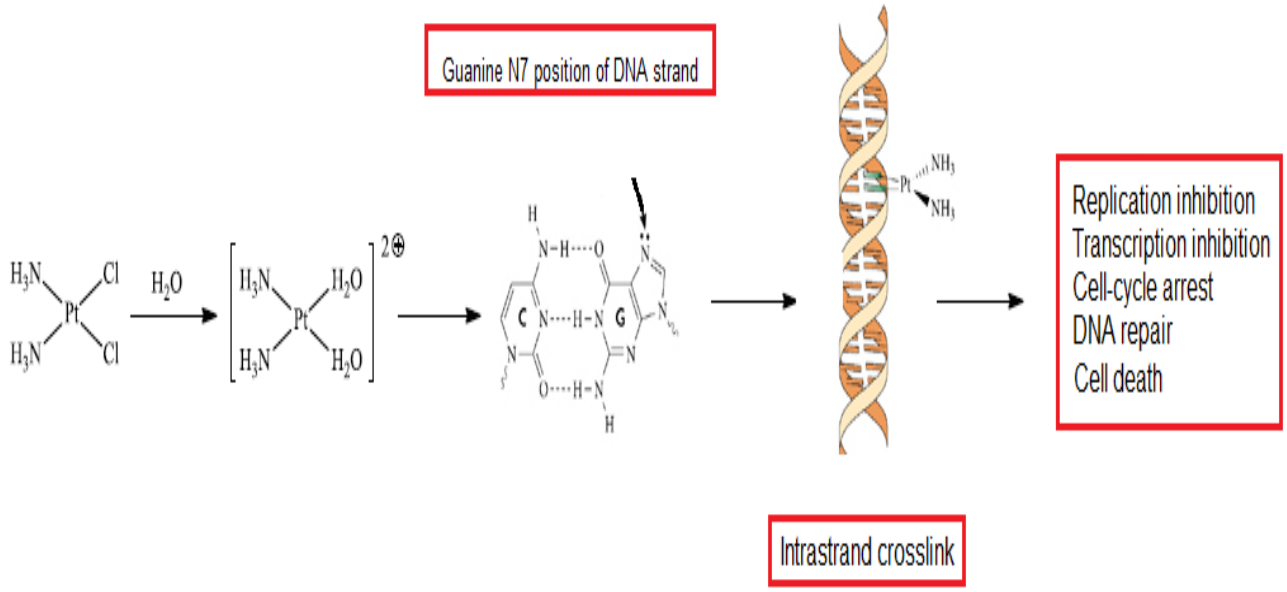

Scheme 1.1: Mode of action of cisplatin.

Despite the success of cisplatin and its analogues as clinical antitumor drugs marked side effects still accompany its administration, to circumvent the side effects novel thioplatin **12** and picoplatin **13** (figure 1.7), third generation platinum compounds have been developed and growing interest in other metal complexes are being investigated.[23-24]

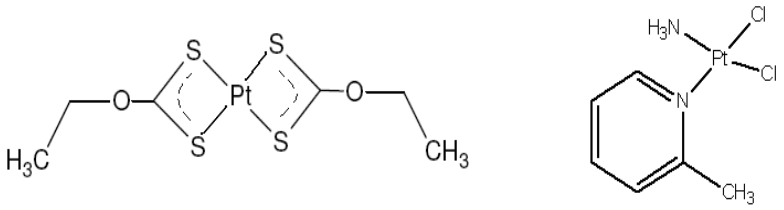

12 **13**

Figure 1.7: Structures of thioplatin **12** and picoplatin **13.**

The picoplatin analogue is under clinical trials, because it exhibits reduced reactivity towards biomolecules and a lower susceptibility to become activated allows oral administration of this drug which is effective against non small cell lung cancer.
Clinically the platinum agents are widely used as a first line treatment for SCLC, either as a single agent or in combination with etopside **5**, whilst for NSCLC, the platinum agent are used in combination with a second agent, usually gemcitabine **3.**[4]

1.2.1.2 Titanium derivatives as anticancer agents

Since the mode of action of platinum complexes involved a *cis* coordination to DNA, initial research has focused on a variety of transition metals complexes bearing *cis* ligands. Amongst the metals studied, two families of titanium complexes, the titanocene dichloride and derivatives, and budotitane and analogues showed interesting activity towards a number of tumour cells, including those resistant to cisplatin and furthermore they showed reduced toxicity compared to cisplatin. Keppler *et* al. succeeded in synthesizing the first non platinum metal based complex to undergo phase 1 clinical trials.[25] Budotitane **14** (figure 1.8), which consisted of a titanium (IV) metal

centre surrounded by two β-diketone ligands and two good leaving ligands either halides or alkoxide was shown to be effective against Ehrlich ascites tumour cells and it was observed that its asymmetry was considered essential for antitumor activity.[25] Other metal complexes with β-diketone ligands complex structures as in budotitane were studied with metals such as hafnium and zirconium, but their anticancer activities were not as active as the titanium (IV) metal complex.

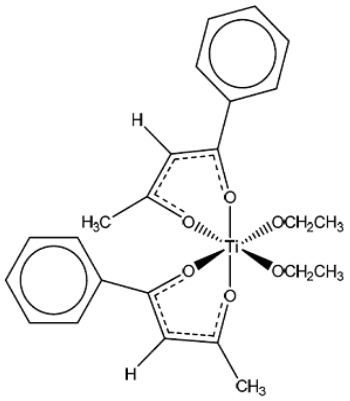

14

Figure 1.8: Structure of budotitane **14.**

However, due to poor water solubility and rapid hydrolysis of first the OR ligands, followed by the more inert ones the two β-diketone, resulted in budotitane being removed from clinical trials due to the drawbacks associated with its use. Another reason that held back any further promising development of budotitane and its analogues as a potential anticancer drug was the discovery of titanocene dichloride. Whilst Kopf-Maier *et* al. were screening the metallocene dichlorides of vanadium, niobium, molybdenium and titanium for anticancer activity in 1979; they discovered that titanocene dichloride **15** (figure 1.9), exhibited the most promising chemotherapeutic activity.[26]

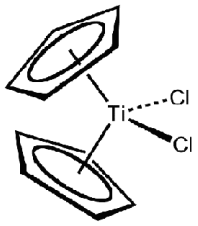

15

Figure 1.9: Structure of titanocene dichloride **15.**

Kopf-Maier *et* al. showed that titanocene dichloride was effective against a wide range of cancer tumors which included B16 melanoma, Ehrlich ascites tumors, colon B adenocarcinoma and sarcoma 189. In phase I clinical trials, titanocene dichloride showed no toxic effects on the kidney as opposed to cisplatin, however, clinical trials for this compound were stopped in phase II.[26] It was shown that upon dissolution in water, the chloride ligands of titanocene dichloride rapidly hydrolyzed which lead to the formation of an insoluble titanium complex which was biologically inactive and showed no antitumor activity. To circumvent this problem of lack of hydrolytic stability, modification of the ligand or encapsulation is an active area of research.[27]

1.2.1.3 Ruthenium derivatives as anticancer drugs

Apart from cisplatin derivatives and titanium complexes that have been widely studied, the antineoplastic potential of ruthenium has been well known for more than 2 decades. Despite exhibiting lower cytotoxic activity than cisplatin they are better tolerated *in vivo* and ruthenium complexes also offer a number of advantageous characteristics for their use as potential anticancer agents such as (i) ruthenium complexes have the ability to mimic iron in binding to biomolecules such as transferrin and human serum which makes them remarkably less toxic than the clinically used cisplatin and its analogues, (ii) ruthenium^{III} complexes maintain their metal oxidation state until they reach the cancer tumor where the low oxygen levels in the cancer turmors permits their reduction to their active state ruthenium^{II}; (iii) their greatest interest is their characteristic inhibition of angiogenesis and matrix metalloproteinases and, hence,

metastasis *in vivo*.[28] The most interesting ruthenium-based drug candidates that have entered clinical trials include the following (figure 1.10) KP1019, indazolium [trans-tetrachlorobis(1H-indazole) ruthenate (III)] **16** and (ii) NAMI-A, imidazole [trans-tetrachloro(dimethylsulfoxide) imidazoleruthenate (III)] **17** NAMI-A was the first ruthenium agent to enter clinical trials and was developed by Alessio *et* al.[29] whilst KP1019 was developed by Keppler *et* al.[30]

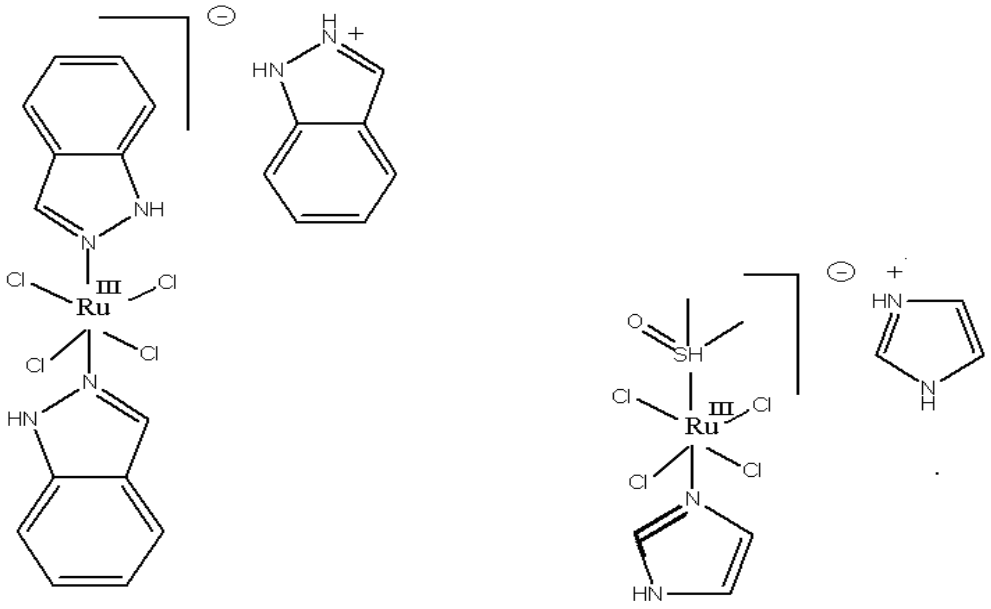

16 **17**

Figure 1.10: Structures of KP1019; indazolium [trans-tetrachlorobis(1H-indazole) ruthenate (III)] **16** and NAMI-A; imidazole [trans-tetrachloro(dimethylsulfoxide)-imidazoleruthenate (III)] **17.**

In vitro tests of KP1019 have shown inhibition effects on cultured cancer cells in contrast to NAMI-A which was shown to have a marginally cytotoxic effect; however, *in vivo*, NAMI-A lowered the growth of lung metastasis in mice bearing mammary carcinoma.[31] Despite NAMI-A not being cyotoxic to primary tumors, it is potentially useful because although great progress has been made in treating primary cancers secondary metastases represents a major clinical challenge and the incorporation of NAMI-A may enhance cancer treatment using the available cancer treatments.[31]

Although the mode of action of NAMI-A is not fully understood, it has been reported that NAMI-A seems to act as an anti-angiogenic, has the ability to scavenge NO produced by epithelial cells in tumour cells and also it acts as an anti-invasive agent which results in its interaction with extracellular or external cell membrane receptor proteins which may result in its antimetastastic properties.[31] Whilst KP1019 is a cytotoxin, which is active against primary tumors, it is thought to cause cancer cell apoptosis via the mitochondrial pathway however the mode of action is not fully understood.[32] With the success of these two ruthenium complexes that have entered clinical trials, more recently, two new classes of ruthenium compounds have been developed.

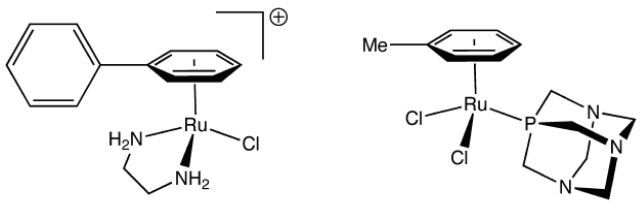

18 **19**

Figure 1.11: Structures of water-soluble ruthenium complex **18** and ruthenium arene 1, 3, 5-triaza-7-phosphaadamantane (RAPTA) **19.**

Sadler *et* al. have reported the synthesis of a new stable water-soluble ruthenium complex **18** (figure 1.11), which was shown to be as potent as cisplatin and its analogues in some primary cell lines and, moreover, they exhibit a wide spectrum of activity and are also active against some tumors which have become resistant to cisplatin.[33] The mode of action is thought to be similar to that of cisplatin, and it may involve coordination to the N-7 of guanine bases in DNA resulting in cell death.[33] The second class of the new ruthenium complexes was developed by Dyson *et* al. the ruthenium arene 1, 3, 5-triaza-7-phosphaadamantane (RAPTA) **19** (figure 1.11). Like NAMI-A, RAPTA was found to be inactive against primary tumors but was found in vivo to have activity against metastases.[34] Although less potent than NAMI-A, RAPTA is less toxic and thus can be administered in higher doses. As a result of these promising results there is ongoing research in the use of ruthenium complexes as potential anticancer agents.[34]

1.2.1.4 Iron derivatives as anticancer drugs

In the last two decades, a range of both charged and neutral ferrocene derivatives have been shown to exhibit antitumour activity. The first iron complexes to exhibit antitumour activity were reported by Kopf-Maier *et* al. in 1984 and these include the salts of ferricenium picrate **20** and ferricenium trichloroacetate **21** (figure 1.12).[35]
The ferricenium salts reported by Kopf-Maier *et* al. showed inhibition in the growth of Ehlrich ascites tumours, B16 melanoma, colon 38 carcinoma and furthermore the cure rate of 100% was obtained in mice bearing Ehlrich ascites tumours.[35]

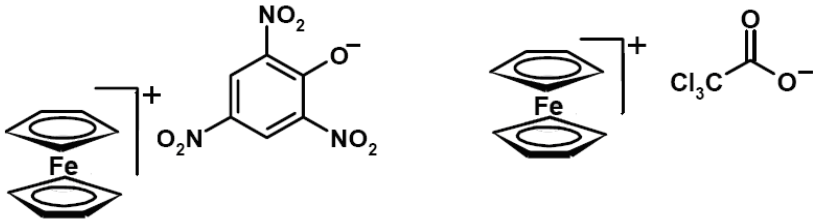

20 **21**

Figure 1.12: Structures of ferricenium picrate **20** and ferricenium trichloroacetate **21.**

These observation of antitumour activity of ferricenium salts prompted further investigation on the use of these salts as potential anticancer agents. Osella *et* al. reported the synthesis of decamethylferriceniumtetrafluoroborate **22** (figure 1.13) another example of a ferricenium salt that showed anticancer activity against MCF-7 breast cancer cells with an IC_{50} value of 35 μM.[36]

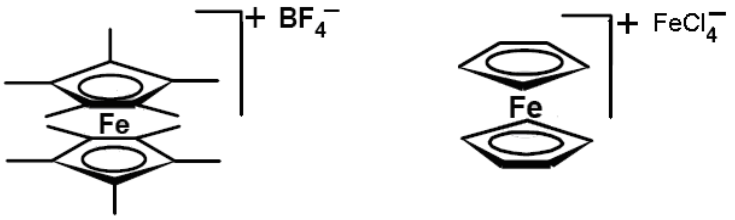

22 **23**

Figure 1.13: Structures of Decamethylferriceniumtetrafluoroborate **22** and ferriceniumtetrachloroferrate **23.**

Osella *et al* proposed that the antitumour activity of ferricenium salts was due to the generation of ·OH radicals under physiological conditions which resulted in oxidative DNA damage to cancer cells. The use of ferricenium salts has been a growing area of research. Houlton *et* al. have also reported the synthesis of ferriceniumtetrachloroferrate **23** (figure 1.13), which showed anticancer activity against CH 1 human ovarian carcinoma cells with an IC_{50} value of 10 µM.[37] Despite the enormous research in the use of ferricenium salts in cancer chemotherapy, it has emerged that neutral ferrocene derivatives also exhibit antitumour activity. It has been known that ferrocene on its own exhibites no antitumour activity; however, neutral ferrocene derivatives have been reported to show anticancer activity or enhance anticancer activity when incorporated into existing therapeutics.[37] The mechanism of action of these ferrocene derivatives in the treatment of cancer has been studied by several groups and they have reported that the ferrocene moiety undergoes metabolism in cancer cells resulting in the formation of ferricenium ions which induces oxidative cleavage.[38]

Romao *et* al. have reported the synthesis of 1,2-disubstituted ferrocene derivatives that have shown antitumour activity in vitro against Ehrlich ascites tumor cells whilst neither ferrocene nor *N,N*-dimethylaminomethylferrocene showed any anticancer activity. With the 1, 2-disubstituted ferrocene derivatives IC_{50} values ranging from 71.2 µM for 2-(*N,N*-dimethylaminomethyl)ferrocene **24** (figure 1.14) to 376.6 µM for 1,2-diformylferrocene **25** (figure 1.14) where observed.[39]

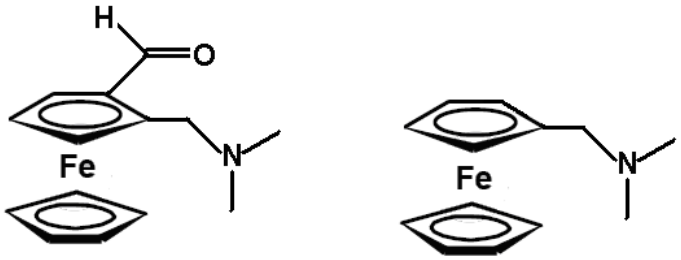

24 **25**

Figure 1.14: Structures of 2-(*N,N*-dimethylaminomethyl)ferrocene **24** and 1, 2- diformylferrocene **25.**

Ling Ming Gao *et al* have reported the preparation of a series of ferrocenyl ester derivatives and the cytotoxicities of the derivatives were tested against colon cancer

cells HT-29 and breast cancer MCF-7 cells and the ferrocenyl ester derivative $Fe(C_5H_4CO_2CH_2CH=CH_2)_2$ **26** (figure 1.15), showed the highest anticancer activity with an IC_{50} value of 180 µM for HT-29 and 190 µM for MCF-7 cell lines.[40]

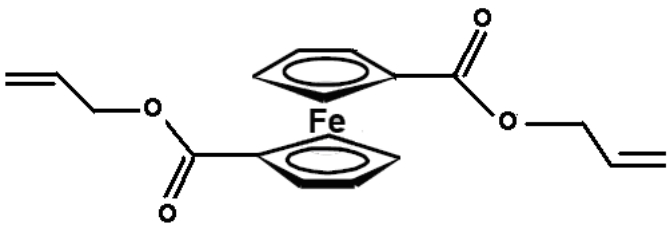

26

Figure 1.15: Structure of $Fe(C_5H_4CO_2CH_2CH=CH_2)_2$ **26.**

The incorporation of a C-F bond is a recognized strategy often employed in the development of pharmaceuticals and this is evident by the success of a large number of fluorinated drugs approved by the FDA which are being used as anticancer, antiviral and antidepressant agents. Kenny *et* al. have reported the preparation of a series of *N*-(ferrocenylmethyl) fluorobenzene carboxamide derivatives which combine the ferrocene moiety with a substituent containing one or more C-F bonds and the cytotoxicities of these derivatives were screened *in vitro* against MDA-MB-435-S-F breast cancer cell lines. The most active derivative found was *N*-(ferrocenylmethyl) 4 fluorobenzene-carboxamide **27** (figure 1.16) with an IC_{50} value in the range of 11-14 µM.[41]

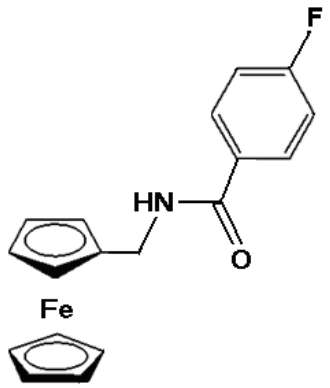

27

Figure 1.16: Structure of *N*-(ferrocenylmethyl) 4-fluorobenzene carboxamide **27**.

Kenny *et* al. have also reported the synthesis of ferrocene derivatives in which various amino acid and dipeptides have been coupled to the ferrocene moiety via a benzoyl spacer moiety. In particular, *N-para*, *N-meta* and *N-ortho*-(ferrocenyl) benzoyl dipeptide esters have been found to possess good anticancer activity against carboplatin resistant variant H1299 lung cancer cells and the most active derivative was *N*-{*meta*-(ferrocenyl) benzoyl} glycine L-alanine ethyl ester **28** (figure 1.17) with an IC_{50} value of 4.0 ± 0.71 μM.[42 - 45]

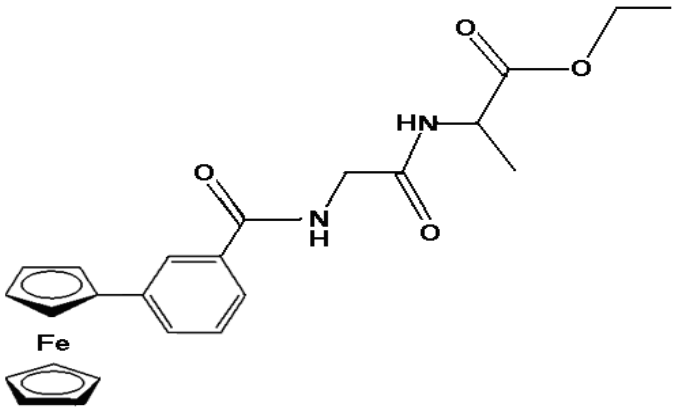

28

Figure 1.17: Structure of *N*-{*meta*-(ferrocenyl) benzoyl} glycine L-alanine ethyl ester **28.**

The *N*-(ferrocenyl) benzoyl dipeptide esters consist of three key components: (i) the electroactive core, the ferrocene moiety; (ii) a conjugated linker that lowers the oxidation potential and (iii) a peptide derivative that can interact with other biomolecules via secondary interactions, such as hydrogen bonding. Kenny *et* al. have reported that the possible mode of action for the anticancer activity of the *N*-(ferrocenyl) benzoyl dipeptide esters is possibly due to their low redox potentials and their ability to form reactive oxygenated species (ROS) under physiological conditions. [42 - 45] It is envisaged that the peptide chain of these derivatives may have a secondary mode of action. The role of the dipeptide is not clear, however, it is plausible that the lipophilic ferrocenyl benzoyl moiety anchors to the cell membrane of the

cancer cell and the peptide chain blocks the opening of the channels in the cell membrane, leading to cell death.[42]

In order to improve the cytotoxicity of the *N*-(ferrocenyl) benzoyl dipeptide esters, Kenny *et* al. have reported the synthesis of *N*-*para*, *N*-*meta* and *N*-*ortho*-(ferrocenyl) benzoyl tri- and tetrapeptide esters. They showed that extending the peptide chain had a negative effect on cytotoxicity as the tri- and tetrapeptide derivatives had IC_{50} values >50 µM for instance *N*-{*ortho*-(ferrocenyl) benzoyl} glycyl glycyl glycine ethyl ester an IC_{50} value of 63 ± 1.11µM.[45]

Kenny *et* al. have shown that the cytotoxicity of the *N*-(ferrocenyl) benzoyl dipeptide esters can be enhanced when the benzoyl conjugate is replaced by a polyaromatic conjugate and they have reported a series of *N*-(ferrocenyl) naphthoyl dipeptide ethyl esters with IC_{50} values against H1299 lung cancer cells ranging from 1.2 – 8.0 µM.[46] The *N*-(6-ferrocenyl-2-naphthoyl) glycine L-alanine ethyl ester **29** (figure 1.18) was found to be the most active derivative of the naphthoyl series to date, displaying an IC_{50} value of 1.3 ± 0.13 µM and this value is slightly lower than that found for the clinically used cisplatin which has an IC_{50} value of 1.5 ± 0.11 µM against the H1299 lung cancer cell line.

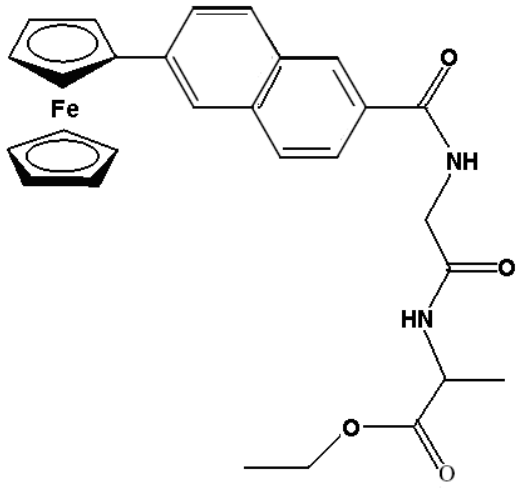

29

Figure 1.18: Structure of *N*-(6-ferrocenyl-2-naphthoyl) glycine L-alanine ethyl ester **29.**

To date, the biological evaluation of *N*-(ferrocenyl) benzoyl and *N*-(ferrocenyl) naphthoyl derivatives has focussed on determining their anti-proliferative effect in the non small cell lung cancer (NSCLC) cell line, H1299. This is due to the fact that lung cancer is the leading cause of cancer mortality worldwide with approximately 75–85% of all lung cancer cases being NSCLC.[47] European national cancer registries have shown a rising incidence of melanoma during the past two decades.[48] Most localised melanoma can be effectively treated early by wide localised excision; however, patients with advanced stage of the disease have a poor prognosis, with a 1 year survival rate of less than 5%. The poor prognosis is due to the resistant of metastatic melanoma to cytotoxic chemotherapy.[49] More efficacious novel chemotherapeutic drugs are urgently required to improve the prognosis for malignant melanoma patients. Thus, Kenny *et* al. have reported the synthesis, characterisation and biological evaluation of a series of *N*-(ferrocenyl) naphthoyl amino acid esters, which have been screened *in vitro* for anti-proliferative effect against NSCLC cell line, H1299 and Sk-Mel-28 malignant melanoma cell line.[50] The *N*-(6-ferrocenyl-2-naphthoyl) γ -aminobutyric acid ethyl ester **30** (figure 1.19) was found to be the most active derivative of the naphthoyl amino acid series displaying a high activity in both the H1299 cell line with an IC_{50} value of 0.62 ± 0.06 μM and in the Sk-Mel-28 cell line an IC_{50} 1.41 ± 0.04 μM .

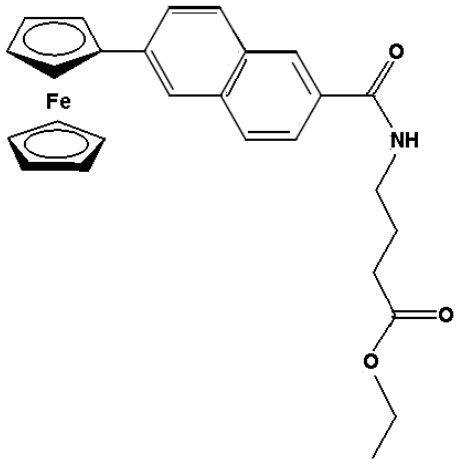

30

Figure 1.19: Structure of *N*-(6-ferrocenyl-2-naphthoyl) γ-aminobutyric acid ethyl ester **30.**

From futher SAR studies of the *N*-(6-ferrocenyl-2-naphthoyl) derivatives, by replacing the alanine amino ethyl ester of compound **30** (figure 1.19) with glycine, Kenny *et* al. have recently reported a three fold improvement in antiproliferative effect in the non small cell lung cancer (NSCLC) cell line, H1299 with the *N*-{6-(ferrocenyl)-2-napthoyl} glycine glycine ethyl ester **31** (figure 1.20) showing an IC_{50} value of 0.13 ± 0.01 µM.[51]

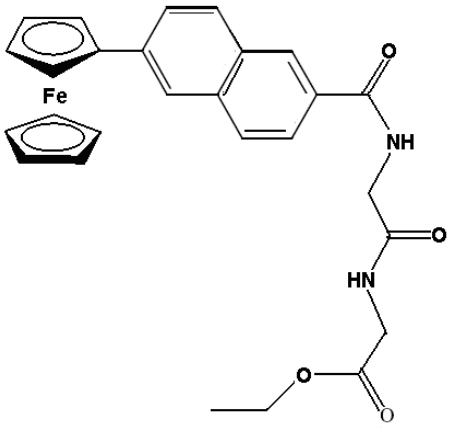

31

Figure 1.20: Structure of *N*-{6-(ferrocenyl)-2-napthoyl} glycine glycine ethyl ester **31.**

Kondopi *et* al. have reported the preparation of several ferrocene derivatives and found out that thiomorpholideamidemethylferrocene **32** (figure 1.21) showed the highest antiproliferative activity against colo 205 colon adenocarcinoma compared to the other derivatives prepared with IC_{50} an value of 50 µM.[52]

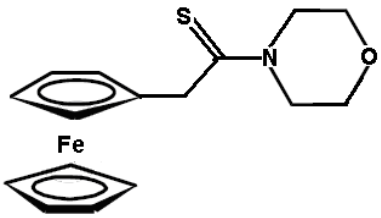

32

Figure 1.21: Structure of thiomorpholideamidemethylferrocene **32.**

Kondopi *et* al. also suggested that the mode of action was as a result of a competitive binding between ATP to the catalytic enzyme topoisomerase II which resulted in its inhibition. Topoisomerase II is an enzyme responsible for maintaining the topology of DNA and it is well known that, in cancer cells, there is an increased topoisomerase II activity, hence, the inhibition of topoisomerase II results in antiproliferative activity.[53] In addition to the reported ferrocene derivatives that have shown anticancer activity, the incorporation of ferrocene into large bioactive molecules have been explored as promising strategy against cancer activity. The incorporation of a metallocene into compounds with medicinal applications was rare prior to the 1980s. To date there has been several reported successes of increased efficacy of ferrocenyl analogues of known drugs. Jaouen *et* al. reported that the incorporation of a ferrocene moiety in tamoxifen showed antitumour activity in both hormone-dependent and hormone-independent breast cancer.[54] Breast cancer is the most common cancer in women and it affects one in every eight women in the world. It is classified into two types, which are distinguished by the presence or absence of estrogen receptors (ER); ER(+) is used to distinguish breast cancer that is dependent on the presence of the estrogen receptor, which account for two-thirds of breast cancer, whilst ER(-) is used to distinguish breast cancer which is independent of the estrogen receptor. Tamoxifen **33** (figure 1.22) is widely prescribed to patients diagnosed with ER(+) breast cancer. The antiproliferative effect arises from the competitive binding of hydroxytamoxifen **34** (the active form of tamoxifen) to the estrogen receptor instead of estradiol **35** (figure 1.22) which results in the repression of the estradiol-mediated DNA transcription.[55]

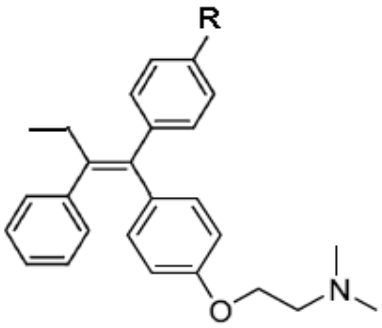

33: R=H**; 34:** R=OH

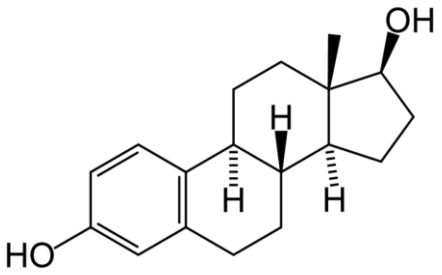

35

Figure 1.22: Tamoxifen **33** and hydroxytamoxifen **34** and estradiol **35.**

Although the administration of tamoxifen is well tolerated, unfortunately some drawbacks are associated with its use, for instance long term use of tamoxifen increases the risk of uterine cancer and blood clotting in the lungs. Overtime, some cancer cells develop resistance to tamoxifen administration and, furthermore, tamoxifen is not effective against the ER(-) breast cancer form. In trying to find better alternatives to tamoxifen, Jaouen *et* al. investigated ferrocifen **36** (figure 1.23), a tamoxifen analogs that contained an organometallic moiety. Whilst they were studying the effects of hydroxyferrocifen (active form of ferrocifen) on the proliferation of the ER(+) and ER(-) breast cancer cell lines they observed the following. In ER(+) MCF-7 cells, hydroxyferrocifen showed an antiestrogenic effect similar in ER(-) MDA-MB-231 cell lines, the hydroxyferrocifen showed antiproliferative activity with an IC_{50} value in the order of 0.5 µM, whereas, there was no anticancer activity observed when hydroxytamoxifen **34** (figure 1.22) was used. The hydroxyferrocifen **37** (figure 1.23), which is the ferrocenyl analogue of hydroxytamoxifen synthesized by Jaouen *et* al. was the first molecule that have been shown to be to be active in both hormone-dependent and hormone-independent breast cancer tumours and furthermore showed a wide therapeutic window against kidney cancer, ovarian and prostate cancer.

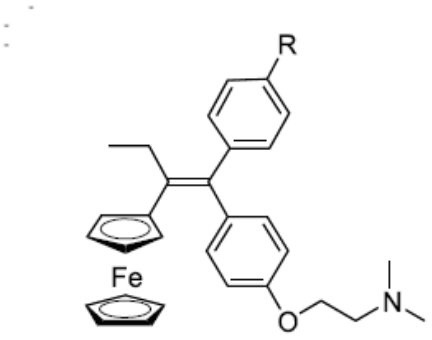

36: R=H; **37**: R=OH

Figure 1.23: Structure of ferrocifen **36** and hydroxyferrocifen **37.**

Jaouen *et al* have also reported the incorporation of ferrocene to a polyphenolic system yielding compound **38** (figure 1.24) which also showed antiproliferation effects in both hormone-dependent and hormone-independent tumours in ER(+) MCF-7 cells and in ER(-) MDA-MB-231 cell lines. The antiproliferative effect observed was stronger than that observed for hydroxytamoxifen. This high effect may lead to the generation of a potent cytotoxic compound.[56]

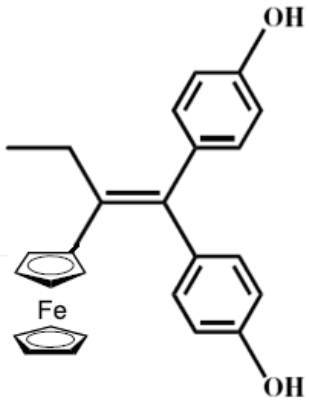

38

Figure 1.24: Structure of ferrocenyl polyphenolic **38.**

1.2.2 Antimalarial organometallic therapeutics

For many years, malaria has continued to be a major cause of death in many developing countries. According to reports from the World Health Organization (WHO), approximately 40 % of the world's population is at risk of malaria infection.[57]

To date, chloroquine **39**, and quinine **40** and mefloquine **41** (figure 1.25) have been the most effective antimalarial agents used against the four known malaria parasites namely *Plasmodium falciparum, P. vixax, P. ovale and P. malariae*, of which *P. falciparum* is the most dangerous and accounts for 90% of all deaths from malaria because it is becoming more resistant to existing therapeutics.[58] As a result of the increased resistance by the malaria parasites, some novel organometallic antimalarial drugs have been synthesized.

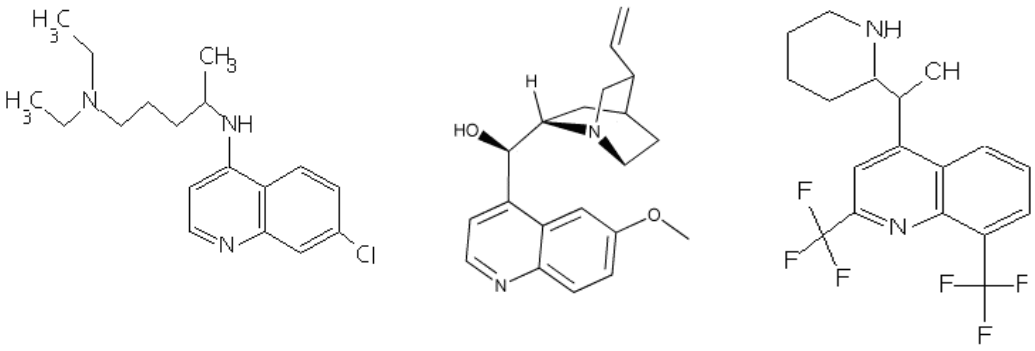

39 **40** **41**

Figure 1.25: Structures of chloroquine **39**, quinine **40** and mefloquine **41.**

Brocard *et* al. discovered that the insertion of a ferrocenyl group to chloroquine resulted in the chemotherapeutic activity of chloroquine being altered.[59] They showed that for ferroquine **42** (figure 1.26) an analogue of chloroquine, the incorporation of a ferrocenyl moiety as an integral part of the side chain of chloroquine between the two N atoms had superior efficacy to other analogues in which the moiety was terminal on the side chain or bonded to the quinoline. *In vitro* assays showed that ferroquine was more potent than chloroquine in the inhibition of the growth of *P. falciparium.*

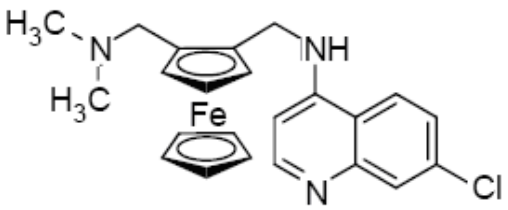

42

Figure 1.26: Structure of ferroquine **42.**

To date, the use of ferroquine as a potential antimalarial agent has made it possible to avoid the relapse in the long term which is associated with conventional antimalaria therapeutics and as a result ferroquine is in phase 1 clinical trials. Biot *et al*. recently demonstrated that the mode of action of ferroquine is similar to that of chloroquine, in that ferroquine forms complexes with haematin found in infected red blood cells and ferroquine is an even stronger inhibitor of β-haematin formation than chloroquine.[60] When chloroquine is administered to chloroquine resistant malaria parasites, the chloroquine is expelled rapidly from red blood cells and this is catalyzed by a *P. falciparum* transmembrane protein. However, when ferroquine is administered Biot *et* al. reported that ferroquine may block the *P. falciparium* transmembrane protein through its lipophilic properties, acting like a resistance reversing agent; hence, this could be the reason why ferroquine is effective against chloroquine-resistant malaria. Biot *et al.* also have shown the preparation of a series of ferrocenyl mefloquine analogues **43** and **44** (figure 1.27). When tested on *P. falciparium* strains, the results showed that the ferrocenyl analogue compounds exhibited a lower antimalarial activity than existing mefloquine and quinine therapeutics.[61]

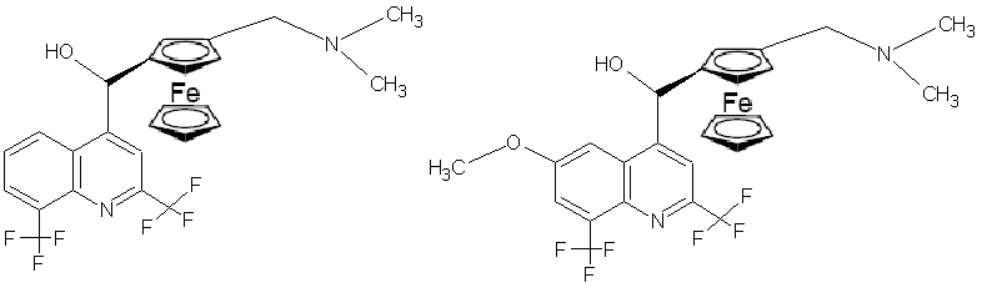

43 **44**

Figure 1.27: Structures of ferrocenyl mefloquine analogues **43** and **44.**

Go *et* al. prepared a series of ferrocenyl chalcones an example of which is compound **45** (figure 1.28)**.** These antimalarial ferrocene derivatives did not involve any incorporation of any of the existing conventional therapeutics previously discussed.[62] *In vitro* assays against *Plasmodium falciparium* showed that the most active compound was 1-ferrocenyl-3-(4-nitrophenyl)prop-2-en-1-one and the location of the ferrocene moiety and the polarity of the carbonyl linkage influenced the ease of oxidation of Fe^{2+} in ferrocene which enhanced the antiplasmodial activity.

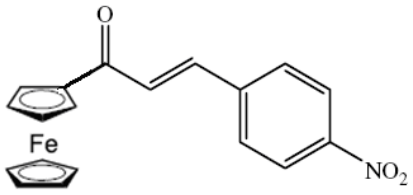

45

Figure 1.28: Structure of 1-ferrocenyl-3-(4-nitrophenyl)prop-2-en-1-one **45.**

Go *et al* also reported that the incorporation of ferrocene may enhance the antimalarial activity through the generation of free radicals from the redox cycling of the ferrocene moiety which may contribute to the antiplasmodial activity observed with ferrocenyl chalcones. However, the extent to which this property is manifested is also influenced by other physicochemical properties such as polarity, planarity and lipophilicity of the compounds.[62]

1.2.3 Antibacterial therapeutics

Antibiotics have been critical in the fight against infectious diseases caused by bacteria; however, bacterial resistance to existing antibiotics continues to develop and poses a significant threat. For instance, diseases such as gonorrhoea and tuberculosis have become hard to treat with current antibiotics.[63] Antibacterial resistance over the years has developed as a result of the natural consequence of the ability of the bacterial cell to adapt as a result of the prolonged usage of the existing antibiotics. To complicate matters there has been a decline in antibacterial research by many large pharmaceutical companies and this has led to a shortfall in the development of new and better antibacterial agents to fight the present threat of drug resistance. Penicillin V **46** (figure 1.29) historically was the first antibacterial drug that was effective against many previously serious diseases such as syphilis and staphylococcus infections. Penicillin V is still widely used today, although many types of bacteria are now resistant to its administration such as *Eschericia. coli.*[64-65]

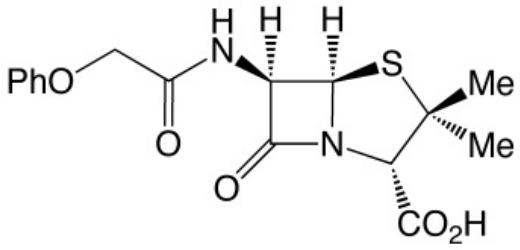

46

Figure 1.29: Structure of Penicillin V **46.**

Resistance to penicillin V in *Eschericia. coli* was first reported by Abraham *et* al. in 1940 and, later on in 1952, Lederberg *et* al. reported the ability for bacterial to transfer genetic information on antibiotic resistance to other bacterial species.[64-65]

Despite the years of exhaustive medicinal chemical studies on the modification of known antibacterial scaffolds, it is becoming increasingly difficult to deliver new leads on this approach. The recent focus on antibacterial research has, therefore, moved to the identification of novel therapeutics. The use of organometallic compounds as potential antibacterial agents is now an active area of research. The first reported antibiotic that

contained an organometallic moiety was ferrocenyl penicillin **47** (figure 1.30). In 1975 Edward *et al* reported the synthesis of ferrocenyl penicillin.[66] They reported that when a ferrocenyl moiety is incorporated into penicillin, the antibacterial properties of the penicillin V derivative increased significantly.

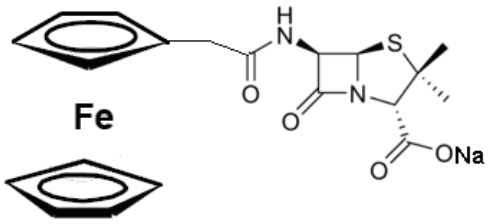

47

Figure 1.30: Structure of ferrocenyl penicillin **47.**

The observed increased antibacterial activity of ferrocenyl penicillin as a result of the incorporation of a ferrocene metal complex and the successful organometallic therapeutics that are in clinical use in cancer treatment has prompted the exploration of organometallics as antibacterial agents.[67] Dyson *et* al. have recently reported the synthesis of a series of water soluble ruthenium (II) arene complexes, which were screened for antibacterial activity, The ruthenium complex, {Ru(η^6-p-cymene)I_2(1,3,5-triaza-7-phosphatricylo[3.3.1.1]decane)} **48** (figure 1.31) showed the highest antibacterial activity against *Bacillus subtilis* compared to the other water soluble ruthenium (II) arene complexes.

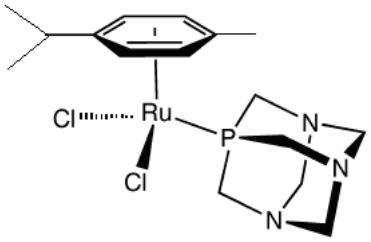

48

Figure 1.31: Structure of {Ru(η^6-p-cymene)I_2(1,3,5-triaza-7-phosphatricylo [3.3.1.1] decane)}**48.**

Kabbani *et* al. have also reported the synthesis of copper and cobalt complexes with 4-chloro-3-nitrobenzoate (ClNBz) and the nitrogen ligands 1,3-diaminopropane (1,3-DAP) or *o*-phenylenediamine (*o*-PDA) and they have shown that the copper complex [Cu(ClNBz)(*o*-PDA)]Cl **49** (figure 1.32) showed the highest antibacterial activity compared to the other complexes studied as indicated by its ability to inhibit the growth of *Staphylococcus aureus* and *Enterococcus faecalis.*[68]

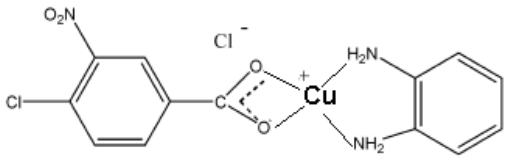

49

Figure 1.32: Structure of [Cu(ClNBz)(*o*-PDA)]Cl **49.**

1.3 Summary

Despite the years of exhaustive medicinal chemistry studies on the modification of known therapeutic scaffolds, it is becoming increasingly difficult to deliver new leads on this approach and as a result the use of organometallics in biomedical applications has become an active area of research. The use of organometallics as potential therapeutics commenced with the discovery of cisplatin by Rosenberg in 1965 which marked the genesis of bioorganometallic chemistry due to the success of cisplatin against various types of cancer. Furthermore, the incorporation of organometallics into compounds with medicinal applications has resulted in increased efficacy of existing therapeutics, for example ferrocifen, the ferrocenyl analogue of tamoxifen, has shown antiproliferative effects in both hormone-dependent and hormone-independent tumours which was not shown by tamoxifen an established chemotherapeutic. Furthermore the use of ferroquine, the ferrocenyl analogue of chloroquine as a potential antimalarial agent has made it possible to avoid the relapse in the long term which is associated with conventional antimalarial therapeutics.

References:

1 http://www.cancer.gov/cancertopics/cancerlibrary/what-is-cancer

2 Valko, M., Rhodes, C.J., Moncol, J., Izakovic, M., Mazur, M., *Chemico.Bio. Inter.*, **2006**, *160*, 1–40.

3 World Health Organization, http://www.who.int.

4 Amarasena, U I., Walters J.A.E., Wood-Baker, R., and Fong, K., In *Cochrane Database of Systematic Reviews*; John Wiley & Sons, Ltd: Chichester, UK, 2008.

5 Burdett, S., L. Stewart, L., and Rydzewska, L., In *Cochrane Database of Systematic Reviews*; John Wiley & Sons, Ltd: Chichester, UK., **2007**.

6 N.-S. C. L. C. C. Group In., *Cochrane Database of Systematic Reviews*., John Wiley & Sons, Ltd: Chichester., UK, **2000**.

7 http://www.cancer.gov/cancertopics/treatment/types-of-treatment.

8 Gogas, H.J., Kirkwood, J.M., and Sondak, V.K., *Cancer.*, **2007**, *109*, 455-464.

9 Reid, J.M., Kuffel, M.J., Miller, J.K,, *Clin Cancer Res.*, **1999**, *5*, 2192-2197.

10 Patrick, G.L., *An Introduction to Medicinal Chemistry*, 3rd ed., Oxford University Press, **2005**.

11 http://chemoth.com/types/antimetabolites.

12 http://www.cancer.org/treatment/treatmentsandsideeffects/guidetocancerdrugs/gemcitabine.

13 http://www.drugs.com/mmx/gemzar.html.

14 http://www.ebi.ac.uk/interpro/potm/2006_1/Page1.htm.

15 Giaccone, G., Pinedo, H.M., *The Oncologist* ., **1996**, *1*, 82-87.

16 Rosenberg, B., Vancamp, L., Trosko, J.E., Mansour, V.H., *Nature*., **1969**, *222*, 385-386.

17 De Champdore, M., Fabio, G., Messere, A., Montesarchio, D., Piccialli, G., Loddo, R., Collad, M., *Tetrahedron.*, **2004**, *60*, 6555- 6563.

18 Fouda, M.F.R., Abd-Elzaher, M.M., Abdelsamaia, R.A., Labib, A.A., *Applied Organometallic Chemistry.*, **2007**, *21*, 613-625.

19 Long, N.J., *Metallocenes: An Introduction to Sandwich Complexes.*, Blackwell Science., **1998**.

20 Chu, G., *J. Biol. Chem.*, **1994**, *269*, 787-790.

21 Kelland, B., *Chem. Rev*., **2007**, *107*, 1387-1407.

22 Jung, Y., *Chem. Rev*., **2007**, *107*, 1387-1407.

23 Amtmann, E., *Cancer Chemother. Pharmacol*., **2001**, *47*, 461-466.

24 Kelland, L., *Expert Opin. Investigation. Drugs*., **2007**, *16*, 1009-1021.

25 Meléndez, E., *Critical Reviews in Oncology/Heamatology*., **2002**, *42*, 309-315.

26 Kopf, H., Kopf-Maier, P., *Angew. Chem. Int. Ed. Eng*., **1979**, *18*, 477-478.

27 Lu, Z., Lu, C., Ren X. and Meng, Q., *J. Organomet. Chem.*, **2006**, *691*, 5895-5899.

28 Kostova, J., Curr. *Med. Chem*., **2006**, *13*, 1085-1107.

29 Alessio, E., Mestroni, G., Bergamo, A., Sava, G., *Met. Ions Biol. Syst.*, **2004**, *42*, 323-351.

30 Kung, A., Pieper, T., Wissiack, R., Rosenberg, E., Keppler, B. K., *J. Biol. Inorg. Chem.*, **2001**, *6*, 292-299.

31 Pluim, D., van Waardenberg, R.C.A.M., Beijnen, J.H., Schellens, J.H.M., *Cancer Chemother. Pharmacol.*, **2004**, *54*, 71-78.

32 Kapitza, S., Jakupec, M.A., Uhl, M., Keppler, B.K., Marian, B., *Cancer Lett*., **2005**, *226*, 115-121.

33 Morris, R. E., Aird, R. E., Murdoch, P. D., Chen, H. M., Cummings, J., Hughes, N.D., Parsons, S., Parkin, A., Boyd, G., Jodrell, D. I., Sadler, P. J., *J. Med. Chem., 2* **2001**, *44*, 3616-3621.

34 Allardyce, C. S., Dyson, P. J., Ellis, D. J., Heath, S. L., *Chem. Commun.*, **2001**, *8*, 1396-1397.

35 Kopf-Maier, P., Kopf, H., Neuse, E., *Angew. Chem. Int. Ed. Eng*., **1984**, *23*, 456-458

36 Osella, D., Ferrali, M., Zanello, P., Laschi, F., Fontani, M., Nervi, C., Cavigiolio, G., *Inorganica Chimica. Acta.*, **2000**, *306*, 42-48

37 Houlton, A., Roberts, R.M.G., Silver, J., *J. Organomet. Chem.*, **1991**, *418*, 107-112

38 Tamura, H., Miwa, M., *Chem. Letts*., **1997**, *11*, 1177- 1178.

39 Romao, C.C., Alves, P.M., Pillinger, M., Goncalves, I.S., Matos, M.L., Pereira, C.C.L., Braga, S.S., Norton de Matos, M.R.P., Petrovski, Z., *J. Organomet. Chem.*, **2008**, *693*, 675-684.

40 Gao, M.L., Hernandez, R., Matta, J., Melendez, E., *Hindawi. Pub. Corp*., **2009**, *420*, 784-788.

41 Kelly, P.N., Prêtre, A., Devoy, S., O'Rielly, I., Devery, R., Goel, A., Gallagher, J.F., Lough, A.J., and Kenny, P.T.M., *J. Organomet. Chem.*, **2007**, *692*, 1327-1331.

42 Goel, A., Savage, D., Alley, S.R., Kelly, P.N., O'Sullivan, D., Mueller-Bunz, H., and Kenny, P.T.M., *J. Organomet. Chem.*, **2007**, *692*, 1292-1299.

43 Corry, A.J., Goel, A., Alley, S.R., Kelly, P.N., O'Sullivan, D., Savage, D., and Kenny, P.T.M., *J. Organomet. Chem.*, **2007** *692*, 1405-1410.

44 Goel, A., Savage, D., Alley, S.R., Hogan, T., Kelly, P.N., Draper, S., Fitchett C.M., and Kenny P.T.M., *J. Organomet. Chem.*, **2006**, *691*, 4686-4693.

45 Corry, A.J., Mooney, A., O'Sullivan, D., and Kenny, P.T.M., *Inorganica Chimica. Acta.*, **2009**, *362*, 2957-2961.

46 Mooney, A., Corry, A.J., O'Sullivan, D., Rai, D.K., and Kenny, P.T.M., *J. Organomet. Chem.*, **2009**, *694*, 886-894.

47 Ferlay, J., Autier, P., Boniol, M., Heanue, M., Colombet, M., and Boyle, P., *Ann. Oncol.*, **2006,** *18*, 581–592.

48 Mckie, R.M., Hauschild, A., and Eggermont A.M.M., *Ann. Oncol.*, **2009**, *20*, 1-7.

49 Eustance, A.J., Crown, J., Clynes, M., O'Donovan, N., *J. Transl. Med.*, **2008**, *6*, 53–64.

50 Mooney, A., Corry, A.J., Ni' Ruairc, C., Mahgoub, T., O'Sullivan, D., O'Donovan, N., Crown, J., Varughese, S., Draper, S.M., Rai, D.K., and Kenny, P.T.M., *Dalton. Trans.*, **2010**, *39*, 8228–8239.

51 Mooney, A., Tiedt, R., Maghoub, T., O'Sullivan, D., O'Donovan, N., Crown, J., Varughese, S., White, B., and Kenny, P.T.M., *J. Med. Chem.*, **2012**, *55*, 5455−5466.

52 Gopal, Y.N.V., Jayaraju, D., Kondapi, A.K., *Arch. Biochem. Biophys.*, **2000,** *376*, 229-235.

53 Krishna, A.D.S., Panda, G., Kondapi, A.K., *Arch. Biochem. Biophys.*, **2005,** *438*, 206-216

54 Top, S., Dauer, B., Vaisserman, J., Jaouen, G., *J. Organomet. Chem.*, **1997**, *541*, 355-361

55 Huynh, H., Yang, X., Pollak, M., *J. Biol. Chem.*, **1996**, *271*, 1016.-1021

56 Vessieres, A., Top, S., Pigeon, P., Hillard, E., Boubeker, L., Spera, D., Jaouen, G., *J. Med. Chem.*, **2005**, *48*, 3937-3940

57 World Health Organization, http://www.who.int.

58 WHO., *Weekly Epidemiol. Rep*., **1996**, *3*, 53-80

59 Biot, C., Glorian, G., L. A. Maciejewski, L.A., J. S. Brocard, J.S., *J. Med. Chem*., **1997,** *23*, 3715-3718.

60 Biot, C., Taramelli, D., Forfar-Bares, I., Maciejewski, L., Boyce, M., Nowogrocki, G., Brocard, J., Basilico, N., Olliaro, P., Egan, T.J., *Mol. Pharm.*, **2005**, *2***,** 185-193.

61 Biot, C., Delhaes, L., Maciejewski, L.A., Mortuaire, M., Camus, D., Dive, D., Brocard, J.S., *Eur. J. Med. Chem.*, **2000**, *35*, 707-714

62 Wu, X., Wilairat, P., Go M.L., *Bioorg. Med. Chem. Lett.*, **2002**, *12*, 2299-2302

63 World Health Organization, http://www.who.int.

64 Abraham, E.P., Chain, E., *Nature.*, **1940**, 51, *3713*-837.

65 Lederberg, J., Lederberg, E., 1952. *J. Bact*., **1952**, *63*, 399-406.

66 Edwards, E.I., Epton, R., Marr, G., *J. Organomet. Chem*., **1975**, *85*, 223-225.

67 Dyson, P.J., Allardyce, C.S., Ellis, D.J., Salter, P.A., Scopelliti, R., *J. Organomet. Chem.*, **2003**, *668*, 35-42**.**

68 Kabbani, A.T., Hammud, H.H., Ghahannoum, A.M., *Chem. Pharm. Bull.*, **2007**, *55*, 446–450.

Chapter 2: Synthesis and structural characterisation of 1-alkyl-1'-*N-para*, *N-meta* and *N-ortho*-(ferrocenyl) benzoyl dipeptide esters

2.1 Introduction

Organometallic compounds containing transition metals, such as cobalt, copper, iron and platinum are known to have antiproliferative (*in vitro*) and antineoplastic (*in vivo*) activities.[1] Platinum coordination compounds, such as cisplatin and carboplatin are currently being used in the treatment of a variety of tumours.[1] However, problems with toxicity, harsh side effects during administration, together with acquired drug resistance, has lead to increased research, to find alternatives to cisplatin and its analogues.

Ferrocene is a particularly useful organometallic compound for biological applications due to its electrochemical properties, its stability and its aromatic nature which allows for derivatization. As a result of these factors, ferrocene research has received an increased level of interest over the past decade.[1] Ferricenium salts are known to inhibit tumour growth through the formation of hydroxyl radicals under physiological conditions, leading to the oxidative damage of DNA.[2] Therefore, ferrocenyl derivatives that possess redox potentials which fall within the range of biologically accessible potentials, offer a desirable and alternative method to target and kill cancer cells. The aim of this research is to develop novel ferrocenyl dipeptide bioconjugates for use as potential anticancer agents.

Previous studies within the group have been carried out on the non small cell lung cancer (NSCLC) cell line, H1299 to evaluate the *in vitro* activity of novel ferrocenyl benzoyl amino acid and dipeptide esters. The effect of these compounds on H1299 cell growth was expressed as IC_{50} values. The IC_{50} value is the concentration of a drug required for 50% inhibition of cell growth. *N*-{*ortho*-(ferrocenyl) benzoyl} glycine ethyl ester was initially tested for its *in vitro* anti-proliferative activity against H1299 lung cancer cells. This compound was found to be cytotoxic and had an IC_{50} value of 48 ± 1.01 μM, whereas the starting material, *ortho*-ferrocenyl ethyl benzoate, was completely inactive against the cell line. Therefore, other derivatives were prepared and evaluated for their anticancer activity against H1299 lung cancer cells. The dipeptide

derivative *N*-{*ortho*-(ferrocenyl) benzoyl} glycine glycine ethyl ester was shown to have an IC_{50} value of approximately 20 ± 1.72 µM, while *N*-{*ortho*-(ferrocenyl) benzoyl} glycine L-alanine ethyl ester had an IC_{50} value of 5.3 ± 1.23 µM. The *N*-{*meta*-(ferrocenyl) benzoyl} glycine L-alanine ethyl ester **28** and *N*-{para-(ferrocenyl)-benzoyl} glycine L-alanine ethyl ester were also tested and gave results of 4.0 ± 0.71 µM and 6.6 ± 1.03 µM respectively.[3-7]

As an extension of this study we now report the synthesis and structural characterization of novel 1-alkyl-1'-*N-para*, *N-meta* and *N-ortho*-(ferrocenyl) benzoyl dipeptide esters. These compounds (figure 2.1) consist of four key moieties:

(i) A redox active centre
(ii) A conjugate linker
(iii) A alkyl chain (further lowers the oxidation potential of the ferrocene moiety)
(iv) A dipeptide chain

These novel derivatives differ from the *N-para*, *N-meta* and *N-ortho*-(ferrocenyl) benzoyl dipeptide esters by having an alkyl moiety on the previously unsubstituted cyclopentadiene ring (figure 2.1). The primary objective of this research is to explore a structure-activity relationship (SAR) study of the incorporation of alkyl chains moieties on the unsubstituted ring of the *N-para*, *N-meta* and *N-ortho*-(ferrocenyl) benzoyl dipeptide esters.[3-7] The dipeptides employed in this investigation were Glycine Glycine (Gly Gly), Glycine L-Alanine (Gly L-Ala), Glycine L-Leucine (Gly L-Leu) and Glycine L-Phenylalanine (Gly L-Phe) ethyl esters. A tripeptide or tetrapeptide chain was shown to have a negative effect on biological activity.[6] Thus, a series of novel 1-alkyl-1'-*N-para*, *N-meta* and *N-ortho*-(ferrocenyl) benzoyl dipeptide esters **64–99** (figure 2.1) were prepared by coupling alkyl ferrocenyl benzoic acids to the dipeptide ethyl esters using the conventional *N*-(3-dimethylaminopropyl)-*N*'-ethylcarbodiimide hydrochloride (EDC) and 1-hydroxybenzotriazole (HOBt) coupling protocol. All the compounds were fully characterized using a combination of nuclear magnetic resonance techniques (^{1}H, ^{13}C & DEPT-135), ^{1}H-^{13}C COSY and electrospray ionization mass spectrometry (ESI-MS).

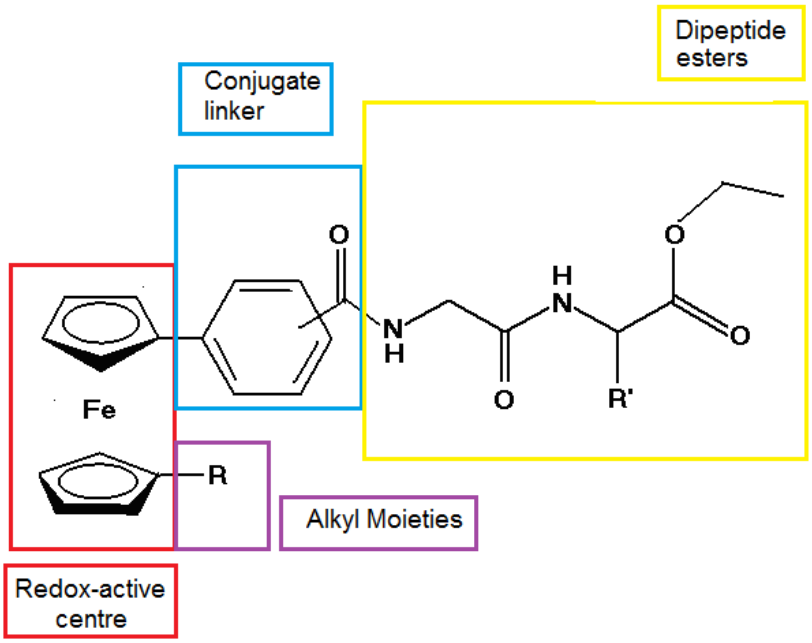

64–99

R = CH_3 , CH_2CH_3 , $CH_2CH_2CH_3$
R' = H, CH_3 , C_4H_9, C_7H_7,

Figure 2.1 General structure of the 1-alkyl-1'-*N-para*, *N-meta* and *N-ortho*-(ferrocenyl) benzoyl dipeptide esters **64–99.**

2.2 The synthesis of the alkylferrocene derivatives

For the synthesis of the alkylferrocenes, three synthetic pathways were considered as shown in scheme 2.1. The most direct approach for the preparation of alkylferrocenes involves the Friedel Crafts alkylation of ferrocene (scheme 2.1a). However, these reactions proceed with a low degree of regiocontrol and invariably produce mixtures of mono- and poly-alkylated derivatives in low yields.[8] The reason for such undesired polyalkylation is that the introduction of one alkyl group to the ferrocene results in the alkylferrocene ring being more activated than the ferrocene starting material resulting in further alkylation, leading to the almost inevitable second alkylation and hence, its use as a synthetic pathway was not investigated.

The synthesis of alkylferrocene utilising catalytic palladium cross coupling using ferrocene boronic acid and alkylhalides (Scheme 2.1b) offered a potential synthetic pathway which was evaluated in this study.[9] Initial work involved the optimisation of the experimental protocol and it was observed that reflux of reactants at 80 ^{o}C for 144 hr resulted in the synthesis of alkylferrocene, however, the yields for these reactions varied from 15–20%. The reflux period was time consuming and the yields were relatively low, hence, other feasible synthetic pathways were considered. The Friedel Crafts acylation reaction of ferrocene and Vilsmeir formylation are well established methods and furnish good yields of mono- and di-acylated ferrocenes (scheme 2.1c) with a remarkable degree of regioselectivity compared to the direct approach for the preparation of alkylferrocenes via Friedel Crafts alkylations.[10-11] Accordingly, a two-step protocol involving regioselective acylation followed by hydrogenation of the acylated ferrocene constituted a method of choice for the preparation of the alkylferrocenes. The hitherto reported general methods for the deoxygenation of acylferrocenes include Clemmensen reduction and reductive deoxygenation using lithium aluminium hydride in the presence of anhydrous aluminium trichloride.[12-14]

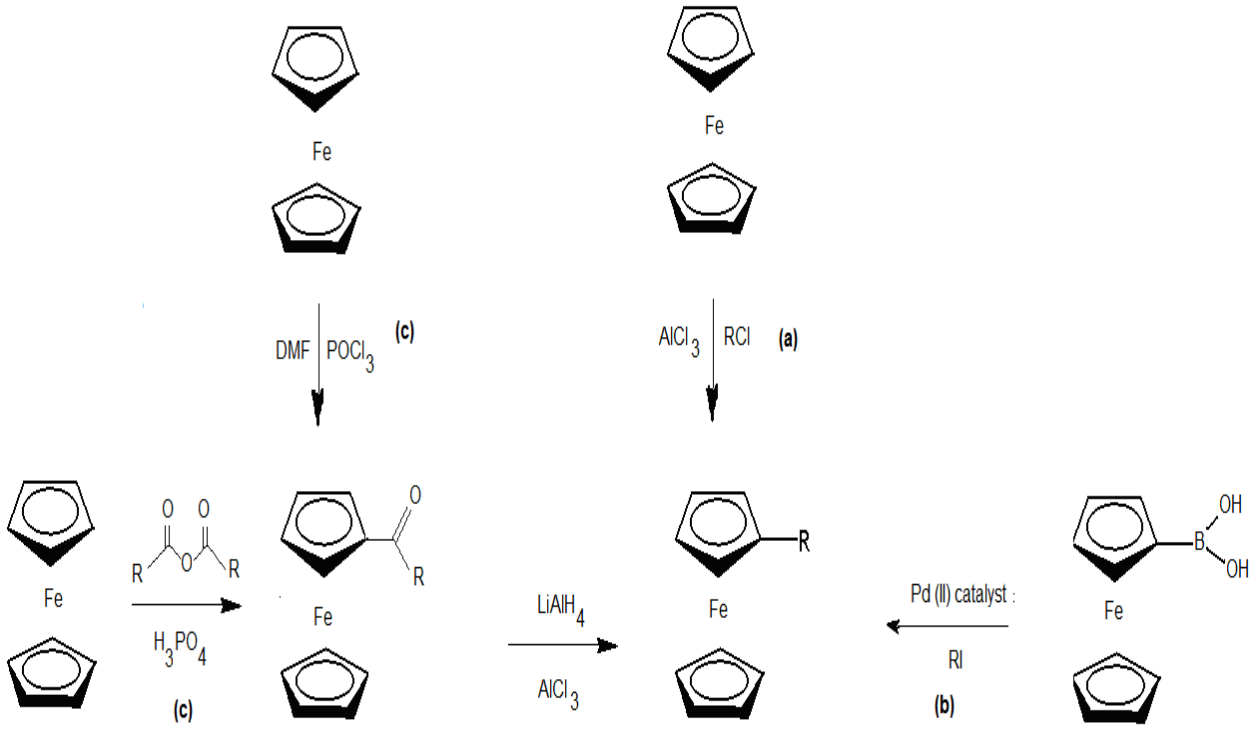

Scheme 2.1. Synthesis of alkylferrocene via three pathways **(a), (b)** and **(c).**

These methods were both evaluated as potential synthetic pathways for the formation of the alkylferrocenes. It was observed that the deoxygenation of acylferrocenes using lithium aluminium hydride in the presence of anhydrous aluminium chloride resulted in the formation of alkylferrocenes and the yields for these reactions varied from 75-95% whilst the Clemmensen reduction protocol was not successful on initial evaluation, hence, it was not investigated further.

2.2.1 The synthesis of alkylferrocene derivatives via palladium catalysed cross coupling.

The preparation of the alkylferrocene derivatives via palladium catalysed cross coupling involved the refluxing of ferrocene boronic acid in dimethoxyethane (DME) in the presence of 1,1-*bis*-(diphenylphosphino)ferrocene dichloropalladium(II) catalyst, 3M NaOH solution and iodoethane yielded ethylferrocene as shown in scheme 2.2.[15]

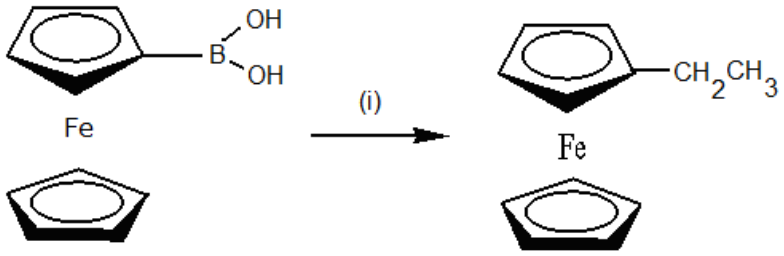

56

(i) 1,1-*bis*-(diphenylphosphino)ferrocene dichloropalladium(II),
DME, NaOH, Iodoethane

Scheme 2.2: The synthesis of ethylferrocene via palladium catalysed cross coupling.

The catalytic cycle for the formation of alkylferrocene derivatives via palladium cross coupling proceeds *via* three steps, (i) oxidative addition of a carbon electrophile to the zero valent palladium followed by (ii) the transmetallation of a nucleophilic carbon from boron to the palladium complex. Which is then followed by (iii) the rapid reductive elimination of the cross coupled product to regenerate the zero valent palladium, Pd(0) as shown in scheme 2.3.[15]

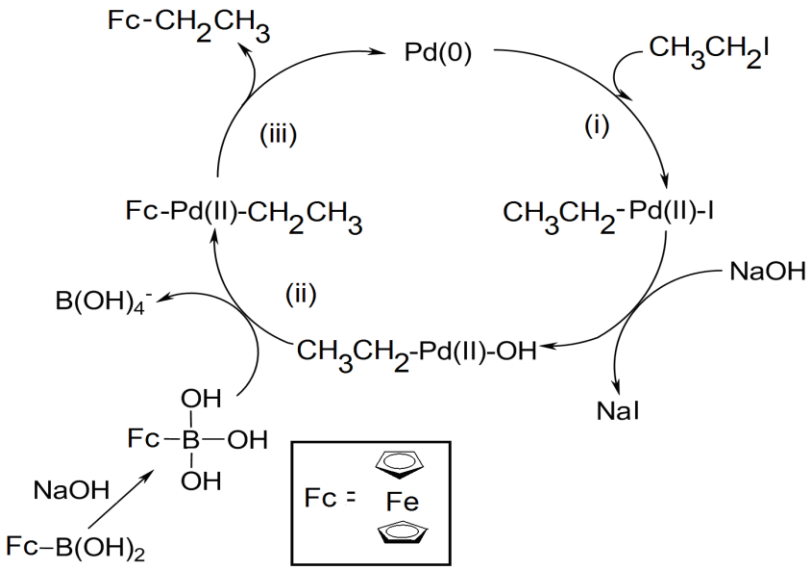

Scheme 2.3: Palladium catalysed cross coupling mechanism for the synthesis of ethyl ferrocene.

2.2.2 The synthesis of alkylferrocene derivatives via reductive deoxygenation of acylferrocenes derivatives

2.2.2.1 The synthesis of the acylferrocene derivatives

For the synthesis of acylferrocene derivatives two synthetic protocols reported in the literature were used. For the preparation of ferrocene carboxyaldehyde, Vilsmeir formylation was used.[11] For the synthesis of acetylferrocene and propionyl ferrocene Friedel Crafts acylation was the method of choice.[10]

2.2.2.1.1 Synthesis of ferrocene carboxaldehyde

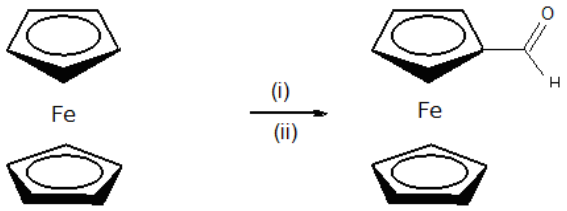

48

(i) $POCl_3$, DMF; (ii) NaOH, H_2O

Scheme 2.4: Synthesis of ferrocene carboxaldehyde **48**.

In the mechanism for the formation of ferrocene carboxaldehyde the initial step is the formation of the Vilsmeir reagent.[11] Today it is well established that the reaction proceeds via the formation of a chloromethylene iminium cation from the reaction between the DMF and phosphorus oxychloride as shown in scheme 2.5.

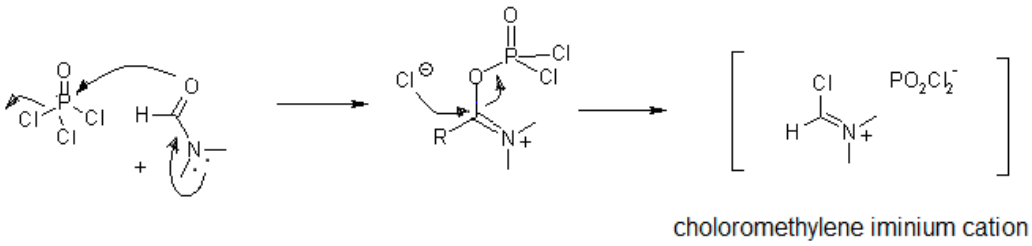

Scheme 2.5: Formation of choloromethylene iminium cation.

The chloromethylene iminium cation in the presence of an electron rich species in this case ferrocene undergoes iminoalkylation which is essentially an electrophilic substitution reaction. Hydrolysis of the iminoalkylation product is carried out using NaOH and water. This is a particularly useful method as it removes any acid formed and results in the formation of ferrocene carboxyaldehyde as shown in scheme 2.6.

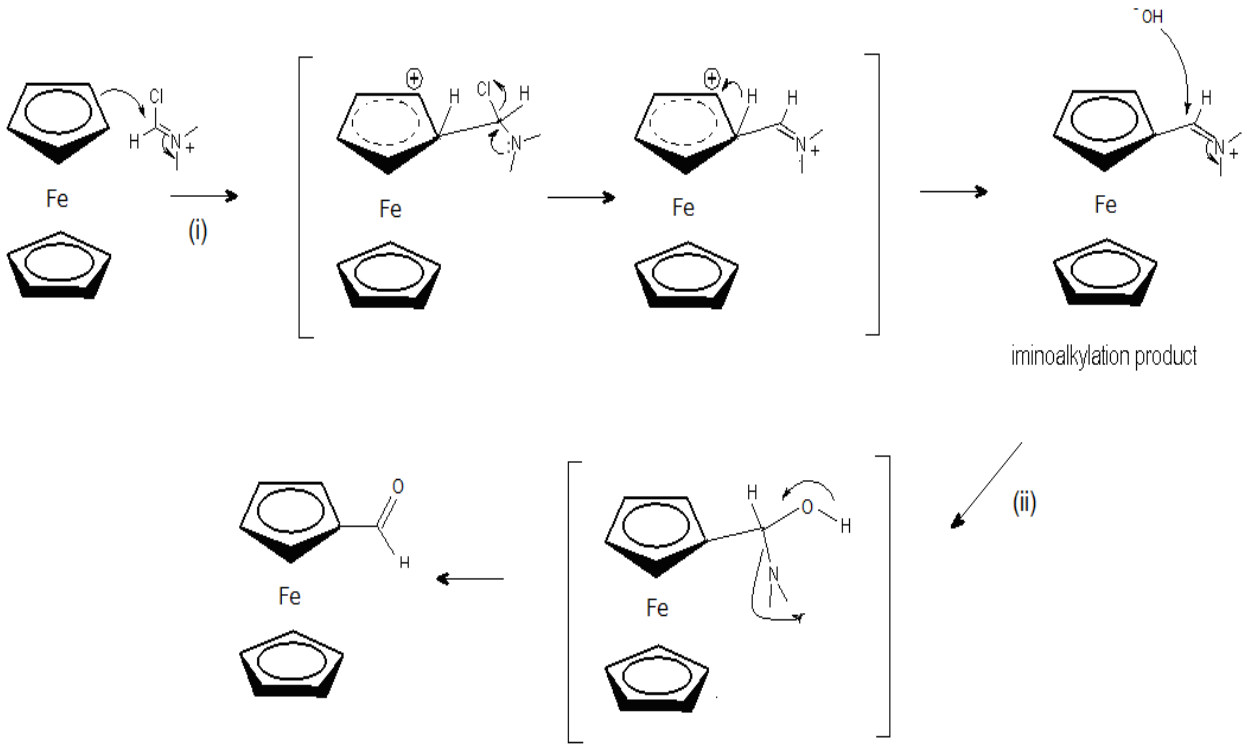

Scheme 2.6: Iminoalkylation (i) and base induced hydrolysis (ii).

In the synthesis of ferrocene carboxaldehyde via Vilsmeir formylation, low percentage yields of 11% were obtained. These low percentage yields were due to the fact the formylation is not substrate specific. Di-formylated ferrocene was formed in the reaction and unreacted ferrocene was recovered which showed that the reaction conditions employed did not result in the reaction going to completion. As a result of these limitations large scale synthesis was employed in order to get sufficient amounts of ferrocene carboxylaldehyde required for the reductive deoxygenation reaction to obtain methylferrocene.

2.2.2.1.2 Synthesis of acetylferrocene

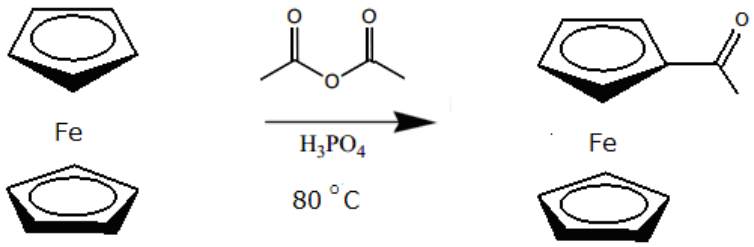

49

Scheme 2.7: Synthesis of acetylferrocene **49**.

Friedel Crafts acylation is a well known effective synthetic pathway of introducing new carbon-carbon bonds into aromatic compounds.[10] The most common catalyst for acylation of an aromatic ring is aluminum trichloride. Aluminium trichloride is a strong Lewis acid, and it is used in Friedel Crafts acylation. It is often associated with a few limitations, for example aluminum trichloride gives off HCl gas upon contact with moist air and is required in greater than stoichiometric amounts. This leads to the generation of considerable quantities of acidic and aluminum waste. For the Friedel Crafts acylation of ferrocene when aluminium trichloride is used, the activation of the ferrocene ring, leads to a large amount of disubstitution product being formed.[10] Therefore for the synthesis of acetyl ferrocene a benign catalyst, phosphoric acid, was used instead to catalyze the Friedel Crafts acylation reaction in the presence of acetic anhydride. This acylation reaction affords a higher yield of primarily the mono-substituted product, acetylferrocene. From numerous Friedel Crafts acylation reactions carried out, it was observed that slow addition of phosphoric acid over 30 min resulted in the generation of high yields of acetylferrocene, greater than 80%, as opposed to spontaneous addition of the catalyst which resulted in low yields being obtained. The mechanism for the synthesis of acetylferrocene involves the generation of an acylium ion electrophile by protonation of the acetic anhydride by phosphoric acid (scheme 2.8).[14]

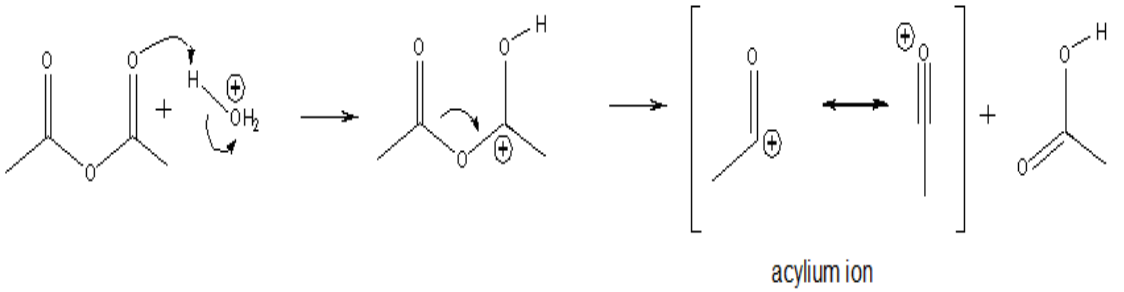

Scheme 2.8: Formation of acylium ion.

The π electrons on the cyclopentadiene ring of ferrocene act as a nucleophile, attacking the positively charge acylium carbon. This step destroys the aromaticity giving rise to a ferrocenyl cation intermediate. Removal of the proton from the carbon atom bearing the acyl group reforms the aromatic system, generating HCl and regenerating the active catalyst (scheme 2.9).

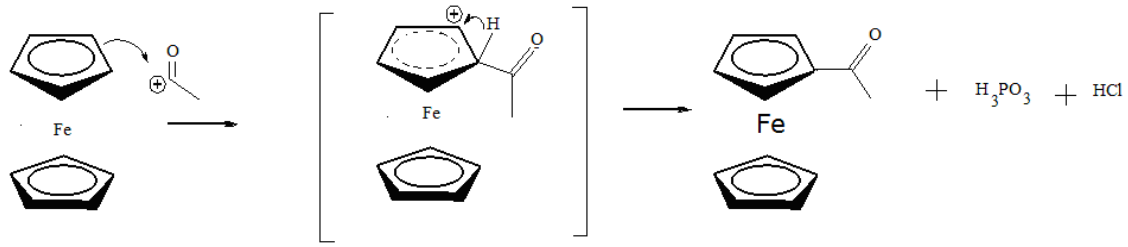

Scheme 2.9: Fridel crafts acylation mechanism for synthesis of acetyl ferrocene.

2.2.2.1.3 Synthesis of propionyl ferrocene

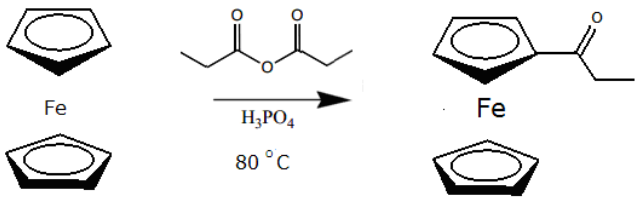

50

Scheme 2.10: Synthesis of propionyl ferrocene **50**.

The mechanism for the synthesis of propionyl ferrocene is similar to that used for the synthesis of acetylferrocene (scheme 2.8 and 2.9).[14] The only difference is that

propionic anhydride is used instead of acetic anhydride. The percentage yield of propionyl ferrocene was greater than 50%. These percentage yields were lower than those obtained for the acetylferrocene; the reason for the low yield was a result of steric hindrance associated with the size of acylium ion electrophile formed in the Friedel Crafts acylation reaction.

2.2.2.1.4 Reductive deoxygenation of acylferrocenes derivatives

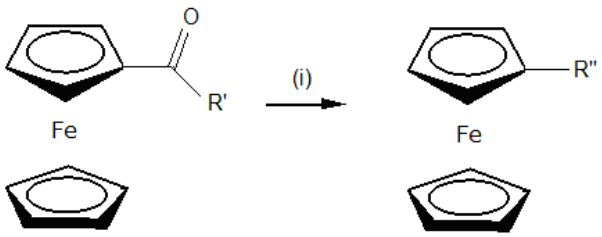

(i) $LiAlH_4$, $AlCl_3$, diethyl ether

48.R'= H; **49**. R'= CH_3 : **50.** R'= CH_2CH_3

51. R'' = CH_3; **56.** R''= CH_2CH_3; **60.** R''= $CH_2CH_2CH_3$

Scheme 2.11: Reductive deoxygenation of acylferrocenes derivatives.

The reductive deoxygenation of acylferrocenes to the corresponding hydrocarbons via the combined action of lithium aluminium hydride and the use of the strong Lewis acid aluminium trichloride in diethyl ether, as shown in scheme 2.11 yielded the desired alkylated ferrocene derivatives with percentage yields varying between 75-95%.

2.3 Synthesis of 1-alkyl-1'-*para, meta* and *ortho*-(ferrocenyl) benzoic acids

Following already established protocols for the synthesis of *para*-(ferrocenyl) benzoic acid, the synthesis of 1-alkyl-1'-*para*, *meta* and *ortho*-(ferrocenyl) benzoic acids involved the diazonium coupling of the alkylferrocene to 2, 3, 4-ethylamino benzoate followed by hydrolysis to yield the desired products (scheme 2.12).[3-7] However, the percentage yields were less than 8%. When 2,3,4-amino benzoic acids were used

instead of 2,3,4-ethylamino benzoates, yields greater than 15% were obtained for the 1-alkyl-1'-*para*, *meta* and *ortho*-(ferrocenyl) benzoic acids (scheme 2.13).

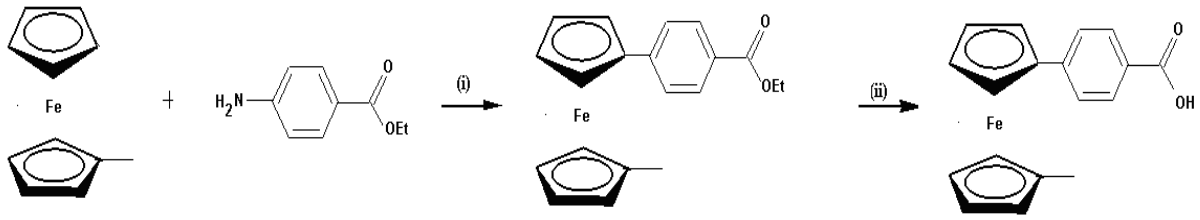

51. **52.** **53.**

(i) $NaNO_2$, HCl, (ii) NaOH, MeOH, HCl

Scheme 2.12: The synthesis of 1-methyl-1'-*para*-ferrocenyl benzoic acid via a two step reaction scheme.

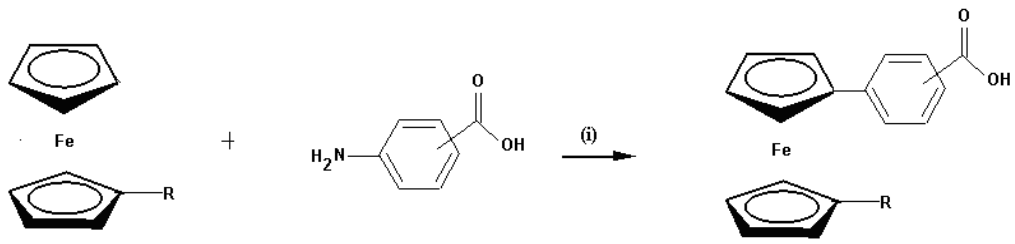

(i) $NaNO_2$, HCl

51: R = CH_3; **56:** R = CH_2CH_3; **60:** R = $CH_2CH_2CH_3$

53, 54, 55: R = CH_3; **57, 58, 59:** R = CH_2CH_3; **61, 62, 63:** R = $CH_2CH_2CH_3$

Scheme 2.13: The synthesis of 1-alkyl-1'-*para*, *meta* and *ortho*-(ferrocenyl) benzoic acids.

The mechanism for the diazonium coupling using 2,3,4-amino benzoic acids is shown is shown in scheme 2.14. [13]

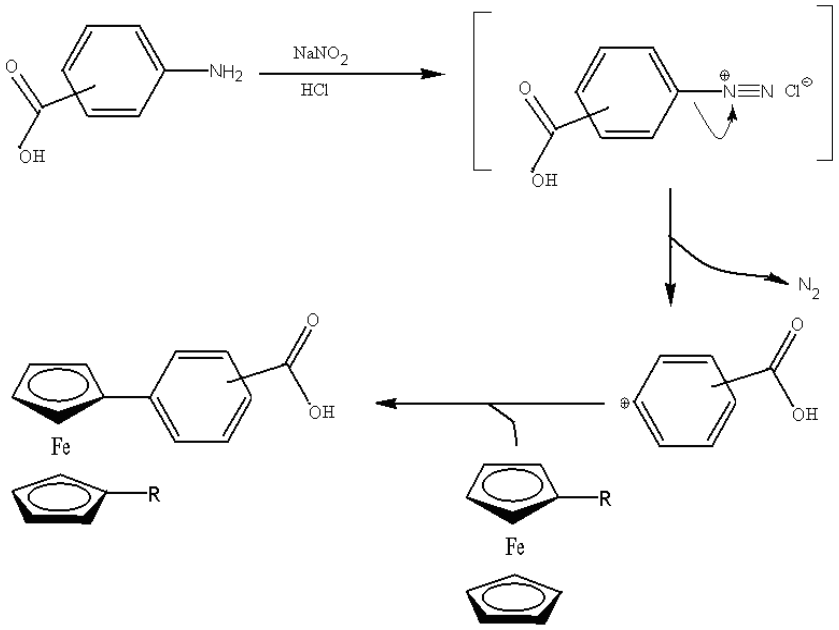

R = CH_3; CH_2CH_3; $CH_2CH_2CH_3$

Scheme 2.14: The mechanism for the diazonium coupling reaction.

2.4 The synthesis of 1-alkyl-1'-*N-para, N-meta* and *N-ortho*-(ferrocenyl) benzoyl dipeptide esters

The synthesis of 1-alkyl-1'-*N-para*, *N-meta* and *N-ortho*-(ferrocenyl) benzoyl dipeptide esters **64–99** involved the coupling of the dipeptide ethyl ester hydrochloride salts of Gly Gly, Gly L-Ala, Gly L-Leu and Gly L-Phe to 1-alkyl-1'-*para*, *meta* and *ortho*-(ferrocenyl) benzoic acids using *N*-(3-dimethylaminopropyl)-*N*'-ethylcarbodiimidehydrochloride (EDC), 1-hydroxybenzotriazole (HOBt) and triethylamine (TEA) in dichloromethane shown in scheme 2.15.[3-7] The 1-alkyl-1' derivatives were isolated following the coupling procedure and purified by column chromatography, using a 1:1 mixture of hexane and ethyl acetate as the eluent. The pure 1-alkyl-1'-*N-para*, *N-meta* and *N-ortho*-(ferrocenyl) benzoyl dipeptide esters **64–99** was furnished as either an orange solid or a red oil, with yields of 12-28%. All compounds gave spectroscopic and analytical data in accordance with their proposed structures.

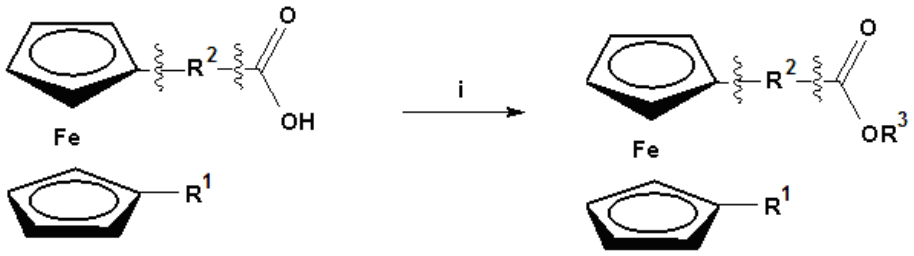

(i) EDC, HOBt, Triethylamine and dipeptides ethyl esters (R^3)

R^1	R^2	R^3	Compound no.
$-CH_3$		Gly Gly(OEt)	**64**
		Gly L-Ala(OEt)	**65**
		Gly L-Leu(OEt)	**66**
		Gly L-Phe(OEt)	**67**
	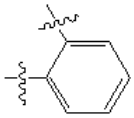	Gly Gly(OEt)	**68**
		Gly L-Ala(OEt)	**69**
		Gly L-Leu(OEt)	**70**
		Gly L-Phe(OEt)	**71**
	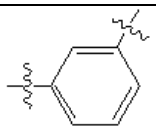	Gly Gly(OEt)	**72**
		Gly L-Ala(OEt)	**73**
		Gly L-Leu(OEt)	**74**
		Gly L-Phe(OEt)	**75**
$-CH_2CH_3$		Gly Gly(OEt)	**76**
		Gly L-Ala(OEt)	**77**
		Gly L-Leu(OEt)	**78**
		Gly L-Phe(OEt)	**79**
	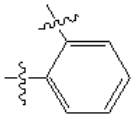	Gly Gly(OEt)	**80**
		Gly L-Ala(OEt)	**81**
		Gly L-Leu(OEt)	**82**
		Gly L-Phe(OEt)	**83**
	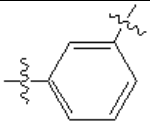	Gly Gly(OEt)	**84**
		Gly L-Ala(OEt)	**85**
		Gly L-Leu(OEt)	**86**
		Gly L-Phe(OEt)	**87**
$-CH_2CH_2CH_3$		Gly Gly(OEt)	**88**
		Gly L-Ala(OEt)	**89**
		Gly L-Leu(OEt)	**90**
		Gly L-Phe(OEt)	**91**
	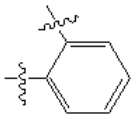	Gly Gly(OEt)	**92**
		Gly L-Ala(OEt)	**93**
		Gly L-Leu(OEt)	**94**
		Gly L-Phe(OEt)	**95**
	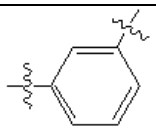	Gly Gly(OEt)	**96**
		Gly L-Ala(OEt)	**97**
		Gly L-Leu(OEt)	**98**
		Gly L-Phe(OEt)	**99**

Scheme 2.15: The synthesis of 1-alkyl-1'-*N-para*, *N-meta* and *N-ortho*-(ferrocenyl) benzoyl dipeptide esters **64–99.**

Of the compounds synthesized, the *ortho* derivatives (**72-75, 84-87, 96-99**) and *meta* derivatives (**68-71, 80-83, 92-95**) gave the lowest yields, while the *para* derivatives (**64-67, 76-79, 88-91**) gave the highest yields. The difference in percentage yield can be rationalized by considering the respective orientations of the *ortho* and *meta*-ferrocenyl benzoic acids. The 1-alkyl-1'- *meta* and *ortho*-(ferrocenyl) benzoic acids are more sterically hindered than the 1-alkyl-1'-*para*-(ferrocenyl) benzoic acid starting material which give arise to the low yields. This is consistent with previously reported observations by Corry *et* al. for the *N*-(ferrocenyl) benzoyl dipeptide derivatives.[3-7] The side chains of the reacting α-amino acids and the alkyl chain incorporated can also have an influence on the overall yield. Yields are lower in cases where both the side chain of the α-amino acids and alkyl group are large enough to exert steric hindrance. This is clearly observed for 1-methyl and 1-propyl-1'–*N*-{*para*-(ferrocenyl) benzoyl} glycine L-phenylalanine ethyl esters. The increase of the alkyl chain length from a methyl (**67**) to a propyl (**91**) resulted in a drop of the percentage yield from 16% to 14% respectively.

In the standard coupling protocol (EDC/HOBt), the first step towards the amide bond formation involves the addition of the carboxyl group to the carbodiimide to give an *O*-acylisourea ester intermediate. This intermediate is highly reactive and is prone to intramolecular acyl transfer to form an *N*-acylurea by-product (scheme 2.16). The formation of this by-product contributes to the low yields observed for compounds **64-99.** Previously reported in the literature, it has been shown that the addition of HOBt stabilizes the *O*-acylisourea ester intermediate, by converting it to an amine-reactive HOBt ester. This reduces intramolecular acyl transfer of *O*-acylisourea to form *N*-acylurea.[7] In comparison to the previously reported *N*-(ferrocenyl) benzoyl dipeptide esters [3-7] the yields of the compounds synthesized are lower as a result of the presences of the alkyl groups. For instance, the 1-methyl-1'–*N*-{*meta*-(ferrocenyl) benzoyl} glycine L-alanine ethyl (**69**) had a percentage yield of 22%, whilst the *N*-{*meta*-(ferrocenyl) benzoyl} glycine L-alanine ethyl ester (**28**) had a yield of 42%. [3]

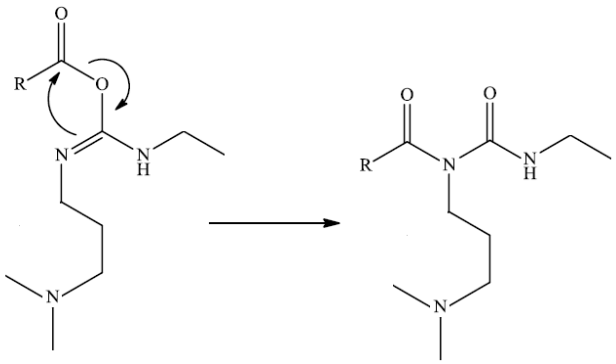

Scheme 2.16: Intramolecular acyl transfer of *O*-acylisourea to form *N*-acylurea.

As depicted in scheme 2.17, the EDC/HOBt mediated coupling of the 1-alkyl-1'-*para*, *meta* and *ortho*-(ferrocenyl) benzoic acids (i) with the dipeptide ethyl ester hydrochloride salts of Gly Gly, Gly L-Ala, Gly L-Leu and Gly L-Phe (vi), progresses through a formation of an unstable intermediate; an O-acylisourea ester (iii). This compound is formed by the reaction of the EDC (ii) with the 1-alkyl-1'-*para*, *meta* and *ortho*-(ferrocenyl) benzoic acids (i). Due to the instability of this intermediate, it is prone to intramolecular acyl transfer. The addition of HOBt (iv) stabilizes the the O-acylisourea intermediate by converting it to an amine-reactive HOBt ester (v), which is a much more stable compound and remains reactive with the amine moiety of the dipeptide ethyl ester hydrochloride salts. Upon addition of the dipeptide ethyl ester hydrochloride salts of Gly Gly, Gly L-Ala, Gly L-Leu and Gly L-Phe (vi), the HOBt is displaced resulting in the formation of 1-alkyl-1'-*N-para*, *N-meta and N-ortho*-(ferrocenyl) benzoyl dipeptide esters (**64**–**99**).[7]

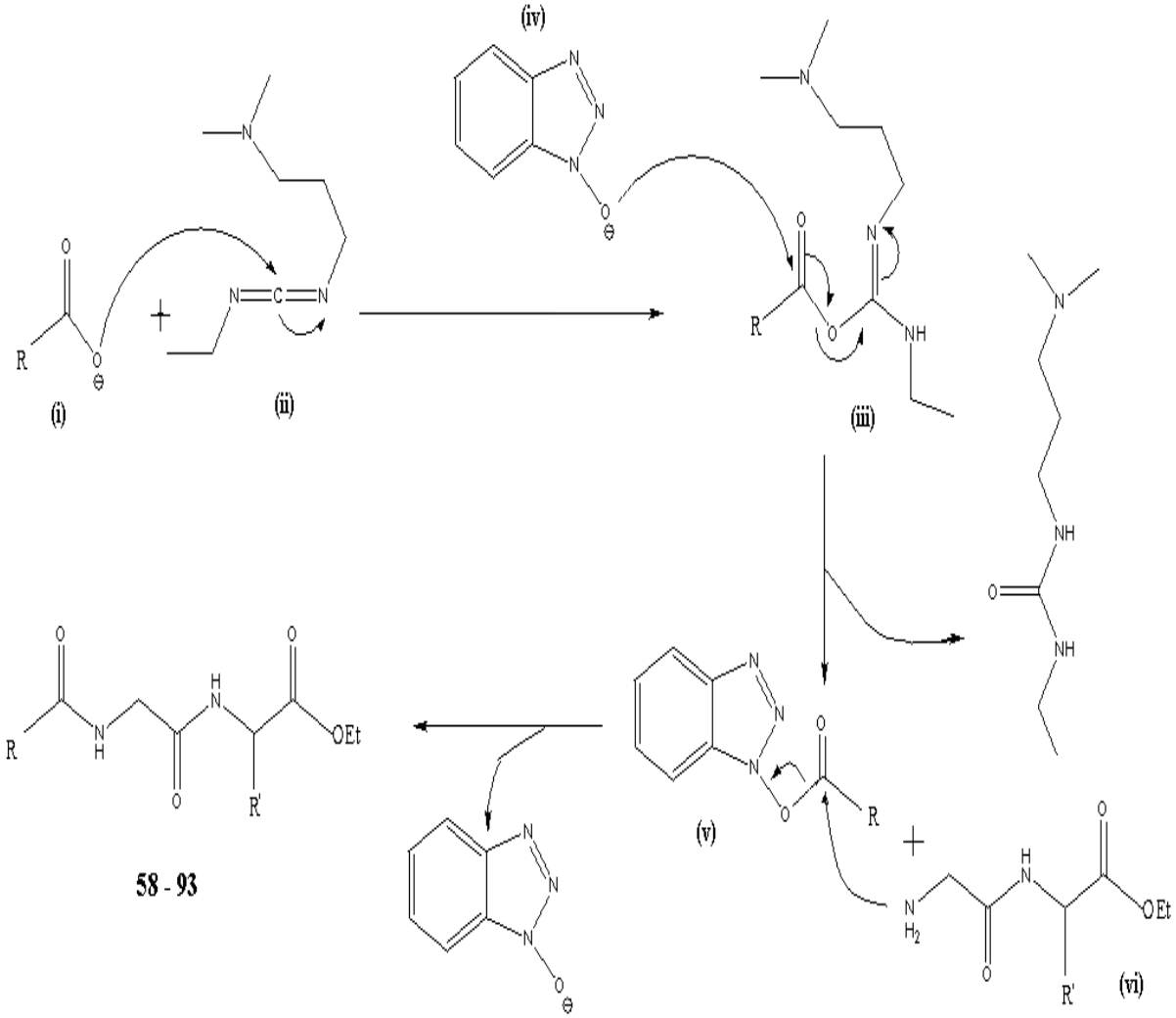

R= 1-alkyl-1'-*N-para, N-meta and N-ortho*-(ferrocenyl) benzoic acids

R'= H; CH_3; C_4H_9; C_7H_7

Scheme 2.17: Mechanism of the synthesis of 1-alkyl-1'-*N-para*, *N-meta* and *N-ortho*-(ferrocenyl) benzoyl dipeptide esters **64**–**99** using EDC and HOBt.

2.5 ^{1}H NMR spectroscopic studies of 1-alkyl-1'-*N-para*, *N-meta* and *N-ortho*-(ferrocenyl) benzoyl dipeptide esters

All the ^{1}H NMR experiments were performed in DMSO-d_6 as the 1-alkyl-1'-*N-para*, *N-meta* and *N-ortho*-(ferrocenyl) benzoyl dipeptide esters showed limited solubility in other deuterated solvents. In DMSO-d_6 the two amide protons appear between δ 8.80 and δ 8.20 (figure 2.2**)**. The appearance of these signals in the downfield region of the ^{1}H NMR spectrum is due to hydrogen bond interactions between the amide proton and the S=O bond of DMSO-d_6. If $CDCl_3$ was used to obtain the spectra, the amide protons would most likely appear more upfield since $CDCl_3$ does not possess the same ability to form hydrogen bonds.[7] The splitting pattern of the hydrogens on the benzoyl linker and the cyclopentadiene rings do not follow first order (n+1) splitting patterns. The splitting pattern of the benzoyl linker of the 1-alkyl-1' derivatives in the literature is shown to follow second order splitting pattern.[7] This is due to the extended coupling of magnetically inequivalent hydrogens on the benzoyl linker.[7] These signals are reported in table 2.1.

Table 2.1: Splitting pattern of the aromatic hydrogens on the benzyol linker.

Orientation of benzoyl linker	**Splitting pattern for the four aromatic hydrogens**
para-disubstituted derivatives	2 signals observed (apparent doublets peaks)
meta-disubstituted derivatives	3 signals observed (apparent singlet, multiplet and doublet peaks)
Ortho-disubstituted derivatives	4 signals observed (apparent doublet, triplet, triplet and doublet peaks)

In general, the protons on the benzoyl linker appear between δ 8.15 and δ 7.10. For the disubstituted ferrocene moiety, three splitting patterns are observed. For the cyclopentadiene ring attached to the benzoyl linker ($\eta^5C_5\underline{H}_4$-benzoyl), the protons appear as either apparent singlet or triplet signals in the region of δ 4.89 and δ 4.20.

This complexity is due to four protons being magnetically inequivalent, thus, following the second order splitting pattern. The protons on the alkylated cyclopentadiene ring (η^5-$C_5\underline{H}_4$-alkyl) overlap with the signals of the methylene groups of the glycine moiety, resulting in a multiplet being observed between δ 4.05 - 3.79. The typical chemical shifts of the 1-alkyl-1'-*N-para*, *N-meta* and *N-ortho*-(ferrocenyl) benzoyl dipeptide esters that follow the (n+1) rule, include the methylene protons of the ethyl ester (-O$\underline{CH_2}CH_3$) which appear as a quartet in the region δ 4.20 - 3.96, whilst the methyl protons (-$OCH_2\underline{CH_3}$) appear as a triplet in the region δ 1.26 - 1.04.

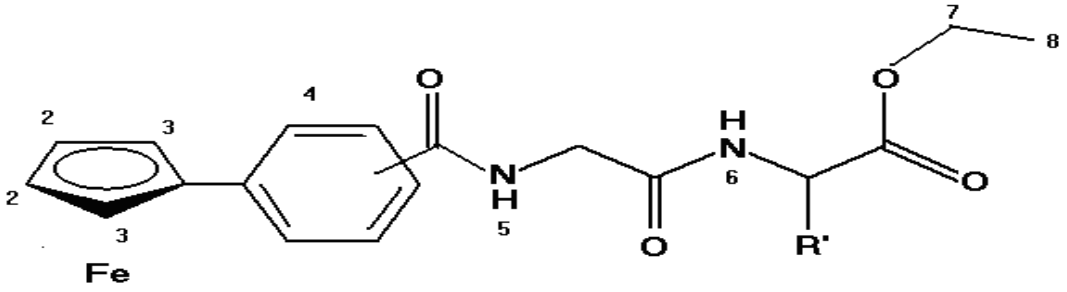

Proton location	Proton source	δ (DMSO- d_6)
1	η^5–C_5H_4-R	4.05 - 3.79
2,3	η^5–C_5H_4- benzoyl	4.89 - 4.20
4	Aromatic H	8.15 - 7.10
5,6	NH	8.80 – 8.20
7	-O$\underline{CH_2}CH_3$	4.20 - 3.96
8	-$OCH_2\underline{CH_3}$	1.26 - 1.04

Figure 2.2: Typical chemical shifts observed for the 1-alkyl-1'-*N-para*, *N-meta* and *N-ortho*-(ferrocenyl) benzoyl dipeptide esters **64–99**.

2.5.1 ^{1}H NMR spectroscopic study of 1-propyl-1'-*N*-{*para*-(ferrocenyl) benzoyl} glycine L-phenylalanine ethyl ester 91

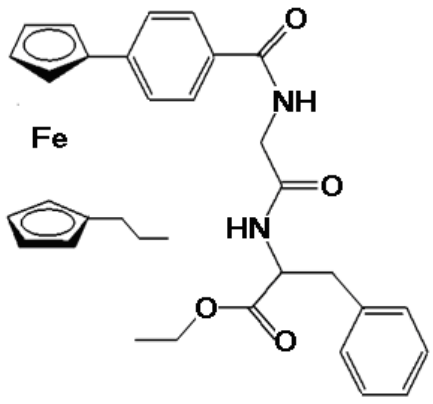

91

The ^{1}H NMR spectrum of the 1-propyl-1'-*N*-{*para*-(ferrocenyl) benzoyl} glycine L-phenylalanine ethyl ester **(91)** is shown in figure 2.3**.** The two amide protons appear as a triplet at δ 8.56 and as a doublet at δ 8.27 with coupling constants of 6.0 Hz and 7.6 Hz respectively. The four aromatic protons present between δ 7.71 and δ 7.51 are observed as two apparent doublet signals with coupling constant of 8.0 Hz respectively. The protons of the phenyl ring appear as a multiplet between δ 7.18 - 7.12 which integrates for 5 protons. The *ortho* and *meta* protons on the cyclopentadiene ring ($\eta^5C_5\underline{H}_4$-benzoyl) attached to the benzoyl spacer moiety appear as apparent singlets at δ 4.74 and δ 4.27. The methine group {-$\underline{CH}(CH_2Ph)$} appears as a multiplet between δ 4.40 - 4.38. The methylene protons of the ethyl ester (-O$\underline{CH_2}CH_3$) appear as a quartet at δ 3.96 with a coupling constant of 7.2 Hz. The protons on the alkylated cyclopentadiene ring ($\eta^5C_5\underline{H}_4$-alkyl) overlap with the protons of the methylene groups of (-NH$\underline{CH_2}$CO-), resulting in a multiplet being observed between δ 3.84 - 3.79, which has an overall integration of six. The protons of the methylene group {-CH($\underline{CH_2}$Ph)} is observed as a multiplet between δ 2.92 - 2.85. For the propyl chain attached to the cyclopentadiene ring, the protons of the methylene groups (-$\underline{CH_2}\underline{CH_2}CH_3$) appear as a triplet at δ 1.90 and a multiplet between δ 1.30 - 1.29 whilst the protons on the methyl group (-$CH_2CH_2\underline{CH_3}$) appear as a triplet at δ 0.66. The methyl group of the ethyl ester (-$OCH_2\underline{CH_3}$) is observed as a triplet at δ 1.04.

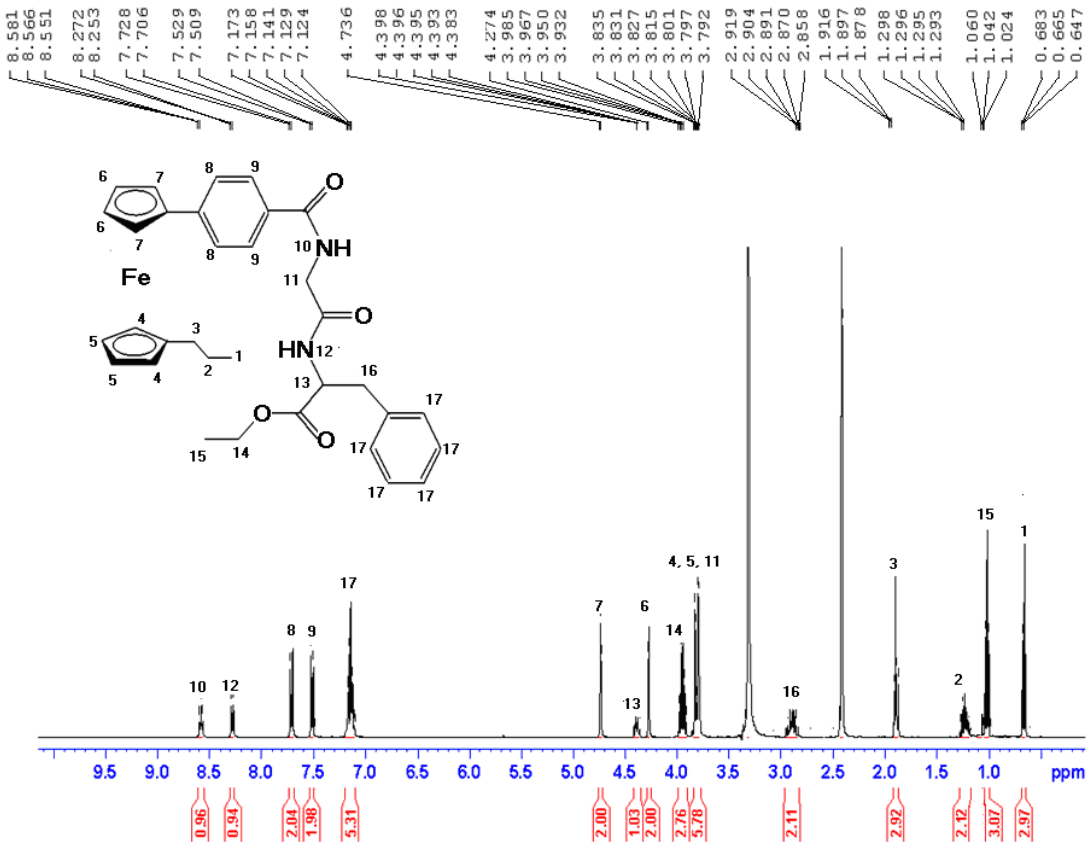

Figure 2.3: ^{1}H NMR spectrum of 1-propyl-1'-*N*-{*para*-(ferrocenyl) benzoyl} glycine L-phenylalanine ethyl ester **91.**

2.6 H^1-H^1 COSY spectroscopic studies of 1-alkyl-1'-*N*-*para*, *N*-*meta* and *N*-*ortho*-(ferrocenyl) benzoyl dipeptide esters

The COSY experiment (Correlation Spectroscopy) is a standard technique that provides a means of identifying mutually coupled protons in the structure of a compound. The experiment presents a two-dimensional contour map, with each dimension representing proton chemical shifts and the contours representing signal intensity. In the spectrum the diagonal running bottom left to top right shows peaks that correspond with those in the usual 1D spectrum. The peaks of interest are the crosspeaks which represent the coupling between the protons that are correlated to each other.[17]

2.6.1 H^1-H^1COSY spectrum of 1-ethyl-1'-*N*-{*para*-(ferrocenyl) benzoyl} glycine glycine ethyl ester 76

In the H^1-H^1 COSY spectrum (figure 2.4) of 1-ethyl-1'-*N*-{*para*-(ferrocenyl) benzoyl} glycine glycine ethyl ester **(76)** the two amide protons 8 and 10 (-$\underline{NH}CH_2CO$-) correlate with the adjacent methylene protons 9 and 11 (-NH$\underline{CH_2}$CO-) of the glycine glycine ethyl ester. Correlation is also present between the protons of the *para* disubstituted benzoyl spacer, 6 and 7. The *ortho* protons 5 and *meta* protons 4 on the cyclopentadiene ring ($\eta^5C_5\underline{H_4}$-benzoyl) attached to the benzoyl spacer, correlate. The methylene of the ethyl ester (-O$\underline{CH_2}CH_3$) 12 correlates to the methyl protons 13. These correlations observed for this derivative is consistent with previously reported observations for the *N*-(ferrocenyl) benzoyl dipeptide derivatives.[3-7]

For the protons on the alkylated cyclopentadiene ring ($\eta^5C_5\underline{H_4}$-alkyl), the methylene protons 2 correlate to the methyl protons 1. This correlation is not observed in the *N*-(ferrocenyl) benzoyl dipeptide derivatives because the derivatives do not have an alkylated cyclopentadiene ring.

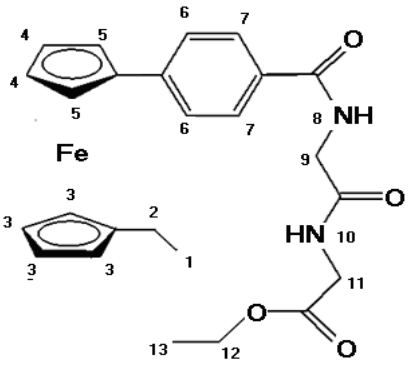

76

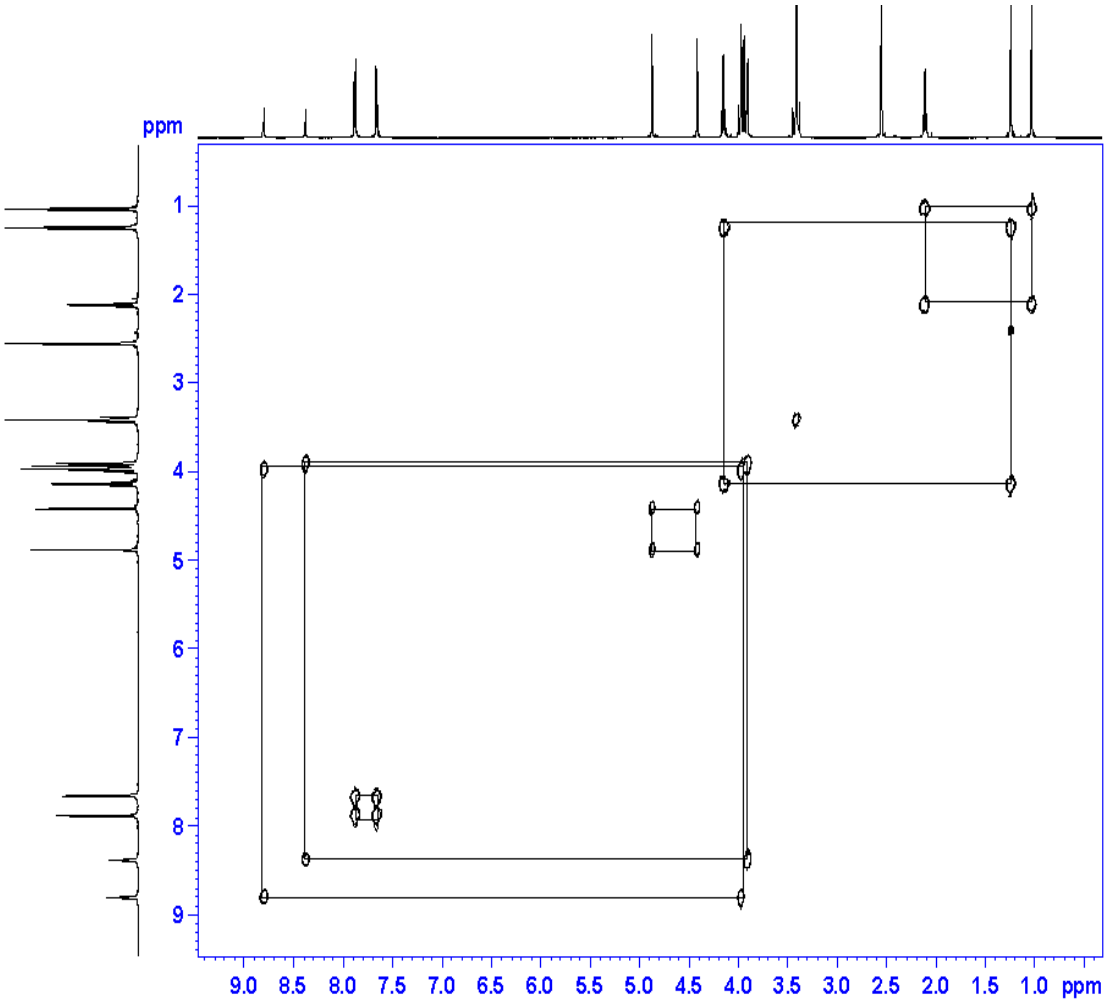

Figure 2.4: H^1-H^1 COSY spectrum of 1-ethyl-1'-*N*-{*para*-(ferrocenyl) benzoyl} glycine glycine ethyl ester **76.**

2.7 ^{13}C NMR and DEPT-135 spectroscopic studies of 1-alkyl-1'-*N-para*, *N-meta* and *N-ortho*-(ferrocenyl) benzoyl dipeptide esters

^{13}C and DEPT-135 NMR spectroscopic studies were carried out on all of the compounds synthesized. In the ^{13}C NMR spectra of 1-alkyl-1'-*N-para*, *N-meta* and *N-ortho*-(ferrocenyl) benzoyl dipeptide esters, the typical peaks observed include the appearance of three carbonyl signals between δ 173.0 - 166.0 (figure 2.5). The aromatic region of the spectrum in the 1-alkyl-1'-*N-para*, *N-meta* and *N-ortho*-(ferrocenyl) benzoyl dipeptide esters is dependent on whether the ferrocenyl moiety and the dipeptide chain are in the *ortho, meta* or *para* positions. *Ortho* and *meta* derivatives give rise to six peaks due to the six non-equivalent carbon atoms on the aromatic ring. Whilst the *para* derivatives have four peaks representing four unique carbons. Typically the carbon atoms on the benzoyl linker appear between δ 145 and δ 125. The two quaternary carbon atoms present on the benzoyl linker appear between δ 145 and δ 135. These quaternary carbons can be easily identified by their absence in the DEPT-135 spectrum.

For the 1-alkyl-1' derivatives, six unique carbon signals are observed for the disubstituted ferrocene moiety with two *ipso* carbons being present. The *ipso* carbon (η^5-$\underline{C}_5H_4$-benzoyl) appears between δ 84.3 - 80.0, whilst the *ipso* carbon (η^5-$\underline{C}_5H_4$-alkyl) appears between δ 95.3 – 88.0.

The signals of *ortho* carbons on the substituted cyclopentadiene rings appear more downfield compared to the *meta* carbons due to deshielding by the benzoyl linker and the alkyl chain attached. The methylene carbon of the ethyl ester (-O$\underline{C}H_2CH_3$) appears between δ 64.0 - 60.0 whilst the methyl carbon appears at δ 14.5 - 14.0. In a DEPT-135 spectrum, methine and methyl carbons appear as positive peaks, whereas methylene carbons appear as negative peaks *i.e.* below the resonance line. Quaternary carbons are absent in a DEPT-135 spectrum.

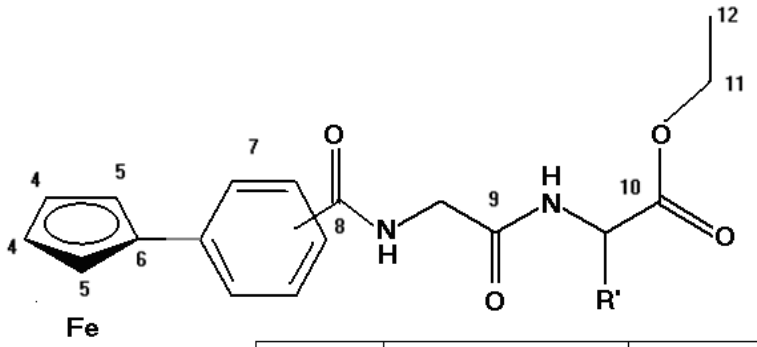

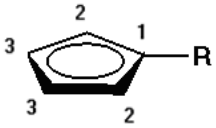

Carbon location	Carbon source	δ, (*d6*-DMSO)
1	Ipso (η^5-C_5H_4- R)	95.3 - 88.0
2, 3	η^5- C_5H_4- R	72.0 - 66.0
4, 5	η^5- C_5H_4- benzoyl	72.0 - 66.0
6	Ipso (η^5-C_5H_4- benzoyl)	84.3 - 80.0
7	Aromatic carbons	142.6 -125.6
8, 9 ,10	C=O	173.0 - 166.0
11	- $O\underline{CH_2}CH_3$	64.0 - 60.0
12	- $OCH_2\underline{CH_3}$	14.5 - 14.0

Figure 2.5: Typical chemical shifts observed for the 1-alkyl-1'-*N-para*, *N-meta* and *N-ortho*-(ferrocenyl) benzoyl dipeptide esters **64–99**.

2.7.1 ^{13}C NMR and DEPT-135 spectroscopic studies of 1-methyl-1'-*N*-{*para*-(ferrocenyl) benzoyl} glycine L-leucine ethyl ester 66

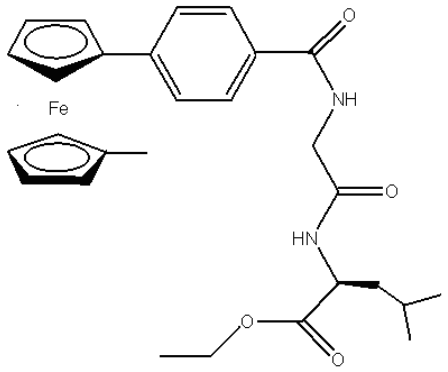

66

The ^{13}C NMR spectrum of 1-methyl-1'-*N*-{*para*-(ferrocenyl) benzoyl} glycine L-leucine ethyl ester displays three carbonyl carbon signals between δ 172.5 and δ 166.2 (figure 2.6). These are absent in the DEPT-135 spectrum. The aromatic region shows 4 unique signals between δ 142.4 and δ 125.2. The two quaternary carbon atoms at δ 142.2 and δ 130.8 from the benzoyl spacer moiety can be easily identified by their absence in the DEPT-135 spectrum. The *ipso* carbon atom on (η^5-$\underline{C}_5H_4$-alkyl) ring appears at δ 90.4 whilst the *ipso* on (η^5-$\underline{C}_5H_4$-benzoyl) ring appears at δ 84.2. These are absent in the DEPT-135 spectrum. The remaining carbon atoms on the cyclopentadiene rings are present between δ 70.1 - 66.9. The methylene and methyl carbon atoms of the ethyl ester (-O$\underline{CH_2}\underline{CH_3}$) appear at δ 60.4 and δ 14.0 respectively. The two methylene carbon atoms from (-NH$\underline{CH_2}$CO-) and {-$\underline{CH_2}$CH$(CH_3)_2$} appear at δ 42.0 and δ 39.4 respectively and display negative resonances in the DEPT-135 spectrum. The two methine carbon atoms from (-NH$\underline{CH}$CO-) and {-$CH_2\underline{CH}(CH_3)_2$} of the glycine leucine ethyl ester appear at δ 50.3 and δ 24.2 respectively. The two methyl carbon atoms of the glycine leucine ethyl ester appear at δ 22.7 and δ 21.4. The carbon atom of the methyl group (-$\underline{CH_3}$) attached to the cyclopentadiene ring appears at δ 13.2.

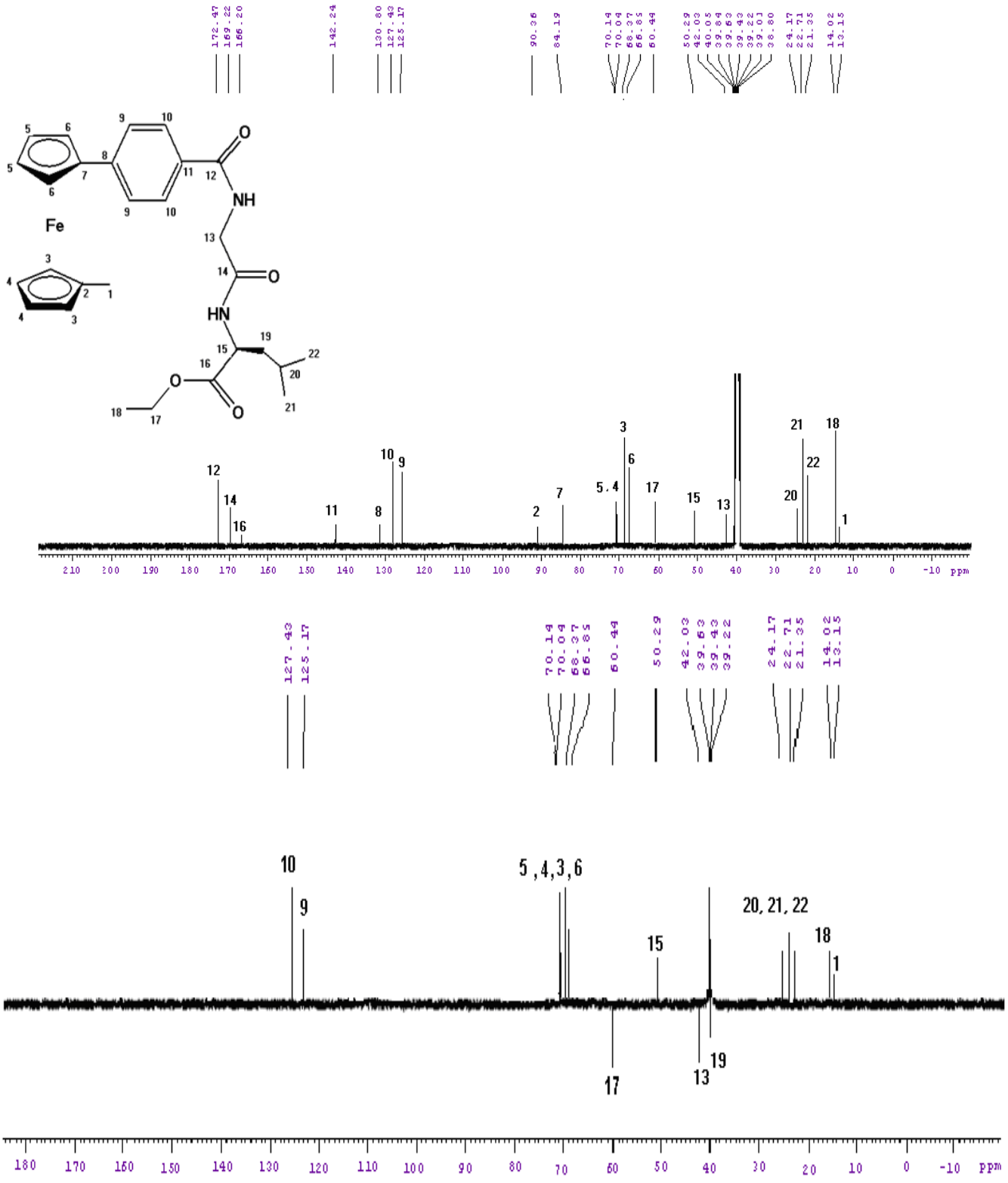

Figure 2.6: ^{13}C NMR and DEPT-135 spectra of 1-methyl-1'-*N*-{*para*-(ferrocenyl) benzoyl} glycine L-leucine ethyl ester **66.**

2.8 HMQC spectroscopic studies of 1-alkyl-1'-*N*-*para*, *N*-*meta* and *N*-*ortho*-(ferrocenyl) benzoyl dipeptide esters

HMQC (Heteronuclear Multiple Quantum Coherence) is a 2D NMR technique that correlates each carbon atom to the proton to which it is directly attached.[18] Thus, HMQC allows the assignment of proton and carbon spectra which aids in structure elucidation. This correlation is achieved by using a pulse sequence with a delay time set at half the value of the C- H coupling constant, usually in the region of 100 - 200 Hz. This results in a correlation between the carbon atom and the proton to which it is attached. In the HMQC spectrum (figure 2.7) of 1-ethyl-1'-*N*-{*para*-(ferrocenyl) benzoyl} glycine glycine ethyl ester **(76)**, the following C-H correlations were observed:

(i) Aromatic C-H correlations

(ii) Cyclopentadiene ring C-H correlations for (η^5-$\underline{C}_5\underline{H}_4$-alkyl) and ($\eta^5$-$\underline{C}_5\underline{H}_4$-benzoyl)

(iii) C-H correlations of methylene groups and C-H correlations of the methyl groups on the ethyl alkyl chain moiety and on the ethyl ester

(iv) C-H correlation of methylene groups on the glycine glycine moiety

The positions of the C-H correlation are listed in (table 2.2). The aromatic C-H correlations, C-H correlations of the methylene groups on the glycine moiety and the C-H correlations on the (η^5-$\underline{C}_5\underline{H}_4$-benzoyl) are consistent to those observed for the *N*-{*para*-(ferrocenyl) benzoyl} glycine glycine ethyl ester.[3]

However, for the alkylated cyclopentadiene ring (η^5-$\underline{C}_5\underline{H}_4$-alkyl) two C-H correlations are observed for the two unique C-H bonds in the *ortho* and *meta* positions. For the unsubstituted ring (η^5-$\underline{C}_5\underline{H}_5$) for the *N*-(ferrocenyl) benzoyl derivatives, one C-H correlation signal is observed because the C-H bonds are equivalent giving rise to one C-H correction signal.[3]

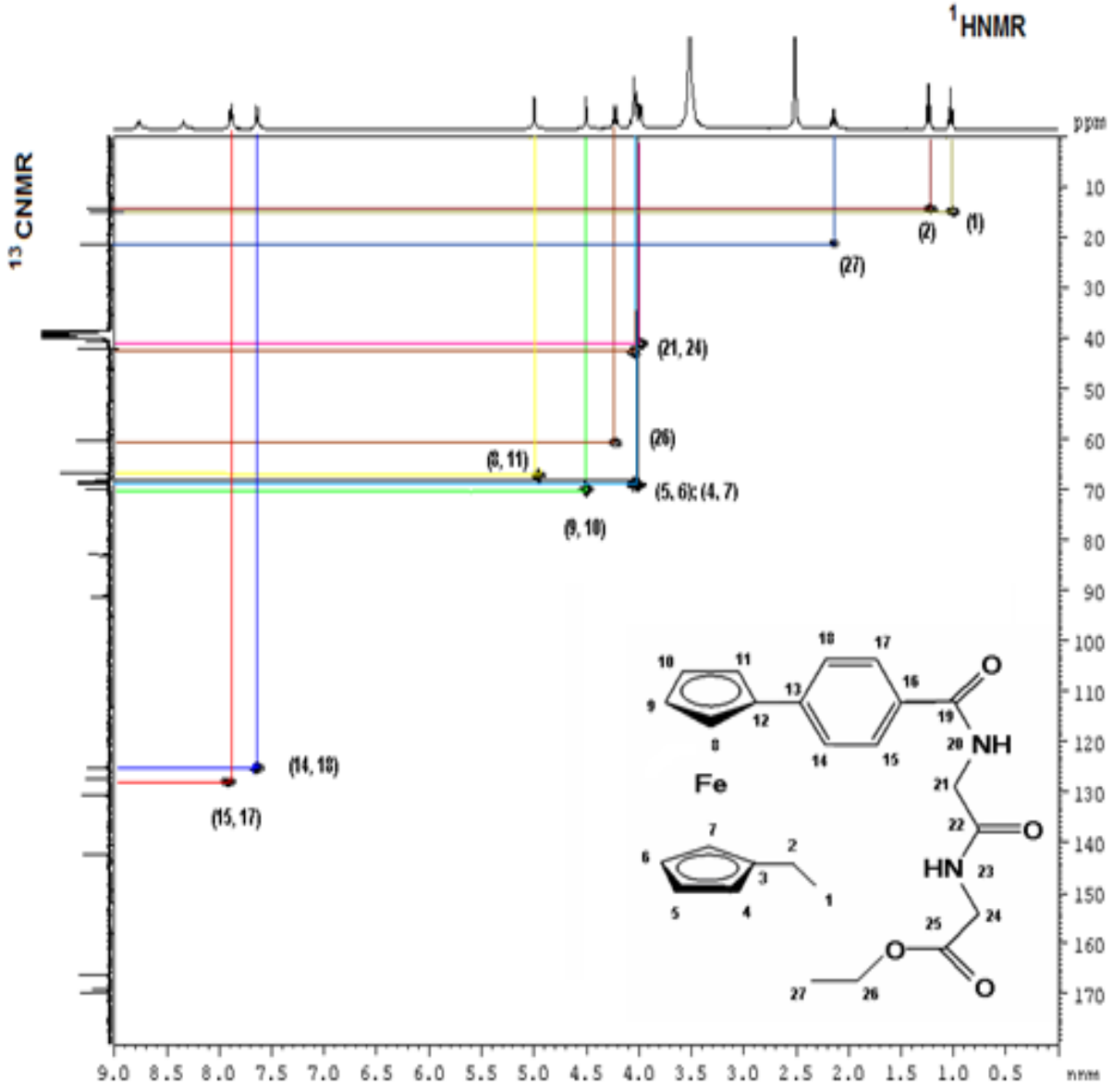

Figure 2.7: HMQC spectrum of 1-ethyl-1'-*N*-{*para*-(ferrocenyl) benzoyl} glycine glycine ethyl ester **76.**

Table 2.2: C-H correlation data from HMQC spectrum of 1-ethyl-1'-*N*-{*para*-(ferrocenyl) benzoyl} glycine glycine ethyl ester **76.**

Site	^{1}H NMR	^{13}C NMR
1*	1.02	14.0
2*	2.12	20.8
3*		91.3
(4 and 7)*	4.05 – 3.90	68.5
(5 and 6)*	4.05 – 3.90	68.8
(8 and 11)*	4.89	66.9
(9 and 10)*	4.42	69.9
12		83.0
13		130.8
(14 and 18)*	7.65	125.2
(15 and 17)*	7.87	127.5
16		142.6
19		169.8
20	8.80	
21*	4.05 – 3.90	42.4
22		169.7
23	8.38	
24*	4.05 – 3.90	40.7
25		166.3
26*	4.15	60.4
27*	1.23	14.5

* C-H correlation site

2.9 UV-Vis spectroscopic studies of the 1-alkyl-1'-*N-para, N-meta* and *N-ortho*-(ferrocenyl) benzoyl dipeptide esters

In organic molecules the absorption of ultraviolet and visible radiation is restricted to certain functional groups (chromophores) that contain valence electrons of low excitation energy.[20] These transitions are usually between a bonding or a lone pair orbital and an unfilled non-bonding or anti-bonding orbital. From a molecular orbital diagram, the possible electronic transition that occurs, gives rise to absorption bands for selective chromophores shown in figure 2.8.[20] The spectrum of a molecule containing many chromophores can be limited as dominant absorption bands can overlap with weak absorption bands and as a result the use of UV in determination of functional groups present is restricted.[20]

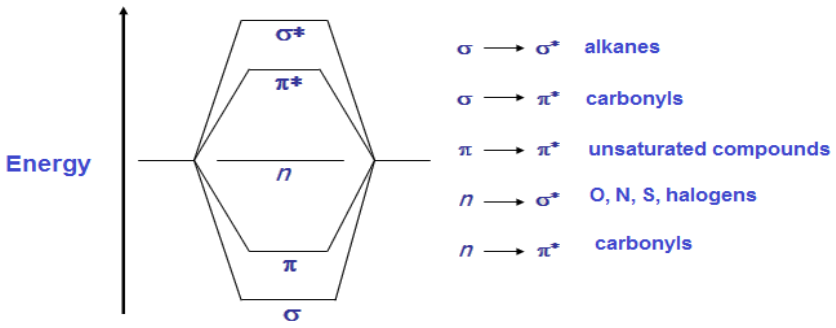

Figure 2.8: Electronic transition that occur that give rise to absorption bands for selective chromophores.

In this UV-Vis study, the spectra of all compounds were obtained at a concentration of 4 x 10^{-4} M in ethanol. In the UV spectra of the 1-alkyl-1'-*N-para*, *N-meta* and *N-ortho*-(ferrocenyl) benzoyl dipeptide esters **64–99,** low energy bands observed in the visible region, from approximately 390 to 545 nm with a distinct λ_{max} value can be assigned as metal to ligand charge transfer (MLCT) band transitions arising from the ferrocene moiety. The high energy band between 310 and 390 nm, with distinct λ_{max} values are due to the π - π^* transitions of the benzoyl moiety (table 2.3).

In the literature it is well know that the addition of a conjugate system to ferrocene causes the λ_{max} value of ferrocene (400 nm) to shift toward the red region as a result of extended conjugation.[8]

In the UV-Vis spectra of the synthesised compounds **64-99**, all the derivatives cause the ferrocene to undergo a red shift to lower energies as shown for selected compounds in table 2.3. In general the *para* derivatives give rise to lower energy bands compared to the *meta* and *ortho* derivatives. This is due to the benzoyl linker being coplanar to the disubstituted cyclopentadiene rings thus, imposing extended conjugation. These observations are in accordance with the observations made for the *N*-(ferrocenyl) benzoyl dipeptide derivatives.[3-7]

For the *meta* and *ortho* derivatives steric hindrance, contributed by the position of the dipeptide derivatives, forces the atoms in these derivatives to adopt a strained conformation resulting in a loss of co-planarity of the conjugating groups.[4-5]

From the UV-Vis data for selected 1-methyl-1'-*N-para*, *N-meta* and *N-ortho* (ferrocenyl) benzoyl} glycine glycine ethyl esters shown in figure 2.9 and table 2.3 the following observations were observed; the *para* derivatives have maxima at approximately 360 nm and 450 nm, corresponding to the π-π* transition of the benzoyl moiety and the metal to ligand charge transfer (MLCT) of the ferrocene moiety (figure 2.9) respectively. For the *ortho* and *meta* derivatives the λ_{max} values (table 2.3) are lower due to the loss of co-planarity between the ferrocenyl moiety and the benzoyl linker. Thus, the *ortho* derivatives have λ_{max} at 325 nm and 445 nm, while the *meta* derivatives have λ_{max} at 330 nm and 447 nm. From the UV-Vis spectra (figure 2.9) it can be seen that the substitution pattern of the benzoyl linker on the ferrocene induces the π-π* transition to undergo a red shift to lower energies, compared to the *ortho* and *meta* derivatives (figure 2.9).

Extinction coefficient (ε) values were calculated using the Beer-Lambert Law, $A = \varepsilon Cl$ where A is absorbance, C is concentration in mol/L and l is the path length of the cell in centimetres.[7]

Table 2.3: UV-Vis data for selected 1-methyl-1'-*N-para*, *N-meta* and *N-ortho* (ferrocenyl) benzoyl} glycine glycine ethyl esters.

Compound	Chromophore			
	Ferrocene moiety		Aromatic linker	
	λ_{max} (nm)	ε (L mol^{-1} cm^{-1})	λ_{max} (nm)	ε (L mol^{-1} cm^{-1})
64	451	(ε 1075)	360	(ε 3250)
68	447	(ε 1015)	333	(ε 1750)
72	445	(ε 675)	330	(ε 1063)

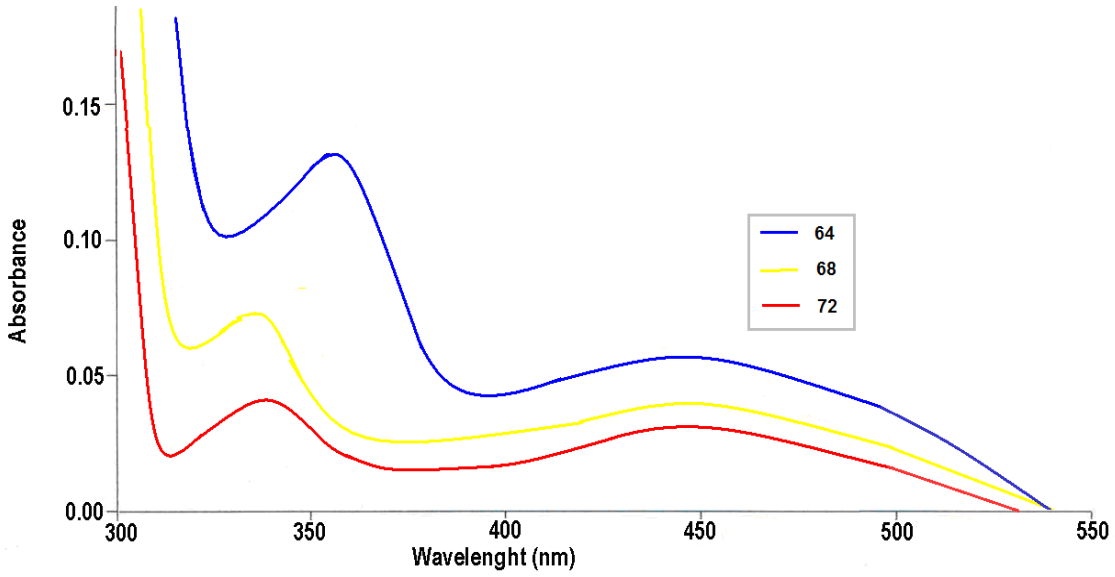

Figure 2.9: UV-Vis data for selected 1-methyl-1'-*N-para*, *N-meta* and *N-ortho* (ferrocenyl) benzoyl} glycine glycine ethyl esters **64, 68** and **72**.

2.10 Mass spectrometric studies of 1-alkyl-1'-*N*-*para*, *N*-*meta* and *N*-*ortho*-(ferrocenyl) benzoyl dipeptide esters

Mass spectrometry enables the determination of the relative molecular mass of many different types of compounds. The mass spectrometer is composed of three distinct parts, namely the ion source, the analyser and the detector. The sample is introduced into the ion source and this allows ionisation to occur. These ions are then extracted into the analyser, where they are separated according to their mass (*m*) to charge (*z*) ratios (*m/z*). The separated ions are detected and displayed as a mass spectrum. Electrospray ionization mass spectrometry (ESI-MS) was employed in the analysis of 1-alkyl-1'-*N*-*para*, *N*-*meta* and *N*-*ortho*-(ferrocenyl) benzoyl dipeptide esters. Examination of the mass spectra revealed the presence of sodium ion adducts, $[M+Na]^+$. In the mass spectra, sequence specific fragment ions were not observed, therefore tandem mass spectrometry was employed to determine the fragmentation pattern of 1-methyl-1'-*N*- {*para* -(ferrocenyl) benzoyl} glycine glycine ethyl ester **64**, 1-ethyl-1'-*N*-{*para*-(ferrocenyl) benzoyl} glycine glycine ethyl ester **76** and 1-propyl-1'-*N*-{*para*-(ferrocenyl) benzoyl} glycine glycine ethyl ester **88**.

In the MS/MS spectrum of compound **64,** the sequence specific fragment ions are present at *m/z* 275, *m/z* 303, *m/z* 331 and *m/z* 359 (figure 2.10). The product ions at *m/z* 275 and *m/z* 303 correspond to the 1-methyl-1'-*N*-{*para*-(ferrocenyl) benzyl and 1-methyl-1'-*N*-{*para*-(ferrocenyl) benzoyl subunits respectively. However, the expected a_1 and b_1 product ions at *m/z* 332 and *m/z* 360 were not observed, instead a_1-1 and b_1-1 product ions were observed at *m/z* 331 and *m/z* 359 respectively. The formation of a_1-1 and b_1–1 ions in the mass spectrum of *N*-{*para*-(ferrocenyl) benzoyl} glycine L-alanine ethyl ester was investigated previously within the group by tandem mass spectrometry and deuterium labelling studies. The results showed that b_1-1 product ions arise from the loss of a hydrogen atom attached to the nitrogen atom and not to the α-carbon atom of the glycine residue.[22] The fragment ion at *m/z* 434 is due to a loss of C_2H_4 from the ethyl ester group by a McLafferty rearrangement (scheme 2.18).[23]

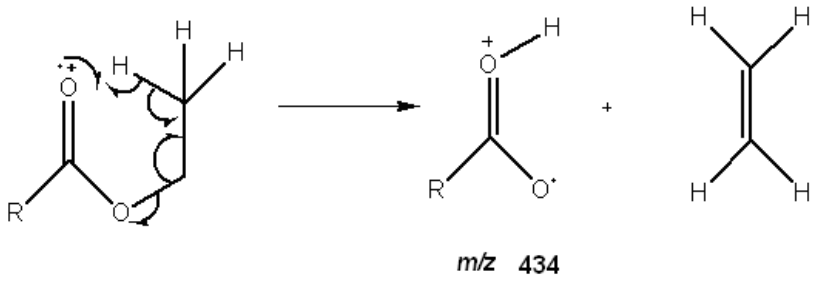

R =1-methyl-1'-*N*- {*para* -(ferrocenyl) benzoyl}glycine glycine

Scheme 2.18: McLafferty rearrangement resulting in the *m/z* 434 fragment ion.

The sequence specific fragment ions are also observed for derivatives **76** and **88** which differ by 14 mass units respectively as shown in figure 2.11 - 2.12. For compound **76** the sequence specific fragment ions are observed 14 mass units higher at *m/z* 289, *m/z* 317, *m/z* 345 and *m/z* 373 (figure 2.11). The product ions at *m/z* 289 and *m/z* 317 correspond to the 1-ethyl-1'-*N*-{*para*-(ferrocenyl) benzyl and 1-ethyl-1'-*N*-{*para*-(ferrocenyl) benzoyl subunits respectively whilst the product ion a_1-1 and b_1-1 are observed at *m/z* 345 and *m/z* 373 respectively. The fragment ion at *m/z* 448 is due to a loss of C_2H_4 from the ethyl ester group by McLafferty rearrangement. The sequence specific fragment ions for **88** are present at *m/z* 303, *m/z* 331, *m/z* 359 and *m/z* 387 (figure 2.12). The product ions at *m/z* 303 and *m/z* 331 correspond to the 1-propyl-1' -*N*-{*para*-(ferrocenyl) benzyl and 1-propyl-1'-*N*-{*para*-(ferrocenyl) benzoyl subunits respectively. The product ion a_1-1 and b_1-1 are observed at *m/z* 359 and *m/z* 387 respectively. The fragment ion at *m/z* 462 is due to a loss of C_2H_4 from the ethyl ester group by McLafferty rearrangement.

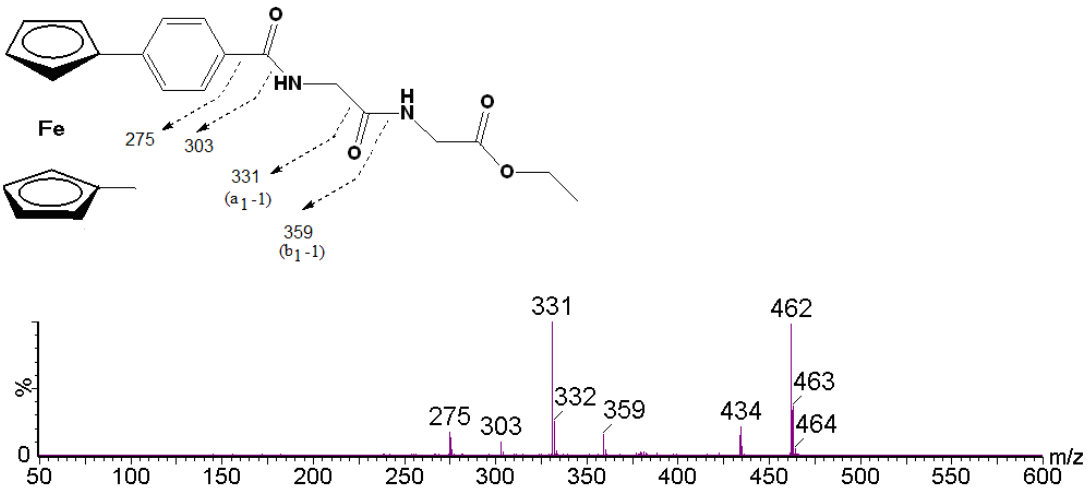

Figure 2.10. Product ions observed in the MS/MS spectrum of 1-methyl-1' -*N*- {*para*-(ferrocenyl)-benzoyl} glycine glycine ethyl ester **64.**

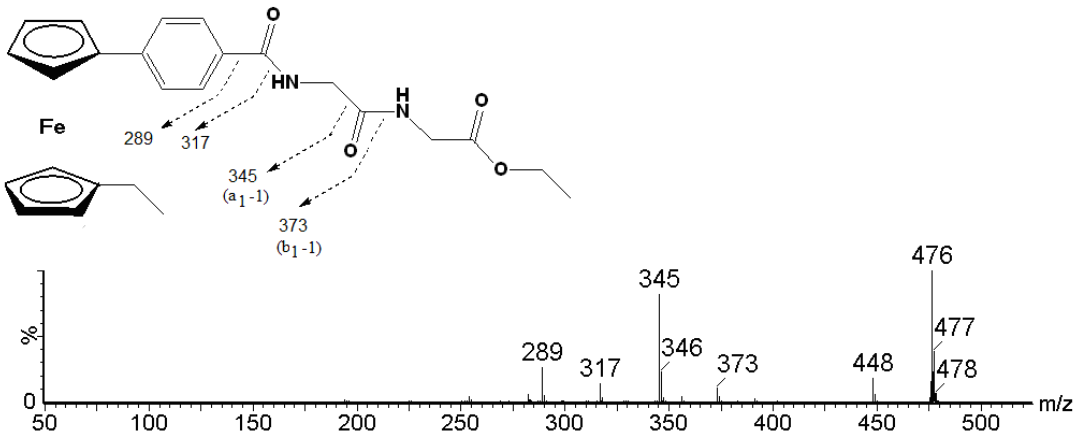

Figure 2.11. Product ions observed in the MS/MS spectrum of 1-ethyl-1' -*N*- {*para*-(ferrocenyl)-benzoyl} glycine glycine ethyl ester **76.**

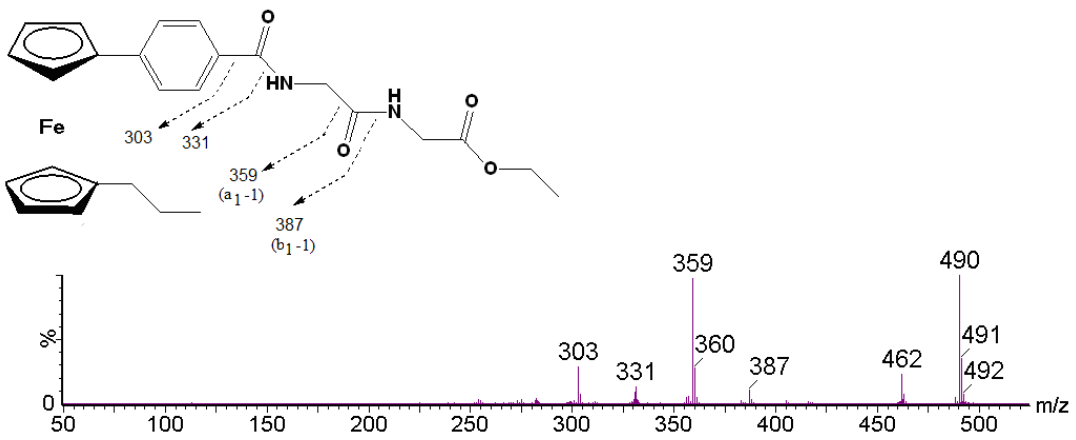

Figure 2.12. Product ions observed in the MS/MS spectrum of 1-propyl-1' -*N*- {*para*-(ferrocenyl) benzoyl} glycine glycine ethyl ester **88.**

2.11 A comparative study of *N-para*, *N-meta* and *N-ortho*-(ferrocenyl) benzoyl dipeptide esters and the novel 1-alkyl-1' derivatives

2.11.1 Introduction

The synthesis and structural characterization of biologically active *N*-ferrocenyl benzoyl dipeptide esters has been previously reported.[3-7] In an extension of that study we now report the synthesis and structural characterization of novel 1-alkyl-1'-*N-para*, *N-meta* and *N-ortho*-(ferrocenyl) benzoyl dipeptide esters

64–99 (figure 2.13). In the literature incorporation of electron donating groups is a well know strategy to lower oxidation potentials of ferrocene moieties.[8] Thus, the incorporation of the various alkyl chain groups (electron donating groups) to the unsubstituted cyclopentadiene ring of the *N-para*, *N-meta* and *N-ortho*-(ferrocenyl) benzoyl dipeptide esters should improve the cytotoxicity of these derivatives. In addition, the alkyl chain should also increase the lipophilicity of the reported derivatives.[3-7]

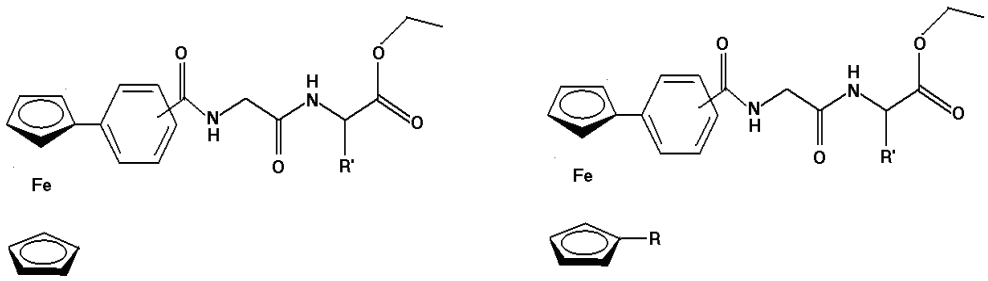

$R = CH_3, CH_2CH_3, CH_2CH_2CH_3$

$R' = H, CH_3, C_4H_9, C_7H_7,$

Figure 2.13 General structures of the *N-para, N-meta* and *N-ortho*-(ferrocenyl) benzoyl dipeptide esters and the novel 1-alkyl-1' derivatives.

2.11.2 Synthetic route comparison

For the synthesis of *N-para*, *N-meta* and *N-ortho*-(ferrocenyl) benzoic acid the synthetic protocol involved the diazonium coupling of ferrocene to 2,3,4-ethylamino benzoate followed by a base hydrolysis.[3-7] However, when this protocol was employed in the synthesis of 1-alkyl-1' benzoic acid derivatives, yields of less than 8% where obtained. To improve the selectivity for the synthesis of monoarylferrocene it was observed that when 2,3,4-amino benzoic acids were used, yields greater than 15% were obtained. For the synthesis of 1-alkyl-1' dipeptide derivatives **(64–99),** the yields obtained were lower than the *N-para, N-meta* and *N-ortho* -ferrocenyl benzoyl dipeptide esters previously reported.[3-7] The low yields obtained were due to steric hindrance from the incorporation of the alkyl chains and the competing reaction in the EDC/HOBt coupling protocol (section 2.4)

2.11.3 ^{1}H NMR, ^{13}C NMR and DEPT-135 spectroscopic studies of *N-para*, *N-meta* and *N-ortho*-(ferrocenyl) benzoyl dipeptide esters and their 1-alkyl-1' derivatives.

For the ^{1}H NMR spectra of both classes of compounds (figure 2.14) the two amide protons of the dipeptide chain appear between δ 8.89 and δ 8.14. The four aromatic protons on the benzyol linker occur between δ 8.15 and δ 7.10 for both classes of compounds. The splitting pattern of the benzoyl spacer for both classes follows the second order splitting pattern, due to extended coupling of magnetically inequivalent hydrogens on the benzoyl linker.[7] Thus, they are reported as apparent signals, as shown in table 2 in section 2.5. These typical proton signals do not show any significant difference in the chemical shift between the two classes of compounds (figure 2.14).
The protons on the monosubstituted ferrocene ring in the *N-para*, *N-meta* and *N-ortho*-(ferrocenyl) benzoyl dipeptide esters occur as three signals in the region δ 4.95 and δ 4.00. For the 1-alkyl-1'derivatives (**64–99)** the protons on the disubstituted ferrocene moiety appear as three signals between δ 4.89 and δ 3.79. For both classes three splitting patterns are observed.[3-7] The cyclopentadiene ring attached to the benzoyl linker ($\eta^5C_5\underline{H}_4$-benzoyl) appears as either apparent singlets or triplets for both classes. This complexity has already been discussed in Section 2.5. The protons on the unsubstituted cyclopentadiene ring of the *N-para*, *N-meta* and *N-ortho*-(ferrocenyl) benzoyl dipeptide esters appear as a singlet due to the hydrogens being magnetically equivalent. However the protons on the alkylated cyclopentadiene ring (η^5-$C_5\underline{H}_4$-alkyl) which are not magnetically equivalent overlap with the signals of the methylene groups of the glycine moiety, resulting in a multiplet being observed. The overlapping of the cyclopentadiene proton signals is not observed in the monosubstituted ferrocene derivatives. For both classes of compounds the methylene protons of the ethyl ester (-O$\underline{CH_2}CH_3$) appear between δ 4.20 - 3.96 as a quartet, whilst the methyl protons (-$OCH_2\underline{CH_3}$) appear between δ 1.30 - 1.04 as a triplet.

The difference between the two classes of compounds are the presence of the methyl, ethyl or propyl groups on the cyclopentadiene ring for the 1-alkyl-1' derivatives (**64–99**). For the methyl (-$\underline{CH_3}$) group, the proton signals are present between δ 1.46 - 1.70 as a singlet. The methylene and methyl protons of the ethyl group appear as a quartet

between δ 2.15 - 1.96 and as a triplet between δ 1.05 - 0.70 respectively. For the propyl group the protons on the methylene groups (-$\underline{CH_2}\underline{CH_2}CH_3$) appear as a triplet between δ 2.08 - 1.88 and as a multiplet between δ 1.45 - 1.25, whilst the protons on the methyl group (-$CH_2CH_2\underline{CH_3}$) appear as a triplet between δ 0.76 - 0.66.

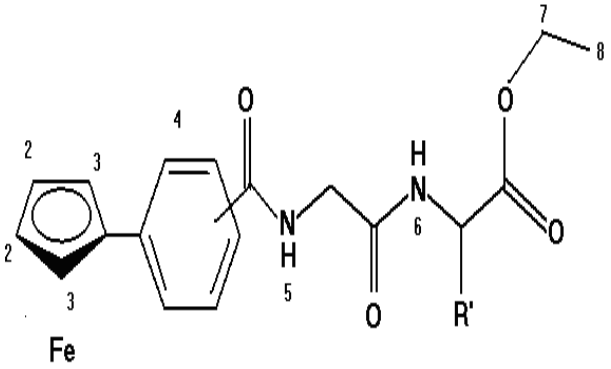

Proton location	Proton source	δ (DMSO- d_6)
1	η^5- C_5H_5	4.00 - 4.10
2,3	η^5- C_5H_4- benzoyl	4.95 - 4.38
4	Aromatic H	7.80 – 7.10
5,6	NH	8.89 - 8.14
7	-$O\underline{CH_2}CH_3$	4.15 - 4.00
8	-$OCH_2\underline{CH_3}$	1.30 – 1.10

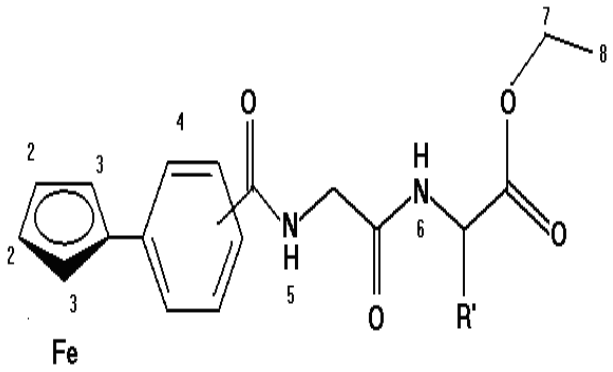

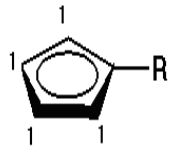

Proton location	Proton source	δ (DMSO- d_6)
1	η^5- C_5H_4-R	4.05 - 3.79
2,3	η^5- C_5H_4- benzoyl	4.89 - 4.20
4	Aromatic H	8.15 - 7.10
5,6	NH	8.80 – 8.20
7	-$O\underline{CH_2}CH_3$	4.20 - 3.96
8	-$OCH_2\underline{CH_3}$	1.26 - 1.04

64–99

Figure 2.14: Typical chemical shifts observed for *N-para*, *N-meta* and *N-ortho*-(ferrocenyl) benzoyl dipeptide esters and the 1-alkyl-1'-*N-para*, *N-meta* and *N-ortho*-(ferrocenyl) benzoyl dipeptide esters (**64–99).**

In the ^{13}C NMR spectra of *N-para*, *N-meta* and *N-ortho*-(ferrocenyl) benzoyl dipeptide esters and their 1-alkyl-1' derivatives (**64-99),** the typical carbon signals (figure 2.15) observed include the presence of carbonyl carbons between δ 172.7 and δ 166.0. The carbon atoms on the benzyol linker appear between δ 145 and δ 125 for both classes. The methylene and methyl carbon atoms of the ethyl ester (-O$\underline{CH_2}\underline{CH_3}$) present in both classes of compounds appear between δ 64.0 - 60.0, whilst the methyl carbon appears between δ 14.5 - 14.0. These typical carbon signals do not show any significant difference in the chemical shift between the two classes of compounds.

However, for the *N*-(ferrocenyl) benzoyl derivatives, four unique carbon signals are observed for a monosubstituted cyclopentadiene ring. The *ipso* carbon (η^5-$\underline{C_5}H_4$-benzoyl) appears between δ 84.3 - 80.0 and the remaining three unique carbon signals on the monosubstituted ring appear between δ 70.5 - 68.5.

For the 1-alkyl-1' derivatives, six unique carbon signals are observed for the disubstituted ferrocene moiety; two *ipso* carbons are present, which can be easily identified as a difference between the two classes of compounds. The *ipso* carbon (η^5-$\underline{C_5}H_4$-benzoyl) appears between δ 84.3 - 80.0, whilst the *ipso* carbon (η^5-$\underline{C_5}H_4$-alkyl) appears between δ 95.3 - 88.0. The remaining four unique carbons on the disubstituted cyclopentadiene rings appear between δ 72.0 - 66.0.

The main difference between the two classes of compounds is the presence of the alkyl moieties attached on the cyclopentadiene ring. These alkyl moieties give rise to distinct carbon signals which can be easily identified from the ^{13}C and DEPT-135 spectra of compounds **64-99,** which are absent in the *N-para*, *N-meta* and *N-ortho*-(ferrocenyl) benzoyl dipeptide esters.[3-7]

The carbon atom of the methyl group (-$\underline{CH_3}$) appears between δ 14.0 - 13.2. The methylene carbon atoms of the ethyl group (-$\underline{CH_2}CH_3$) appear between δ 24.0 - 20.5, whilst the methyl carbon atoms (-$CH_2\underline{CH_3}$) appear between δ 14.0 - 13.8. The two methylene carbon atoms of the propyl group (-$\underline{CH_2}\underline{CH_2}CH_3$) appear between δ 36.8 - 30.0 and between δ 24.0 - 20.5 respectively. The methyl group of the propyl group (-$CH_2CH_2\underline{CH_3}$) appears between δ 14.0 - 13.0.

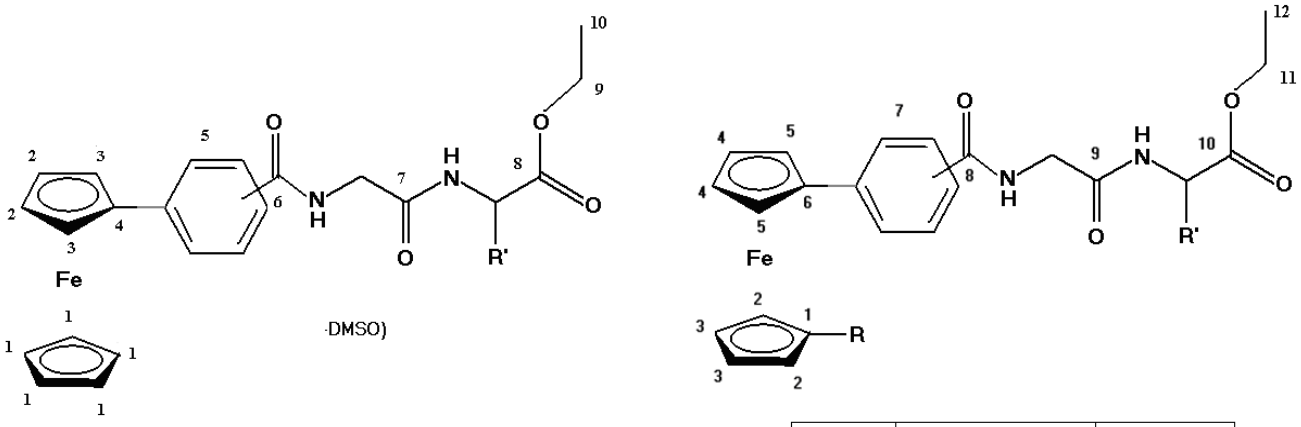

Carbon location	Carbon source	δ, (d_6-DMSO)
1	(η^5-C_5H_4)	70.0 - 66.0
2, 3	η^5-C_5H_4- benzoyl	68.5 - 66.8
4	Ipso (η^5-C_5H_4- benzoyl)	84.3 - 80.0
5	Aromatic carbons	142.6 -125.6
6, 7, 8	C=O	173.0 - 166.0
9	- $O\underline{CH_2}CH_3$	64.0 - 60.0
10	- $OCH_2\underline{CH_3}$	14.5 - 14.0

Carbon location	Carbon source	δ, (d_6-DMSO)
1	Ipso (η^5-C_5H_4- R)	95.3 - 88.0
2, 3	η^5 -C_5H_4- R	72.0 - 66.0
4, 5	η^5-C_5H_4- benzoyl	72.0 - 66.0
6	Ipso (η^5-C_5H_4- benzoyl)	84.3 - 80.0
7	Aromatic carbons	142.6 -125.6
8, 9 ,10	C=O	173.0 - 166.0
11	- $O\underline{CH_2}CH_3$	64.0 - 60.0
12	- $OCH_2\underline{CH_3}$	14.5 - 14.0

64–99

Figure 2.16: Typical chemical shifts observed for *N-para*, *N-meta* and *N-ortho*-(ferrocenyl) benzoyl dipeptide esters and the 1-alkyl-1'-*N-para*, *N-meta* and *N-ortho*-(ferrocenyl) benzoyl dipeptide esters **64–99.**

2.12 Conclusion

A series of 1-alkyl-1'-*N-para*, *N-meta* and *N-ortho*-(ferrocenyl) benzoyl dipeptide esters **64–99** were prepared and structurally characterized. Each novel compound contains an electroactive alkylated ferrocene core, a conjugated aromatic linker and a dipeptide chain These novel compounds were characterized by a combination of ^{1}H NMR, ^{13}C NMR, DEPT-135 and ^{1}H-^{13}C COSY (HMQC) spectroscopy, electrospray ionization mass spectrometry (ESI-MS).

References:

1. Togni, A., Hayashi, T., *Ferrocenes*, **1994**, Wiley, VCH publications.
2. Savage, D., Gallagher, J. F., Ida, Y., Kenny, P. T. M., *Inorg. Chem. Comm.*, **2002**, *5*, 1034-1040.
3. Goel, A., Savage, D., Alley, S.R., Kelly, P.N., O'Sullivan, D., Mueller-Bunz, H., and Kenny, P.T.M., *J. Organomet. Chem.*, **2007**, *692*, 1292-1299.
4. Goel, A., Savage, D., Alley, S.R., Hogan, T., Kelly, P.N., Draper, S., Fitchett C.M., and Kenny P.T.M, *J. Organomet. Chem.*, **2006**, *691*, 4686-4693.
5. Corry, A.J., Goel, A., Alley, S.R., Kelly, P.N., O'Sullivan, D., Savage, D., and Kenny, P.T.M., *J. Organomet. Chem*., **2007** *692*, 1405-1410
6. Corry, A.J., Mooney, A., O'Sullivan, D., and Kenny, P.T.M., *Inorganica Chimica Acta.*, **2009**, *362*, 2957-2961.
7. Corry, A.J., O'Donovan, N., Mooney, A., O'Sullivan, D., Rai, D.K., Kenny, P.T.M., *J. Organomet. Chem.*, **2009**, *694*, 880-885.
8. Vogel , M., Rausch, M.D., Rosenberg, H., *J. Organomet. Chem.*, **1957**, *22*, 1016-1019
9. Miyaura, N., Yamada, K., Suzuki, A., *Tetrahedron Letters.*, **1979**, *20***,** 3437-3440.
10. http://faculty.swosu.edu/william.kelly/pdf/fc.pdf
11. Jones, G., Stanforth, S. P., *Org. React*., **2000**, *56*, 355-659.
12. Buchanan, J. G., Woodgate, P. D., *Quart. Rev.* **1969,** *23*, 522-527
13. Nystron, R, F., Berger C. R. A., *J. Amer. Chem. Soc*., **1958**, *80*, 2896-2898.
14. http://cnx.org/content/m15238/latest/
15. Rosenblum, M., Glenn-Howells, W., Banerjee, A. K., Bennett, C., *J. Am. Chem. Soc*., **1962**, *84*, 2726-2732.
16. Corry, A.J., *'The Synthesis and Characterization of Novel Ferrocenyl benzoyl peptide esters as anti-cancer agents and Ferrocenoyl self assembled monolayers as anion sensors,'* DCU, Ph.D, Thesis, **2009**.
17. Breitmaier, E., '*Structure Elucidation by NMR in Organic Chemistry'*, Wiley, **1993**.
18. http://www2.chemistry.msu.edu/facilities/nmr/HMQC.html

19. http://www2.chemistry.msu.edu/faculty/reusch/VirtTxtJml/Spectrpy/UV-Vis/spectrum.htm
20. McMurry, J., *'Organic Chemistry'*, Brooks/Cole, **2000** 5th edition.
21. Goel, A. and Kenny, P.T.M, *Rapid Communications in Mass Spectrometry*, **2008**, *22*, 2398-2401.
22. http://lsc.ucdavis.edu/~holliste/Jim118C/Mass_Spec.pdf
23. http://www.chem.wisc.edu/areas/reich/nmr/05-hmr-09-2ndorder.htm

Chapter 3: Biological evaluation of 1-alkyl-1'-*N-para*, *N-meta* and *N-ortho*-(ferrocenyl) benzoyl dipeptide esters

3.1 Introduction

Chemotherapy plays a significant role in the control of metastatic cancers that can not be cured by surgery. However, cancer is associated with poor prognosis and an increase in drug resistance to existing chemotherapy treatments.[1] Hence, there is an urgent need for new anticancer therapies. The development of the resistance to a particular or a combination of unrelated cancer drugs is a major impediment in the treatment of cancer.[2] This multiple drug resistance (MDR) is a result of a variety of changes in the cell which result in the increased activity of drug pumps like P-glycoprotein (Pgp) which expel the chemotherapeutics out of the cancer cells.[2] In cancer cells there is a accumulation of high concentrations of hydrogen peroxide due to the over expression of superoxide dismutase (SOD) that transforms superoxide ions into hydrogen peroxide.[3] Ferrocene based compounds reported in the literature are well know to exploit the overproduction of hydrogen peroxide in cancer cells to produce hydroxyl radicals (•OH) which cause oxidative DNA damage.

In previous studies carried out to evaluate the *in vitro* anticancer activity of *N-para*, *N-meta* and *N-ortho*-(ferrocenyl) benzoyl dipeptide esters (figure 3.1) in non small cell lung cancer cell line, H1299, the general trend in cytotoxicity was *para* < *ortho* < *meta*. The dipeptide derivative *N*-{ortho-(ferrocenyl) benzoyl} glycine L-alanine ethyl ester was shown to have an IC_{50} value of 5.3 ± 1.23 µM. The *N*-{para-(ferrocenyl) benzoyl} glycine L-alanine ethyl ester and the *N*-{meta-(ferrocenyl) benzoyl} glycine L-alanine ethyl ester had IC_{50} values of 6.6 ± 1.03 µM and 4.0 ± 0.71 µM respectively.[3-7]

In a further SAR study a series of 1-alkyl-1'-*N-para*, *N-meta* and *N-ortho*-(ferrocenyl) benzoyl dipeptide esters were synthesised, structurally characterised and biologically evaluated. In total, 36 compounds were tested for their anti-proliferative effect on the non small cell lung cancer cell line, H1299. These novel derivatives differ from the *N-para*, *N-meta* and *N-ortho*-(ferrocenyl) benzoyl dipeptide esters by having an alkyl moiety on the previously unsubstituted ferrocene ring.

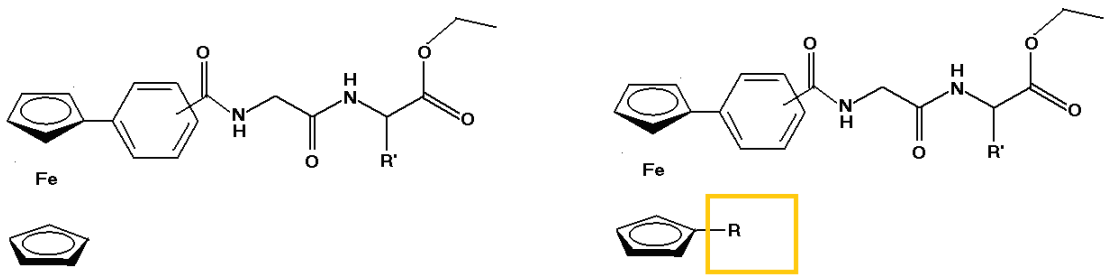

alkyl moiety (R) = CH_3; CH_2CH_3; $CH_2CH_2CH_3$

R' = H; CH_3; C_4H_9; C_7H_7

Figure 3.1: General structure of the *N-para*, *N-meta* and *N-ortho*-(ferrocenyl) benzoyl dipeptide esters and the 1-alkyl-1'-*N-para*, *N-meta* and *N-ortho*-(ferrocenyl) benzoyl dipeptide esters.

3.2 *In vitro* anti-cancer activity of 1-alkyl-1'-*N-para*, *N-meta* and *N-ortho*-(ferrocenyl) benzoyl dipeptide esters

The *in vitro* cytotoxicity of the 1-alkyl-1' derivatives **64–99** were evaluated by performing a comprehensive screen of every compound at a single dose (10 μM) in the H1299 cell line and the endpoint of the growth inhibition was evaluated by the acid phosphatase assay.[7] The screening of the compounds was performed in collaboration with Dr. Norma O'Donovan and James Murphy of the National Institute for Cellular Biotechnology (NICB), Dublin City University. The comprehensive screen was performed in triplicate by treating individual wells of a 96-well plate containing H1299 cells with a 10 μM solution of each test compound prepared in DMSO. A reference control *N-meta*-(ferrocenyl) benzoyl glycine L-alanine ethyl ester (**28**), a DMSO control and a control for normal (untreated) cell growth were included in the assays. The cells were then incubated for 5 days, until cell confluency was reached. At this point, cell survival was established through determination of the acid phosphatase activity of surviving cells.

In the acid phosphatase assay, a solution of the *p*-nitrophenyl phosphate substrate is added at the end-point of the assay. This substrate is dephosphorylated by the acid phosphatase enzyme, which is located in the lysosomes of cells, to yield

p-nitrophenol.[8] In the presence of strong alkali, the *p*-nitrophenol chromophore can be quantified by measuring the absorbance at 405 nm (figure 3.2).

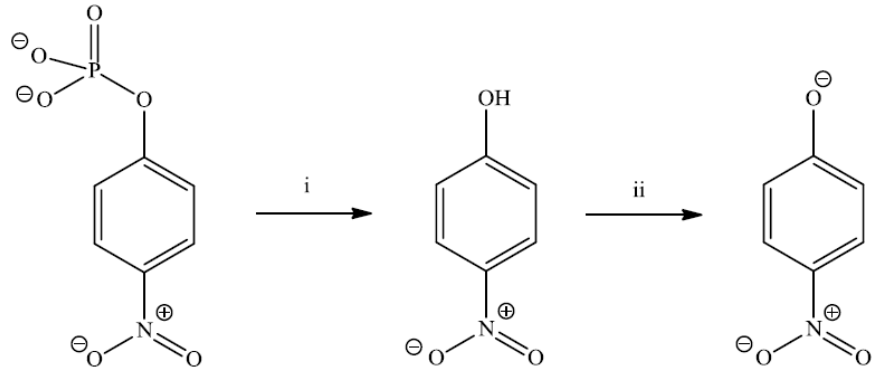

Figure 3.2 Acid phosphatase end-point assay: (i) Phosphatase catalysed reaction (in water); (ii) Colour reaction in strong base (NaOH).

This colorimetric end-point assay is an indirect measure of cytotoxicity which evaluates the enzyme activity of cells after a given treatment period. The results of the comprehensive screens are expressed as the percentage growth inhibition ± standard deviation (relative to the DMSO controls). Standard deviations have been calculated using data obtained from three independent experiments. The results for the preliminary screen of compounds **64–99** are depicted in figures 3.3-3.5.

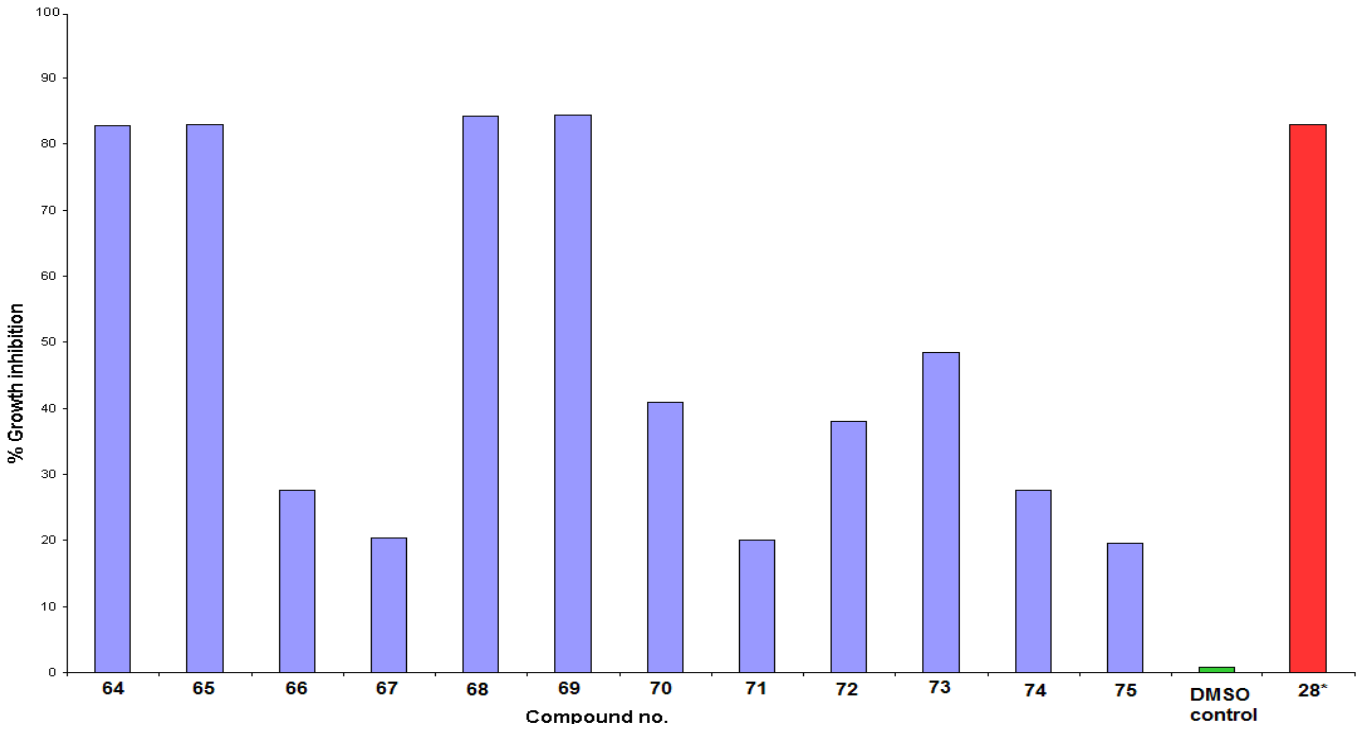

Alkyl	Benzoyl	Dipeptide ethyl ester	Compound No.	% growth inhibition at 10 µM
-CH_3	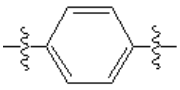	Gly Gly(OEt)	**64**	83 ± 4.35
		Gly L-Ala(OEt)	**65**	83 ± 0.97
		Gly L-Leu(OEt)	**66**	28 ± 1.57
		Gly L-Phe(OEt)	**67**	20 ± 2.86
	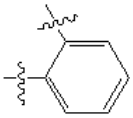	Gly Gly(OEt)	**68**	84 ± 3.80
		Gly L-Ala(OEt)	**69**	84 ± 1.26
		Gly L-Leu(OEt)	**70**	41 ± 1.01
		Gly L-Phe(OEt)	**71**	20 ± 2.92
	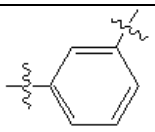	Gly Gly(OEt)	**72**	38 ± 2.40
		Gly L-Ala(OEt)	**73**	48 ± 1.48
		Gly L-Leu(OEt)	**74**	28 ± 2.61
		Gly L-Phe(OEt)	**75**	20 ± 3.68
No alkyl chain incorporation	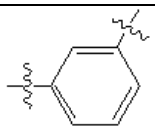	Gly L-Ala(OEt)	**28***	83 ± 0.87

Note: **28*** Originally prepared by Alan Corry [7]

Figure 3.3: % Growth inhibition at 10 µM on H1299 lung cancer cells for 1-methyl-1'-*N-para*, *N-meta* and *N-ortho*-(ferrocenyl) benzoyl dipeptide esters **64–75** and reference compound **28.**

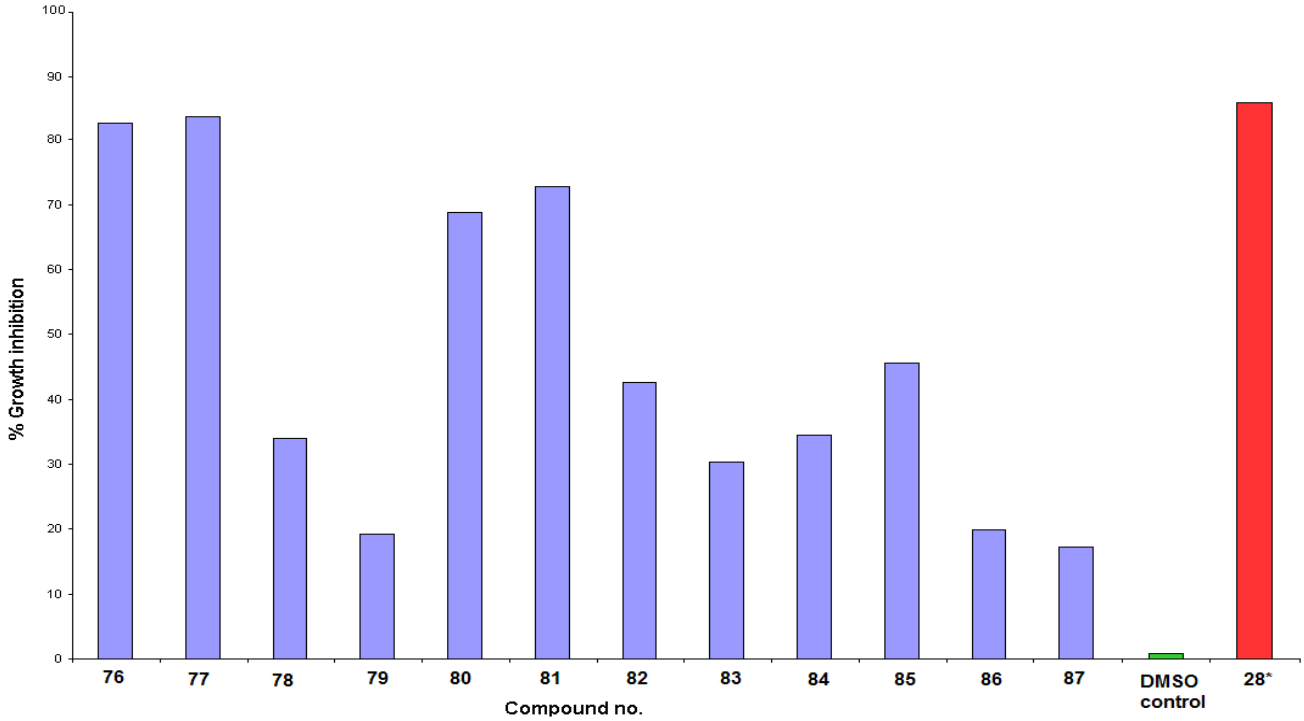

Alkyl	Benzoyl	Dipeptide ethyl ester	Compound no.	% growth inhibition at 10 µM
-CH_2CH_3	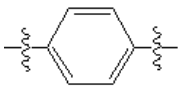	Gly Gly(OEt)	**76**	83 ± 1.48
		Gly L-Ala(OEt)	**77**	84 ± 2.32
		Gly L-Leu(OEt)	**78**	34 ± 1.55
		Gly L-Phe(OEt)	**79**	19 ± 3.62
	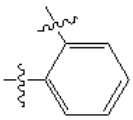	Gly Gly(OEt)	**80**	70 ± 2.61
		Gly L-Ala(OEt)	**81**	73 ± 1.65
		Gly L-Leu(OEt)	**82**	43 ± 0.76
		Gly L-Phe(OEt)	**83**	30 ± 2.42
	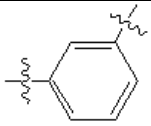	Gly Gly(OEt)	**84**	34 ± 1.94
		Gly L-Ala(OEt)	**85**	46 ± 1.79
		Gly L-Leu(OEt)	**86**	20 ± 2.47
		Gly L-Phe(OEt)	**87**	17 ± 1.33
No alkyl chain incorporation	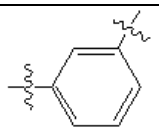	Gly L-Ala(OEt)	**28***	83 ± 0.87

Note: **28*** Originally prepared by Alan Corry [7]

Figure 3.4: % Growth inhibition at 10 µM on H1299 lung cancer cells for 1-ethyl-1'-*N-para*, *N-meta* and *N-ortho*-(ferrocenyl) benzoyl dipeptide esters **76-87** and reference compound **28.**

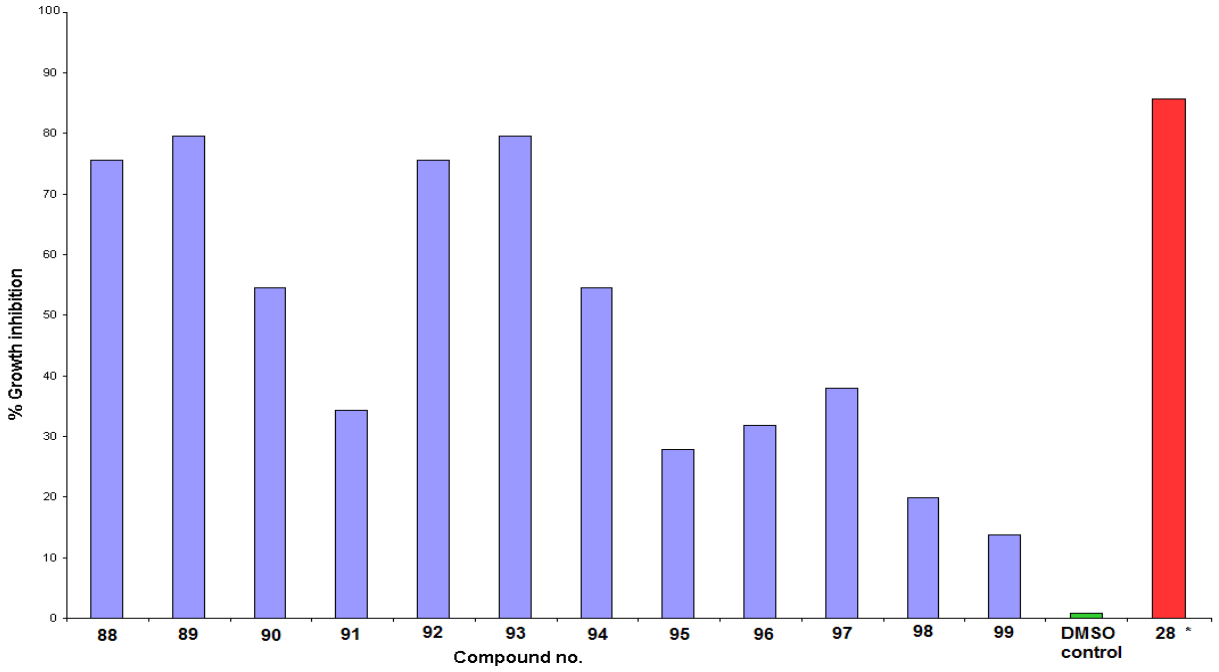

Alkyl	Benzoyl	Dipeptide ethyl ester	Compound No.	% growth inhibition at 10 µM
-$CH_2CH_2CH_3$		Gly Gly(OEt)	**88**	76 ± 3.42
		Gly L-Ala(OEt)	**89**	80 ± 4.50
		Gly L-Leu(OEt)	**90**	55 ± 1.91
		Gly L-Phe(OEt)	**91**	34 ± 2.50
	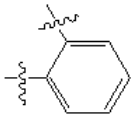	Gly Gly(OEt)	**92**	76 ± 3.12
		Gly L-Ala(OEt)	**93**	80 ± 4.07
		Gly L-Leu(OEt)	**94**	55 ± 0.91
		Gly L-Phe(OEt)	**95**	28 ± 2.32
	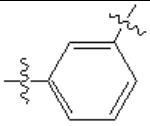	Gly Gly(OEt)	**96**	32 ± 1.56
		Gly L-Ala(OEt)	**97**	38 ± 0.58
		Gly L-Leu(OEt)	**98**	20 ± 2.57
		Gly L-Phe(OEt)	**99**	14 ± 3.43
No alkyl chain incorporation	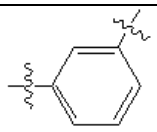	Gly L-Ala(OEt)	**28***	83 ± 0.87

Note: **28*** Originally prepared by Alan Corry [7]

Figure 3.5: % Growth inhibition at 10 µM on H1299 lung cancer cells for 1-propyl-1'-*N-para*, *N-meta* and *N-ortho*-(ferrocenyl) benzoyl dipeptide esters **88-99** and reference compound **28.**

From the preliminary screen at 10 μM a general trend can be observed, the 1-alkyl-1'-*N*-*ortho*- derivatives exhibited lower percentage growth inhibition values compared to the *meta* and *para* derivatives for the dipeptides employed in the SAR study. For instance, the 1-methyl-1'-*N*-{*ortho*-(ferrocenyl) benzoyl} glycine glycine ethyl ester **72** showed a percentage growth inhibition value of 38 ± 2.40 whilst the 1-methyl-1'-*N*-*para* and *meta*-(ferrocenyl) benzoyl} glycine glycine ethyl ester **(64** and **68)** showed percentage growth inhibition values of 84 ± 4.35 and 83 ± 2.86 respectively. The *ortho* derivatives were not investigated further.

A general trend was also observed in these compounds, that is, the Gly Gly (OEt) and Gly L-Ala (OEt) derivatives are more active than the Gly L-Leu and Gly L-Phe ethyl esters which display percentage growth inhibition values ≤ 55 %. For instance the 1-ethyl-1'-*N*-{*para*-(ferrocenyl) benzoyl} glycine glycine ethyl ester and glycine L-alanine ethyl ester displayed percentage growth inhibition values of 83 % ± 1.48 and 84 % ± 2.32 respectively, whilst the Gly L-Leu(OEt) and Gly L-Phe(OEt) displayed percentage growth inhibition values of 34 % ± 1.55 and 19 % ± 3.62 respectively. Thus, the Gly L-Leu and Gly L-Phe ethyl ester derivatives were not investigated further. As a result, it can be concluded that when chiral α-amino acids with bulky side chains are used as the second amino acid in the dipeptide moiety a loss of anti-proliferative activity is observed.

For the 1-alkyl-1'-*N*-*para*, *N*-*meta*-(ferrocenyl) benzoyl dipeptide esters, 12 lead compounds were identified which showed percentage growth inhibition values ≥ 70 % and therefore, IC_{50} values were determined for these compounds.

3.3 IC_{50} value determination

To determine the IC_{50} values of the 12 target compounds, individual 96-well plates containing H1299 cells were treated with the test compounds at concentrations ranging from 0.1 μM to 100 μM. The cells were then incubated for 5-6 days, until cell confluency was reached. Cell survival was determined by performing the acid phosphatase assay. The IC_{50} value for each compound was calculated using Calcusyn software, and standard deviations have been calculated using data obtained from three independent experiments. The values obtained are listed in table 3.1 and figure 3.6.

Table 3.1. IC_{50} values for selected compounds, carboplatin and cisplatin against human lung carcinoma cell line H1299.

Compound Name	**No.**	**IC_{50}**
Cisplatin	**8**	1.5 ± 0.10
Carboplatin	**9**	10 ± 1.60
N- {*meta*-(ferrocenyl)-benzoyl} Gly L-Ala(OEt)	**28***	4.0 ± 0.71
1-methyl- 1' -*N*- {*para*-(ferrocenyl)-benzoyl} Gly Gly(OEt)	**64**	2.8 ± 1.23
1-methyl-1' –*N*- {*para*-(ferrocenyl)-benzoyl} Gly L-Ala(OEt)	**65**	4.5 ± 0.40
1-methyl-1' –*N*- {*meta*-(ferrocenyl)-benzoyl} Gly Gly(OEt)	**68**	2.6 ± 0.62
1-methyl- 1' -*N*- {*meta*-(ferrocenyl)-benzoyl} Gly L-Ala(OEt)	**69**	6.7 ± 0.31
1-ethyl- 1' -*N*- {*para*-(ferrocenyl)-benzoyl} Gly Gly(OEt)	**76**	3.5 ± 0.82
1-ethyl-1' –*N*- {*para*-(ferrocenyl)-benzoyl} Gly L-Ala(OEt)	**77**	5.6 ±1.63
1-ethyl- 1' -*N*- {*meta*-(ferrocenyl)-benzoyl} Gly Gly(OEt)	**80**	6.1 ± 1.09
1-ethyl- 1' -*N*- {*meta*-(ferrocenyl)-benzoyl} Gly L-Ala(OEt)	**81**	13.3 ± 1.10
1-propyl-1' –*N*- {*para*-(ferrocenyl)-benzoyl} Gly Gly(OEt)	**88**	5.4 ±1.21
1-propyl- 1' -*N*- {*para*-(ferrocenyl)-benzoyl}Gly L-Ala(OEt)	**89**	6.6 ± 2.10
1-propyl- 1' -*N*- {*meta*-(ferrocenyl)-benzoyl} Gly Gly(OEt)	**92**	11.3 ± 2.10
1-propyl- 1' -*N*- {*meta*-(ferrocenyl)-benzoyl} Gly L-Ala(OEt)	**93**	20.1 ± 2.46

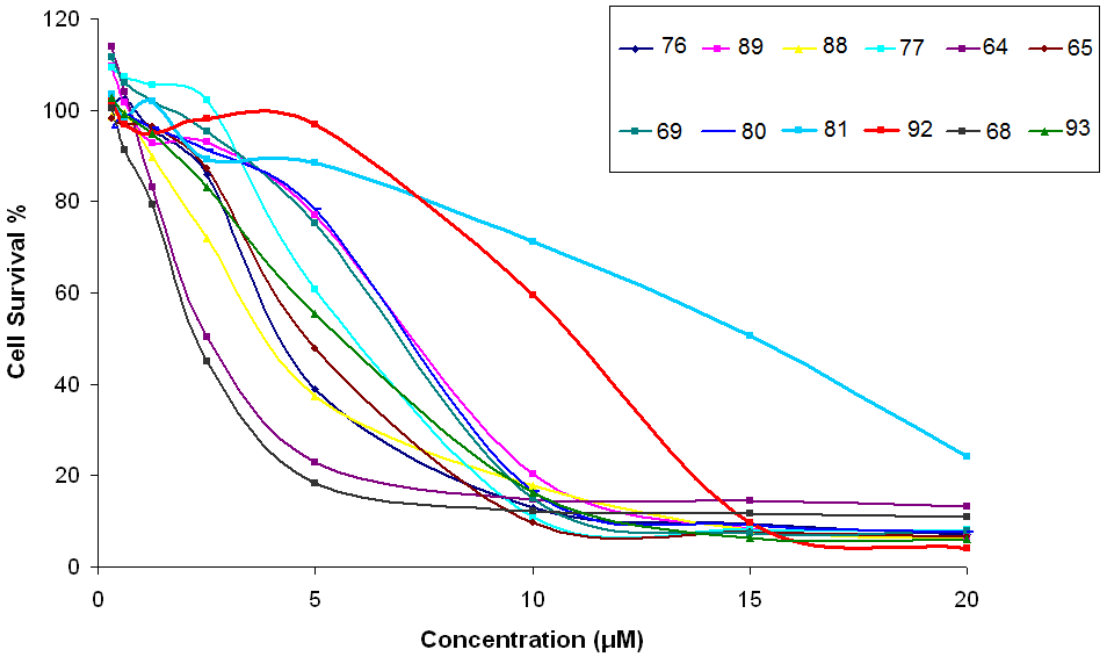

Figure 3.6: IC_{50} plot for selected compounds in the H1299 cell line.

From the IC_{50} values (Table 3.1) of the 1-alkyl-1'-*N*-*para*, *N*-*meta* -(ferrocenyl) benzoyl Gly Gly and Gly L-Ala ethyl esters **64, 65, 68, 69, 76, 77, 80, 81, 88, 89, 92** and **93,** it can be seen that the cytotoxicity of the derivatives decreases with the increase of the size of the alkyl moiety incorporated (propyl < ethyl < methyl). Indeed, all the methyl and ethyl derivatives display IC_{50} values that are lower than 14 µM. The *in vitro* cytotoxicity of the platinum (II) based anticancer drug carboplatin was also evaluated against the H1299 cell line and was found to have an IC_{50} value of 10.0 ± 1.60 µM (Table 3.1). Thus, compounds **64, 65, 68, 69, 76, 77, 80, 88** and **89** are more cytotoxic *in vitro* than the clinically employed anticancer drug carboplatin. In addition, the 1-methyl-1'-*N*-{*para*-(ferrocenyl) benzoyl} glycine glycine ethyl ester **64** displays an IC_{50} value of 2.8 ± 1.23 µM, the 1-ethyl-1'–*N*-{*para*-(ferrocenyl) benzoyl} glycine glycine ethyl ester **76** displays an IC_{50} value of 3.5 ± 0.82 µM and the 1-methyl- 1' -*N*-{*meta*-(ferrocenyl)-benzoyl} glycine glycine ethyl ester **68** shows an IC_{50} value of 2.6 ± 0.62 µM. These compounds display improved bioactivity in comparison to the most active ferrocenyl benzoyl analogues, the *N*-{meta-(ferrocenyl) benzoyl} glycine L-alanine ethyl ester **28** which displayed an IC_{50} values of 4.0 ± 0.71 µM.[6]

From these results incorporation of methyl and ethyl alkyl groups results in an improved cytotoxicity of the *para* derivatives of the glycine glycine ethyl esters and an improved cytotoxicity of the methyl *meta* glycine glycine derivative. However, when the size of the chain length increased to ethyl, the 1-ethyl-1'-*N*-{meta-(ferrocenyl)-benzoyl} glycine L-alanine ethyl ester displayed an IC_{50} of 13.3 ± 1.10 µM. This IC_{50} value was *ca.* three times higher than the unsubstituted analogue.[6] Thus, the increase in alkyl chain length resulted in a drastic decrease in the cytotoxicity of the 1-alkyl-1'-*N-para*, *N-meta* and *N-ortho*-(ferrocenyl) benzoyl dipeptide esters. Although compounds **64** and **68** are the most active derivatives of the 1-alkyl-1'-*N-para*, *N-meta* and *N-ortho*-(ferrocenyl) benzoyl dipeptide esters, they are less active compared to cisplatin which displays an IC_{50} value of 1.5 ± 0.10 µM against human H1299 lung cancer cells.

It was previously shown that the *N*-(6-ferrocenyl-2-naphthoyl) glycine glycine ethyl ester **31**, induced DNA damage through the generation of •OH radicals via a Fenton-type reaction.[9] In the Fenton-type reaction, the ferrocene moiety of the ferrocenyl bioconjugates is oxidised to a higher oxidised state, by donating an electron to a hydrogen peroxide species, which results in the formation of a hydroxyl radical and a hydroxyl ion (scheme 3.1).[9]

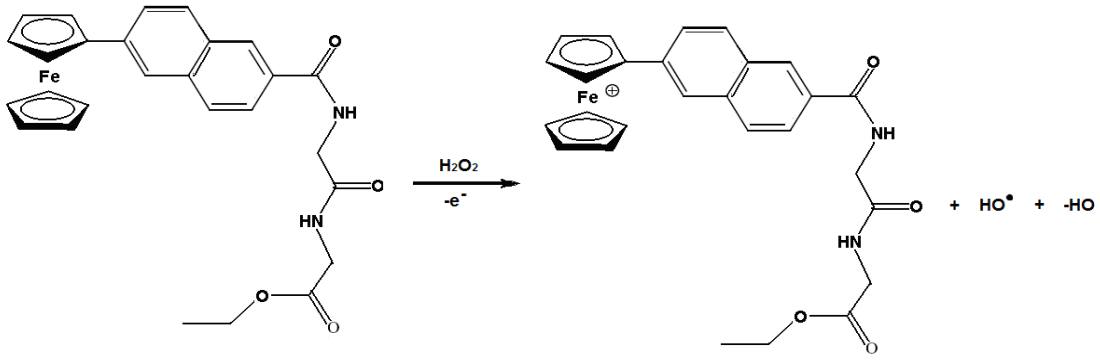

31

Scheme 3.1: Fenton reaction generation of ·OH radical species.

The hydroxyl radical (HO•) generated oxidises guanine to oxo-8-guanine (scheme 3.2), thus altering the base pairing sequence to Adenine which results in DNA damage leading to cell apoptosis.[9]

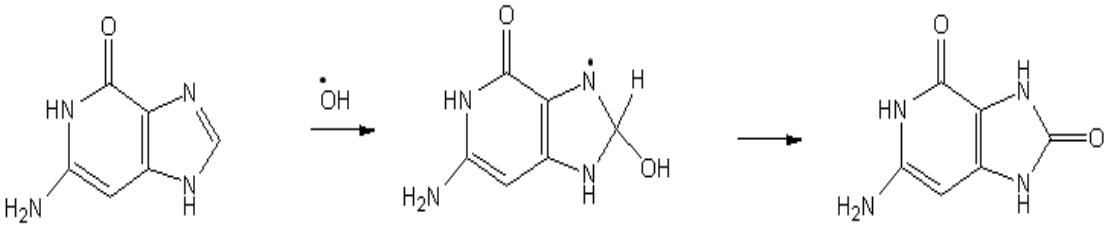

Guanine oxo-8-guanine

Scheme 3.2: Oxidation of guanine to oxo-8-guanine.

3.4 Conclusions

Cytotoxicity of the 1-alkyl-1'-*N*-*para*, *N*-*meta* and *N*-*ortho*-(ferrocenyl) benzoyl dipeptide esters, decreases with the increase of the size of the alkyl group incorporated (propyl < ethyl < methyl) on the ferrocene moiety. All the methyl and ethyl derivatives have IC_{50} values that are lower than 14 µM. The order of the amino acids in the dipeptide chain is crucial for activity, the trend being Gly Gly > Gly L-Ala > Gly L-Leu > Gly L-Phe. The most active derivatives of the 1-alkyl-1'-*N*-*para*, *N*-*meta* and *N*-*ortho*-(ferrocenyl) benzoyl dipeptide esters are the 1-methyl-1'-*N*-{*para*-(ferrocenyl) benzoyl} glycine glycine ethyl ester **64** and the 1-methyl-1'-*N*-{*meta*-(ferrocenyl) benzoyl} glycine glycine ethyl ester **68** which display IC_{50} values of 2.8 ± 1.23 µM and 2.6 ± 0.62 µM respectively. These compounds are more active than carboplatin but are less effective against cisplatin which are clinically employed anticancer drugs.

References

1. Bree, L., Murphy, L., Keenan, J., Clynes, M., *Toxicology in Vitro*, **2008**, *22*, 1234-1241
2. Kinnula, V. L., Crapo, J. D., *Free Rad. Bio. Med.*, **2004**, *36*, 718-744
3. Goel, A., Savage, D., Alley, S.R., Kelly, P.N., O'Sullivan, D., Mueller-Bunz, H., and Kenny, P.T.M., *J. Organomet. Chem.*, **2007**, *692*, 1292-1299.
4. Goel, A., Savage, D., Alley, S.R., Hogan, T., Kelly, P.N., Draper, S., Fitchett C.M., and Kenny P.T.M, *J. Organomet. Chem.*, **2006**, *691*, 4686-4693.
5. Corry, A.J., Goel, A., Alley, S.R., Kelly, P.N., O'Sullivan, D., Savage, D., and Kenny, P.T.M., *J. Organomet. Chem*., **2007** *692*, 1405-1410.
6. Corry, A.J., Mooney, A., O'Sullivan, D., and Kenny, P.T.M., *Inorganica Chimica Acta.*, **2009**, *362*, 2957-2961.
7. Corry, A.J., O'Donovan, N., Mooney, A., O'Sullivan, D., Rai, D.K., Kenny, P.T.M., *J. Organomet. Chem.*, **2009**, *694*, 880-885.
8. Martin, A., Clynes, M., *In Vitro Cell. Dev. Biol*., **1991**, *27A*, 183-184
9. Mooney, A., Tiedt, R., Maghoub, T., O'Sullivan, D., O'Donovan, N., Crown, J., Varughese, S., White, B., and Kenny, P.T.M., *J. Med. Chem*., **2012**, *55*, 5455−5466

Chapter 4: Synthesis and structural characterisation of *N*-{*para*-(ferrocenyl) ethynyl benzoyl}, *N*-{6-(ferrocenyl) ethynyl-2-naphthoyl} and *N*-{5-(ferrocenyl) ethynyl-2-furanoyl} amino acid and dipeptide esters

4.1 Introduction

To date we have shown that the replacement of the conjugated linker of *N*-(ferrocenyl) benzoyl dipeptide esters with a naphthoyl linker leads to an improvement in antiproliferative effect in the non small cell lung cancer (NSCLC) cell line, H1299.[1-3] From the series of *N*-(ferrocenyl) naphthoyl amino acid and dipeptide ethyl esters reported, the *N*-{6-(ferrocenyl)-2-napthoyl} glycine glycine ethyl ester **31** displayed an IC_{50} value of 0.13 ± 0.01 μM in the H1299 lung cancer cell line.[3]

From the promising results obtained from the 1-alkyl-1'-*N-para*, *N-meta* and *N-ortho*-(ferrocenyl) benzoyl dipeptide esters **64–99.** It has been clearly demonstrated in the SAR study of the 1-alkyl-1' derivatives that employing the incorporation of a methyl derivative to the unsubstituted cyclopentadiene ring enhances the anti-proliferative effect of the ferrocenyl dipeptide bioconjugates relative to the *N*-(ferrocenyl) benzoyl dipeptide derivatives in the H1299 lung cancer cell line.[4-8] The most active derivative was the 1-methyl-1'-*N*-{*meta*-(ferrocenyl) benzoyl} glycine glycine ethyl ester **68** which displayed an IC_{50} values of 2.6 ± 0.62 μM.

In a continuation to this SAR study in search for novel compounds with increased anti-proliferative effect, a new library of ferrocenyl based bioconjugates **105-138**, which consist of four key moieties (figure 4.1):

(i) An electroactive core
(ii) An ethynyl moiety
(iii) Three different aromatic linkers
(iv) A series of amino acid and dipeptide esters

This SAR study involves the biological evaluation of the incorporation of an ethynyl moiety between the ferrocene moiety and the conjugate linker. Furthermore, the incorporation of L-leucine and L-phenylalanine into the dipeptide chains have been

shown in the preliminary screen of the 1-alkyl-1' derivatives (**64-69**) (section 3.2) to display low percentage growth inhibition values in H1299 lung cancer cell line. The dipeptides and the amino acid employed were Glycine Glycine (Gly Gly), Glycine L-Alanine (Gly L-Ala), Glycine D-Alanine (Gly D-Ala), Sarcosine Glycine (Sar Gly), Sarcosine L-Alanine (Sar L-Ala), L-Proline L-Alanine (L-Pro L-Ala), L-Proline Glycine (L-Pro Gly), Glycine L-Leucine (Gly L-Leu) and Glycine L-Phenylalanine (Gly L-Phe) and γ-aminobutyric acid **(**GABA).

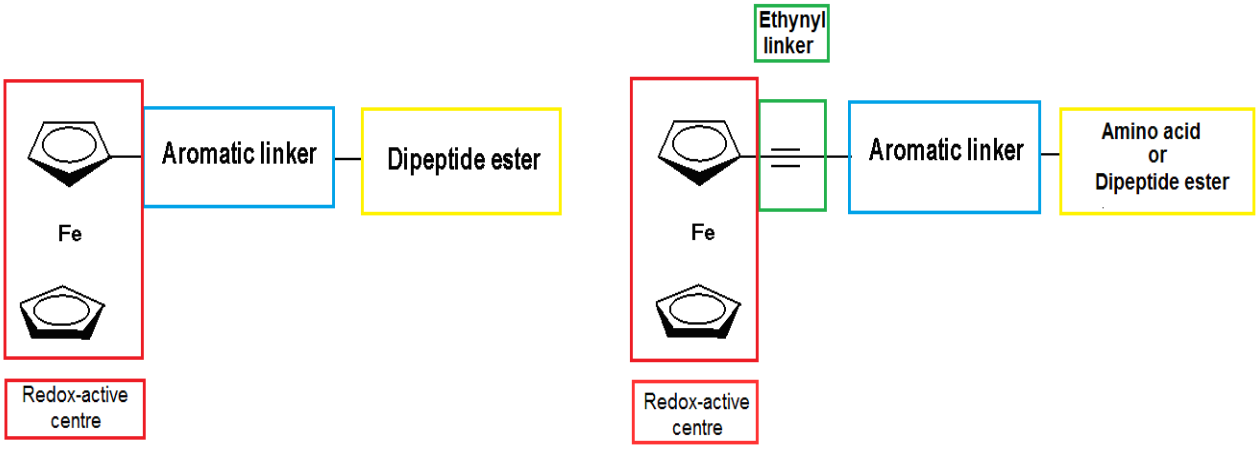

Figure 4.1: General structure of the *N*-(ferrocenyl) benzoyl and naphthoyl bioconjugates and *N*-{*para*-(ferrocenyl) ethynyl benzoyl}, *N*-{6-(ferrocenyl) ethynyl-2-naphthoyl} and *N*-{5-(ferrocenyl) ethynyl-2-furanoyl} amino acid and dipeptide esters.

The synthesis of the new ferrocenyl conjugates involved Sonogashira coupling of an ethynyl ferrocene to three bromo acylated acids to generate *para*-(ferrocenyl) ethynyl benzoic acid, naphthoic acid and 2-furanoic acid. A series of amino acid and dipeptide esters were coupled to the *N*-(ferrocenyl) ethynyl acids generating new classes of compounds, which were characterized by a combination of ^{1}H NMR, ^{13}C NMR, DEPT-135, ^{1}H-^{13}C COSY spectroscopy and electrospray ionization mass spectrometry.

4.2 Synthesis of ethynyl ferrocene 101

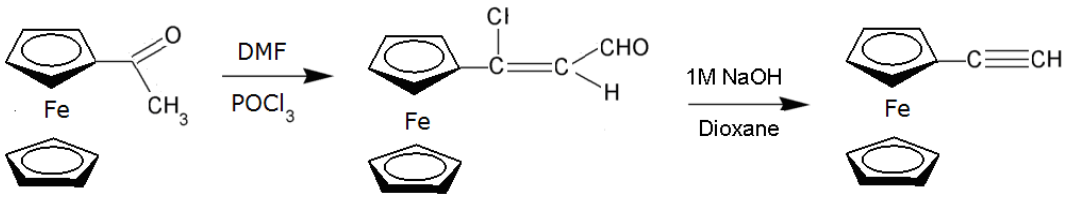

49 **100** **101**

Scheme 4.1: Synthesis of ethynyl ferrocene.

The synthesis of ethynyl ferrocene is well document in the literature.[9-10] Despite being commercially available, it is expensive to purchase for use on a large scale. Rosenblum *et* al. have reported the synthesis of ethynyl ferrocene which was prepared via formation of (2-formyl-1-chlorovinyl) ferrocene from acetyl ferrocene using *N*,*N*-dimethylformamide and phosphorus oxychloride.[10] Dehalogenation of (2-formyl-1-chlorovinyl) ferrocene using 1M sodium hydroxide yields ethynyl ferrocene as shown in scheme 4.1. The yields obtained from this synthetic protocol are high, but it requires aggressive reagents like $POCl_3$; however, this was the protocol chosen to synthesis ethynyl ferrocene.

4.2.1 Synthesis of (2-formyl-l-chlorovinyl) ferrocene intermediate

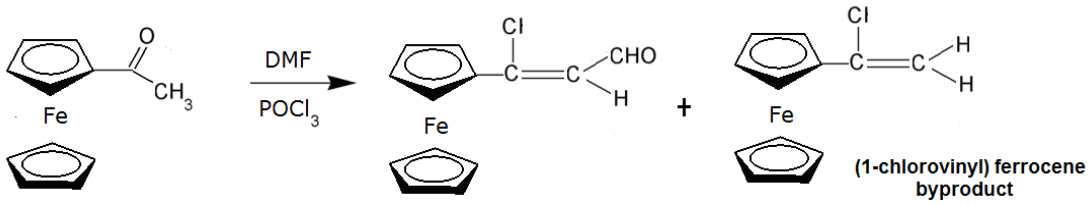

49 **100**

Scheme 4.2: Synthesis of (2-formyl-l-chlorovinyl) ferrocene intermediate.

The treatment of a ketone with Vilsmeir reagent leads generally to the formation of halovinyl aldehydes and it is referred to as a Vilsmeir haloformylation. For a Vilsmeir haloformylation to occur it requires a ketone that can undergo enolisation that is (scheme 4.3).

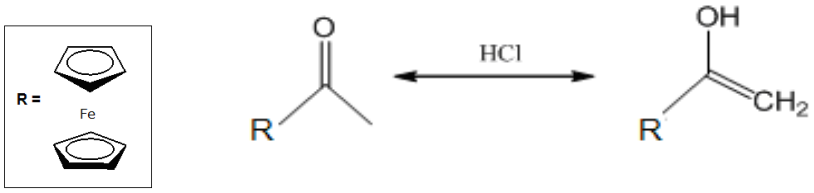

Scheme 4.3: Enolisation of ketone.

The treatment of acetylferrocene with a Vilsmeir reagent, prepared by the reaction of phosphorus oxychloride in *N,N*-dimethylformamide as reported by Rosenblum *et* al., leads to the formation of a mixture of (2-formyl-1-chlorovinyl) ferrocene and a unwanted unstable (1-chlorovinyl)ferrocene (scheme 4.2. In continuation of this work, Polin *et* al. have shown that the formation of (1-chlorovinyl) ferrocene can be suppressed by using excess phosphorus oxychloride, *N,N*-dimethylformamide and solid sodium acetate.[11] From numerous reactions carried out, it was observed that if the Vilsmeir reagent was added over 2 hr as opposed to 30 min as reported by Polin *et* al., it favoured the formation of (2-formyl-l-chlorovinyl) ferrocene. In the mechanism for the formation of (2-formyl-l-ch1orovinyl) ferrocene the initial step is the formation of the Vilsmeir reagent **(i)** in scheme 4.4. Once the Vilsmeir reagent **(i)** is formed it reacts with the enolised ketone **(ii)** to form a β – *N-N*- dimethylaminovinyl ketone **(iii)** (scheme 4.4).

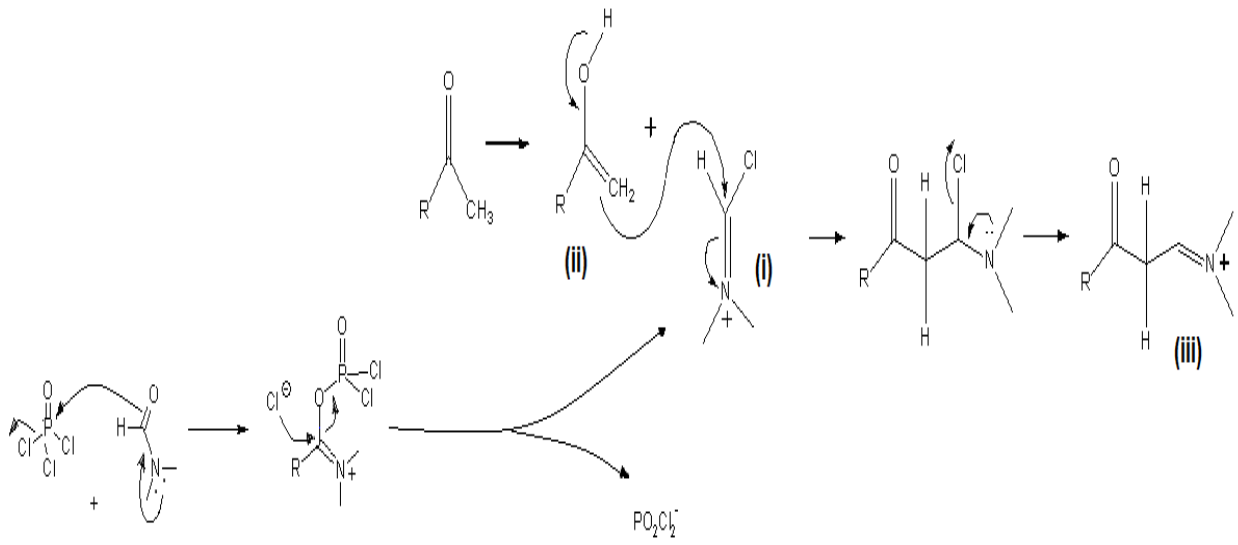

Scheme 4.4: Formation of β – *N-N*- dimethylaminovinyl ketone **(iii).**

The β – *N*-*N*- dimethylaminovinyl ketone **(iii)** further reacts with a Vilsmeir reagent to give rise to a bisiminium chloride **(iv).** This intermediate is liable and undergoes nucleophillic substitution with a chloride ion to give rise to the iminium intermediate **(v).** Base hydrolysis of the intermediate **(v)** with sodium acetate gives rise to (2-formyl-l-ch1orovinyl) **(vi)** as outlined in scheme 4.5.[11]

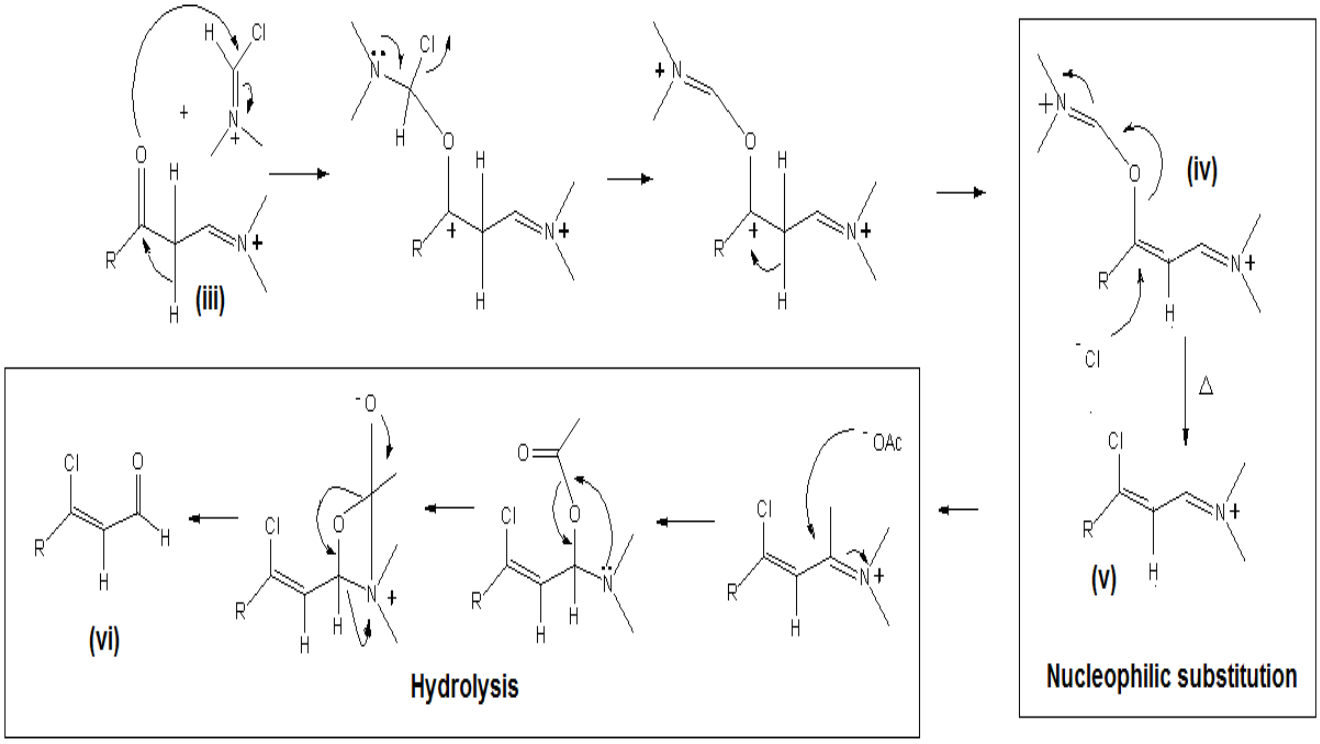

Scheme 4.5: Formation of (2-formyl-l-ch1orovinyl) ferrocene.

In the synthesis of (2-formyl-l-ch1orovinyl) ferrocene via Vilsmeier haloformylation the spectral data obtained for the isolated (2-formyl-l-ch1orovinyl) ferrocene was in agreement with that reported previously for this compound and a yield greater than 60% was obtained.[11]

4.2.2 Dehalogenation of (2-formyl-l-ch1orovinyl) ferrocene to obtain ethynylferrocene

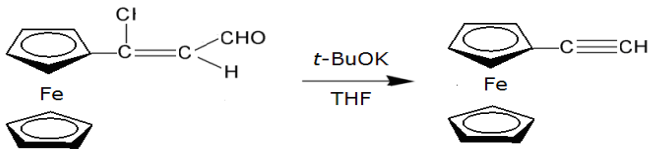

100 **101**

Scheme 4.6: Dehalogenation of (2-formyl-l-ch1orovinyl) ferrocene to obtain ethynylferrocene.

In the base induced dehalogenation of (2-formyl-l-ch1orovinyl) ferrocene to obtain ethynylferrocene according to Polin *et* al., initial attempts were not successful as the reaction required anhydrous conditions which could not have been attained. As a result an alternative pathway had to be established which did not require adverse anhydrous conditions. By using potassium *tert*-butoxide as an alternative base in dry THF at 0 ^{o}C resulted in the dehalogenation of (2-formyl-l-ch1orovinyl) ferrocene to ethynylferrocene with yields greater than 45%.

4.3 Synthesis of *para*-(ferrocenyl) ethynyl benzoic acid, 6-(ferrocenyl) ethynyl-2-naphthoic acid and 5-(ferrocenyl) ethynyl-2-furanoic acid via Sonogashira cross coupling reaction

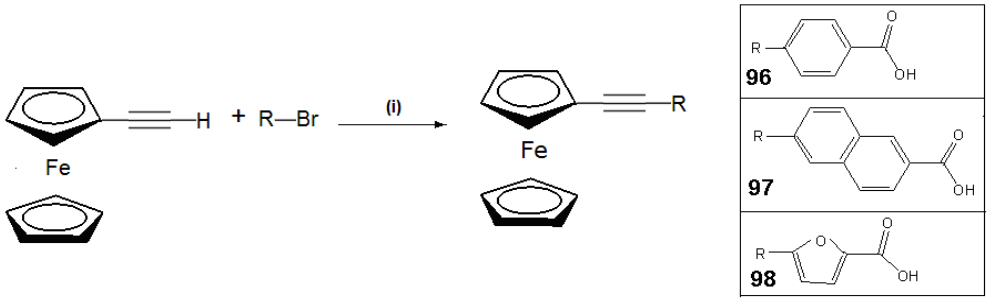

(i) TEA, PPh_3, *Bis*(triphenylphosphine)palladium(II) dichloride, THF, Cu(I)

Scheme 4.7: Synthesis of *para*-(ferrocenyl) ethynyl benzoic acid **102**, 6-(ferrocenyl) ethynyl-2-naphthoic acid **103** and 5-(ferrocenyl) ethynyl-2-furanoic acid **104** via Sonogashira cross coupling reaction.

The Sonogashira cross coupling reaction is a transition metal-catalysed cross-coupling reaction used in organic synthesis to form carbon-carbon bonds.[13] The coupling reaction involves the use of a palladium catalyst, a copper (I) iodine co-catalyst and an amine base to form a carbon–carbon bond between a terminal alkyne and an aryl halide. Sonogashira cross-coupling of an ethynyl ferrocene to the three bromo acylated acids was employed to generate *para*-(ferrocenyl) ethynyl benzoic acid **102**, 6-(ferrocenyl) ethynyl-2-naphthoic acid **103** and 5-(ferrocenyl) ethynyl-2-furanoic acid **104** in yields greater than 60%. These high yields are largely due to the fact that the Sonogashira cross coupling reaction is a substrate specific reaction between an alkyne and an aryl halides. The mechanism for the Sonogashira cross coupling consist of two catalytic cycles namely a palladium cycle and a copper cycle as shown in scheme 4.8.[14]

To enhance the formation of activation of *bis*(triphenylphosphine)palladium(II) dichloride, anhydrous conditions are required. It was observed that the incorporation of triphenylphosphine enhances Sonogashira reaction because it is oxidised by any oxygen in the reaction vessel to triphenylphosphine oxide which enhances the reduction of the Pd (II) catalyst to its active form Pd (0).[15]

In the palladium catalytic cycle the active palladium catalyst Pd (0) reacts with the aryl bromide in an oxidative addition to form a Pd (ll) intermediate complex (i). The generated complex (i) reacts in a transmetallation reaction with the copper acetylide, which is produced in the copper catalytic cycle to give rise to complex (ii). In complex (ii) both organic ligands are *trans*-oriented. The ligands undergo a *trans-cis* isomerisation to produce complex (iii). In the final step of the catalytic cycle complex (iii) undergoes reductive elimination to produce the required compounds (iv) with regeneration of the palladium catalyst.[15]

In the copper catalytic cycle the ethynylferrocene reacts with the copper (I) iodine in the presence of triethylamine to produce a copper (I) acetylide, which acts as an activated species for the coupling reactions hence the copper (I) iodine acts as a co-catalyst to increase the rate of the Sonogashira cross-coupling reaction.

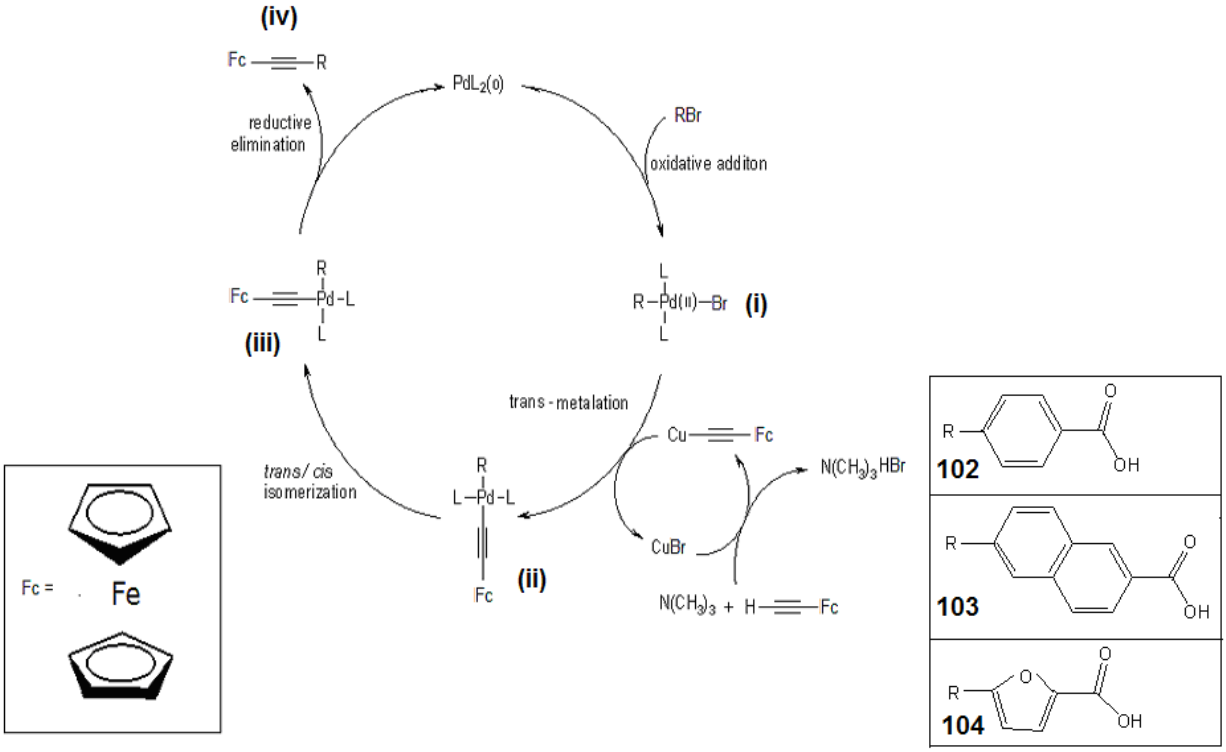

Scheme 4.8: Catalytic cycles in the Sonogashira coupling reaction.

4.4 Synthesis of *N*-{*para*-(ferrocenyl) ethynyl benzoyl}, *N*-{6-(ferrocenyl) ethynyl-2-naphthoyl}, *N*-{5-ferrocenyl ethynyl-2-furanoyl} amino acid and dipeptide esters

The synthesis of *N*-{*para*-(ferrocenyl) ethynyl benzoyl}, *N*-{6-(ferrocenyl) ethynyl-2-naphthoyl}, *N*-{5-ferrocenyl ethynyl-2-furanoyl} amino acid and dipeptide esters was carried by coupling of the dipeptide ethyl and methyl ester hydrochloride salts of Gly Gly, Gly L-Ala, Gly D-Ala, Gly L-Leu and Gly L-Phe, Sar Gly, Sar L-Ala, L-Pro L-Ala, L-Pro Gly and the amino acid GABA, to *N*-para-(ferrocenyl) ethynyl benzoic acid, *N*-6-(ferrocenyl) ethynyl-2-naphthoic acid and *N*-5-(ferrocenyl) ethynyl-2-furanoic acid using the *N*-(3-dimethylaminopropyl)-*N*'-ethylcarbodiimidehydrochloride (EDC), 1-hydroxybenzotriazole (HOBt) protocol as shown in scheme 4.9. The synthesised pure ethynyl derivatives **105-138** was furnished as either an orange solid or a red oil with yields of 8-38%. All compounds gave spectroscopic and analytical data in accordance with their proposed structures.

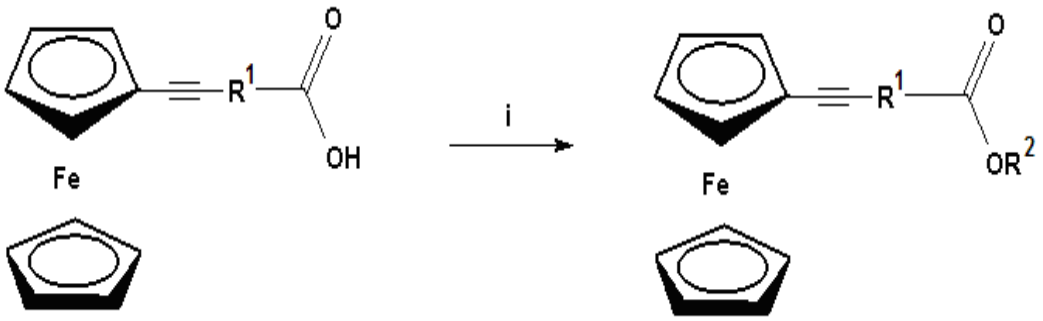

(i) EDC, HOBt, triethylamine, dipeptide ethyl esters and free *N*-terminal γ-Amino butyric acid esters

R^1	R^2	Compound no.
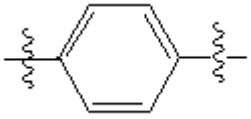	Gly Gly(OMe)	**105**
	GlyGly(OEt)	**106**
	Gly L-Ala(OMe)	**107**
	Gly L-Ala(OEt)	**108**
	Gly D-Ala(OMe)	**109**
	Gly D-Ala(OEt)	**110**
	GABA(OMe)	**111**
	GABA(OEt)	**112**
	Gly L-Phe(OEt)	**113**
	Gly L-Leu(OEt)	**114**
	Sar Gly(OEt)	**115**
	Sar Gly(OMe)	**116**
	Sar L-Ala(OEt)	**117**
	L-Pro Gly(OEt)	**118**
	L-Pro L-Ala(Oet)	**119**
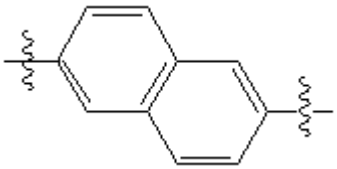	Gly Gly(OEt)	**120**
	Gly L-Ala(OEt)	**121**
	Sar L-Ala(OEt)	**122**
	L-Pro Gly(OEt)	**123**
	GABA(OEt)	**124**
	L-Pro L-Ala(Oet)	**125**
	Gly L-Leu(OEt)	**126**
	Sar Gly(OEt)	**127**
	Gly L-Phe(OEt)	**128**
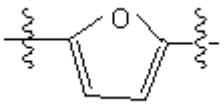	Gly Gly(OEt)	**129**
	Gly L-Ala(OEt)	**130**
	Gly D-Ala(OEt)	**131**
	Gly L-Phe(OEt)	**132**
	Gly L-Leu(OEt)	**133**
	Sar Gly(OEt)	**134**
	L-Pro Gly(OEt)	**135**
	L-Pro L-ala(OEt)	**136**
	Sar L-ala(OEt)	**137**
	GABA(OEt)	**138**

Scheme 4.9: Synthesis of *N*-{*para*-(ferrocenyl) ethynyl benzoyl} amino acid and dipeptide esters **105-138.**

The carbodiimide-mediated coupling reaction follows the mechanism depicted in scheme 2.12 for the synthesis of 1-alkyl-1 derivatives. The yields for the 34 compounds prepared varied from 8-38%. The reasons for the low yields for the compounds **105-138** are similar to those outlined in section 2.4. The low yields can also be rationalized by considering the respective orientations of the terminal amine moiety on the dipeptide amino acid and ethyl esters. Generally 1^{o} amines are more reactive than 2^{o} amines and more reactive than 3^{o} tertiary. Thus in the EDC/HOBt coupling reactions when 1^{o} amine dipeptide amino acid and ethyl esters {GABA(OEt), Gly Gly(OEt) and Gly L-Ala(OEt)} are used, the yields are generally higher than the 2^{o} amines dipeptide ethyl esters [Sar Gly(OEt), Sar L-Ala(OEt), L-Pro Gly(OEt) and L-Pro L-Ala(OEt)]. For instances the *N*-{6-(ferrocenyl) ethynyl-2-naphthoyl} glycine glycine ethyl ester (**120**) displayed a percentage yield of 32% whilst the *N*-{6-(ferrocenyl) ethynyl-2-naphthoyl} sarcosine glycine ethyl ester (**127**) had a percentage yield of 13%.

4.5 ^{1}H NMR spectroscopic studies of *N*-{*para*-(ferrocenyl) ethynyl benzoyl}, *N*-{6-(ferrocenyl) ethynyl-2-naphthoyl} and *N*-{5-(ferrocenyl) ethynyl-2-furanoyl} amino acid and dipeptide esters

4.5.1 ^{1}H NMR spectroscopic studies of *N*-{*para*-(ferrocenyl) ethynyl benzoyl} amino acid and dipeptide esters

In $CDCl_3$, typical chemical shifts observed for the *N*-{*para*-(ferrocenyl) ethynyl benzoyl} amino acid and dipeptide esters (figure 4.2) include the appearance of amide protons and four aromatic hydrogens on the benzoyl spacer between δ 8.90 and δ 6.50. In the ^{1}H NMR spectra of the Sar Gly, Sar L-Ala, L-Pro Gly and L-Pro L-Ala dipeptide derivatives, the amide protons and the aromatic hydrogens on the benzoyl spacer overlap, resulting in multiplets being observed between δ 8.90 and δ 6.50.

For the Gly Gly, Gly L-Ala and Gly L-Leu derivatives the splitting pattern of the hydrogens on the benzoyl linker follows the second order splitting pattern, which is consistent with the alkyl derivatives described in section 2.5 and do not overlap with the amide proton signals.

The protons on the monosubstituted ferrocene ring in the *N*-{*para*-(ferrocenyl) ethynyl benzoyl derivatives, are expected to occur as three signals between δ 4.70 and δ 4.00. However, these signals usually overlap with the hydrogen signals of either the methylene groups or the methine groups that may be present in the amino acid and dipeptide esters. In the Gly L-Ala derivative (**108**) no overlapping is observed, hence, the *ortho* and *meta* protons on the cyclopentadiene ring attached to the ethynyl spacer (η^5-$C_5\underline{H}_4$-C≡C-) appear as two apparent triplet signals. This complexity of the appearance of the apparent singlet or triplet signals has already been discussed in section 2.5. The protons on the unsubstituted cyclopentadiene ring appear as a singlet as all the hydrogens are magnetically equivalent. The methyl protons (-$OCH_2\underline{CH}_3$) of the ethyl ester derivatives appear as a triplet between δ 1.30 and δ 1.15. The methyl protons (-$O\underline{CH}_3$) of the methyl derivatives appear as a singlet between δ 3.70 and δ 3.60.

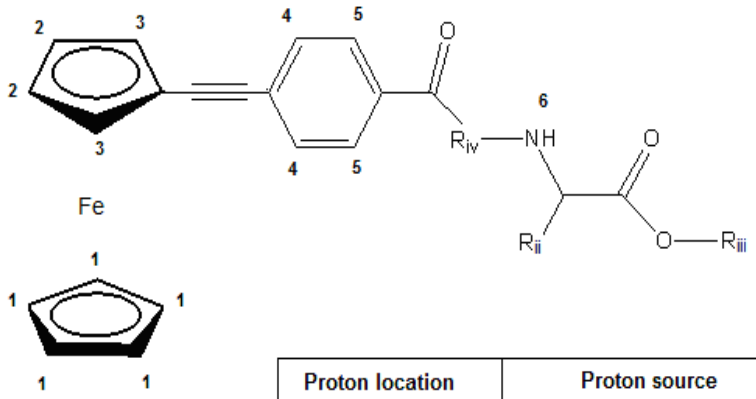

Proton location	Proton source	δ ($CDCl_3$)
1, 2, 3	(η^5-$C_5\underline{H}_4$-C≡C-), (η^5-$C_5\underline{H}_5$)	4.70 - 4.00
4, 5, 6	Aromatic H, NH	8.90 - 6.50
Riii	(-O$\underline{C}H_3$)	3.70 - 3.60
Riii	(-OCH$_2\underline{C}H_3$)	1.30 - 1.15

Figure 4.2: Typical chemical shifts observed for the *N*-{*para*-(ferrocenyl) ethynyl benzoyl} amino acid and dipeptide esters **105-119.**

4.5.1.1 ^{1}H NMR spectroscopic studies of *N*-{*para*-(ferrocenyl) ethynyl benzoyl} glycine D-alanine methyl ester 109

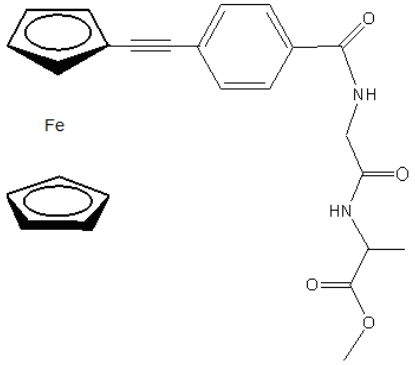

109

The ^{1}H NMR spectrum of compound **109** is shown in figure 4.3. The four aromatic protons present at δ 7.73 and δ 7.46 appear as two apparent doublet signals with a coupling constant of 8.4 Hz. The two amide protons (-CONH-) present at δ 7.25 and δ 7.07 are observed as a triplet and a doublet with constants of 5.6 Hz and 6.8 Hz respectively. The methine group -CH(CH_3) appears as a multiplet between δ 4.55 and δ 4.50. The *ortho* protons (η^5-C_5H_4-C≡C-) on the cyclopentadiene ring attached to the (-C≡C-) spacer moiety appears as an apparent triplet at δ 4.45 whilst the *meta* protons (η^5-C_5H_4-C≡C-) overlap with the protons on the unsubstituted (η^5-C_5H_5) ring, the methylene protons of (-NHCH_2CO-), resulting in a multiplet appearing between δ 4.21 and δ 4.14 with an overall intergration of nine. The methyl group of the methyl ester (-OCH_3) is present as a singlet at δ 3.68. The methyl group (-CHCH_3) on the alanine moiety appears as a doublet at δ 1.38 with a coupling constant of 7.2 Hz.

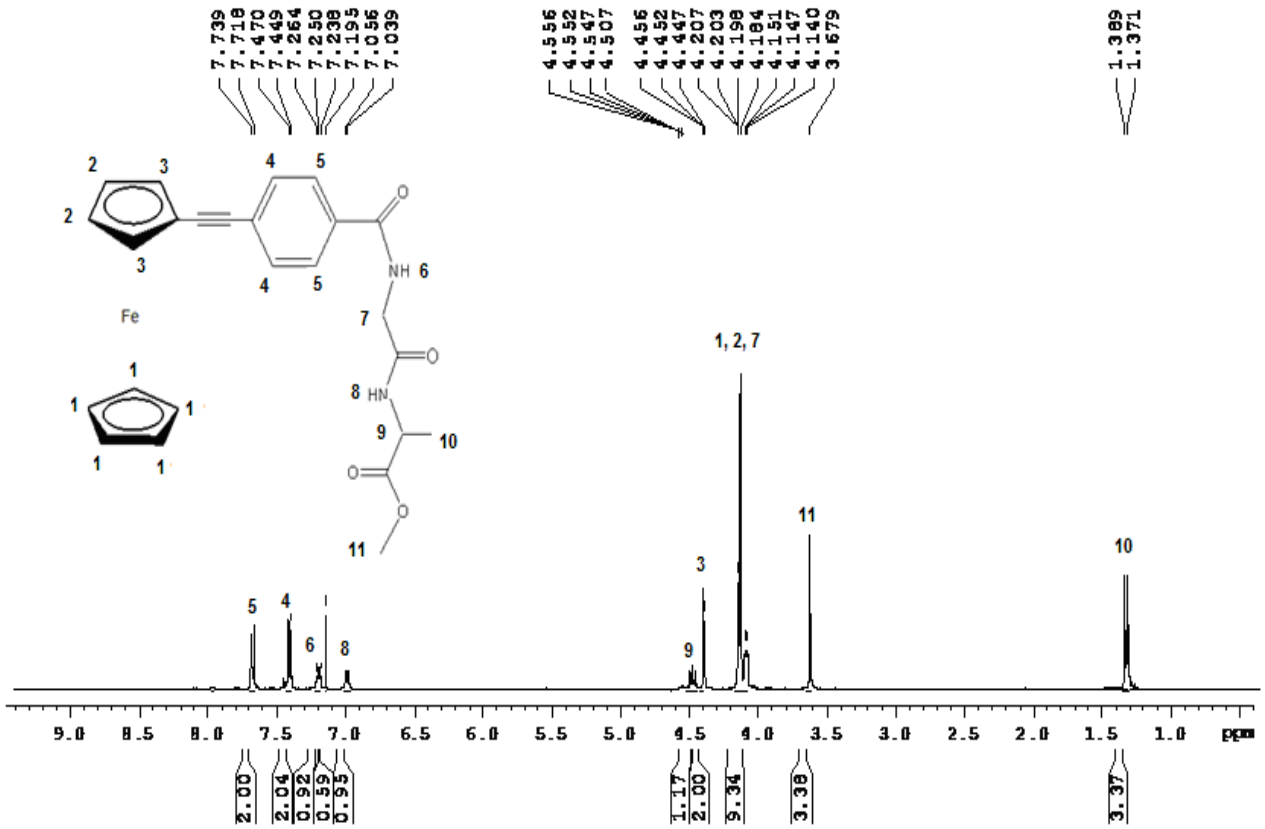

Figure 4.3: ^{1}H NMR spectrum of *N*-{*para*-(ferrocenyl) ethynyl benzoyl} glycine D-alanine methyl ester **109.**

4.5.2 ^{1}H NMR spectroscopic studies of *N*-{6-(ferrocenyl) ethynyl-2-naphthoyl} amino acid and dipeptide esters

The typical chemical shifts observed for the *N*-{6-(ferrocenyl) ethynyl-2-naphthoyl} amino acid and dipeptide esters in $CDCl_3$ include the appearance of amide protons. These signals overlap with the six protons on the naphthoyl spacer group between δ 8.30 and δ 6.70 (figure 4.4). The protons on the monosubstituted ferrocene ring overlap with the hydrogen signals of either the methylene groups or the methine groups that may be present in the amino acid and dipeptide esters. Hence, the expected three signals for a monosubstituted derivative are not observed. For the L-Pro Gly derivative (**123**), the *ortho* protons (η^5-$C_5\underline{H}_4$-C≡C-) on the cyclopentadiene ring attached to the -C≡C- spacer moiety is observed as an apparent singlet signal, whilst the *meta* protons overlap with the protons on the unsubstituted (η^5-C_5H_5) ring resulting in a multiplet being observed between δ 4.21 - 4.18 which has an overall integration of seven. The methyl protons (-$OCH_2\underline{CH}_3$) of the ethyl ester derivatives appear between δ 1.30 and δ 1.00. Due to the overlapping of signals, other spectroscopic techniques were used to provide a more complete picture of the molecular structure of these derivatives. These included ^{13}C NMR, DEPT-135 and ^{1}H-^{13}C COSY (HMQC) spectroscopy and electrospray ionization mass spectrometry (ESI-MS).

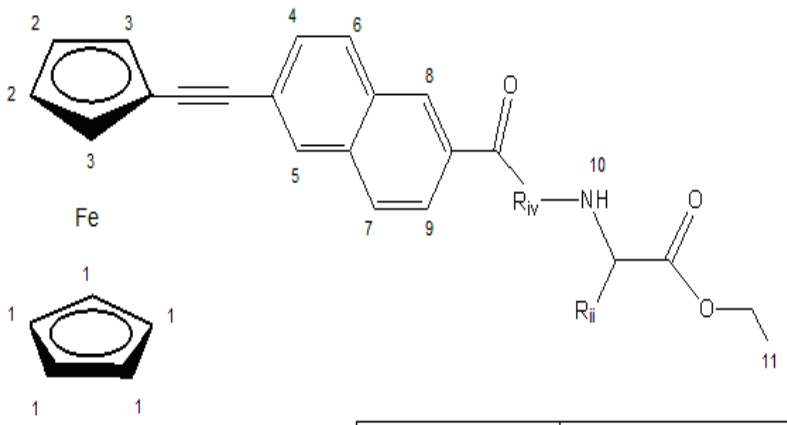

Proton location	Proton source	δ ($CDCl_3$)
1, 2, 3	(η^5-C_5H_4-C≡C-), (η^5-C_5H_5)	4.70 - 4.00
4, 5, 6, 7, 8, 9 , 10	Aromatic H, NH	8.30 - 6.70
11	(-$OCH_2\underline{CH_3}$)	1.30 - 1.00

Figure 4.4: Typical chemical shifts observed for the *N*-{6-(ferrocenyl) ethynyl-2-naphthoyl} amino acid and dipeptide esters **120**-**128**.

4.5.2.1 ^{1}H NMR spectroscopic studies of *N*-{6-(ferrocenyl) ethynyl-2-naphthoyl} glycine glycine ethyl ester 120

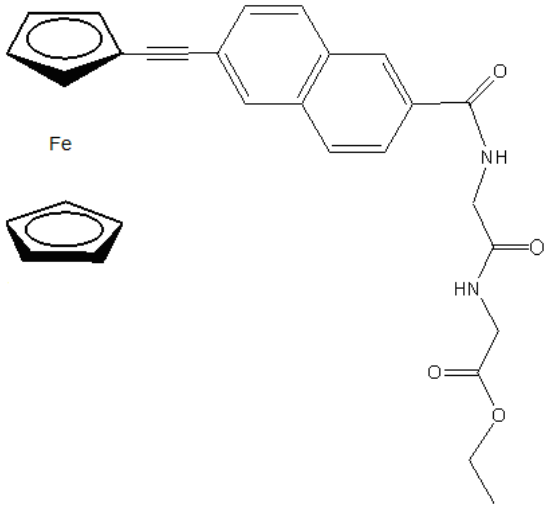

120

The ^{1}H NMR spectrum of compound **120** is shown in figure 4.5. The six protons on the naphthoyl spacer group overlap with the amide protons resulting in a multiplet between δ 8.13 and δ 7.48 with an overall integration of eight. The *ortho* and *meta* protons (η^5-$C_5\underline{H}_4$-C≡C-) on the cyclopentadiene ring attached to the -C≡C- spacer moiety are observed as apparent triplet signals at δ 4.61 and δ 4.30. The protons on the unsubstituted (η^5-C_5H_5) ring overlap with the signals of the methylene groups of (-NH$\underline{CH_2}$CO-), (-O$\underline{CH_2}CH_3$) resulting in a multiplet appearing between δ 4.19 - 4.15 with an overall integration of eleven. The methyl group of the ethyl ester (-OCH$_2\underline{CH_3}$) is present as a triplet at δ 1.23.

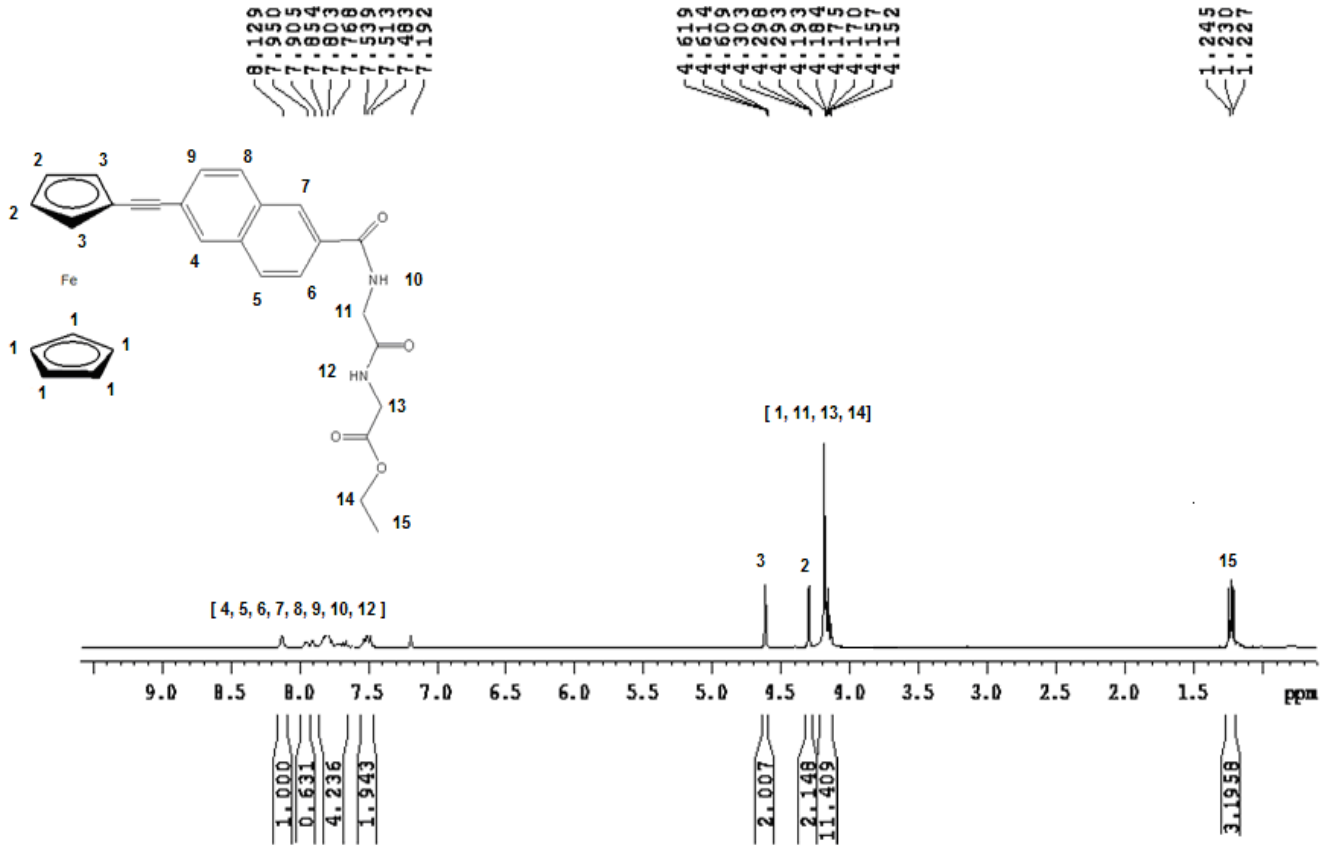

Figure 4.5: ^{1}H NMR spectrum of *N*-{6-(ferrocenyl) ethynyl-2-naphthoyl} glycine glycine ethyl ester **120.**

4.5.3 ^{1}H NMR spectroscopic studies of *N*-{5-(ferrocenyl) ethynyl-2-furanoyl} amino acid and dipeptide esters

In $CDCl_3$, the typical chemical shifts observed for the *N*-{5-(ferrocenyl) ethynyl-2-furanoyl} dipeptide esters include the overlap the signals of amide protons and the aromatic hydrogens of the furanoyl ring spacer group which appear between δ 7.35 and δ 6.50 (figure 4.6). However, for the Sar Gly derivative (**134**), the two aromatic protons on the furanoyl linker appear as two doublets and do not overlap with the amide protons. The splitting pattern of the furanoyl linker for this derivative follows the n+1 splitting pattern which is not observed with the benzoyl and naphthoyl linkers. For the ferrocene moiety, the expected three splitting pattern signals between δ 4.60 and δ 4.10 are usually not seen. These signals usually overlap with the hydrogen signals of either the methylene groups or methine groups that may be present in the *N*-{5-(ferrocenyl) ethynyl-2-furanoyl} amino acid and dipeptide esters.

For the Gly L-Phe derivative (**132**)**,** the *ortho* protons (η^5-$C_5\underline{H}_4$-C≡C-) on the cyclopentadiene ring attached to the -C≡C- spacer moiety is observed as an apparent singlet, whilst the *meta* protons overlap with the protons on the unsubstituted (η^5-C_5H_5). This results in a multiplet with an overall integration of seven. The apparent singlet for the *ortho* protons (η^5-$C_5\underline{H}_4$-C≡C-) follows the second order splitting pattern as described in section 2.5. The methyl protons (-$OCH_2\underline{CH}_3$) of the ethyl ester in this derivative appear between δ 1.30 and δ 1.19. Due to the overlapping of signals, other spectroscopic techniques were used to provide a more complete picture of the molecular structure of these derivatives as described in section 4.5.2

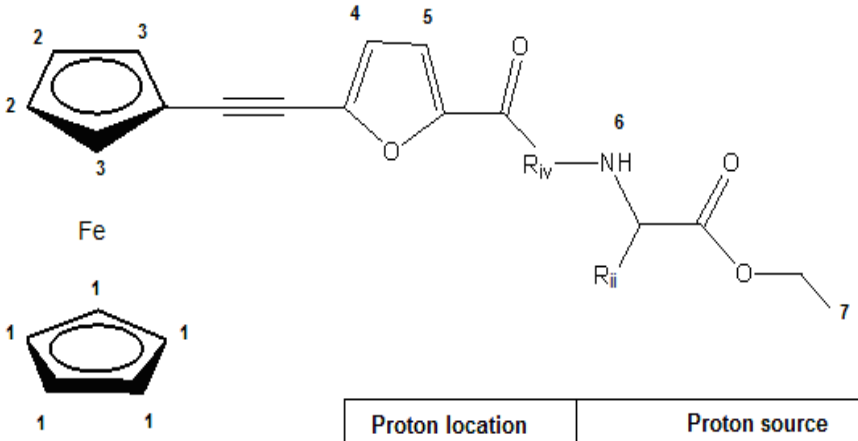

Proton location	Proton source	δ ($CDCl_3$)
1, 2, 3	(η^5-C_5H_4-C≡C-), (η^5-C_5H_5)	4.60 - 4.10
4, 5, 6	Aromatic H, NH	7.35 - 6.50
7	(-OCH_2CH_3)	1.30 - 1.19

Figure 4.6: Typical chemical shifts observed for the *N*-{5-(ferrocenyl) ethynyl-2-furanoyl} amino acid and dipeptide esters **129-138**.

4.5.3.2 ^{1}H NMR spectroscopic studies of *N*-{5-(ferrocenyl) ethynyl-2-furanoyl} L-proline glycine ethyl ester 135

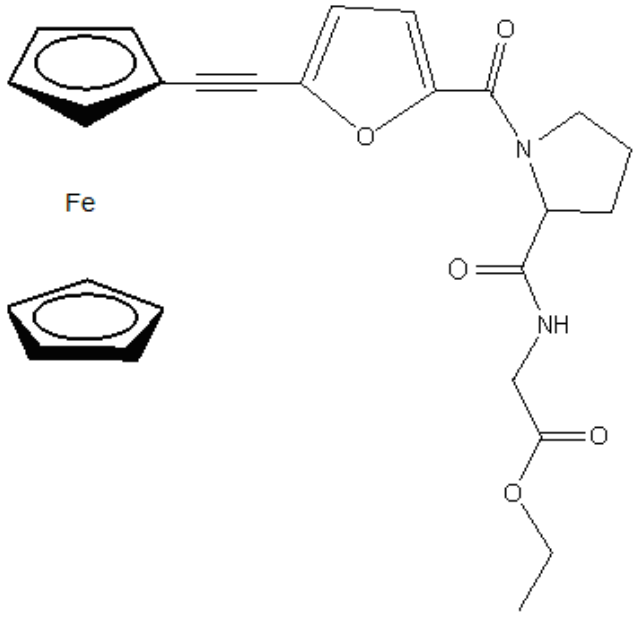

135

The ^{1}H NMR spectrum of compound **135** is shown in figure 4.7. The amide proton appears at δ 7.34 as a triplet with coupling constants of 5.2 Hz. The aromatic region confirms the presence of two protons which are present as two doublets at δ 7.10 and δ 6.56. The methine proton (-N($CH_2CH_2CH_2$)C<u>H</u>CO-) on the proline moiety is present as a broad peak at δ 4.80 - 4.78. The *ortho* protons (η^5-C_5<u>H</u>$_4$-C≡C-) on the cyclopentadiene ring appear as an apparent singlet at δ 4.47, whilst the *meta* protons (η^5-C_5<u>H</u>$_4$-C≡C-) overlap with the protons on the unsubstituted (η^5-C_5H_5) ring, methylene protons of (-O<u>CH_2</u>CH_3), (-NH<u>CH_2</u>CO-) and (-N(<u>CH_2</u>CH_2CH_2)CHCO-) resulting in a multiplet between δ 4.14 - 3.95 which has an overall integration of thirteen. The remaining two methylene protons signals (-N(CH_2<u>CH_2</u><u>CH_2</u>)CHCO-) overlap with each other, resulting in a multiplet being observed between δ 2.36 - 1.88 which has an overall integration of four. The methyl group of the ethyl ester (-OCH_2<u>CH_3</u>) appears as a triplet at δ 1.23 with a coupling constant of 6.4 Hz.

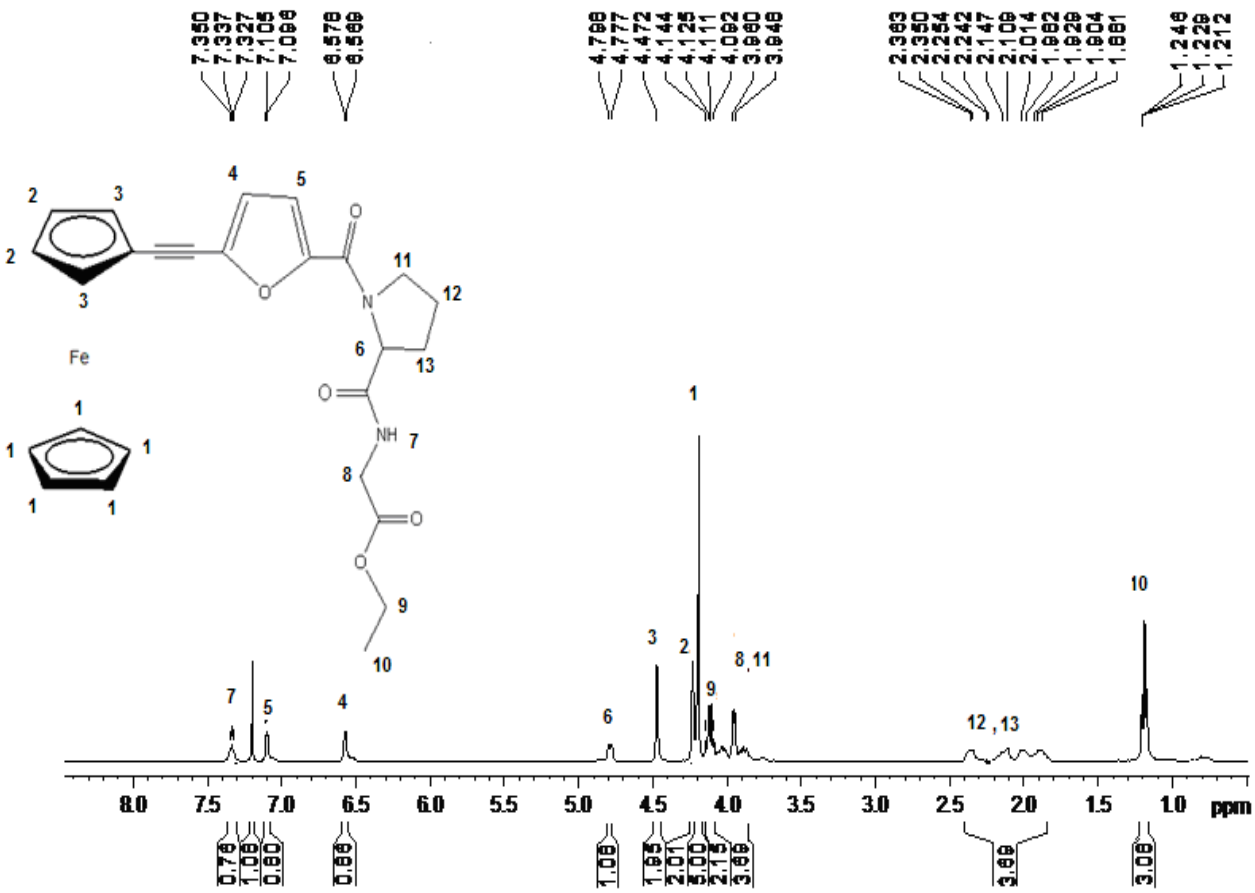

Figure 4.7: ^{1}H NMR spectrum of *N*-{5-(ferrocenyl) ethynyl-2-furanoyl} L-proline glycine ethyl ester **135.**

4.6 H^1-H^1 COSY spectroscopic studies of *N*-{*para*-(ferrocenyl) ethynyl benzoyl}, *N*-{6-(ferrocenyl) ethynyl-2-naphthoyl} and *N*-{5-(ferrocenyl) ethynyl-2-furanoyl} amino acid and dipeptide esters

In the H^1-H^1 COSY spectra of *N*-{*para*-(ferrocenyl) ethynyl benzoyl}, *N*-{6-(ferrocenyl) ethynyl-2-naphthoyl} and *N*-{5-(ferrocenyl) ethynyl-2-furanoyl} amino acid and dipeptide esters, the typical protons that correlate include:

(i) Correlation between the aromatic protons.
(ii) Correlation between the amide protons and adjacent methylene protons
(iii) Correlation between the *ortho* protons and *meta* protons on the cyclopentadiene ring attached to the -C≡C- spacer moiety.

The correlations observed for the ethynyl derivatives is consistent with previously reported correlations for the *N*-(ferrocenyl) benzoyl dipeptide derivatives for the Gly Gly, Gly L-Ala, Gly L-Leu and Gly L-Phe dipeptide ethyl esters derivatives.[4-8]

In the H^1-H^1 COSY spectrum (figure 4.8) of *N*-{5-(ferrocenyl) ethynyl-2-furanoyl} glycine glycine ethyl ester **129** the two amide protons 6 and 8 (-$\underline{NH}CH_2CO$-) correlate with the adjacent methylene protons 7 and 9 (-$NH\underline{CH_2}CO$-) of the glycine glycine ethyl ester. Correlation is also present between the protons of the furanoyl spacer, 4 and 5. The *ortho* protons 3 and *meta* protons 2 on the cyclopentadiene ring attached to the -C≡C- spacer moiety correlate. The methylene of the ethyl ester (-$O\underline{CH_2}CH_3$) 10 correlate to the methyl protons (-$OCH_2\underline{CH_3}$) 11.

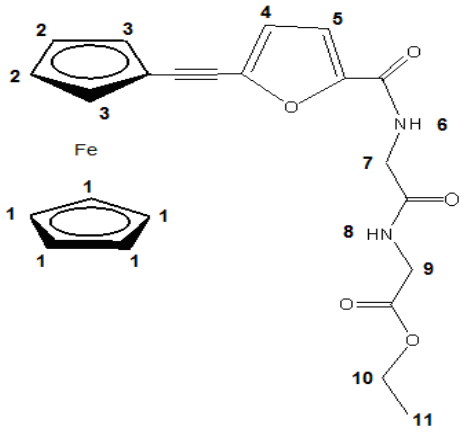

129

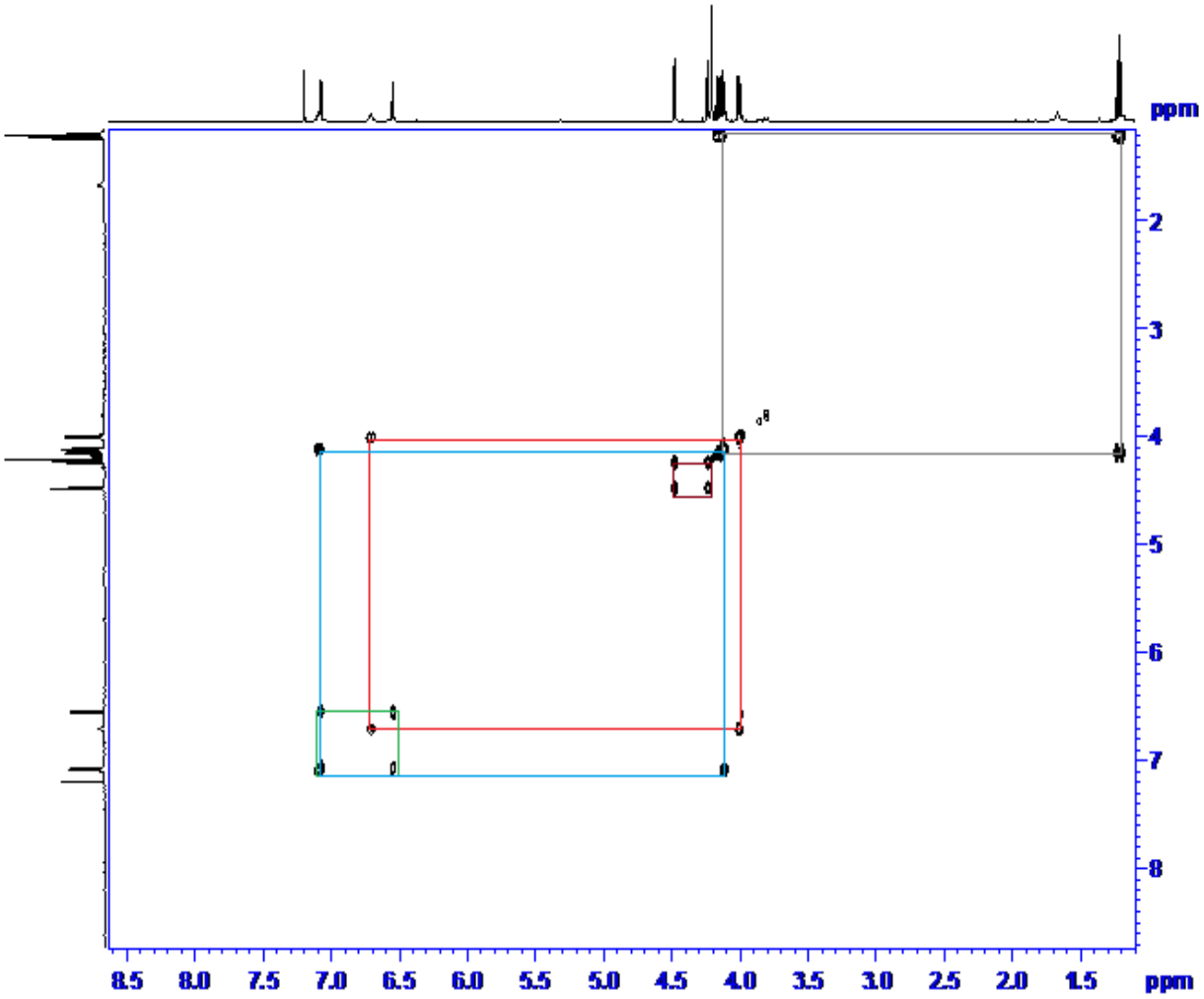

Figure 4.8: H^1-H^1 COSY spectrum of *N*-{5-(ferrocenyl) ethynyl-2-furanoyl} glycine glycine ethyl ester **129.**

4.7. ^{13}C NMR and DEPT-135 spectroscopic studies of *N*-{*para*-(ferrocenyl) ethynyl benzoyl}, *N*-{6-(ferrocenyl) ethynyl-2-naphthoyl} and *N*-{5-(ferrocenyl) ethynyl-2-furanoyl} amino acid and dipeptide esters

4.7.1 ^{13}C NMR and DEPT-135 spectroscopic studies of *N*-{*para*-(ferrocenyl) ethynyl benzoyl} amino acid and dipeptide esters

In the ^{13}C NMR spectra of *N*-{*para*-(ferrocenyl) ethynyl benzoyl} amino acid and dipeptide esters **105-119**, the typical peaks observed include the appearance of carbonyl signals between δ 175.0 - 160.0 (figure 4.9). In the amino acid derivatives only two carbonyl signals are observed whilst for the dipeptide derivatives three carbonyl signals are observed. These carbon signals are absent in the DEPT-135 spectrum. In the aromatic region of the spectrum four unique carbons signals are observed between δ 140.0 - 120.0. The two quaternary carbon atoms present on the benzoyl spacer moiety can be easily identified by their absence in the DEPT-135 spectrum and these signals appear more downfield than the other aromatic carbons, usually between δ 145-135. The carbons on the -C≡C- linker appear between δ 96.0 - 90.0 for (η^5-C_5H_4-C≡$\underline{C}$-) and between δ 87.0 - 84.0 for (η^5-C_5H_4-$\underline{C}$≡C-). These two quaternary carbons can be easily identified by their absence in the DEPT-135 spectrum.

The *ipso* carbon on the cyclopentadiene ring (η^5-$\underline{C}_5H_4$-C≡C-) attached to the -C≡C- appears between δ 68.0 – 64.0 and is absent in the DEPT-135 spectrum. The remaining three unique carbons on the monosubstituted cyclopentadiene rings appear between δ 72.0 - 66.0. The *ortho* carbons on (η^5-$\underline{C}_5H_4$-C≡C-) attached to the *ipso* carbons, appear more downfield than the *meta* carbons (η^5-$\underline{C}_5H_4$-C≡C-) on the substituted cyclopentadiene ring and the unsubstituted ring carbon signal. This indicates that these carbons have become deshielded by the ethynyl moiety attached to the cyclopentadiene rings. The five carbon atoms on the unsubstituted ring give rise to one unique carbon signal because the carbons are equivalent. The methylene carbon of the ethyl ester (-O$\underline{CH_2}CH_3$) appear between δ 64.0 - 60.0 whilst the methyl carbon appears at δ 15.0 - 13.0. In the DEPT-135 spectra methylene carbons appear as a negative resonance.

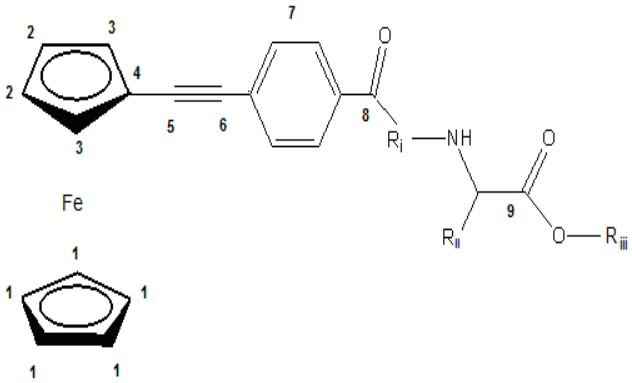

Carbon Location	Carbon source	δ, ($CDCl_3$)
1	η^5-$\underline{C}_5H_5$	70.5 - 68.0
2	η^5-$\underline{C}_5H_4$ – C≡C–	70.5 - 68.0
3	η^5-$\underline{C}_5H_4$ – C≡C–	72.0 - 70.5
4	ipso (η^5-$\underline{C}_5H_4$– C≡C–)	68.0 - 64.0
5	η^5-C_5H_4 – $\underline{C}$≡C–	87.0 - 84.0
6	η^5-C_5H_4 – C≡$\underline{C}$–	96.0 - 90.0
7	Aromatic carbons	140.0 - 120.0
8, 9	C=O	175.0 - 160.0
R_{iii}	-O$\underline{C}H_3$	52.0 - 47.0
R_{iii}	-O$\underline{C}H_2CH_3$	64.0 - 60.0
R_{iii}	-OCH$_2\underline{C}H_3$	15.0 - 13.0

Figure 4.9: Typical chemical shifts observed for the *N*-{*para*-(ferrocenyl) ethynyl benzoyl} amino acid and dipeptide esters **105-119**.

4.7.1.1 ^{13}C NMR and DEPT-135 spectroscopic studies of *N*-{*para*-(ferrocenyl) ethynyl benzoyl} γ-amino butyric acid methyl ester 111

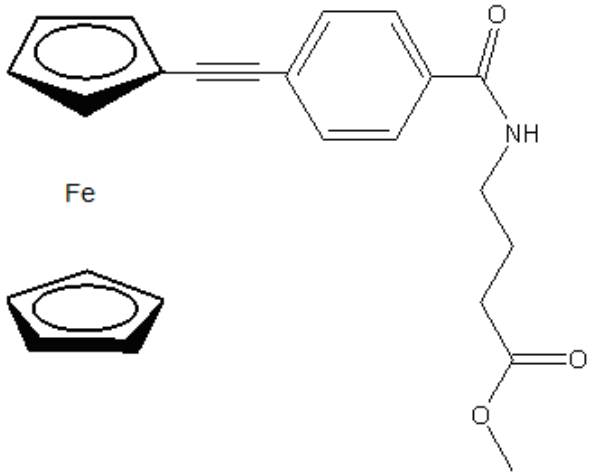

111

The ^{13}C NMR spectrum of *N*-{*para*-(ferrocenyl) ethynyl benzoyl} γ-aminobutyric acid methyl ester displays two carbonyl carbon atoms at δ 174.4 and δ 166.9. These are absent in the DEPT-135 spectrum. The aromatic region shows 4 unique signals between δ 133.0 and δ 126.9. The two quaternary carbon atoms from the benzoyl spacer moiety at δ 133.0 and δ 131.4 can be easily identified by their absence in the DEPT-135 spectrum. The carbon atoms on the -C≡C- linker appear at δ 91.0 for (η^5-C_5H_4-C≡$\underline{C}$-) and at δ 85.1 for (η^5-C_5H_4-$\underline{C}$≡C-). The *ipso* ferrocenyl carbon atom (η^5-$\underline{C}_5H_4$-C≡C-) appears at δ 64.6 and is not present in the DEPT-135 spectrum. The remaining carbon atoms on the cyclopentadiene rings (η^5-$\underline{C}_5H_4$-C≡C-) and (η^5-$\underline{C}_5H_5$) are present between δ 71.6 - 69.1. The methyl carbon atom of the methyl ester (-O$\underline{C}H_3$) appears at δ 51.9. The three methylene carbon atoms (-NH$\underline{C}H_2\underline{C}H_2\underline{C}H_2$-) of the γ-aminobutyric acid appear at δ 39.8, δ 31.8 and δ 24.3 and display negative resonance peaks in the DEPT-135 spectrum.

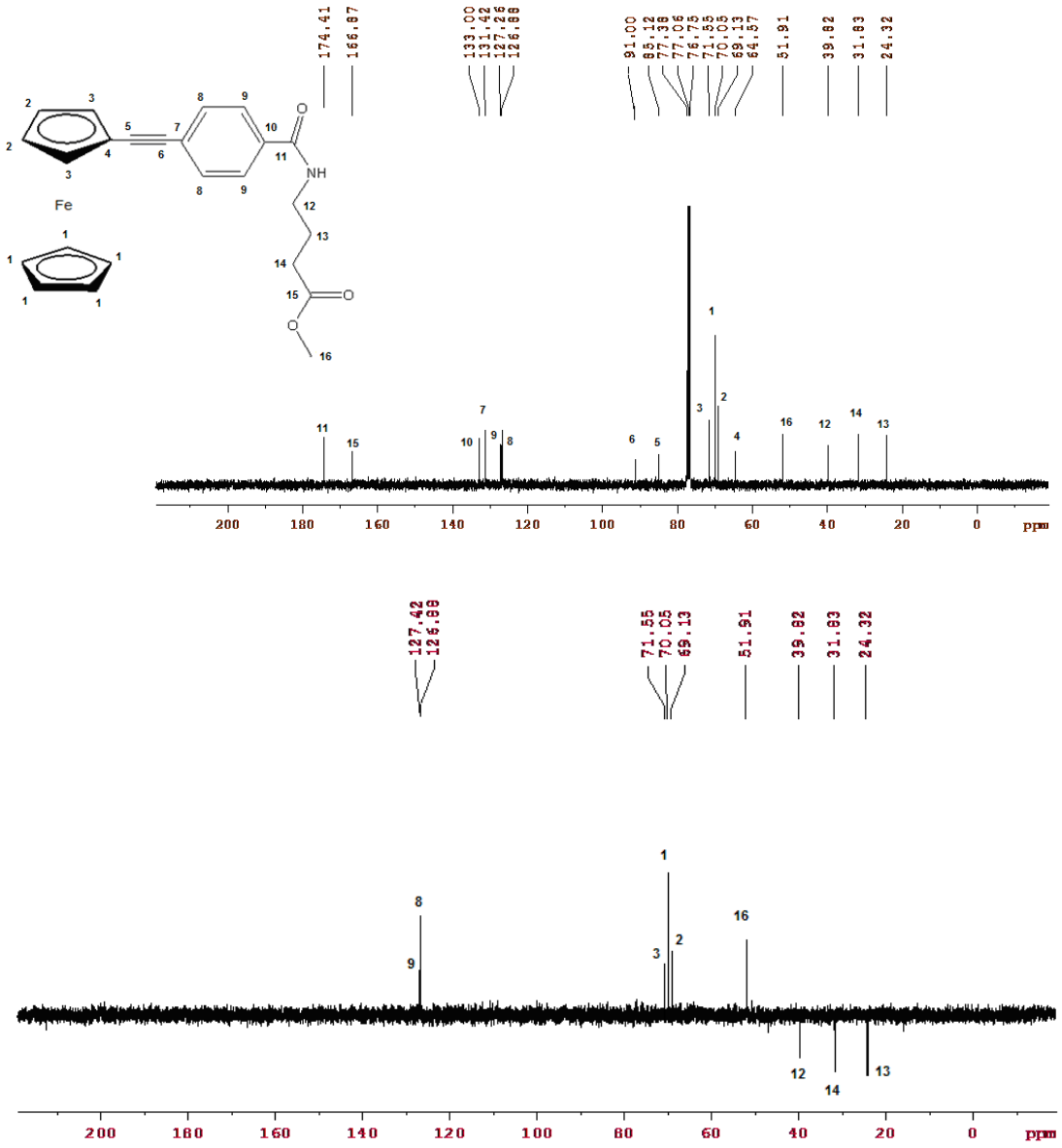

Figure 4.10: ^{13}C NMR and DEPT-135 spectra of *N*-{para-(*ferrocenyl*) ethynyl benzoyl} γ-aminobutyric acid methyl ester **111.**

4.7.2 ^{13}C NMR and DEPT-135 spectroscopic studies of *N*-{6-(ferrocenyl) ethynyl-2-naphthoyl} amino acid and dipeptide esters

In the ^{13}C NMR spectra of *N*-{*para*-(ferrocenyl) ethynyl-2-naphthoyl} amino acid and dipeptide esters, the typical peaks observed include the appearance of carbonyl signals between δ 175.0 - 160.0 (figure 4.11). In the amino acid derivatives only two carbonyl signals are observed whilst for the dipeptide derivatives three carbonyl signals are observed. In the aromatic region of the spectrum of these derivatives, ten unique carbon signals are observed which appear between δ 140.0 - 120.0. The two quaternary carbon atoms present on the naphthoyl moiety can be easily identified by their absence in the DEPT-135 spectrum.

The two quaternary carbons on the -C≡C- linker appear between δ 92.0 - 89.0 for (η^5-C_5H_4-C≡$\underline{C}$-) and between δ 86.0 - δ 84.0 for (η^5-C_5H_4-$\underline{C}$≡C-), can be easily identified by their absence in the DEPT-135 spectrum. The *ipso* carbon on the cyclopentadiene ring (η^5-$\underline{C}_5H_4$-C≡C-) attached to the -C≡C- appears between δ 68.0 - 63.0 whilst the other carbons on the cyclopentadiene rings (η^5-$\underline{C}_5H_4$-C≡C-) and (η^5-$\underline{C}_5H_5$) appear between δ 72.5 - 68.0 with the *ortho* carbons (η^5-$\underline{C}_5H_4$-C≡C-) appearing more downfield than all the carbon atoms present on the cyclopentadiene rings. The *ipso* carbon is easily identified by its absence in the DEPT-135 spectrum. The methylene carbons of the ethyl ester (-O$\underline{CH_2}CH_3$) appear between δ 62.0 - 60.0 whilst the methyl carbon appears between δ 16.0 - 13.0. In the DEPT-135 spectra methylene carbons appear as a negative resonance.

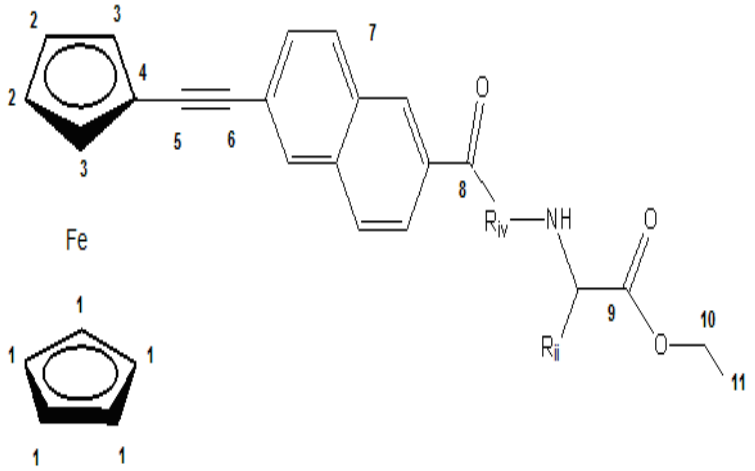

Carbon Location	Carbon source	δ, ($CDCl_3$)
1	η^5-$\underline{C}_5H_5$	70.5 - 68.0
2	η^5-$\underline{C}_5H_4$ -C≡C-	70.5 - 68.0
3	η^5-$\underline{C}_5H_4$ -C≡C-	72.5 - 70.5
4	ipso (η^5-$\underline{C}_5H_4$-C≡C-)	68.0 - 63.0
5	η^5-C_5H_4 -$\underline{C}$≡C-	86.0 - 84.0
6	η^5-C_5H_4 -C≡$\underline{C}$-	92.0 - 89.0
7	Aromatic carbons	140.0 - 120.0
8, 9	C=O	175.0 - 160.0
10	-O$\underline{CH}_2CH_3$	62.0 - 60.0
11	-OCH$_2\underline{CH}_3$	16.0 - 13.0

Figure 4.11: Typical chemical shifts observed for the *N*-{6-(ferrocenyl) ethynyl-2-naphthoyl} amino acid and dipeptide esters **120-128.**

4.7.2.1 ^{13}C NMR and DEPT-135 spectroscopic studies of *N*-{6-(ferrocenyl) ethynyl-2-naphthoyl} glycine L-leucine ethyl ester 126

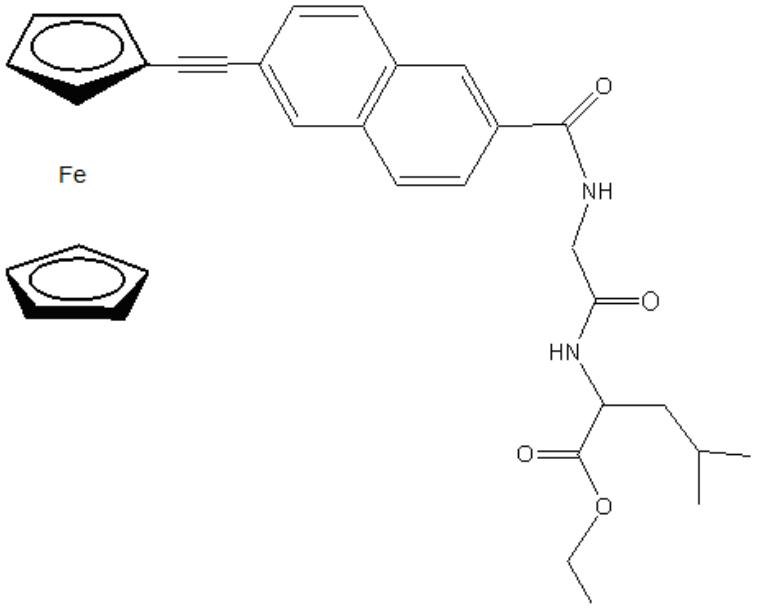

126

The ^{13}C NMR spectrum of *N*-{6-(ferrocenyl) ethynyl-2-naphthoyl} glycine L-leucine ethyl ester displays three carbonyl carbon atoms between δ 172.9 and δ 167.8. These are absent in the DEPT-135 spectrum. The aromatic region shows 10 unique carbon signals between δ 135.0 and δ 120.8. The four quaternary carbon atoms from the naphthoyl spacer moiety at δ 134.8, δ 133.1, δ 130.7 and δ 130.2 can be easily identified by their absence in the DEPT-135 spectrum. The carbon atoms on the -C≡C- linker appear a δ 90.1 for (η^5-C_5H_4-C≡$\underline{C}$-) and at δ 85.6 for (η^5-C_5H_4-$\underline{C}$≡C-). The *ipso* ferrocenyl carbon atom (η^5-$\underline{C}_5H_4$-C≡C-) appears at δ 67.3 and is not present in the DEPT 135 spectrum. The remaining carbon atoms on the cyclopentadiene rings (η^5-$\underline{C}_5H_4$-C≡C-) and (η^5-$\underline{C}_5H_5$) are present between δ 71.1 -69.7. The methylene carbon atom of the ethyl ester (-O$\underline{CH_2}CH_3$) is observed at δ 61.4, whilst the methyl carbon atom appears at δ 14.2. The two methylene carbon atoms from (-NH$\underline{CH_2}$CO-) and {-$\underline{CH_2}$CH$(CH_3)_2$} of the glycine L leucine ethyl ester are observed at δ 43.8 and δ 41.2. The two methine carbon atoms from (-NH$\underline{CH}$CO-) and {-$CH_2\underline{CH}(CH_3)_2$} of the glycine L leucine ethyl ester appear at δ 51.2 and δ 24.9 respectively. The two methyl carbon atoms (-$CH_2CH(\underline{CH_3})_2$) of the glycine L-leucine ethyl ester appear at δ 22.9 and δ 21.9.

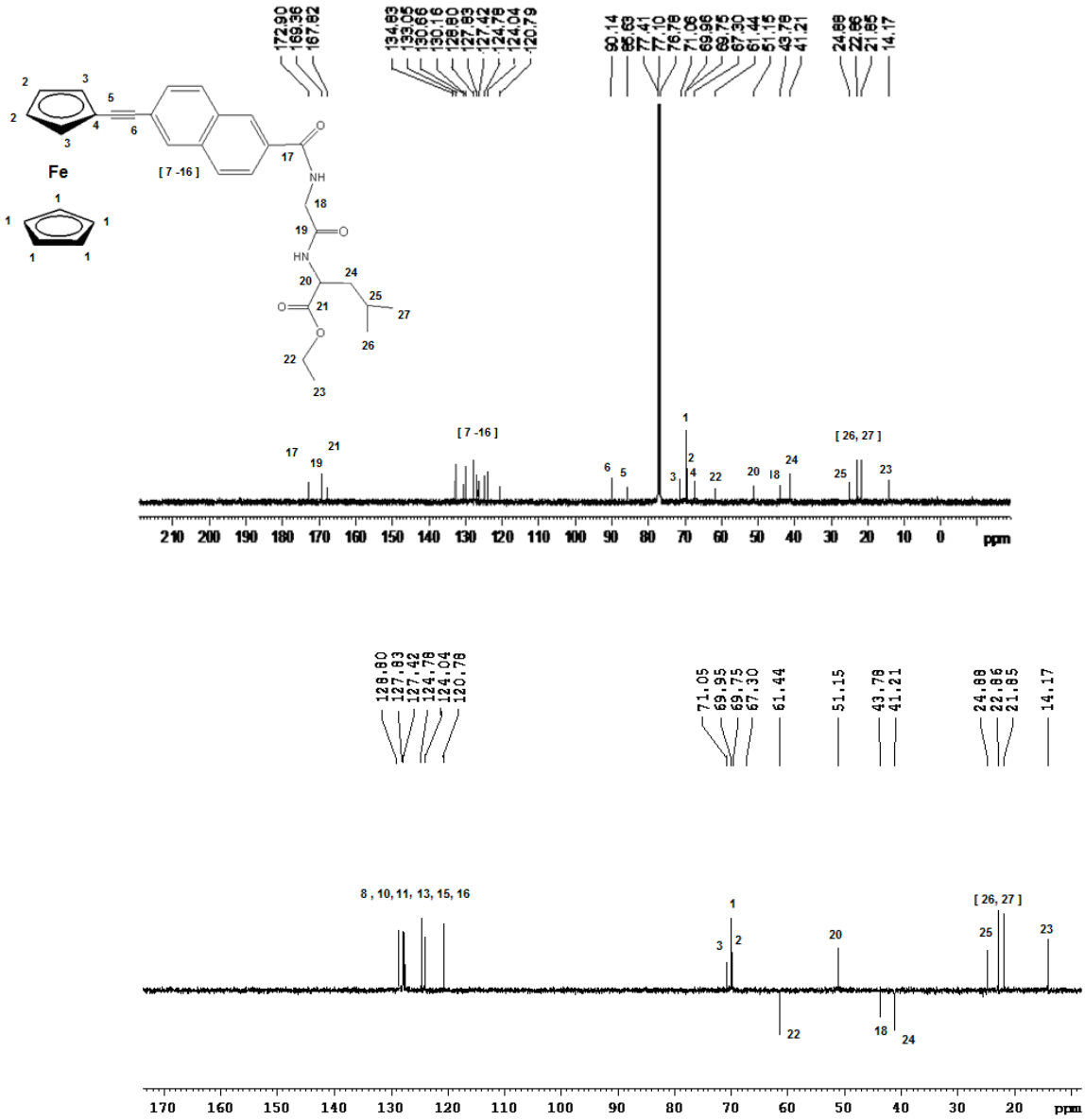

Figure 4.12: ^{13}C NMR and DEPT-135 spectra of *N*-{6-(ferrocenyl) ethynyl-2-naphthoyl} glycine L-leucine ethyl ester **126.**

4.7.3 ^{13}C NMR and DEPT-135 spectroscopic studies of the *N*-{5-(ferrocenyl) ethynyl-2-furanoyl} amino acid and dipeptide esters

In the ^{13}C NMR spectra of *N*-{5-(ferrocenyl) ethynyl-2-furanoyl} amino acid and dipeptide esters, the typical peaks observed include the appearance of carbonyl signals between δ 175.0 - 155.0 which are absent in the DEPT-135 spectrum. In the amino acid derivatives only two carbonyl signals are observed, whilst for the dipeptide derivatives three carbonyl signals are observed. In the aromatic region of the spectrum four unique carbons signals are observed and these signals appear between δ 147.0 - 115.0. The two quaternary carbon atoms present on the furanoyl moiety can be easily identified by their absence in the DEPT-135 spectrum. The carbons on the -C≡C- linker appear between δ 95.0 - 90.0 for (η^5-C_5H_4-C≡$\underline{C}$-) and between δ 76.0 - 73.0 for (η^5-C_5H_4-$\underline{C}$≡C-). The *ipso* carbon on the cyclopentadiene ring (η^5-$\underline{C}_5H_4$-C≡C-) attached to the -C≡C- appears between δ 68.0 - 62.0, whilst the other carbons on the cyclopentadiene rings (η^5-$\underline{C}_5H_4$-C≡C-) and (η^5-$\underline{C}_5H_5$) appear between δ 72.0 – 68.0. The *ipso* carbon (η^5-C_5H_4-C≡$\underline{C}$-) and the two quaternary carbons on the -C≡C- linker can be easily identified by their absence in the DEPT-135 spectrum. The methylene carbon of the ethyl ester (-O$\underline{CH_2}CH_3$) appears between δ 62.0 - 60.0, whilst the methyl carbon appears between δ 15.0 - 13.0. The methylene carbon appears more downfield than the methyl group due to the deshielding effect experienced by the methylene carbon attached to the oxygen atom.

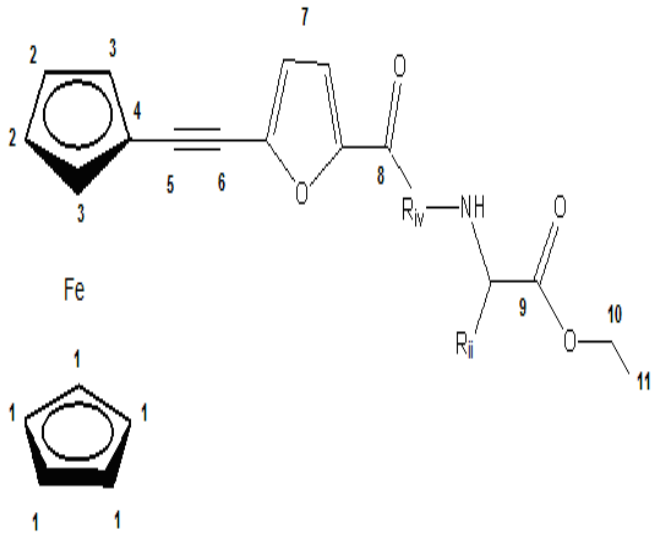

Carbon Location	Carbon source	δ, ($CDCl_3$)
1	η^5-$\underline{C}_5H_5$	70.5 - 68.0
2	η^5-$\underline{C}_5H_4$ - C≡C-	70.5 - 68.0
3	η^5-$\underline{C}_5H_4$ - C≡C-	72.0 - 70.5
4	ipso (η^5-$\underline{C}_5H_4$ - C≡C-)	68.0 - 62.0
5	η^5-C_5H_4 - $\underline{C}$≡C-	76.0 - 73.0
6	η^5-C_5H_4 - C≡$\underline{C}$-	95.0 - 90.0
7	Aromatic carbons	147.0 - 115.0
8, 9	C=O	175.0 - 155.0
10	-O$\underline{CH}_2CH_3$	62.0 - 60.0
11	-$OCH_2\underline{CH}_3$	15.0 - 13.0

Figure 4.13: Typical chemical shifts observed for the *N*-{5-(ferrocenyl) ethynyl-2-furanoyl} amino acid and dipeptide esters **129-138.**

4.7.3.1 ^{13}C NMR and DEPT-135 spectroscopic studies of *N*-{5-(ferrocenyl) ethynyl-2-furanoyl} L-proline L-alanine ethyl ester 136

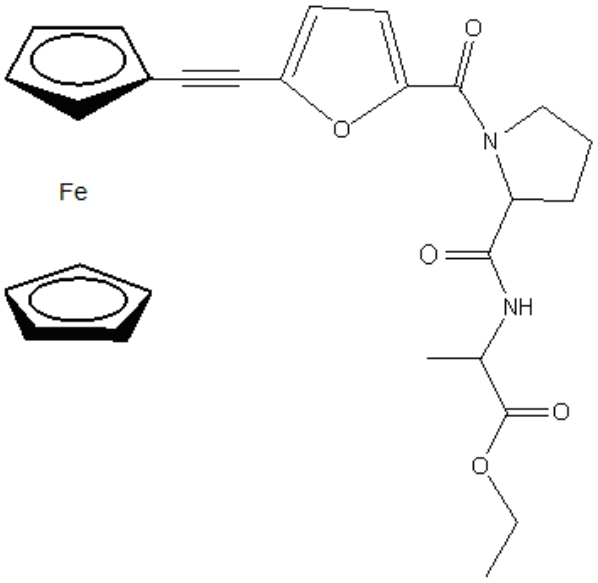

136

The ^{13}C NMR spectrum of *N*-{5-(ferrocenyl) ethynyl-2-furanoyl} L-proline L-alanine ethyl ester displays three carbonyl carbon signals between δ 173.4 and δ 158.5. These are absent in the DEPT-135 spectrum. The aromatic region shows 4 unique carbon atoms present between δ 147.4 and δ 115.7. The two quaternary carbon atoms from the furanoyl spacer moiety at δ 147.4 and δ 140.9 can be easily identified by their absence in the DEPT-135 spectrum. The carbon atoms on the -C≡C- linker appear at δ 94.2 for (η^5-C_5H_4-C≡$\underline{C}$-) and at δ 75.7 for (η^5-C_5H_4-$\underline{C}$≡C-). The *ipso* ferrocenyl carbon atom (η^5-$\underline{C}_5H_4$-C≡C-) appears at δ 63.0 and is not present in the DEPT-135 spectrum. The remaining carbon atoms on the cyclopentadiene rings (η^5-$\underline{C}_5H_4$-C≡C-) and (η^5-$\underline{C}_5H_5$) are present between δ 71.7 - 69.5. The methylene carbon atom of the ethyl ester (-O$\underline{C}H_2CH_3$) appears at δ 61.4 whilst the methyl carbon atom appears at δ 14.2. The methine carbon atoms on the proline moiety (-N($CH_2CH_2CH_2$)$\underline{C}$HCO-) and ($\underline{C}HCH_3$) on the alanine moiety appear at δ 49.8 and δ 46.3 respectively. The three methylene carbon atoms (-N($\underline{CH_2CH_2CH_2}$)CHCO-) of proline moiety are observed at δ 48.7, δ 27.7 and δ 25.5. In the DEPT-135 spectrum the three peaks appear as negative resonances. The methyl carbon (CH$\underline{C}H_3$) on the alanine moiety is observed at δ 18.5.

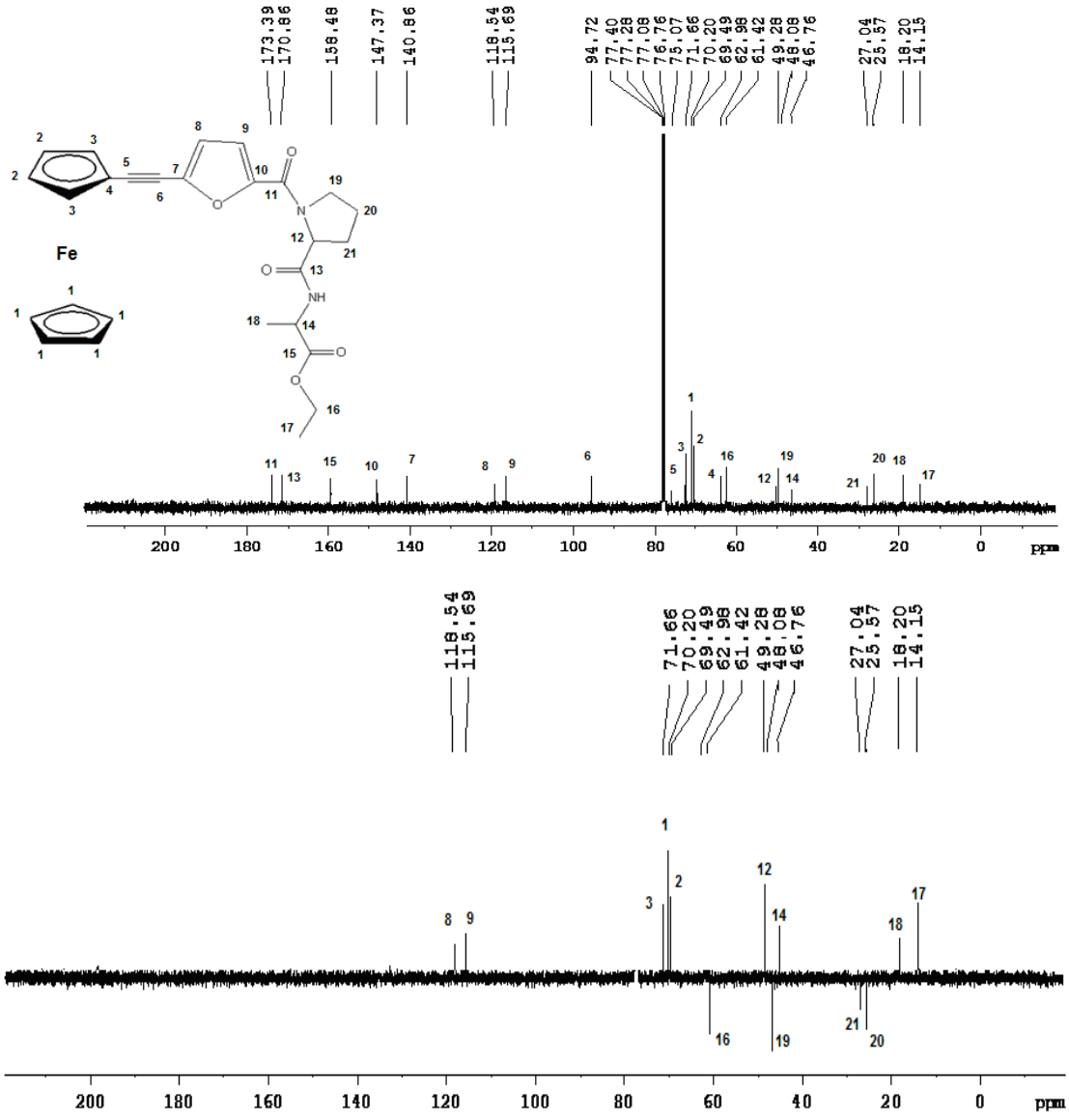

Figure 4.14: ^{13}C NMR and DEPT-135 spectra studies of *N*-{5-(ferrocenyl) ethynyl-2-furanoyl} L-proline L-alanine ethyl ester **136.**

4.8 HMQC spectroscopic studies of *N*-{*para*-(ferrocenyl) ethynyl benzoyl}, *N*-{6-(ferrocenyl) ethynyl-2-naphthoyl} and *N*-{5-(ferrocenyl) ethynyl-2-furanoyl} amino acid and dipeptide esters

In the HMQC spectra of the *N*-{*para*-(ferrocenyl) ethynyl benzoyl}, *N*-{6-(ferrocenyl) ethynyl-2-naphthoyl} and *N*-{5-(ferrocenyl) ethynyl-2-furanoyl} amino acid and dipeptide esters, the typical carbon to proton that correlate include (i) correlation between the aromatic carbon and protons, (ii) correlation between methylene carbon and protons and (iii) correlation between the carbon and protons on the cyclopentadiene rings The correlations observed for the ethynyl derivatives are consistent with previously reported correlations for the *N*-(ferrocenyl) benzoyl dipeptide derivatives for the Gly Gly, Gly L-Ala, Gly L-Leu and Gly L-Phe dipeptide ethyl esters derivatives.[4-8]

In the HMQC spectrum (figure 4.15) of *N*-{*para*-(ferrocenyl) ethynyl benzoyl} glycine D-alanine ethyl ester **110** the following C-H correlations were observed:

(i) Cyclopentadiene ring C-H correlations for (η^5-$\underline{C}_5\underline{H}_5$) and ($\eta^5$-$\underline{C}_5H_4$-C≡C-)

(ii) Aromatic C-H correlations

(iii) C-H correlations of methylene groups and C-H correlations of the ethyl groups on the ethyl ester

(iv) C-H correlation of methylene groups on the glycine L-alanine moiety

The positions of the C-H correlation are listed in (table 4.1). The C-H correlations are consistent to those observed for the *N*-{*para*-(ferrocenyl) benzoyl} glycine glycine ethyl ester.[4]

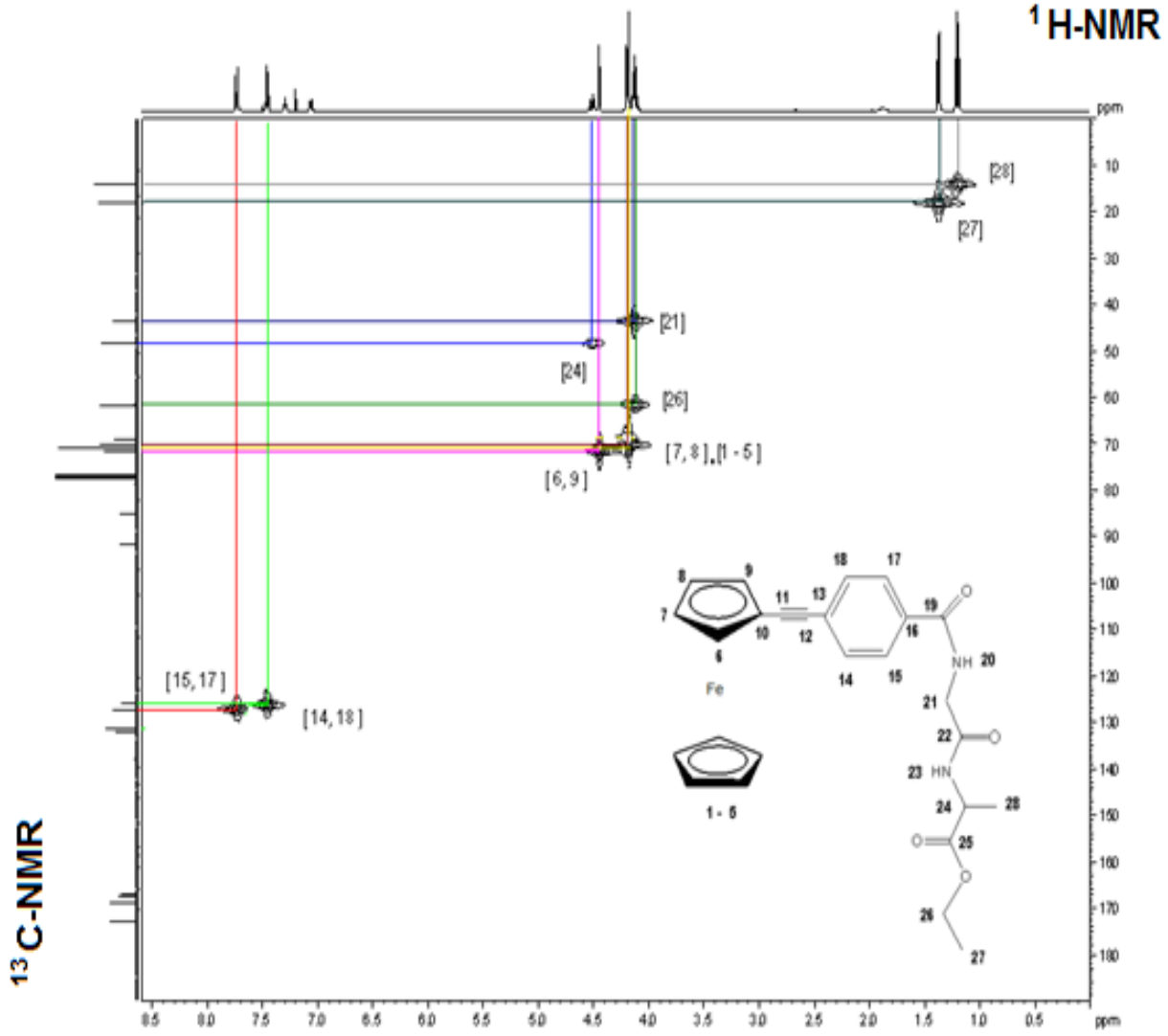

Figure 4.15: HMQC spectrum of *N*-{*para*-(ferrocenyl) ethynyl benzoyl} glycine D-alanine ethyl ester **110.**

Table 4.1: C-H correlation data from HMQC spectrum of *N*-{*para*-(ferrocenyl) ethynyl benzoyl} glycine D-alanine ethyl ester **110.**

Site	^{1}H NMR	^{13}C NMR
(1-5)*	4.20 – 4.18	70.0
(6 and 9)*	4.42	71.6
(7 and 8)*	4.20 – 4.18	69.1
10		68.5
11		85.1
12		91.6
13		131.4
(14 and 18)*	7.45	126.5
(15 and 17)*	7.72	127.7
16		
19		172.7
20	7.30	
21*	4.15 – 4.10	43.5
22		168.7
23	7.05	
24*	4.53	48.4
25		167.1
26*	4.15 – 4.10	61.6
27*	1.20	18.2
28*	1.37	14.1

***C-H correlation site**

4.9 UV-Vis spectroscopic studies of *N*-{*para*-(ferrocenyl) ethynyl benzoyl}, *N*-{6-(ferrocenyl) ethynyl-2-naphthoyl} and *N*-{5-(ferrocenyl) ethynyl-2-furanoyl} amino acid and dipeptide esters

All the UV-Vis spectra were obtained at a concentration of 4 x 10^{-4} M in ethanol. In the UV spectra of the *N*-{*para*-(ferrocenyl) ethynyl benzoyl}, *N*-{6-(ferrocenyl) ethynyl-2-naphthoyl} and *N*-{5-(ferrocenyl) ethynyl-2-furanoyl} amino acid and dipeptide esters **105-138**, metal to ligand charge transfer (MLCT) band transitions arising from the ferrocene moiety are observed at low energy bands between 430 to 560 nm, with distinct λ_{max} values. The high energy band between 340 and 450 nm, with distinct λ_{max} values are due to the π - π^* transitions of aromatic linker (table 2.3). The presence of the π - π^* transitions and the MLCT band transitions are constistent to those seen in the alkyl derivatives (section 2.9) and the previously reported *N*-(ferrocenyl) benzoyl and naphthoyl derivatives.[1-8]

In the literature it is know that the presences of a ethynyl moiety on a ferrocene moiety causes the λ_{max} of ferrocene to shift toward the red region as a result of extendend conjugation.[7]

In the UV-Vis spectra of the synthesised compounds **105-138**, all the derivatives cause the ferrocene moiety to undergo a red shift to lower energies due to the presence of both ethynyl moiety and the aromatic linkers. The ethynyl naphthoyl derivatives gave rise to lower energy bands compared to the ethynyl benzoyl and ethynyl furanoyl. This is due to the ethynyl naphthoyl linker being more conjugated than the other aromatic linkers.

For selected *N*-{*para*-(ferrocenyl) ethynyl benzoyl}, *N*-{6-(ferrocenyl) ethynyl-2-naphthoyl} and *N*-{5-(ferrocenyl) ethynyl-2-furanoyl} glycine glycine ethyl esters the λ_{max} values and their extinction coefficient (ε) values, corresponding to the π-π^* transition and MLCT band transition are shown in table 4.2.

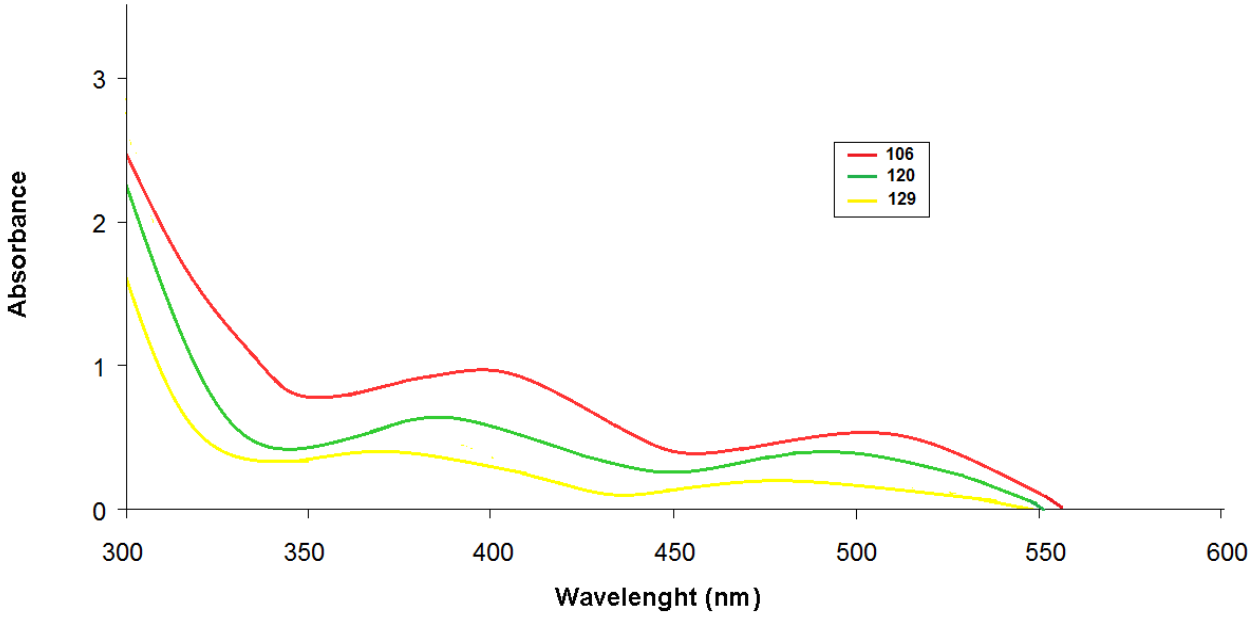

Table 4.2: Selected UV-Vis spectroscopic data for *N*-{*para*-(ferrocenyl) ethynyl benzoyl}, *N*-{6-(ferrocenyl) ethynyl-2-naphthoyl} and *N*-{5-(ferrocenyl) ethynyl-2-furanoyl} glycine glycine ethyl esters **106**, **120** and **129**

Compound	**Chromophore**			
	Ferrocene moiety		**Aromatic linker**	
	λ_{max} (nm)	ε (L mol^{-1} cm^{-1})	**λ_{max}** (nm)	ε (L mol^{-1} cm^{-1})
106	490	(ε 1550)	385	(ε 2500)
120	500	(ε 1025)	400	(ε 1550)
129	476	(ε 525)	370	(ε 1025)

Figure 4.16: The UV-Vis spectra of selected compounds **106, 120 and 129.**

4.10 Mass spectrometric studies of *N*-{*para*-(ferrocenyl) ethynyl benzoyl}, *N*-{6-(ferrocenyl) ethynyl-2-naphthoyl} and *N*-{5-(ferrocenyl) ethynyl-2-furanoyl} amino acid and dipeptide esters 105-138.

Electrospray ionization (ESI) mass spectrometry of compounds **105-138** revealed the presence of sodium adducts, $[M+Na]^+$ whilst tandem mass spectrometry was employed to determine the fragmentation pattern of compounds.

In the MS/MS spectrum of compound **106,** the sequence specific fragment ions are present at *m/z* 285, *m/z* 313, *m/z* 341 and *m/z* 369 (figure 4.16a). The product ions at *m/z* 285 and *m/z* 313 correspond to the *N-para*-(ferrocenyl) ethynyl benzyl and *N-para*-(ferrocenyl) ethynyl benzoyl subunits respectively. The a_1-1 and b_1-1 product ions were observed at *m/z* 341 and *m/z* 369 respectively. The fragment ion at *m/z* 444 is due to a loss of C_2H_4 from the ethyl ester group by a McLafferty rearrangement as already described in section 2.10 in scheme 2.11.

In the MS/MS spectrum of **120** the sequence specific fragment ions are present at *m/z* 335, *m/z* 363, *m/z* 391 and *m/z* 419 (figure 4.16b). The product ions at *m/z* 335 and *m/z* 363 correspond to the *N*-6-(ferrocenyl) ethynyl-2-naphthyl and *N*-6-(ferrocenyl) ethynyl-2-naphthoyl subunits respectively. The a_1-1 and b_1-1 product ions were observed at *m/z* 391 and *m/z* 419 respectively. The fragment ion at *m/z* 494 is due to a loss of C_2H_4 from the ethyl ester group by the McLafferty rearrangement.

For compound **129** the sequence specific fragment ions are observed at *m/z* 275, *m/z* 303, *m/z* 331 and *m/z* 359 (figure 4.16c). The product ions at *m/z* 275 and *m/z* 303 correspond to the *N*-5-(ferrocenyl) ethynyl-2-furanyl and *N*-5-(ferrocenyl) ethynyl-2-furanoyl subunits respectively. The a_1-1 and b_1-1 product ions are observed at *m/z* 331 and *m/z* 359 respectively. For compound **129** a unique product ion is observed at *m/z* 397, corresponding to the loss of the unsubstituted (η^5-C_5H_5) ring. This product ion is not observed in the ethynyl benzoyl or ethynyl-2-naphthoyl analogues**.** The fragment ion at *m/z* 434 is due to a loss of C_2H_4 from the ethyl ester group by the McLafferty rearrangement.

(a)

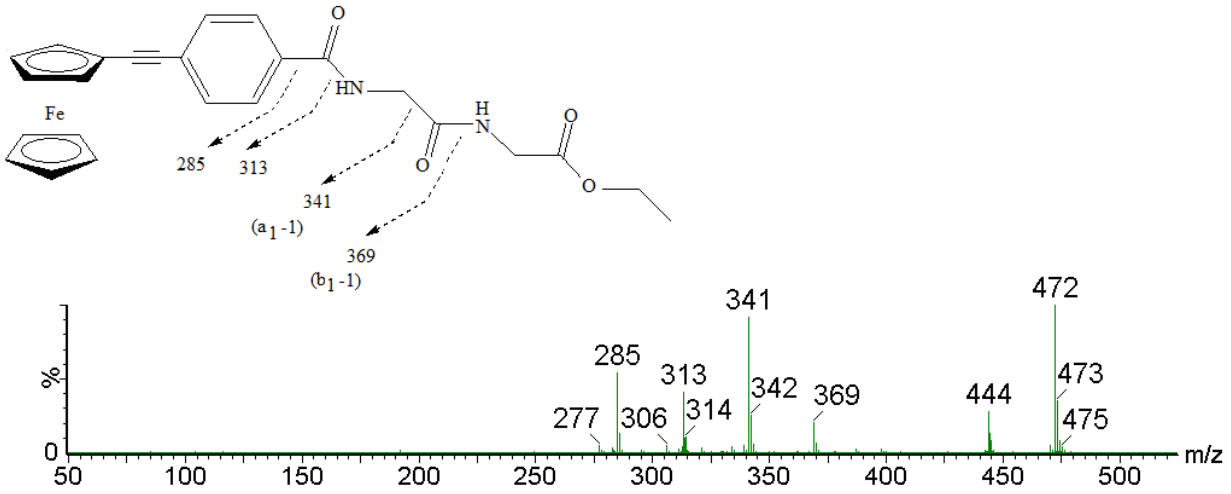
Fe
O
HN
H
N
O
O
O
285
313
341
(a1 -1)
369
(b1 -1)
%
0
341
472
285
313
277
306
314
342
369
444
473
475
50
100
150
200
250
300
350
400
450
500
m/z

(b)

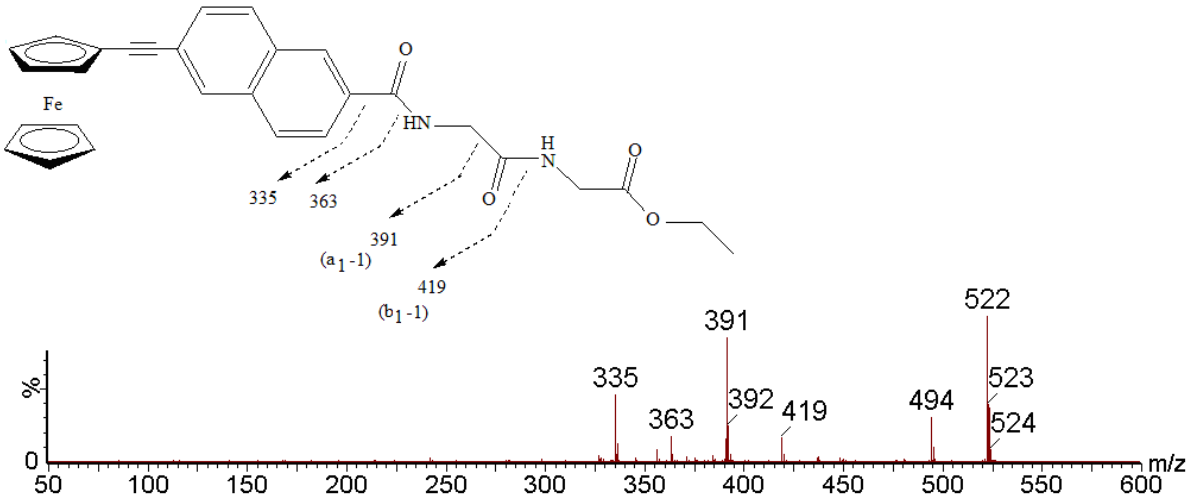
Fe
O
HN
H
N
O
O
O
335
363
391
(a1 -1)
419
(b1 -1)
%
0
391
522
335
363
392
419
494
523
524
50
100
150
200
250
300
350
400
450
500
550
600
m/z

(c)

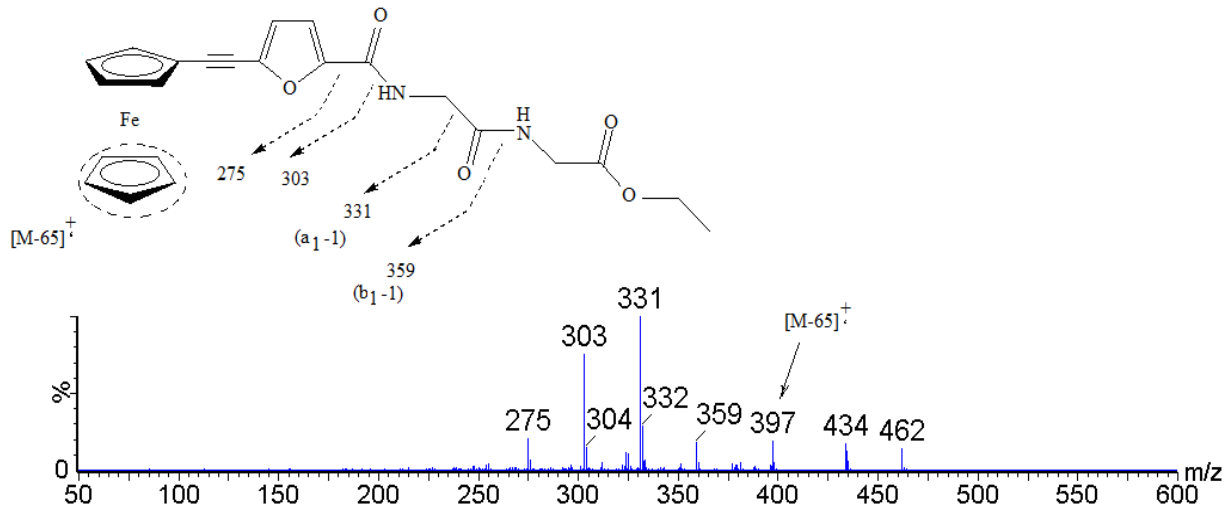

Figure 4.16. MS/MS spectra of (a) *N*-{*para*-(ferrocenyl) ethynyl benzoyl} glycine glycine ethyl ester **106 (b)** *N*-{6-(ferrocenyl) ethynyl-2-naphthoyl} glycine glycine ethyl ester **120** and **(c)** *N*-{5-(ferrocenyl) ethynyl-2-furanoyl} glycine glycine ethyl ester **129.**

4.11 A comparative study of *N-para*, *N-meta* and *N-ortho*-(ferrocenyl) benzoyl dipeptide esters and the novel ethynyl analogues 105-138.

4.11.1 Introduction

In a further extension to ferrocenyl benzoyl and naphthoyl bioconjugates reported, a new library of ferrocenyl based bioconjugates **105-138,** which consist of four key moieties (i) an electroactive core (ii) a -C≡C- moiety (iii) three different aromatic linkers and (iv) and a series of amino acid and dipeptide esters are now reported here. The incorporation of the -C≡C- moiety between the ferrocene moiety and the aromatic spacer and the use of three different aromatic rings are attempts to further improve the cytotoxicity of the previously prepared *N-para*, *N-meta* and *N-ortho*-(ferrocenyl) benzoyl dipeptide esters.

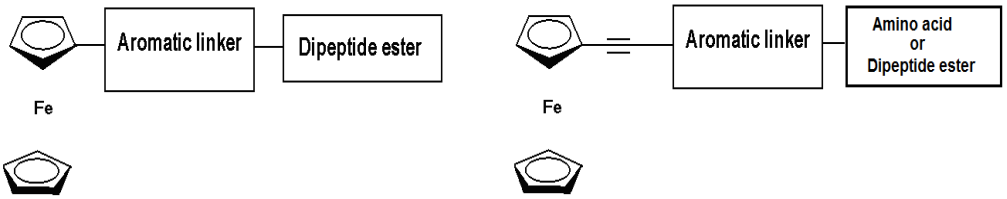

Figure 4.17: General structure of the *N*-(ferrocenyl) benzoyl and naphthoyl bioconjugates and the *N*-{*para*-(ferrocenyl) ethynyl benzoyl}, *N*-{6-(ferrocenyl) ethynyl-2-naphthoyl} and *N*-{5-(ferrocenyl) ethynyl-2-furanoyl} amino acid and dipeptide esters.

4.11.2 Synthetic pathways employed

For the synthesis of *para*, *meta* and *ortho*-(ferrocenyl) benzoic acid the synthetic protocol involved the diazonium coupling of ferrocene to 2, 3, 4-ethylamino benzoate followed by basic hydrolysis.[4-8] The use of the diazonium coupling reaction in the preparation of the monoarylferrocenes derivatives proceeds with a low degree of regiocontrol and produces intractable mixtures of mono-, di- and poly-arylferrocene derivatives with low yields of less than 8% for the desired monoarylferrocene

derivatives. For the synthesis of the ethynyl analogues **105-138,** the synthetic protocol involved the use of Sonogashira cross coupling of ethynyl ferrocene to three bromo acylated acids to generate *para*-(ferrocenyl) ethynyl benzoic acid, 6-(ferrocenyl) ethynyl-2-naphthoic acid, and 5-(ferrocenyl) ethynyl-2-furanoic acids. In this coupling reaction, yields greater than 60% were obtained. These high yields are largely due to the fact that Sonogashira cross coupling is a substrate specific reaction between an alkyne and an aryl halides employed in the coupling reaction which involves the use of palladium catalyst and copper iodine co catalyst.

4.11.3 ^{1}H NMR, ^{13}C NMR and DEPT-135 studies of *N-para, N-meta* and *N-ortho*-(ferrocenyl) benzoyl dipeptide esters and the novel ethynyl analogues 105-138.

In the ^{1}H NMR, ^{13}C NMR and DEPT-135 studies of the *N-para*, *N-meta* and *N-ortho*-(ferrocenyl) benzoyl dipeptide esters and the novel *N*-{*para*-(ferrocenyl) ethynyl benzoyl}, *N*-{6-(ferrocenyl) ethynyl-2-naphthoyl} and *N*-{5-(ferrocenyl) ethynyl-2-furanoyl} amino acid and dipeptide esters, clear similarities and differences can be identified. Typical signals observed in the ^{1}H NMR spectra in both classes of compounds include the appearance of amide protons of the peptide chain which appear between δ 8.89 and δ 8.14, whereas the aromatic protons appear between δ 8.00 and δ 7.00. The protons on the monosubstituted ferrocene ring appear between δ 4.95 and δ 4.00. However with the ethynyl analogues overlapping of the proton signals occurs with these derivatives, which makes the assignment of the proton chemical shift a challenge. For instance the amide proton and aromatic proton overlap resulting in mutiplets being observed which is not observed with in the *N-para*, *N-meta* and *N-ortho*-(ferrocenyl) benzoyl dipeptide esters.[4-8] Furthermore the protons on the monosubstituted ferrocene ring of the ethynyl analogues tend to overlap with each other or with other signals from methylene groups and the methine groups that may be present in the amino acid and dipeptide esters. Hence, the expected three signals for a monosubstituted derivative are not observed. Due to this limited scope of information observed from the proton chemical shifts, other spectroscopic techniques where used to provide a more complete picture of the molecular structure of these derivatives which

included ^{13}C NMR, DEPT-135 and ^{1}H-^{13}C COSY (HMQC) spectroscopy and electrospray ionization mass spectrometry (ESI-MS).

The presence of the -C≡C- unit in the new ethynyl ferrocenyl bioconjugates can be identified in the ^{13}C NMR spectra. The carbons on the -C≡C- linker for the benzoyl derivatives appear between δ 96.0 - 90.0 for (η^5-C_5H_4-C≡<u>C</u>-) and between δ 87.0 - 85.0 for (η^5-C_5H_4-<u>C</u>≡C-). For the naphthoyl derivatives the -C≡C- linkers appear between δ 90.0 -89.0 for (η^5-C_5H_4-C≡<u>C</u>-) and between δ 85.0 - 84.0 for (η^5-C_5H_4-<u>C</u>≡C-) whilst for the furanoyl derivatives it appears between δ 95.0 - 90.0 for (η^5-C_5H_4-C≡<u>C</u>-) and between δ 76.0 - 73.0 for (η^5-C_5H_4-<u>C</u>≡C-). The typical carbon signals present in the two classes of compounds include the presence of carbonyl atoms present between δ 172.7 and δ 155.0. The aromatic carbons occur between δ 145.0 - 115.0. The carbon atoms on the ferrocenyl rings appear between δ 71.5 and δ 63.0. In the DEPT-135 spectrum the presence of the methylene carbon atoms in both classes can be easily identified as they appear as negative resonances.

4.12 Conclusions

A series of *N*-{*para*-(ferrocenyl) ethynyl benzoyl}, *N*-{6-(ferrocenyl) ethynyl-2-naphthoyl} and *N*-{5-(ferrocenyl) ethynyl-2-furanoyl} amino acid and dipeptide esters were prepared and structurally characterized. Each novel compound incorporated an electroactive ferrocene core, a -C≡C-, a conjugated aromatic linker and a dipeptide chain with each part exerting a specific effect on biological activity. The ferrocene moiety is required for the possible production of hydroxyl radicals, the -C≡C- and conjugated aromatic linkers facilitates this process by lowering the redox potential of the ferrocene and the peptide fragment can interact with other molecules *via* hydrogen bonding. These novel compounds were characterized by a combination of ^{1}H NMR, ^{13}C NMR, DEPT-135 and ^{1}H-^{13}C COSY (HMQC) spectroscopy, electrospray ionization mass spectrometry (ESI-MS).

References

1 Mooney, A., Corry, A.J., O'Sullivan, D., Rai, D.K., and Kenny, P.T.M., *J. Organomet. Chem*., **2009**, *694*, 886-894

2 Mooney, A., Corry, A.J., N'i Ruairc, C., Mahgoub, T., O'Sullivan, D., O'Donovan, N., Crown, J., Varughese, S., Draper, S.M., Rai, D.K., and Kenny, P.T.M., *Dalton. Trans*., **2010**, *39*, 8228–8239

3 Mooney, A., Tiedt, R., Maghoub, T., O'Sullivan, D., O'Donovan, N., Crown, J., Varughese, S., White, B., and Kenny, P.T.M., *J. Med. Chem*., **2012**, *55*, 5455−5466

4 Goel, A., Savage, D., Alley, S.R., Kelly, P.N., O'Sullivan, D., Mueller-Bunz, H., and Kenny, P.T.M., *J. Organomet. Chem*., **2007**, *692*, 1292-1299.

5 Goel, A., Savage, D., Alley, S.R., Hogan, T., Kelly, P.N., Draper, S., Fitchett C.M., and Kenny P.T.M, *J. Organomet. Chem*., **2006**, *691*, 4686-4693.

6 Corry, A.J., Goel, A., Alley, S.R., Kelly, P.N., O'Sullivan, D., Savage, D., and Kenny, P.T.M., *J. Organomet. Chem*., **2007** *692*, 1405-1410

7 Corry, A.J., Mooney, A., O'Sullivan, D., and Kenny, P.T.M., *Inorganica Chimica Acta*., **2009**, *362*, 2957-2961.

8 Corry, A.J., O'Donovan, N., Mooney, A., O'Sullivan, D., Rai, D.K., Kenny, P.T.M., *J. Organomet. Chem*., **2009**, *694*, 880-885.

9 Brunner, H., Reimer, A., *Bull. Soc. Chem*. Fr., **1997**, *134*, 307-314

10 Rosenblum, M., Brawn, N., Papenmeier, J., Applebaum, M., *J. Organomet. Chem*. **1966**, *6*, 173-177

11 Polin, J., Schottenberger, H., Organic Syntheses., **1996**, *73*, 262-269.

12 Lilienkampf, A., Johansson, M, P., Wahala, K., *Organic Letters*., **2003**, *5*, 3387-3390

13 Vogel , M., Rausch, M.D., Rosenberg, H., *J. Organomet. Chem*., **1957**, *22*, 1016-1024

14 http://www.organic-chemistry.org/namedreactions/sonogashira-coupling.shtm

15 Chinchilla, R., Najera, C., *Chem. Soc. Rev*., **2011**, *40*, 84–5121

16 http://www.chem.wisc.edu/areas/reich/handouts/nmr-h/hdata.htm

17 McMurry, J., *'Organic Chemistry'*, Brooks/Cole, **2000** 5th edition.

Chapter 5: The biological evaluation of *N*-{*para*-(ferrocenyl) ethynyl benzoyl}, *N*-{6-(ferrocenyl) ethynyl-2-naphthoyl} and *N*-{5-(ferrocenyl) ethynyl-2-furanoyl} amino acid and dipeptide esters

5.1 Introduction

This research group has reported the anti-proliferative effects of ferrocenyl benzoyl and ferrocenyl naphthoyl bioconjugates (figure 5.1) in the H1299 lung cancer cell line.[1-8] In an effort to further improve the cytotoxicity of these derivatives, a series of *N*-{*para*-(ferrocenyl) ethynyl benzoyl}, *N*-{6-(ferrocenyl) ethynyl-2-naphthoyl} and *N*-{5-(ferrocenyl) ethynyl-2-furanoyl} amino acid and dipeptide esters **105-138** (figure 5.1) were synthesised, structurally characterised and biologically evaluated. In total 34 compounds were tested for their anti-proliferative effects on the non-small cell, lung cancer cell line, H1299. These novel derivatives differ from the ferrocenyl benzoyl and ferrocenyl naphthoyl bioconjugates by having an ethynyl linker between the ferrocene moiety and the aromatic linkers (benzoyl and naphthoyl) and furthermore, a new aromatic linker furanoyl has been incorporated.

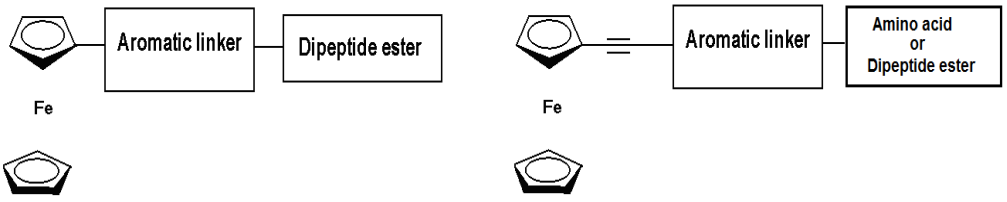

Figure 5.1: General structure of the *N*-(ferrocenyl) benzoyl and naphthoyl bioconjugates and the *N*-{*para*-(ferrocenyl) ethynyl benzoyl}, *N*-{6-(ferrocenyl) ethynyl-2-naphthoyl} and *N*-{5-(ferrocenyl) ethynyl-2-furanoyl} amino acid and dipeptide esters.

5.2 Preliminary biological evaluation of *N*-{*para*-(ferrocenyl) ethynyl benzoyl}, *N*-{6-(ferrocenyl) ethynyl-2-naphthoyl} and *N*-{5-(ferrocenyl) ethynyl-2-furanoyl} amino acid and dipeptide esters

5.2.1 Preliminary biological evaluation of the *N*-{*para*-(ferrocenyl) ethynyl benzoyl} amino acid and dipeptide esters

The *in vitro* cytotoxicity of the derivatives **105-119** against the H1299 lung cancer cells was evaluated by the acid phosphatase assay as previously described in section 3.1. The results for the percentage growth inhibition of the derivatives are depicted in figure 5.2 and table 5.1.

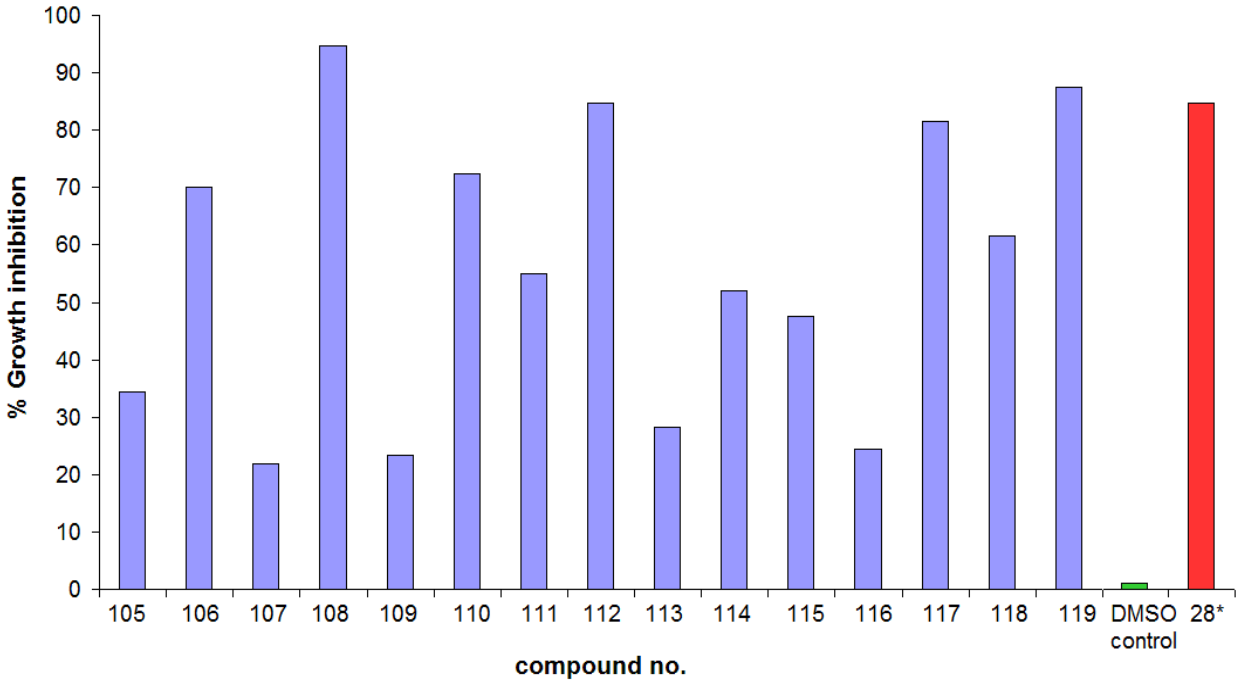

Figure 5.2: % Growth inhibition at 10 µM on H1299 lung cancer cells for *N*-{*para*-(ferrocenyl) ethynyl benzoyl} amino acid and dipeptide esters **105-119** and reference compound **28.**

Table 5.1: % Growth inhibition at 10 μM on H1299 lung cancer cells for *N*-{*para*-(ferrocenyl) ethynyl benzoyl} amino acid and dipeptide esters **105-119** and reference compound **28.**

Ferrocenyl bioconjugate	R	Compound no.	% growth inhibition at 10 μM
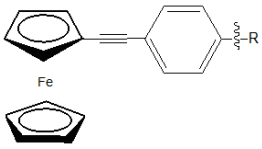	Gly Gly(OMe)	**105**	34 ± 2.49
	Gly Gly(OEt)	**106**	70 ± 2.84
	Gly L-Ala(OMe)	**107**	22 ± 5.47
	Gly L-Ala(OEt)	**108**	95 ± 1.62
	Gly D-Ala(OMe)	**109**	23 ± 4.89
	Gly D-Ala(OEt)	**110**	72 ± 2.01
	GABA(OMe)	**111**	55 ± 3.35
	GABA(OEt)	**112**	85 ± 1.07
	Gly L-Phe(OEt)	**113**	28 ± 1.74
	Gly L-Leu(OEt)	**114**	53 ± 3.17
	Sar Gly(OEt)	**115**	47 ± 4.03
	Sar Gly(OMe)	**116**	25 ± 4.10
	Sar L-Ala(OEt)	**117**	82 ± 4.75
	L-Pro Gly(OEt)	**118**	62 ± 5.06
	L-Pro L-Ala(OEt)	**119**	87 ± 1.12
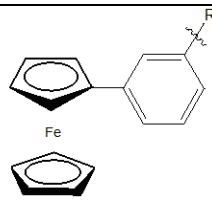	Gly-L-Ala(OEt)	**28***	84 ± 0.33

Note: **28*** Originally prepared by Alan Corry [5]

From the preliminary screen at 10 μM a general trend can be observed, the methyl ester derivatives exhibited lower percentage growth inhibition values between 22 % ± 5.47 to 55 % ± 3.35 compared to the ethyl ester derivatives which exhibited percentage growth inhibition values between 47 % ± 4.03 to 95 % ± 1.62. Generally, the lower the percentage growth value, the lower the anti-proliferative activity. Thus, the methyl ester derivatives were not investigated further.

A general trend was also observed in these derivatives, that is, the Gly L-Leu and Gly L-Phe ethyl esters display percentage growth inhibition values ≤ 53 %. For instance, the *N*-{*para*-(ferrocenyl) ethynyl benzoyl} glycine L-phenylalanine ethyl ester **113** displayed % growth inhibition value of 28 % ± 1.74 whilst the *N*-{*para*-(ferrocenyl) ethynyl benzoyl} glycine L-leucine ethyl ester **114** displayed a percentage growth

inhibition values of 53 % ± 3.17. Thus, the Gly L-Leu and Gly L-Phe ethyl ester derivatives were not investigated further. As a result, it can be concluded that when chiral α-amino acids with bulky side chains are used as the second amino acid in the dipeptide moiety, a loss of anti-proliferative activity is observed. Compounds **106, 108, 110, 112, 117, 118** and **119**, showed percentage growth inhibition values ≥ 60 %. Therefore, IC_{50} values were determined for these compounds.

5.2.2 Preliminary biological evaluation of the *N*-{6-(ferrocenyl) ethynyl-2-naphthoyl} amino acid and dipeptide esters

The *in vitro* anti-proliferative effect of compounds **120-128** were studied at a concentration of 10 μM in the H1299 lung cancer cells. The results of this biological study are shown in figure 5.3 and table 5.2. From the preliminary screen a general trend was observed, the Gly L-Leu and Gly L-Phe ethyl esters displayed percentage growth inhibition values ≤ 34 %. Thus, the Gly L-Leu and Gly L-Phe ethyl ester derivatives were not investigated further. Compounds **120, 121, 122, 123, 124, 125** and **127** showed percentage growth inhibition values ≥ 68 %. Therefore, IC_{50} values were determined for these compounds.

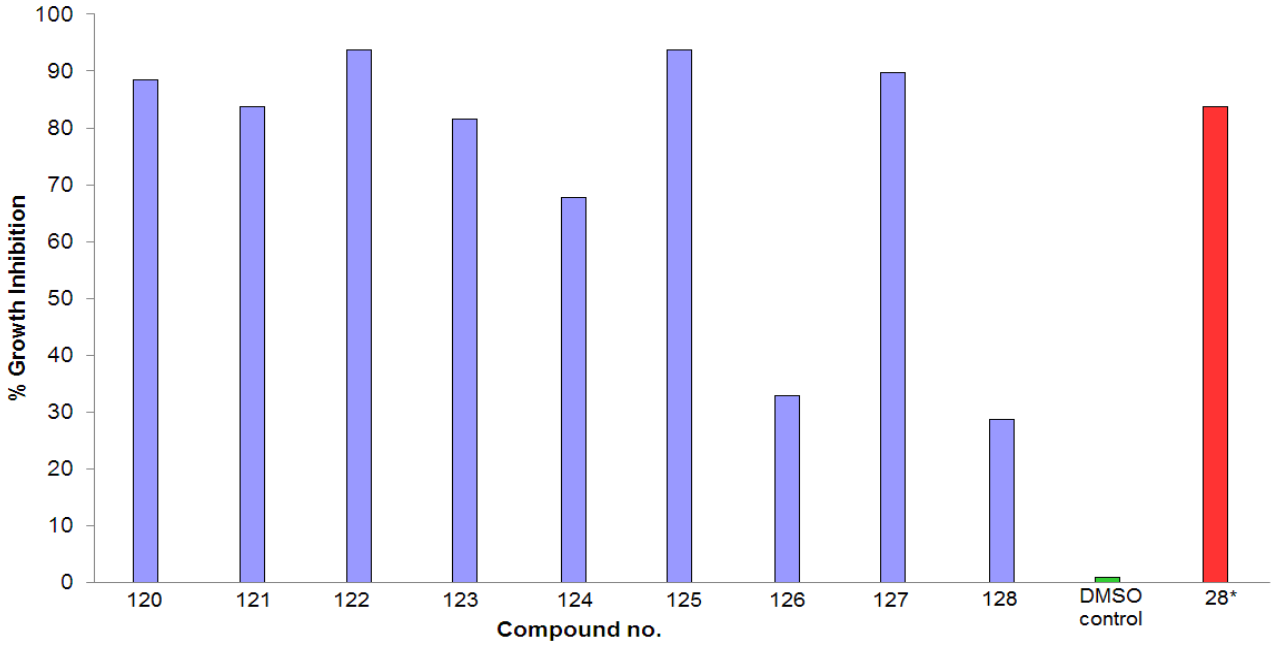

Figure 5.3: Percentage Growth inhibition at 10 µM on H1299 lung cancer cells for *N*-{*para*-(ferrocenyl) ethynyl naphthoyl} amino acid and dipeptide esters **120-128** and reference compound **28.**

Table 5.2: Percentage Growth inhibition at 10 µM on H1299 lung cancer cells for *N*-{*para*-(ferrocenyl) ethynyl naphthoyl} amino acid and dipeptide esters **120-128** and reference compound **28.**

Ferrocenyl bioconjugate	R	Compound no.	% growth inhibition at 10 µM
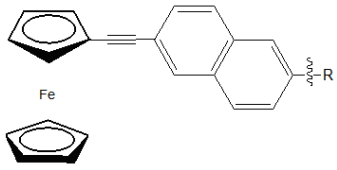	Gly Gly(OEt)	**114**	89 ± 1.23
	Gly L-Ala(OEt)	**115**	84 ± 5.33
	Sar L-Ala(OEt)	**116**	94 ± 1.02
	L-Pro Gly(OEt)	**117**	82 ± 1.92
	GABA(OEt)	**118**	68 ± 5.81
	L-Pro L-Ala(Oet)	**119**	94 ± 0.61
	Gly L-Leu(OEt)	**120**	33 ± 4.72
	Sar Gly(OEt)	**121**	90 ± 1.40
	Gly L-Phe(OEt)	**122**	29 ± 2.53
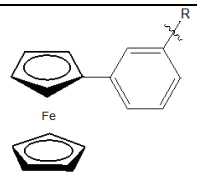	Gly L-Ala(OEt)	**28***	84 ± 0.33

Note: **28*** Originally prepared by Alan Corry [5]

5.2.3 Preliminary biological evaluation of the *N*-{5-(ferrocenyl) ethynyl-2-furanoyl} amino acid and dipeptide esters

The *in vitro* cytotoxicity of the derivatives **129-138** against the human lung carcinoma cell line H1299 was evaluated by the acid phosphatase assay and the % growth inhibition of the derivatives are depicted in figure 5.4 and table 5.2.

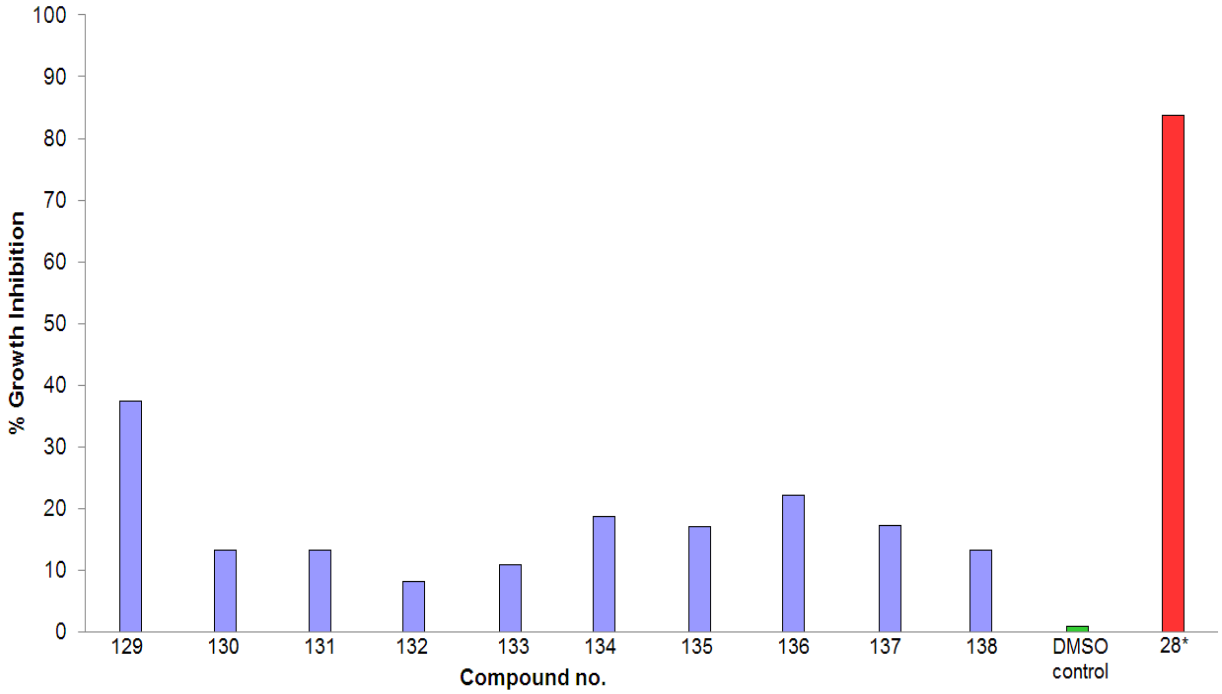

Figure 5.4: Percentage Growth inhibition at 10 µM on H1299 lung cancer cells for *N*-{*para*-(ferrocenyl) furanoyl naphthoyl} amino acid and dipeptide esters **129-138** and reference compound **28.**

Table 5.2: Percentage Growth inhibition at 10 μM on H1299 lung cancer cells for *N*-{*para*-(ferrocenyl) furanoyl naphthoyl} amino acid and dipeptide esters **129-138** and reference compound **28.**

Ferrocenyl bioconjugate	R	Compound no.	% growth inhibition at 10 μM
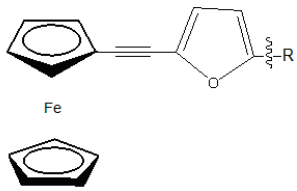	Gly Gly(OEt)	**129**	38 ± 2.62
	Gly L-Ala(OEt)	**130**	13 ± 3.41
	Gly D-Ala(OEt)	**131**	13 ± 4.37
	Gly L-Phe(OEt)	**132**	9 ± 3.30
	Gly L-Leu(OEt)	**133**	11 ± 3.70
	Sar Gly(OEt)	**134**	18 ± 5.43
	L-Pro Gly(OEt)	**135**	17 ± 2.33
	L-Pro L-ala(Oet)	**136**	22 ± 2.60
	Sar L-ala(OEt)	**137**	17 ± 1.50
	GABA(OEt)	**138**	13 ± 1.38
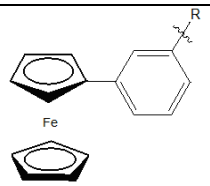	Gly L-Ala(OEt)	**28***	84 ± 0.33

Note: **28*** Originally prepared by Alan Corry [5]

From the preliminary screen at 10 μM, all derivatives exhibited lower percentage growth inhibition values between 9 % ± 3.30 to 38 % ± 2.62. In the case of the *N*-{5-(ferrocenyl) ethynyl-2-furanoyl} glycine glycine ethyl ester **129,** it exhibited the highest percentage growth inhibition value of 38 % ± 2.62 and thus, an IC_{50} value for **129** was determined. For compounds **130-138** no further investigation were carried out.

5.3 IC_{50} value determination of *N*-{*para*-(ferrocenyl) ethynyl benzoyl}, *N*-{6-(ferrocenyl) ethynyl-2-naphthoyl} and *N*-{5-(ferrocenyl) ethynyl-2-furanoyl} amino acid and dipeptide esters

5.3.1 IC_{50} value determination of *N*-{*para*-(ferrocenyl) ethynyl benzoyl} amino acid and dipeptide esters

Further studies were conducted as described in Chapter 3 (Section 3.2), to determine IC_{50} values for in the H1299 cell line. The IC_{50} value for each compound was calculated using Calcusyn software, and standard deviations have been calculated using data obtained from three independent experiments. The values obtained are listed in figure 5.5 and table 5.3.

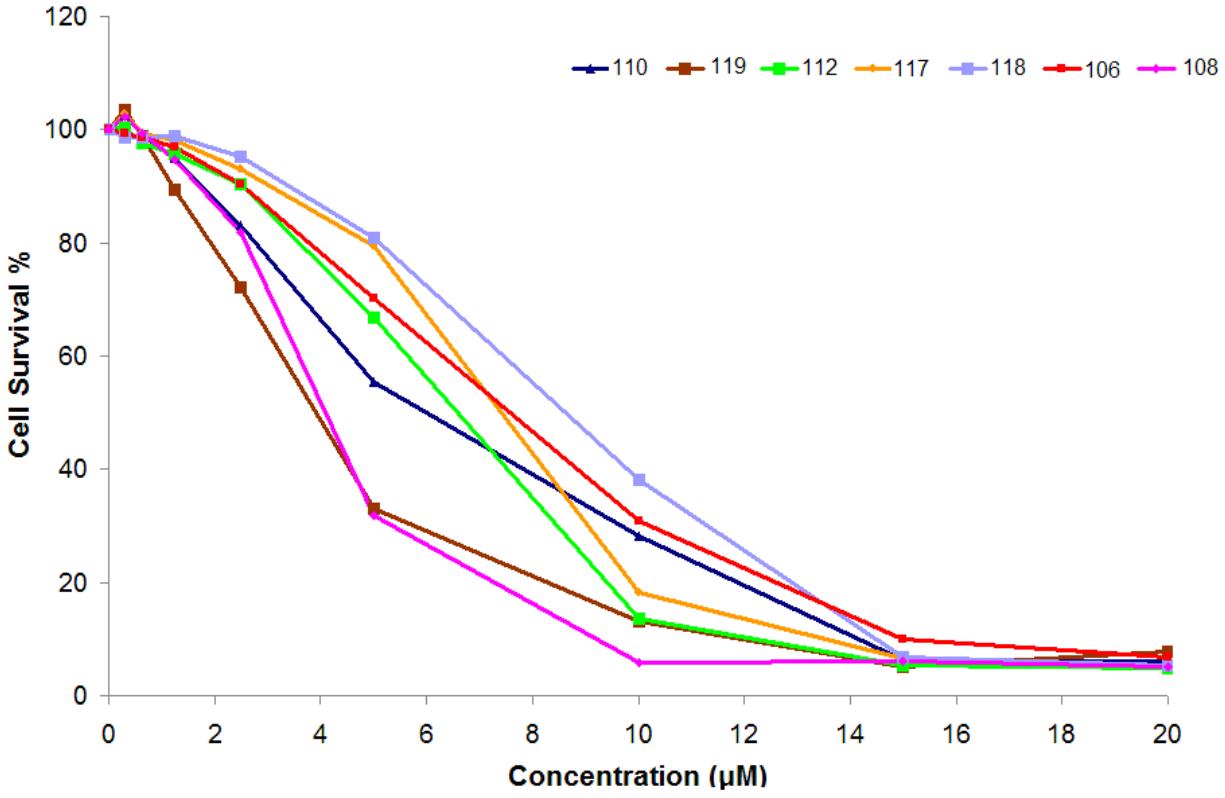

Figure 5.5: IC_{50} plot for selected compounds in the H1299 cell line.

Table 5.3: IC_{50} values for selected compounds, reference compound **28**, carboplatin and cisplatin against human lung carcinoma cell line H1299.

Compound Name	**No.**	**IC_{50}**
Cisplatin	**8**	1.5 ± 0.10
Carboplatin	**9**	10 ± 1.60
N- {*meta*-(ferrocenyl)-benzoyl} Gly L-Ala(OEt)	**28***	4.0 ± 0.71
N-{*para*-(ferrocenyl) ethynyl benzoyl} Gly Gly(OEt)	**106**	6.9 ± 2.14
N-{*para*-(ferrocenyl) ethynyl benzoyl} Gly L-Ala(OEt)	**108**	3.8 ± 1.92
N-{*para*-(ferrocenyl) ethynyl benzoyl} Gly D-Ala(OEt)	**110**	6.1 ± 3.41
N-{*para*-(ferrocenyl) ethynyl benzoyl} GABA(OEt)	**112**	4.9 ± 4.12
N-{*para*-(ferrocenyl) ethynyl benzoyl} Sar L-Ala(OEt)	**117**	7.1 ± 2.46
N-{*para*-(ferrocenyl) ethynyl benzoyl} L-Pro Gly(OEt)	**118**	8.3 ± 3.10
N-{*para*-(ferrocenyl) ethynyl benzoyl} L-Pro L-Ala(OEt)	**119**	5.7 ± 2.91

From the IC_{50} values of compounds **106, 108, 110, 112, 117, 118** and **119** all exert a cytotoxic effect on the H1299 lung cancer cell line. All seven derivatives have an IC_{50} value that is lower than 9 μM and more cytotoxic *in vitro* than the clinically employed anticancer drug carboplatin. In addition, the most active compound was *N*-{*para*-(ferrocenyl) ethynyl benzoyl} glycine L-alanine ethyl ester **108** which had an IC_{50} value of 3.8 ± 1.92 μM. This compound displays a slight improvement in biological activity in comparison to the most active ferrocenyl benzoyl analogue **28** which displayed an IC_{50} value of 4.0 ± 0.71 μM.[5]

The *in vitro* cytotoxicity of the platinum (II) based anticancer drug cisplatin was also evaluated against the H1299 cell line and was found to have an IC_{50} value of 1.5 ± 0.10 μM. Thus, compounds **106, 108, 110, 112, 117, 118** and **119** are less cytotoxic *in vitro* than the clinically employed anticancer drug cisplatin.

Previously, *in vitro* cytotoxic effects have shown the *N*-(ferrocenyl) naphthoyl derivatives to be more active than the *N*-(ferrocenyl) benzoyl derivatives with the most active derivative, *N*-{6-(ferrocenyl)-2-napthoyl} glycine glycine ethyl ester displaying an IC_{50} value of 0.13 ± 0.01 μM.[8] For the *N*-{*para*-(ferrocenyl) ethynyl benzoyl} glycine glycine ethyl ester, an IC_{50} value of 6.9 ± 5.14 μM was obtained. Thus, it can be concluded that the presence of the ethynyl moiety did not result in any marginal increase in the cytoxicity of the *N*-{*para*-(ferrocenyl) ethynyl benzoyl} amino acid and dipeptide esters, when compared to the *N*-(ferrocenyl) benzoyl and naphthoyl analogues previously reported.[1-8] A potential mechanism by which these compounds induce DNA damage is by the catalytic generation of $HO^{\bullet}$ radical as described in section 3.2 in scheme 3.1.

5.3.2 IC_{50} value determination of *N*-{6-(ferrocenyl) ethynyl-2-naphthoyl} amino acid and dipeptide esters

The IC_{50} values for derivatives **120-128** were determined by the acid phosphatase assay as previously described in section 3.3. The IC_{50} values for derivatives **120-128**, cisplatin and carboplatin are depicted in figure 5.6 and table 5.4.

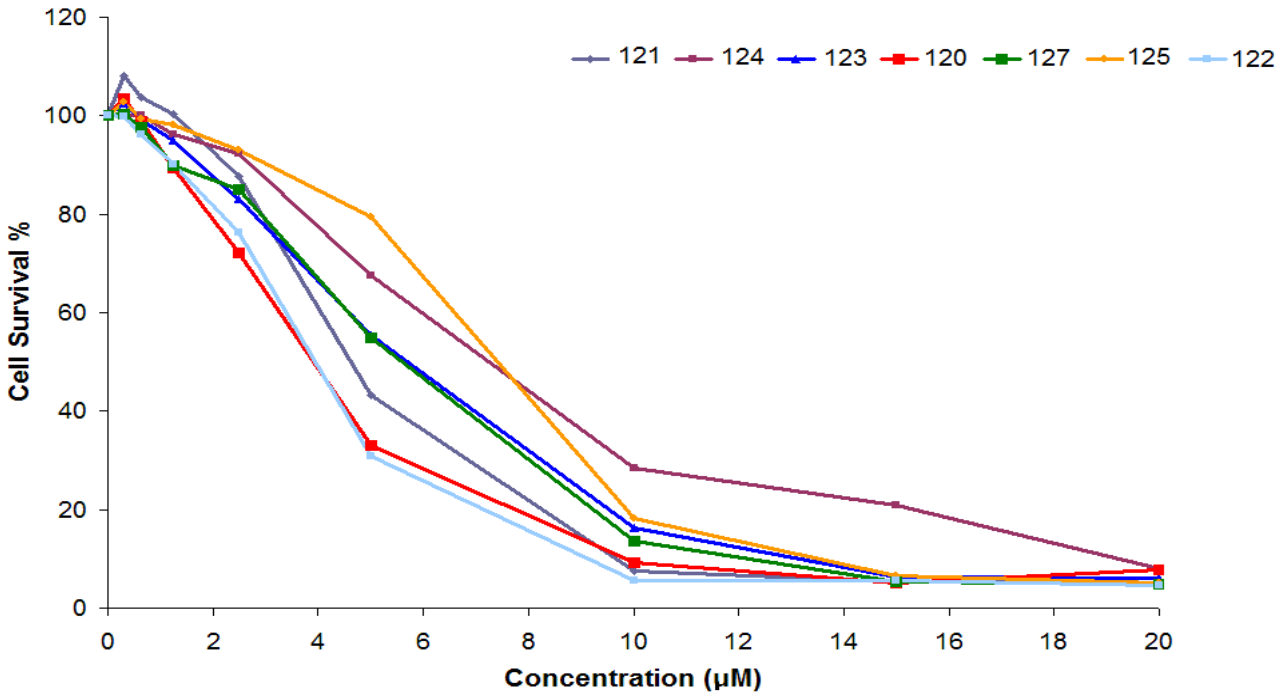

Figure 5.6: IC_{50} plot for selected compounds in the H1299 cell line.

Table 5.4: IC_{50} values for selected compounds, reference compound **28**, carboplatin and cisplatin against human lung carcinoma cell line H1299.

Compound Name	**No.**	**IC_{50}**
Cisplatin	**8**	1.5 ± 0.10
Carboplatin	**9**	10 ± 1.60
N- {*meta*-(ferrocenyl)-benzoyl} Gly L-Ala(OEt)	**28***	4.0 ± 0.71
N-{6-(ferrocenyl) ethynyl-2-naphthoyl} Gly Gly(OEt)	**120**	5.0 ± 4.12
N-{6-(ferrocenyl) ethynyl-2-naphthoyl} Gly L-Ala(OEt)	**121**	5.0 ± 3.61
N-{6-(ferrocenyl) ethynyl-2-naphthoyl} Sar L-Ala(OEt)	**122**	3.2 ± 2.64
N-{6-(ferrocenyl) ethynyl-2-naphthoyl} L-Pro Gly(OEt)	**123**	5.1 ± 1.35
N-{6-(ferrocenyl) ethynyl-2-naphthoyl} GABA(OEt)	**124**	7.2 ± 1.51
N-{6-(ferrocenyl) ethynyl-2-naphthoyl} L-Pro L-Ala(OEt)	**125**	3.8 ± 2.02
N-{6-(ferrocenyl) ethynyl-2-naphthoyl} Sar Gly(OEt)	**127**	4.7 ± 3.71

From the IC_{50} values of the *N*-{6-(ferrocenyl) ethynyl-2-naphthoyl} amino acid and dipeptide ethyl esters **120, 121, 122, 123, 124, 125** and **127,** all exert a cytotoxic effect on the H1299 lung cancer cell line. All seven derivatives have an IC_{50} value that is lower than 7.2 μM and more cytotoxic *in vitro* than the clinically employed anticancer drug carboplatin. The most active compound was *N*-{6-(ferrocenyl) ethynyl-2-naphthoyl} sarcosine L-alanine ethyl ester **122** which had an IC_{50} value of 3.2 ± 2.64 μM. However, for compounds **120, 121, 124** and **127** the presence of the ethynyl moiety had a negative effect of anti-proliferative effect compared to analogous compounds prepared previously lacking the ethynyl group.[6-8] For example for *N*-{6-(ferrocenyl) ethynyl-2-naphthoyl} γ-aminobutyric acid ethyl ester **124** the IC_{50} value is 7.2 ± 1.51 μM, whereas for *N*-(6-ferrocenyl-2-naphthoyl) γ-aminobutyric acid ethyl ester the IC_{50} value was 0.62 ± 0.17 μM. The *in vitro* cytotoxicity of the platinum (II) based anticancer drug cisplatin was also evaluated against the H1299 cell line, and was

found to have an IC_{50} value of 1.5 ± 0.10 μM (Table 4). Thus, compounds **120-128** are less cytotoxic *in vitro* than the clinically employed anticancer drug cisplatin. A potential mechanism by which these novel organometallic anticancer compounds may induce DNA damage is by the catalytic generation of ROS. This is possible *via* a Fenton-type reaction, in which $HO^{\bullet}$ radicals are generated from the superoxide dismutation product, hydrogen peroxide (H_2O_2). It was shown that the generation of 8-oxoGua by a compound prepared in a previous SAR study, *N*-(6-ferrocenyl-2-naphthoyl) glycine glycine ethyl ester, that the oxidation was occurring by Fenton chemistry and that *N*-(6-ferrocenyl-2-naphthoyl) glycine glycine ethyl ester is generating oxidative damage via a ROS-mediated mechanism. Therefore, guanine oxidation studies confirmed that *N*-(6-ferrocenyl-2-naphthoyl) glycine glycine ethyl ester was capable of causing oxidative damage to guanine, and it does so by the generation of $HO^{\bullet}$ radicals from H_2O_2.[8] However, the introduction of the ethynyl group reduces the IC_{50} value from 0.13 ± 0.01 μM for *N*-(6-ferrocenyl-2-naphthoyl) gly gly(OEt) to 5.0 ± 4.12 μM for *N*-{6-(ferrocenyl) ethynyl-2-naphthoyl}gly gly(OEt). Therefore, it is possible that some other feature of these derivatives may play an important role, such as the ability to interact with DNA in other ways. It is plausible that these polyaromatic derivatives could intercalate with DNA, as observed for many polyaromatic drugs including the anthracycline class of chemotherapeutics. The hydrogen bond donor and acceptor atoms present in the peptide side chain, could then interact with the nucleotide bases positioned in the centre of the helix. Although the bulky ferrocene substituent (10.5 Å) is too large to fit into the major groove of DNA (depth = 8.5 Å), the oxidation potentials of these derivatives supports the possibility that the ferrocene moiety in its oxidized Fe^{3+} state, could interact with the negatively charge phosphate backbone positioned on the outside of the helix. However, for the *N*-{6-(ferrocenyl) ethynyl-2-naphthoyl} amino acid and dipeptide ethyl esters the presence of the ethynyl group could disrupt this interaction. Thus, it is possible for the naphthoyl ferrocenyl bioconjugates to possess two distinct modes of action: the ability to cause oxidative damage to DNA through ROS production and the ability to intercalate with DNA, both of which would result in the disruption of cancer cell replication. A general trend can be seen between the *N*-{6-(ferrocenyl) ethynyl-2-naphthoyl} and *N*-{*para*-(ferrocenyl) ethynyl benzoyl} amino acid and dipeptide esters.

The Gly Gly, Sar L-Ala, L-Pro Gly, L-Pro L-Ala ethyl esters of the *N*-{6-(ferrocenyl) ethynyl-2-naphthoyl} derivatives are more active than the *N*-{*para*-(ferrocenyl) ethynyl benzoyl}derivatives whilst the Gly L-Ala and GABA esters of the *N*-{*para*-(ferrocenyl) ethynyl benzoyl}derivatives are more active than the *N*-{6-(ferrocenyl) ethynyl-2-naphthoyl}derivatives.

5.3.3 IC_{50} value determination of *N*-{5-(ferrocenyl) ethynyl-2-furanoyl}-glycine-glycine ethyl ester 129.

The IC_{50} value for *N*-{5-(ferrocenyl) ethynyl-2-furanoyl} glycine glycine ethyl ester **129** was the only derivative evaluated by the acid phosphatase assay. The IC_{50} value for the derivative, cisplatin and carboplatin are depicted in figure 5.7 and table 5.5.

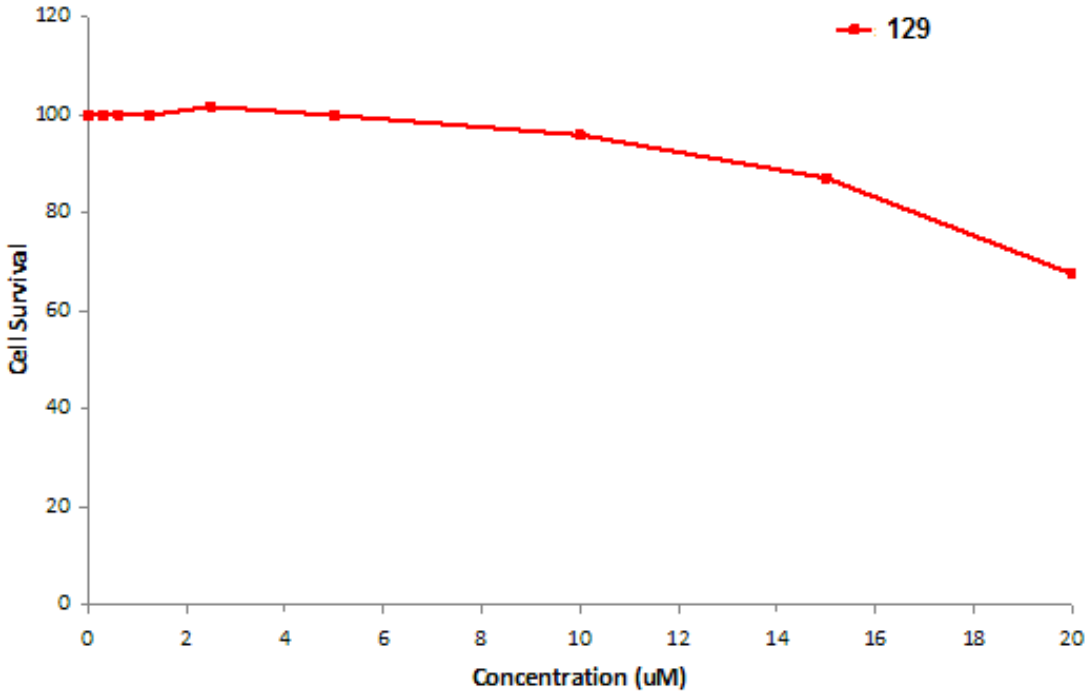

Figure 5.7: IC_{50} plot for compound **129** in the H1299 cell line.

Table 5.5: IC_{50} values for selected compounds, reference compound **28**, carboplatin and cisplatin against human lung carcinoma cell line H1299.

Compound Name	**No.**	**IC_{50}**
Cisplatin	**8**	1.5 ± 0.10
Carboplatin	**9**	10 ± 1.60
N- {*meta*-(ferrocenyl)-benzoyl} Gly L-Ala(OEt)	**28***	4.0 ± 0.71
N-{5-(ferrocenyl) ethynyl-2-furanoyl} Gly Gly(OEt)	**129**	23 ± 5.14

From the results obtained, compound **129** displayed an IC_{50} value of 23 ± 5.14 μM and was less cytotoxic *in vitro* than the clinically employed cisplatin and carboplatin which had IC_{50} values of 1.50 ± 0.10 μM and 10 ± 1.60 μM respectively. In addition, when compared to the *N*-{*para*-(ferrocenyl) ethynyl benzoyl} and *N*-{6-(ferrocenyl) ethynyl-2-naphthoyl} glycine glycine ethyl esters with IC_{50} values of 6.9 ± 2.14 μM and 5.0 ± 4.12 μM respectively, compound **129** was also less cytotoxic than the two derivatives. As a result it can be concluded that the furanoyl ring is not a bioactive aromatic conjugate linker that promotes anti-proliferative effect in H1299 lung cancer line.

5.4 Conclusion

The biological evaluation of *N*-{*para*-(ferrocenyl) ethynyl benzoyl}, *N*-{6-(ferrocenyl) ethynyl-2-naphthoyl} and *N*-{5-(ferrocenyl) ethynyl-2-furanoyl} amino acid and dipeptide esters was carried out in the H1299 lung cancer cell line. The most active derivative *N*-{6-(ferrocenyl) ethynyl-2-naphthoyl} sarcosine L-alanine ethyl ester **122** displayed an IC_{50} value of 3.2 ± 2.64 μM. This compound is more active than the clinically used carboplatin but is less effective than cisplatin. A general trend can be seen between the *N*-{*para*-(ferrocenyl) ethynyl benzoyl} and *N*-{6-(ferrocenyl) ethynyl-2-naphthoyl} amino acid and dipeptide esters. The Gly Gly, Sar L-Ala,
L-Pro Gly, L-Pro L-Ala ethyl esters of the *N*-{6-(ferrocenyl) ethynyl-2-naphthoyl} derivatives are more active than the *N*-{*para*-(ferrocenyl) ethynyl benzoyl}derivatives whilst the Gly L-Ala and GABA esters of the *N*-{*para*-(ferrocenyl) ethynyl benzoyl} derivatives are more active than the *N*-{6-(ferrocenyl) ethynyl-2-naphthoyl} derivatives.

From the SAR studies carried out it has been clearly demonstrated that the presence of the ethynyl moiety does not result in any significant enhancement of the anti-proliferative effect of the *N*-(ferrocenyl) benzoyl and naphthoyl dipeptide derivatives. However, the incorporation of a methyl derivative to the unsubstituted cyclopentadiene ring of the *N*-(ferrocenyl) benzoyl dipeptide derivatives showed an enhancement of the anti-proliferative effect. Thus, the incorporation of a methyl group to the most active *N*-{6-(ferrocenyl)-2-napthoyl} glycine glycine ethyl ester **31** with an IC_{50} value of 0.13 ± 0.01 μM could result in the formulation of a potent novel bioorganometallic anticancer agent.

References

1 Goel, A., Savage, D., Alley, S.R., Kelly, P.N., O'Sullivan, D., Mueller-Bunz, H., and Kenny, P.T.M., *J. Organomet. Chem*., **2007**, *692*, 1292-1299.

2 Goel, A., Savage, D., Alley, S.R., Hogan, T., Kelly, P.N., Draper, S., Fitchett C.M., and Kenny P.T.M, *J. Organomet. Chem*., **2006**, *691*, 4686-4693.

3 Corry, A.J., Goel, A., Alley, S.R., Kelly, P.N., O'Sullivan, D., Savage, D., and Kenny, P.T.M., *J. Organomet. Chem*., **2007** *692*, 1405-1410

4 Corry, A.J., Mooney, A., O'Sullivan, D., and Kenny, P.T.M., *Inorganica Chimica* Acta., **2009**, *362*, 2957-2961.

5 Corry, A.J., O'Donovan, N., Mooney, A., O'Sullivan, D., Rai, D.K., Kenny, P.T.M., *J. Organomet. Chem*., **2009**, *694*, 880-885.

6 Mooney, A., Corry, A.J., O'Sullivan, D., Rai, D.K., and Kenny, P.T.M., *J. Organomet. Chem*., **2009**, *694*, 886-894

7 Mooney, A., Corry, A.J., N'i Ruairc, C., Mahgoub, T., O'Sullivan, D., O'Donovan, N., Crown, J., Varughese, S., Draper, S.M., Rai, D.K., and Kenny, P.T.M., *Dalton. Trans*., **2010**, *39*, 8228–8239

8 Mooney, A., Tiedt, R., Maghoub, T., O'Sullivan, D., O'Donovan, N., Crown, J., Varughese, S., White, B., and Kenny, P.T.M., *J. Med. Chem*., **2012**, *55*, 5455−5466

Chapter 6: Experimental data

Experimental note

Chemicals used were purchased from Sigma-Aldrich and TCI. Commercial grade reagents were used without further purification and where necessary solvents were dried over magnesium sulphate ($MgSO_4$) prior to use. Nuclear magnetic resonance spectra (NMR) were obtained using a Bruker AC 400 NMR spectrometer operating at 400 MHz for ^{1}H NMR and 100 MHz for ^{13}C NMR. Chemical shifts are reported as δ-values (ppm) relative to trimethylsilane (δ = 0.00 ppm) and all coupling constants (*J*) are in Hertz. Melting points were determined using a Griffin melting point apparatus and are uncorrected. Infrared spectra were recorded on a Nicolet 405 FT-IR spectrometer and melting points were determined using a Griffin melting point apparatus. The IR spectra for solids were obtained in a potassium bromide matrix, spectra for liquids were obtained from thin films between NaCl discs. Column chromatography was performed on silica gel (40 mesh, 60Å, Fisher). UV-Vis were recorded on a Hewlett-Packard 8452A diode array UV-Vis spectrophotometer. Electrospray ionization mass spectra were performed on a Micromass LCT mass spectrometer or a Brüker Daltonics Esquire-LC ion trap mass spectrometer. Tandem mass spectra were obtained on a Micromass Quattro *micro* ™. LC-MS/MS triple quadrupole mass spectrometer.

General procedure for the synthesis of the starting materials

Ferrocene carboxyaldehyde (48) [1]

Ferrocene (50 g, 268.76 mmol) was dissolved with dry dichloromethane (150 ml) at 0 °C under nitrogen. *N*,*N*-dimethylformamide (38 ml) was added slowly over 10 min. Phosphorus oxychloride (138 ml) was added slowly over 3 hr and the reaction mixture was allowed to reflux at 40 °C for 48 hr under nitrogen. The reaction mixture was poured onto ice and neutralised with conc. sodium hydroxide solution. The resulting solution was extracted with diethyl ether. The solvent was evaporated to yield the crude product which was purified by column chromatography (eluent 9:1 hexane: diethyl ether) yielding the title compound as deep purple crystals. (24 g, 42%), mp. 120 -121 °C (lit. [1] 120 - 122 °C);

^{1}H NMR (400 MHz) δ (DMSO- d_6): 9.88 (1H, s, -C<u>H</u>O), 4.73 (2H, s, *ortho* on η^5-C_5<u>H</u>$_4$-CHO), 4.54 (2H, s, *meta* on η^5-C_5<u>H</u>$_4$-CHO), 4.21 (5H, s, η^5-C_5<u>H</u>$_5$);

^{13}C NMR (100 MHz) δ (DMSO- d_6): 193.5 (C=O), 71.4 (C_{ipso} η^5-<u>C</u>$_5$H$_4$-CHO), 69.9 (C_{meta} η^5-<u>C</u>$_5$H$_4$-CHO), 69.7 (C_{ortho} η^5-<u>C</u>$_5$H$_4$-CHO), 67.8 (η^5-<u>C</u>$_5$H$_5$).

Acetylferrocene (49) [2]

Ferrocene (50 g, 268.76 mmol) was dissolved in acetic anhydride (180 ml) and the reaction mixture was allowed to stir for 10 min. Phosphoric acid (50 ml) was added slowly to the reaction mixture over 30 min. Reaction mixture was refluxed at 70 °C for 15 min. The reaction mixture was poured onto ice and neutralised with conc. sodium hydroxide solution. The resulting solution was extracted with diethyl ether. The solvent was evaporated to yield the crude product which was purified by column chromatography (eluent 9:1 hexane: diethyl ether) yielding the title compound as a red solid. (50 g, 82%), mp. 82 - 83 °C (lit. [2] 81 - 83 °C);

^{1}H NMR (400 MHz) δ (DMSO- d_6): 4.78 (2H, t, J =1.2 Hz, *ortho* on η^5-C_5<u>H</u>$_4$-COCH$_3$), 4.57 (2H, t, J =1.2 Hz, *meta* on η^5-C_5<u>H</u>$_4$-COCH$_3$), 4.21 (5H, s, η^5-C_5<u>H</u>$_5$), 2.35 (3H, s, -COC<u>H</u>$_3$);

^{13}C NMR (100 MHz) δ (DMSO- d_6): 200.1 (C=O), 71.8 (C_{ipso} η^5-<u>C</u>$_5$H$_4$-COCH$_3$), 70.1 (C_{meta} η^5-<u>C</u>$_5$H$_4$-COCH$_3$), 68.7 (C_{ortho} η^5-<u>C</u>$_5$H$_4$-COCH$_3$), 63.5 (η^5-<u>C</u>$_5$H$_5$), 27.7 (η^5-C$_5$H$_4$-COC<u>H</u>$_3$).

Propionyl ferrocene (50)

Ferrocene (50 g, 268.76 mmol) was dissolved with propionic anhydride (150 ml) and reaction mixture was allowed to stir for 10 min. Phosphoric acid (38 ml) was added slowly to the reaction mixture over 30 min. Reaction mixture was refluxed at 80 °C for 15 min. The reaction mixture was poured onto ice and neutralised with conc. sodium hydroxide solution. The resulting solution was extracted with with ethyl acetate. The solvent was evaporated to yield the crude product which was purified by column chromatography (eluent 9:1 hexane: diethyl ether) yielding the title compound as a dark brown oil. (34 g, 52%),

^{1}H NMR (400 MHz) δ (DMSO- d_6): 4.71 (2H, s, *ortho* on η^5-$C_5\underline{H}_4$-$COCH_2CH_3$), 4.50 (2H, s, *meta* on η^5-$C_5\underline{H}_4$-$COCH_2CH_3$), 4.19 (5H, s, η^5-$C_5\underline{H}_5$), 2.78 (2H, q, J = 7.2 Hz, -$COC\underline{H}_2CH_3$), 1.27 (3H, t, J = 7.2 Hz, -$COCH_2C\underline{H}_3$);

^{13}C NMR (100 MHz) δ (DMSO- d_6): 200.1 (C=O), 71.8 (C_{ipso} η^5-$\underline{C}_5H_4$-$COCH_2CH_3$), 70.1 (C_{meta} η^5-$\underline{C}_5H_4$-$COCH_2CH_3$), 68.4 (C_{ortho} η^5-$\underline{C}_5H_4$-$COCH_2CH_3$), 65.5 (η^5-$\underline{C}_5H_5$), 60.6 (-$CO\underline{CH}_2CH_3$, -ve DEPT), 17.7 (-$COCH_2\underline{CH}_3$).

Methylferrocene (51)

Lithium aluminum hydride (1.42 g, 37.38 mmol) was dissolved in dry diethyl ether (100 ml) under nitrogen at 0 ^{o}C. Ferrocene carboxyaldehyde (4.00 g, 18.69 mmol) was then added slowly followed by anhydrous aluminum chloride (4.98 g, 37.38 mmol). The reaction mixture was than allowed to reflux at 55 ^{o}C for 12 h. The reaction mixture was then quenched in ice. The ether layer was washed with water and dried over $MgSO_4$. The solvent was removed *in vacuo* to yield the crude product which was purified by column chromatography {eluent 3:2 hexane: diethyl ether} yielding the title product as a red oil (3.20 g, 80%),

^{1}H NMR (400 MHz) δ (DMSO- d_6): 4.12 (5H, s, η^5-$C_5\underline{H}_5$), 4.09 (2H, s, *meta* on η^5-$C_5\underline{H}_4$-alkyl), 4.02 (2H, s, *ortho* on η^5-$C_5\underline{H}_4$-alkyl), 1.95 (3H, s, -$\underline{CH}_3$);

^{13}C NMR (100 MHz) δ (DMSO- d_6): 89.5 (C_{ipso} η^5-$\underline{C}_5H_4$-alkyl), 67.1 (C_{meta} η^5-$\underline{C}_5H_4$-CH_3), 65.1 (C_{ortho} η^5-$\underline{C}_5H_4$-alkyl), 65.8 (η^5-$\underline{C}_5H_5$), 14.0 (-$\underline{CH}_3$).

1-methyl-1'-*para*-ferrocenyl ethyl benzoate (52)

Ethyl-4-aminobenzoate (4.13 g, 25.00 mmol) was dissolved in deionised water (30 ml) at 0 ^{o}C followed by addition of concentrated HCl (7 ml). Sodium nitrite (1.72 g, 25.00 mmol) was dissolved in deionised water (20 ml) at 0 ^{o}C and was then added to the ethyl-4-aminobenzoate solution with stirring at a temperature less than 5 ^{o}C. The resulting pale yellow diazonium salt was then added to a solution of methylferrocene (5.00 g, 25.00 mmol) in dry diethyl ether (100 ml) and the reaction mixture was allowed to stir at room temperature for 48 h. The reaction mixture was then washed with water and brine and the organic layer was dried over $MgSO_4$. The solvent was removed *in vacuo* to yield the crude product. The crude product was purified by column chromatography {eluent 3:2 hexane: diethyl ether} yielding the title product as a red oil (1.45 g, 16%),

^{1}H NMR (400 MHz) δ (DMSO- d_6): 7.87 (2H, d, J = 7.4 Hz, Ar<u>H</u>), 7.62 (2H, d, J = 7.4 Hz, Ar<u>H</u>), 4.82 (2H, s, *ortho* on η^5-C_5<u>H</u>$_4$-benzoyl), 4.38 (2H, s, *meta* on η^5-C_5<u>H</u>$_4$-benzoyl), 4.32 (2H, q, J = 6.8 Hz, -O<u>CH$_2$</u>CH$_3$), 3.90 (4H, dd, η^5-C_5<u>H</u>$_4$-alkyl), 1.60 (3H, s, -C<u>H$_3$</u>), 1.19 (3H, t, J = 6.8 Hz, -OCH$_2$<u>CH$_3$</u>);

^{13}C NMR (100 MHz) δ (DMSO- d_6): 169.0 (C=O), 140.3 (C_q), 128.3 (C_q), 127.0, 125.4, 90.0 (C_{ipso} η^5-<u>C</u>$_5$H$_4$-alkyl), 85.7 (C_{ipso} η^5-<u>C</u>$_5$H$_4$-benzoyl), 71.1 (C_{meta} η^5-<u>C</u>$_5$H$_4$-benzoyl), 69.8 (C_{meta} η^5-<u>C</u>$_5$H$_4$-alkyl), 68.5 (C_{ortho} η^5-<u>C</u>$_5$H$_4$-alkyl), 67.0 (C_{ortho} η^5-<u>C</u>$_5$H$_4$-benzoyl), 61.3 (-O<u>CH$_2$</u>CH$_3$, -ve DEPT), 14.4 (-OCH$_2$<u>CH$_3$</u>), 13.9 (-<u>CH$_3$</u>).

1-methyl-1'-*para*-ferrocenyl benzoic acid (53)

1-methyl-1'-*para*-ferrocenyl ethyl benzoate (1.45 g, 4.00 mmol) was dissolved in methanol (50 ml) and a 10% v/v sodium hydroxide solution (50 ml) was then added. The reaction mixture was then allowed to reflux at 80 ^{o}C for 12 h. The reaction mixture was then cooled to 0 ^{o}C and conc. HCl was added until the solution reached pH 2. The product was isolated by filtration and recrystallisation from chloroform furnished the desired product as an orange solid (0.60 g, 47%),

^{1}H NMR (400 MHz) δ (DMSO- d_6): 12.85 (1H, s, -COO<u>H</u>), 7.89 (2H, d, J = 7.2 Hz, Ar<u>H</u>), 7.68 (2H, t, J = 7.2 Hz, Ar<u>H</u>), 4.89 (2H, s, *ortho* on η^5-C_5<u>H</u>$_4$-benzoyl) , 4.41 (2H, s, *meta* on η^5-C_5<u>H</u>$_4$-benzoyl), 3.95 (4H, dd, η^5-C_5<u>H</u>$_4$-alkyl), 1.62 (3H, s, -C<u>H$_3$</u>);

^{13}C NMR (100 MHz) δ (DMSO- d_6): 169.9 (C=O), 140.3 (C_q), 128.4 (C_q), 127.1, 125.4, 92.6 (C_{ipso} η^5-$\underline{C}_5H_4$-alkyl), 82.7 (C_{ipso} η^5-$\underline{C}_5H_4$-benzoyl), 71.0 (C_{meta} η^5-$\underline{C}_5H_4$-benzoyl), 68.1 (C_{meta} η^5-$\underline{C}_5H_4$-alkyl), 68.6 (C_{ortho} η^5-$\underline{C}_5H_4$-alkyl), 67.2 (C_{ortho} η^5-$\underline{C}_5H_4$-benzoyl), 14.0 (-$\underline{C}H_3$).

1-methyl-1'-*para*-ferrocenyl benzoic acid (53) via diazonium coupling using 4-amino benzoic acid

4-Aminobenzoic acid (3.43 g, 25.00 mmol) was dissolved in deionised water (30 ml) at 0 ^oC followed by the addition of concentrated HCl (7 ml). Sodium nitrite (1.72 g, 25.00 mmol) was dissolved in deionised water (20 ml) at 0 ^oC and was then added to the ethyl-4-aminobenzoic solution with stirring at a temperature less than 5 ^oC. The resulting pale yellow diazonium salt was then added to a solution of methylferrocene (5.00 g, 25.00 mmol) in dry diethyl ether (100 ml) and the reaction mixture was allowed to stir at room temperature for 48 h. The reaction mixture was then washed with water and brine and the organic layer was dried over $MgSO_4$. The solvent was removed *in vacuo* to yield the crude product. The crude product was purified by column chromatography {eluent 1:1 hexane: ethyl acetate} yielding the title product as a red oil (1.65 g, 21%),

^{1}H NMR (400 MHz) δ (DMSO- d_6): 12.80 (1H, s, -COO$\underline{H}$), 7.79 (2H, d, J = 7.2 Hz, Ar$\underline{H}$), 7.67 (2H, d, J = 7.2 Hz, Ar$\underline{H}$), 4.89 (2H, s, *ortho* on η^5-$C_5\underline{H}_4$-benzoyl), 4.41 (2H, s, *meta* on η^5-$C_5\underline{H}_4$-benzoyl), 3.90 (4H, dd, η^5-$C_5\underline{H}_4$-alkyl), 1.62 (3H, s, -$\underline{C}H_3$);

^{13}C NMR (100 MHz) δ (DMSO- d_6): 174.3 (C=O), 140.1 (C_q), 132.4 (C_q), 126.5, 123.9, 91.6 (C_{ipso} η^5-$\underline{C}_5H_4$-alkyl), 80.7 (C_{ipso} η^5-$\underline{C}_5H_4$-benzoyl), 73.2 (C_{meta} η^5-$\underline{C}_5H_4$-benzoyl), 69.8(C_{meta} η^5-$\underline{C}_5H_4$-alkyl), 68.0 (C_{ortho} η^5-$\underline{C}_5H_4$-alkyl), 67.5 (C_{ortho} η^5-$\underline{C}_5H_4$-benzoyl), 13.1(-$\underline{C}H_3$).

1-methyl-1'-*meta*-ferrocenyl benzoic acid (54)

3-Aminobenzoic acid (3.43 g, 25.00 mmol) and methylferrocene (5.00 g, 25.00 mmol) was used as starting materials. The title product was isolated by filtration and recrystallisation from chloroform furnished the desired product as an orange solid (1.46 g, 18%),

^{1}H NMR (400 MHz) δ (DMSO- d_6): 12.85 (1H, s, -COOH), 8.00 (1H, s, ArH), 7.69 (2H, m, ArH), 7.36 (1H, t, J = 7.2 Hz, ArH), 4.87 (2H, s, *ortho* on η^5-C_5H_4-benzoyl), 4.41 (2H, s, *meta* on η^5-C_5H_4-benzoyl), 3.96 (4H, dd, η^5-C_5H_4-alkyl), 1.62 (3H, s, -CH_3);

^{13}C NMR (100 MHz) δ (DMSO- d_6): 170.3 (C=O), 136.5 (C_q), 135.8 (C_q), 129.4, 128.2, 127.3, 125.1, 90.0 (C_{ipso} η^5-C_5H_4-alkyl), 83.2 (C_{ipso} η^5-C_5H_4-benzoyl), 72.2 (C_{meta} η^5-C_5H_4-benzoyl), 68.8 (C_{meta} η^5-C_5H_4-alkyl), 68.0 (C_{ortho} η^5-C_5H_4-alkyl), 67.3 (C_{ortho} η^5-C_5H_4-benzoyl), 13.9 (-CH_3).

1-methyl-1'-*ortho*-ferrocenyl benzoic acid (55)

2-Aminobenzoic acid (3.43 g, 25.00 mmol) and methylferrocene (5.00 g, 25.00 mmol) was used as starting materials. The title product was isolated by filtration and recrystallisation from chloroform furnished the desired product as an orange solid (1.26 g, 16%),

^{1}H NMR (400 MHz) δ (DMSO- d_6): 12.85 (1H, s, -COOH), 7.95 (1H, d, J = 7.6 Hz, ArH), 7.77 (1H, t, J = 7.2 Hz, ArH), 7.65 (1H, t, J = 6.4 Hz, ArH), 7.40 (1H, d, J = 7.6 Hz, ArH), 4.89 (2H, s, *ortho* on η^5-C_5H_4-benzoyl), 4.41 (2H, s, *meta* on η^5-C_5H_4-benzoyl), 3.95 (4H, dd, η^5-C_5H_4-alkyl), 1.62 (3H, s, -CH_3);

^{13}C NMR (100 MHz) δ (DMSO- d_6): 171.3 (C=O), 140.3 (C_q), 137.5 (C_q), 130.4, 128.7, 126.3, 125.9, 92.6 (C_{ipso} η^5-C_5H_4-alkyl), 80.7 (C_{ipso} η^5-C_5H_4-benzoyl), 73.9 (C_{meta} η^5-C_5H_4-benzoyl), 68.2 (C_{meta} η^5-C_5H_4-alkyl), 67.9 (C_{ortho} η^5-C_5H_4-alkyl), 67.0 (C_{ortho} η^5-C_5H_4-benzoyl), 13.5 (-CH_3).

Ethylferrocene (56)

For compound **56** acetyl ferrocene (4.00 g, 17.54 mmol) was used as a starting material. The crude product was purified by column chromatography {eluent 3:2 hexane: diethyl ether} yielding the titled product as a red oil (3.12 g, 83%),

^{1}H NMR (400 MHz) δ (DMSO- d_6): 4.12 (5H, s, η^5-C_5H_5), 4.10 (2H, t, J = 1.6 Hz, *meta* on η^5-C_5H_4-alkyl), 4.09 (2H, t, J =1.6 Hz, η^5-C_5H_4-alkyl), 2.31 (2H, q, J =7.6 Hz, -CH_2CH_3), 1.14 (3H, t, J = 7.6 Hz, -CH_2CH_3);

^{13}C NMR (100 MHz) δ (DMSO- d_6): 90.5 (C_{ipso} η^5-$\underline{C}_5H_4$-alkyl), 68.1 (C_{meta} η^5-$\underline{C}_5H_4$-alkyl), 67.1 (C_{ortho} η^5-$\underline{C}_5H_4$-alkyl), 66.8 (η^5-$\underline{C}_5H_5$), 21.7 (-$\underline{C}H_2CH_3$, -ve DEPT), 14.5 (-$CH_2\underline{C}H_3$).

Ethylferrocene (56) via Suzuki cross coupling

Ferroceneboronic acid (0.50 g, 2.17 mmol), iodoethane (0.34 g, 2.17 mmol), {1,1-bis-(diphenylphosphino) ferrocene}dichloropalladium(II) (0.08 g) was dissolved in dimethoxyethane (40 ml) and 5 ml of 3M NaOH was added. The reaction was refluxed for 72 h. Water (30 ml) was added and the reaction was extracted with chloroform (150 ml). The combined organic layers were then washed with water (150 ml) and dried over $MgSO_4$. The solvent was removed *in vacuo* to yield the crude product. The crude product was purified by column chromatography {eluent 3:2 hexane: diethyl ether} yielding the titled product as a red oil (0.10 g, 20%)

1-ethyl-1'-*para*-ferrocenyl benzoic acid (57)

4-Aminobenzoic acid (3.20 g, 23.36 mmol) was dissolved in deionised water (30 ml) at 0 ^oC followed by the addition of concentrated HCl (7 ml). Sodium nitrite (1.61 g, 23.36 mmol) was dissolved in deionised water (20 ml) at 0 ^oC and was then added to the ethyl-4-aminobenzoic solution with stirring at a temperature less than 5 ^oC. The resulting pale yellow diazonium salt was then added to a solution of ethylferrocene (5.00 g, 23.36 mmol) in dry diethyl ether (100 ml) and the reaction mixture was allowed to stir at room temperature for 48 h. The reaction mixture was then washed with water and brine and the organic layer was dried over $MgSO_4$. The solvent was removed *in vacuo* to yield the crude product. The title product was isolated by filtration and recrystallisation from chloroform furnished the desired product as an orange solid (1.80 g, 23%),

^{1}H NMR (400 MHz) δ (DMSO- d_6): 12.85 (1H, s, -COO$\underline{H}$), 7.86 (2H, d, J = 7.6 Hz, Ar$\underline{H}$), 7.62 (2H, d, J = 7.6 Hz, Ar$\underline{H}$), 4.82 (2H, t, J =1.6 Hz, *ortho* on η^5-$C_5\underline{H}_4$-benzoyl), 4.31 (2H, t, J =1.6 Hz, *meta* on η^5-$C_5\underline{H}_4$-benzoyl), 3.91 (4H, dd, η^5-$C_5\underline{H}_4$-alkyl), 2.04 (2H, q, J = 7.2 Hz, -$\underline{C}H_2CH_3$), 0.97 (3H, t, J = 7.2 Hz, -$CH_2\underline{C}H_3$);

^{13}C NMR (100 MHz) δ (DMSO- *d*$_6$): 167.3 (C=O), 144.3 (C_q), 129.4 (C_q), 127.5, 125.4, 91.6 (C_{ipso} η^5-$\underline{C}_5H_4$-alkyl), 81.3 (C_{ipso} η^5-$\underline{C}_5H_4$-benzoyl), 70.2 (C_{meta} η^5-$\underline{C}_5H_4$-benzoyl), 68.8 (C_{meta} η^5-$\underline{C}_5H_4$-alkyl), 68.6 (C_{ortho} η^5-$\underline{C}_5H_4$-alkyl), 67.0 (C_{ortho} η^5-$\underline{C}_5H_4$-benzoyl), 20.7 (-$\underline{CH_2}CH_3$, -ve DEPT), 14.4 (-$CH_2\underline{CH_3}$).

1-ethyl-1'-*meta*-ferrocenyl benzoic acid (58)

3-Aminobenzoic acid (3.20 g, 23.36 mmol) and ethylferrocene (5.00 g, 23.36 mmol) was used as starting materials. The title product was isolated by filtration and recrystallisation from chloroform furnished the desired product as an orange solid (1.48 g, 19%),

^{1}H NMR (400 MHz) δ (DMSO- *d*$_6$): 12.85 (1H, s, -COO$\underline{H}$), 8.05 (1H, s, Ar$\underline{H}$), 7.70 - 7.66 (2H, m, Ar$\underline{H}$), 7.39 (1H, t, *J* = 7.2 Hz, Ar$\underline{H}$), 4.89 (2H, t, *J* =1.6 Hz, *ortho* on η^5-$C_5\underline{H}_4$-benzoyl), 4.41 (2H, t, *J* =1.6 Hz, *meta* on η^5-$C_5\underline{H}_4$-benzoyl), 3.95 (4H, dd, η^5-$C_5\underline{H}_4$-alkyl), 2.31 (2H, q, *J* =7.6 Hz, -$\underline{CH_2}CH_3$), 1.14 (3H, t, *J* = 7.6 Hz, -$CH_2\underline{CH_3}$);

^{13}C NMR (100 MHz) δ (DMSO- *d*$_6$): 169.3 (C=O), 139.5 (C_q), 135.8 (C_q), 132.4, 128.7, 127.7, 125.9, 91.6 (C_{ipso} η^5-$\underline{C}_5H_4$-alkyl), 81.7 (C_{ipso} η^5-$\underline{C}_5H_4$-benzoyl), 71.2 (C_{meta} η^5-$\underline{C}_5H_4$-benzoyl), 68.8 (C_{meta} η^5-$\underline{C}_5H_4$-alkyl), 68.6 (C_{ortho} η^5-$\underline{C}_5H_4$-alkyl), 66.9 (C_{ortho} η^5-$\underline{C}_5H_4$-benzoyl), 23.0 (-$\underline{CH_2}CH_3$,-ve DEPT), 13.5 (-$CH_2\underline{CH_3}$).

1-ethyl-1'-*ortho*-ferrocenyl benzoic acid (59)

2-Aminobenzoic acid (3.20 g, 23.36 mmol) and ethylferrocene (5.00 g, 23.36 mmol) was used as starting materials. The title product was isolated by filtration and recrystallisation from chloroform furnished the desired product as an orange solid (1.29 g, 17%),

^{1}H NMR (400 MHz) δ (DMSO- *d*$_6$): 12.85 (1H, s, -COO$\underline{H}$), 7.97 (1H, d, *J* = 7.6 Hz, Ar$\underline{H}$), 7.74 (1H, t, *J* = 7.2 Hz, Ar$\underline{H}$), 7.62 (1H, t, *J* = 6.4 Hz, Ar$\underline{H}$), 7.44 (1H, d, *J* = 7.6 Hz, Ar$\underline{H}$), 4.89 (2H, t, *J* =1.6 Hz, *ortho* on η^5-$C_5\underline{H}_4$-benzoyl), 4.41 (2H, t, *J* =1.6 Hz, *meta* on η^5-$C_5\underline{H}_4$-benzoyl), 3.95 (4H, dd, η^5-$C_5\underline{H}_4$-alkyl), 2.32 (2H, q, *J* =7.6 Hz, -$\underline{CH_2}CH_3$), 1.13 (3H, t, *J* = 7.6 Hz, -$CH_2\underline{CH_3}$);

^{13}C NMR (100 MHz) δ (DMSO- *d*$_6$):169.3 (C=O), 140.3 (C_q), 135.8 (C_q), 131.4, 127.2, 126.3, 125.1, 89.6 (C_{ipso} η^5-$\underline{C}_5H_4$-alkyl), 80.7 (C_{ipso} η^5-$\underline{C}_5H_4$-benzoyl), 70.2 (C_{meta} η^5-

$\underline{C}_5H_4$-benzoyl), 68.8 (C_{meta} η^5-$\underline{C}_5H_4$-alkyl), 68.6 (C_{ortho} η^5-$\underline{C}_5H_4$-alkyl), 67.0 (C_{ortho} η^5-$\underline{C}_5H_4$-benzoyl), 22.7 (-$\underline{CH_2}CH_3$, -ve DEPT), 14.0 (-$CH_2\underline{CH_3}$).

Propylferrocene (60)

For compound **60** propionyl ferrocene (4.00 g, 16.53 mmol) was used as a starting material. The crude product was purified by column chromatography {eluent 3:2 hexane: diethyl ether} yielding the titled product as a red oil (3.16 g, 84%),

^{1}H NMR (400 MHz) δ (DMSO- d_6): 4.13 (5H, s, η^5-$C_5\underline{H}_5$), 4.09 (2H, s, *meta* on η^5-$C_5\underline{H}_4$-alkyl), 4.05 (2H, s, *ortho* on η^5-$C_5\underline{H}_4$-alkyl), 2.31 (2H, t, J = 7.6 Hz, -$\underline{CH_2}CH_2CH_3$), 1.54 - 1.45 (2H, m, -$CH_2\underline{CH_2}CH_3$), 0.92 (3H, t, J = 7.2 Hz, -$CH_2CH_2\underline{CH_3}$);

^{13}C NMR (100 MHz) δ (DMSO- d_6): 91.5 (C_{ipso} η^5-$\underline{C}_5H_4$-alkyl), 69.1 (C_{meta} η^5-$\underline{C}_5H_4$-alkyl), 68.1 (C_{ortho} η^5-$\underline{C}_5H_4$-alkyl), 66.8 (η^5-$\underline{C}_5H_5$), 30.3 (-$\underline{CH_2}CH_2CH_3$, -ve DEPT), 22.7 (-$CH_2\underline{CH_2}CH_3$, -ve DEPT), 14.4 (-$CH_2CH_2\underline{CH_3}$).

1-propyl-1'-*para*-ferrocenyl benzoic acid (61)

4-Aminobenzoic acid (3.01 g, 21.93 mmol) was dissolved in deionised water (30 ml) at 0 ^oC followed by the addition of concentrated HCl (7 ml). Sodium nitrite (1.51 g, 21.93 mmol) was dissolved in deionised water (20 ml) at 0 ^oC and was then added to the ethyl-4-aminobenzoic solution with stirring at a temperature less than 5 ^oC. The resulting pale yellow diazonium salt was then added to a solution of propyl ferrocene (5.00 g, 21.93 mmol) in dry diethyl ether (100 ml) and the reaction mixture was allowed to stir at room temperature for 48 h. The reaction mixture was then washed with water and brine and the organic layer was dried over $MgSO_4$. The solvent was removed *in vacuo* to yield the crude product. The title product was isolated by filtration and recrystallisation from chloroform furnished the desired product as an orange solid (1.61 g, 21%),

^{1}H NMR (400 MHz) δ (DMSO- d_6): 12.85 (1H, s, -COO$\underline{H}$), 7.86 (2H, d, J = 7.4 Hz, Ar$\underline{H}$), 7.62 (2H, d, J = 7.4 Hz, Ar$\underline{H}$), 4.82 (2H, s, *ortho* on η^5-$C_5\underline{H}_4$-benzoyl), 4.38 (2H, s, *meta* on η^5-$C_5\underline{H}_4$-benzoyl), 3.92 (4H, dd, η^5-$C_5\underline{H}_4$-alkyl), 1.94 (2H, t, J = 7.6 Hz, -

$\underline{CH_2}CH_2CH_3$), 1.40 - 1.27 (2H, m, -$CH_2\underline{CH_2}CH_3$), 0.75 (3H, t, *J* = 7.6 Hz, -$CH_2CH_2\underline{CH_3}$);

^{13}C NMR (100 MHz) δ (DMSO- d_6): 167.3 (C=O), 144.3 (C_q), 129.3 (C_q), 127.5, 125.4, 89.3 (C_{ipso} η^5-$\underline{C_5}H_4$-alkyl), 81.7 (C_{ipso} η^5-$\underline{C_5}H_4$-benzoyl), 70.1 (C_{meta} η^5-$\underline{C_5}H_4$-benzoyl), 68.8 (C_{meta} η^5-$\underline{C_5}H_4$-alkyl), 68.5 (C_{ortho} η^5-$\underline{C_5}H_4$-alkyl), 67.0 (C_{ortho} η^5-$\underline{C_5}H_4$-benzoyl), 32.3 (-$\underline{CH_2}CH_2CH_3$, -ve DEPT), 22.0 (-$CH_2\underline{CH_2}CH_3$, -ve DEPT), 14.4 (-$CH_2CH_2\underline{CH_3}$).

1-propyl-1'-*meta*-ferrocenyl benzoic acid (62)

3-Aminobenzoic acid (3.01 g, 21.93 mmol) and propyl ferrocene (5.00 g, 21.93 mmol) was used as starting materials. The title product was isolated by filtration and recrystallisation from chloroform furnished the desired product as an orange solid (1.48 g, 19%),

^{1}H NMR (400 MHz) δ (DMSO- d_6): 12.85 (1H, s, -COO$\underline{H}$), 8.00 (1H, s, Ar$\underline{H}$), 7.65 (2H, m, Ar$\underline{H}$), 7.30 (1H, t, *J* = 7.2 Hz, Ar$\underline{H}$), 4.89 (2H, s, *ortho* on η^5-$C_5\underline{H_4}$-benzoyl), 4.41 (2H, s, *meta* on η^5-$C_5\underline{H_4}$-benzoyl), 3.95 (4H, dd, η^5 $C_5\underline{H_4}$-alkyl), 2.31 (2H, t, *J* = 7.6 Hz, -$\underline{CH_2}CH_2CH_3$), 1.54 - 1.45 (2H, m, -$CH_2\underline{CH_2}CH_3$), 0.92 (3H, t, *J* = 7.2 Hz, -$CH_2CH_2\underline{CH_3}$);

^{13}C NMR (100 MHz) δ (DMSO- d_6): 168.3 (C=O), 139.5 (C_q), 136.8 (C_q), 132.4, 128.9, 127.5, 125.7, 89.6 (C_{ipso} η^5-$\underline{C_5}H_4$-alkyl), 82.7 (C_{ipso} η^5-$\underline{C_5}H_4$-benzoyl), 72.2 (C_{meta} η^5-$\underline{C_5}H_4$-benzoyl), 68.9 (C_{meta} η^5-$\underline{C_5}H_4$-alkyl), 68.6 (C_{ortho} η^5-$\underline{C_5}H_4$-alkyl), 67.0 (C_{ortho} η^5-$\underline{C_5}H_4$-benzoyl), 31.3 (-$\underline{CH_2}CH_2CH_3$, -ve DEPT), 22.7 (-$CH_2\underline{CH_2}CH_3$, -ve DEPT), 14.4 (-$CH_2CH_2\underline{CH_3}$).

1-propyl-1'-*ortho*-ferrocenyl benzoic acid (63)

2-Aminobenzoic acid (3.01 g, 21.93 mmol) and propyl ferrocene (5.00 g, 21.93 mmol) was used as starting materials. The title product was isolated by filtration and recrystallisation from chloroform furnished the desired product as an orange solid (1.26 g, 17%),

^{1}H NMR (400 MHz) δ (DMSO- d_6): 12.85 (1H, s, -COO$\underline{H}$), 7.95 (1H, d, *J* = 7.6 Hz, Ar$\underline{H}$), 7.77 (1H, t, *J* = 7.2 Hz, Ar$\underline{H}$), 7.65 (1H, t, *J* = 6.4 Hz, Ar$\underline{H}$), 7.40 (1H, d, *J* = 7.6

Hz, Ar<u>H</u>), 4.89 (2H, s, *ortho* on η^5-C_5<u>H</u>$_4$-benzoyl), 4.41 (2H, s, *meta* on η^5-C_5<u>H</u>$_4$-benzoyl), 3.95 (4H, dd, η^5-C_5<u>H</u>$_4$-alkyl), 2.31 (2H, t, *J* = 7.6 Hz, -<u>CH$_2$</u>CH_2CH_3), 1.54 - 1.45 (2H, m, -CH_2<u>CH$_2$</u>CH_3), 0.92 (3H, t, *J* = 7.2 Hz, -CH_2CH_2<u>CH$_3$</u>);

^{13}C NMR (100 MHz) δ (DMSO- d_6): 169.3 (C=O), 138.5 (C_q), 135.8 (C_q), 130.4, 128.2, 126.3, 124.1, 90.6 (C_{ipso} η^5-<u>C</u>$_5H_4$-alkyl), 82.7 (C_{ipso} η^5-<u>C</u>$_5H_4$-benzoyl), 71.2 (C_{meta} η^5-<u>C</u>$_5H_4$-benzoyl), 68.7 (C_{meta} η^5-<u>C</u>$_5H_4$-alkyl), 68.2 (C_{ortho} η^5-<u>C</u>$_5H_4$-alkyl), 67.1 (C_{ortho} η^5-<u>C</u>$_5H_4$-benzoyl), 34.3 (-CH_2<u>CH$_2$</u>CH_3, -ve DEPT), 22.0 (-CH_2<u>CH$_2$</u>CH_3, -ve DEPT), 14.0 (-CH_2CH_2<u>CH$_3$</u>).

General procedure for the synthesis of 1-methyl-1'-*N-ferrocenyl* benzoyl dipeptide ethyl esters

1-methyl-1'-*N*-{*para* -(ferrocenyl) benzoyl} glycine glycine ethyl ester (64)

1-methyl-1'-*N-para* ferrocenyl benzoic acid (0.25 g, 0.78 mmol) was dissolved in dichloromethane (100 ml) at 0 ^oC. *N*-(3-dimethylaminopropyl)-*N*'-ethylcarbodiimide hydrochloride (0.15 g, 0.78 mmol), 1-hydroxybenotriazole (0.11 g, 0.78 mmol), glycine glycine ethyl ester hydrochloride (0.13 g, 0.78 mmol) and triethylamine (3 ml) were added and the reaction mixture was allowed to stir at 0 ^oC for 45 min. The reaction mixture was then allowed to stir at room temperature for 48 h. The reaction mixture was then washed with water and brine. The organic layer was then dried over $MgSO_4$. The solvent was removed *in vacuo* to yield the crude product. The crude product was purified by column chromatography {eluent 1:1 hexane: ethyl acetate} yielding the titled product as an orange solid (0.10 g, 28%), m.p 75 - 77 ^oC;

Mass spectrum: $[M+Na]^+$ found: 485.1289

$C_{24}H_{26}N_2O_4FeNa$ requires: 485.1291

I.R. υ_{max} (KBr): 3300 (NH), 1740 (C=O_{ester}), 1630 (C=O_{amide}), 1608 (C=O_{amide}) cm^{-1};

UV-Vis λ_{max} EtOH: 360, 451 nm;

^{1}H NMR (400 MHz) δ (DMSO- d_6): 8.76 (1H, t, *J* = 6.0 Hz, -CON<u>H</u>-), 8.35 (1H, t, *J* = 6 Hz, -CON<u>H</u>-), 7.82 (2H, d, *J* = 8.4 Hz, Ar<u>H</u>), 7.60 (2H, d, *J* = 8.4 Hz, Ar<u>H</u>), 4.80 (2H, s, *ortho* on η^5-C_5<u>H</u>$_4$-benzoyl), 4.35 (2H, s, *meta* on η^5-C_5<u>H</u>$_4$-benzoyl), 4.09 (2H, q, *J* = 7.2 Hz, -O<u>CH$_2$</u>CH_3), 3.90 - 3.80 {8H, m, (η^5-C_5<u>H</u>$_4$-alkyl), (-NH<u>CH$_2$</u>CHO-), (-NH<u>CH$_2$</u>CHO-)}, 1.58 (3H, s, -CH_3), 1.19 (3H, t, *J* = 7.2 Hz, -OCH_2<u>CH$_3$</u>);

^{13}C NMR (100 MHz) δ (DMSO- d_6): 171.5 (C=O), 168.2 (C=O), 166.5 (C=O), 142.3 (C_q), 130.8 (C_q), 127.4, 125.2, 92.3 (C_{ipso} η^5-$\underline{C}_5H_4$-alkyl), 82.0 (C_{ipso} η^5-$\underline{C}_5H_4$-benzoyl), 70.4 (C_{meta} η^5-$\underline{C}_5H_4$-benzoyl), 69.1 (C_{meta} η^5-$\underline{C}_5H_4$-alkyl), 68.4 (C_{ortho} η^5-$\underline{C}_5H_4$-alkyl), 66.2 (C_{ortho} η^5-$\underline{C}_5H_4$-benzoyl), 61.5 (-O$\underline{CH_2}$$CH_3$, -ve DEPT), 42.6 (-NH$\underline{CH_2}$CHO-, -ve DEPT), 40.7 (-NH$\underline{CH_2}$CHO-, -ve DEPT), 14.5 (-OCH$_2$$\underline{CH_3}$), 14.2 (-$\underline{C}H_3$).

1-methyl-1'-*N*-{*para*-(ferrocenyl) benzoyl} glycine L-alanine ethyl ester (65)

Glycine L-alanine ethyl ester hydrochloride (0.14 g, 0.78 mmol) was used as a starting material. The crude product was purified by column chromatography {eluent 1:1 hexane: ethyl acetate} yielding the titled product as a red oil (0.08 g, 22%),

$[\alpha]_D^{20}$ = -10 ^{o} (*c* 0.1, EtOH);

Mass spectrum: $[M+Na]^+$ found: 499.1394

$C_{25}H_{28}N_2O_4FeNa$ requires: 499.1396

I.R. υ_{max} (KBr): 3295 (NH), 1743 (C=O$_{ester}$), 1636 (C=O$_{amide}$), 1608 (C=O$_{amide}$) cm^{-1};

UV-Vis λ_{max} EtOH: 360, 451 nm;

^{1}H NMR (400 MHz) δ (DMSO- d_6): 8.67 (1H, t, *J* = 6.4 Hz, -CON$\underline{H}$-), 8.41 (1H, d, *J* = 7.0 Hz, -CON$\underline{H}$-), 7.80 (2H, d, *J* = 8.4 Hz, Ar$\underline{H}$), 7.61 (2H, d, *J* = 8.4 Hz, Ar$\underline{H}$), 4.81 (2H, s, *ortho* on η^5-$C_5\underline{H}_4$-benzoyl), 4.36 (2H, s, *meta* on η^5-$C_5\underline{H}_4$-benzoyl), 4.31 - 4.24 (1H, m, -$\underline{CH}$$CH_3$), 4.05 (2H, q, *J* = 6.8 Hz, -O$\underline{CH_2}$$CH_3$) , 3.96 - 3.85 {6H, m, (η^5-$C_5\underline{H}_4$-alkyl), (-NH$\underline{CH_2}$CO-)}, 1.60 (3H, s, -$\underline{CH_3}$), 1.31 (3H, t, *J* = 6.2 Hz, -CH$\underline{CH_3}$), 1.18 (3H, t, *J* = 6.8 Hz, -OCH$_2$$\underline{CH_3}$);

^{13}C NMR (100 MHz) δ (DMSO- d_6): 172.5 (C=O), 169.0 (C=O), 166.5 (C=O), 142.5 (C_q), 130.8 (C_q), 127.4, 125.2, 92.3 (C_{ipso} η^5-$\underline{C}_5H_4$-alkyl), 82.0 (C_{ipso} η^5-$\underline{C}_5H_4$-benzoyl), 71.0 (C_{meta} η^5-$\underline{C}_5H_4$-benzoyl), 69.8 (C_{meta} η^5-$\underline{C}_5H_4$-alkyl), 68.5 (C_{ortho} η^5-$\underline{C}_5H_4$-alkyl), 66.9 (C_{ortho} η^5-$\underline{C}_5H_4$-benzoyl), 60.9 (-O$\underline{CH_2}$$CH_3$, -ve DEPT), 47.6 (-$\underline{CH}$$CH_3$), 42.0 (-NH$\underline{CH_2}$CHO-, -ve DEPT), 17.0 (-CH$\underline{CH_3}$), 14.5 (-OCH$_2$$\underline{CH_3}$), 14.0 (-$\underline{CH_3}$).

1-methyl-1'-*N*-{*para*-(ferrocenyl) benzoyl} glycine L-leucine ethyl ester (66)

Glycine L-leucine ethyl ester hydrochloride (0.17 g, 0.78 mmol) was used as a starting material. The crude product was purified by column chromatography {eluent 1:1

hexane: ethyl acetate} and recrystallisation from hexane: ethyl acetate yield the desired product as an orange solid (0.07 g, 17%), m.p 142 - 144 ^{o}C;

$[\alpha]_D^{20}$ = -17^{o} (*c* 0.1, EtOH);

Mass spectrum: $[M+Na]^+$ found: 541.1884

$C_{28}H_{34}N_2O_4FeNa$ requires: 541.1888

I.R. υ_{max} (KBr): 3267 (NH), 1742 (C=O_{ester}), 1640 (C=O_{amide}), 1610 (C=O_{amide}) cm^{-1};

UV-Vis λ_{max} EtOH: 358, 450 nm;

^{1}H NMR (400 MHz) δ (DMSO- d_6): 8.65 (1H, t, *J* = 6.0 Hz, -CON<u>H</u>-), 8.33 (1H, d, *J* = 7.6 Hz, -CON<u>H</u>-), 7.80 (2H, d, *J* = 8.0 Hz, Ar<u>H</u>), 7.60 (2H, d, *J* = 8.0 Hz, Ar<u>H</u>), 4.82 (2H, s, *ortho* on η^5-C_5<u>H_4</u>-benzoyl), 4.37 - 4.29 {3H, m, (*meta* on η^5-C_5<u>H_4</u>-benzoyl), (-<u>CH</u>($CH_2CH(CH_3)_2$)}, 4.08 (2H, q, *J* = 7.2 Hz, -O<u>CH_2</u>CH_3), 3.96 - 3.85 {6H, m, (η^5-C_5<u>H_4</u>-alkyl), (-NH<u>CH_2</u>CO-)}, 1.63 - 1.40 {6H, m, (-<u>CH_3</u>), (-CH(<u>CH_2</u><u>CH</u>(CH_3)$_2$)}, 1.18 (3H, t, *J* = 7.2 Hz, -OCH_2<u>CH_3</u>), 0.91- 0.89 {6H, m, -CH(CH_2CH(<u>CH_3</u>)$_2$};

^{13}C NMR (100 MHz) δ (DMSO- d_6): 172.5 (C=O), 169.2 (C=O), 166.2 (C=O), 142.2 (C_q), 130.8 (C_q), 127.4, 125.2, 90.4 (C_{ipso} η^5-<u>C_5</u>H_4-alkyl), 84.2 (C_{ipso} η^5-<u>C_5</u>H_4-benzoyl), 70.1 (C_{meta} η^5-<u>C_5</u>H_4-benzoyl), 70.0 (C_{meta} η^5-<u>C_5</u>H_4-alkyl), 68.4 (C_{ortho} η^5-<u>C_5</u>H_4-alkyl), 66.9 (C_{ortho} η^5-<u>C_5</u>H_4-benzoyl), 60.4 (-O<u>CH_2</u>CH_3, -ve DEPT), 50.3 {-<u>CH</u>($CH_2CH(CH_3)_2$}, 42.0 (-NH<u>CH_2</u>CHO-, -ve DEPT), 39.4 {-CH(<u>CH_2</u>$CH(CH_3)_2$), -ve DEPT}, 24.2 {-$CH(CH_2$<u>CH</u>$(CH_3)_2$}, 22.7 (-$CH(CH_2CH$(<u>CH_3</u>)$_2$}, 21.4 {-CH(CH_2CH(<u>CH_3</u>)$_2$}, 14.0 (-OCH_2<u>CH_3</u>), 13.2 (-<u>CH_3</u>).

1-methyl-1'-*N*-{*para*-(ferrocenyl) benzoyl} glycine L-phenylalanine ethyl ester (67)

Glycine L-phenylalanine ethyl ester hydrochloride (0.20 g, 0.78 mmol) was used as a starting material. The crude product was purified by column chromatography {eluent 1:1 hexane: ethyl acetate} and recrystallisation from hexane: ethyl acetate yield the desired product as an orange solid (0.07 g, 16%), m.p 82 - 83 ^{o}C;

$[\alpha]_D^{20}$ = +6^{o} (*c* 0.1, EtOH);

Mass spectrum: $[M+Na]^+$ found: 575.1794

$C_{31}H_{32}N_2O_4FeNa$ requires: 575.1796

I.R. υ_{max} (KBr): 3263 (NH), 1735 (C=O_{ester}), 1663 (C=O_{amide}), 1609 (C=O_{amide}) cm^{-1};

UV-Vis λ_{max} EtOH: 358, 448 nm;

^{1}H NMR (400 MHz) δ (DMSO- d_6): 8.68 (1H, t, *J* = 6.4 Hz, -CONH-), 8.34 (1H, d, *J* = 7.6 Hz, -CONH-), 7.81 (2H, d, *J* = 8.4 Hz, ArH), 7.60 (2H, d, *J* = 8.4 Hz, ArH), 7.27 - 7.21 {5H, m, -CH(CH_2Ph)}, 4.80 (2H, s, *ortho* on η^5-C_5H_4-benzoyl), 4.47 - 4.45 {1H, m, -CH(CH_2Ph)}, 4.35 (2H, s, *meta* on η^5-C_5H_4-benzoyl), 4.04 (2H, q, *J* = 7.2 Hz, -OCH_2CH_3), 3.96 - 3.85 {6H, m, (η^5-C_5H_4-alkyl), (-NHCH_2CO-)}, 3.06 - 2.93 {2H, m, -CH(CH_2Ph)}, 1.57 (3H, s, -CH_3), 1.12 (3H, t, *J* = 7.2 Hz, -OCH_2CH_3);

^{13}C NMR (100 MHz) δ (DMSO- d_6): 172.4 (C=O), 169.2 (C=O), 166.3 (C=O), 142.0 (C_q) 136.9 (C_q), 130.7 (C_q), 129.1, 128.0, 127.4, 126.0, 125.2, 90.2 (C_{ipso} η^5-C_5H_4-alkyl), 82.0 (C_{ipso} η^5-C_5H_4-benzoyl), 71.4 (C_{meta} η^5-C_5H_4-benzoyl), 71.0 (C_{meta} η^5-C_5H_4-alkyl), 68.0 (C_{ortho} η^5-C_5H_4-alkyl), 66.4 (C_{ortho} η^5-C_5H_4-benzoyl), 61.4 (-OCH_2CH_3, -ve DEPT), 53.6 {-CH(CH_2Ph)}, 42.9 (-NHCH_2CHO-, -ve DEPT), 36.7 {-CH(CH_2Ph), -ve DEPT}, 14.0 (-OCH_2CH_3), 13.2 (-CH_3).

1-methyl-1'-*N*-{*meta*-(ferrocenyl) benzoyl} glycine glycine ethyl ester (68)

Glycine glycine ethyl ester hydrochloride (0.13 g, 0.78 mmol) was used as a starting material. The crude product was purified by column chromatography {eluent 1:1 hexane: ethyl acetate} yielding the titled product as a red oil (0.09 g, 25%),

Mass spectrum: $[M+Na]^+$ found: 499.1286

$C_{24}H_{26}N_2O_4FeNa$ requires: 485.1291

I.R. υ_{max} (KBr): 3350 (NH), 1751 ($C=O_{ester}$), 1627 ($C=O_{amide}$), 1602 ($C=O_{amide}$) cm^{-1};

UV-Vis λ_{max} EtOH: 333, 447 nm;

^{1}H NMR (400 MHz) δ (DMSO- d_6): 8.65 (1H, t, *J* = 6.0 Hz, -CONH-), 8.30 (1H, t, *J* = 7.6 Hz, -CONH-), 8.00 (1H, s, ArH), 7.69 - 7.67 (2H, m, ArH), 7.39 (1H, t, *J* = 7.2 Hz, ArH), 4.80 (2H, s, *ortho* on η^5-C_5H_4-benzoyl), 4.31 (2H, s, *meta* on η^5-C_5H_4-benzoyl), 4.10 (2H, q, *J* = 7.2 Hz, -OCH_2CH_3) , 3.91 - 3.82 {8H, m, (η^5-C_5H_4-alkyl), (-NHCH_2CHO-), (-NHCH_2CHO-)}, 1.61 (3H, s, -CH_3), 1.18 (3H, t, *J* = 7.2 Hz, -OCH_2CH_3);

^{13}C NMR (100 MHz) δ (DMSO- d_6): 170.5 (C=O), 167.2 (C=O), 166.5 (C=O), 136.5 (C_q), 135.8 (C_q), 129.4, 128.2, 127.3, 125.1, 92.3 (C_{ipso} η^5-C_5H_4-alkyl), 82.0 (C_{ipso} η^5-C_5H_4-benzoyl), 70.4 (C_{meta} η^5-C_5H_4-benzoyl), 69.1 (C_{meta} η^5-C_5H_4-alkyl), 68.4 (C_{ortho} η^5-C_5H_4-alkyl), 66.2 (C_{ortho} η^5-C_5H_4-benzoyl), 61.5 (-OCH_2CH_3, -ve DEPT), 42.6 (-

NH$\underline{CH_2}$CHO-, -ve DEPT), 40.7 (-NH$\underline{CH_2}$CHO-, -ve DEPT), 14.5 (-OCH$_2\underline{CH_3}$), 14.2 (-$\underline{CH_3}$).

1-methyl-1'-*N*-{meta-(ferrocenyl) benzoyl} glycine L-alanine ethyl ester (69)

Glycine L-alanine ethyl ester hydrochloride (0.14 g, 0.78 mmol) was used as a starting material. The crude product was purified by column chromatography {eluent 1:1 hexane: ethyl acetate} yielding the titled product as a red oil (0.08 g, 22%),

$[\alpha]_D^{20}$ = -13^o (*c* 0.1, EtOH);

Mass spectrum: $[M+Na]^+$ found: 499.1391

$C_{25}H_{28}N_2O_4FeNa$ requires: 499.1396

I.R. υ_{max} (KBr): 3311 (NH), 1751 (C=O$_{ester}$), 1620 (C=O$_{amide}$), 1601 (C=O$_{amide}$) cm^{-1};

UV-Vis λ_{max} EtOH: 333, 447 nm;

^{1}H NMR (400 MHz) δ (DMSO- *d*$_6$): 8.65 (1H, t, *J* = 6.0 Hz, -CON$\underline{H}$-), 8.30 (1H, d, *J* = 7.6 Hz, -CON$\underline{H}$-), 8.05 (1H, s, Ar$\underline{H}$), 7.70 - 7.69 (2H, m, Ar$\underline{H}$), 7.39 (1H, t, *J* = 7.2 Hz, Ar$\underline{H}$), 4.81 (2H, s, *ortho* on η^5-C$_5\underline{H_4}$-benzoyl), 4.34 (2H, s, *meta* on η^5-C$_5\underline{H_4}$-benzoyl), 4.30 - 4.24 (1H, m, -$\underline{CH}$CH$_3$), 4.00 (2H, q, *J* = 6.6 Hz, -O$\underline{CH_2}$CH$_3$) , 3.92 - 3.84 {6H, m, (η^5-C$_5\underline{H_4}$-alkyl), (-NH$\underline{CH_2}$CO-)}, 1.59 (3H, s, -$\underline{CH_3}$), 1.31 (3H, t, *J* = 6.2 Hz, -CH$\underline{CH_3}$), 1.15 (3H, t, *J* = 6.6 Hz, -OCH$_2\underline{CH_3}$);

^{13}C NMR (100 MHz) δ (DMSO- *d*$_6$): 170.5 (C=O), 167.0 (C=O), 166.9 (C=O), 136.5 (C$_q$), 135.8 (C$_q$), 129.0, 128.2, 126.3, 125.1, 90.3 (C$_{ipso}$ η^5-$\underline{C_5}$H$_4$-alkyl), 81.0 (C$_{ipso}$ η^5-$\underline{C_5}$H$_4$-benzoyl), 70.9 (C$_{meta}$ η^5-$\underline{C_5}$H$_4$-benzoyl), 68.4 (C$_{meta}$ η^5-$\underline{C_5}$H$_4$-alkyl), 67.5 (C$_{ortho}$ η^5-$\underline{C_5}$H$_4$-alkyl), 66.4 (C$_{ortho}$ η^5-$\underline{C_5}$H$_4$-benzoyl), 60.8 (-O$\underline{CH_2}$CH$_3$, -ve DEPT), 48.5 (-$\underline{CH}$CH$_3$), 42.2 (-NH$\underline{CH_2}$CHO-, -ve DEPT), 17.0 (-CH$\underline{CH_3}$), 14.9 (-OCH$_2\underline{CH_3}$), 14.5 (-$\underline{CH_3}$).

1-methyl-1'-*N*-{*meta*-(ferrocenyl) benzoyl} glycine L-leucine ethyl ester (70)

For compound **62** glycine L-leucine ethyl ester hydrochloride (0.17 g, 0.78 mmol) was used as a starting material. The crude product was purified by column chromatography {eluent 1:1 hexane: ethyl acetate} yielding the titled product as a red oil (0.07 g, 17%),

$[\alpha]_D^{20}$ = -19^o (*c* 0.1, EtOH);

Mass spectrum: $[M+Na]^+$ found: 541.1883

$C_{28}H_{34}N_2O_4FeNa$ requires: 541.1888

I.R. υ_{max} (KBr): 3287 (NH), 1742 (C=O_{ester}), 1649 (C=O_{amide}), 1610 (C=O_{amide}) cm^{-1};

UV-Vis λ_{max} EtOH: 330, 445 nm;

^{1}H NMR (400 MHz) δ (DMSO- *d_6*): 8.65 (1H, t, *J* = 6.0 Hz, -CONH-), 8.30 (1H, d, *J* = 7.6 Hz, -CONH-), 8.00 (1H, s, ArH), 7.69 - 7.66 (2H, m, ArH), 7.39 (1H, t, *J* = 7.0 Hz, ArH) 4.83 (2H, s, *ortho* on η^5-C_5H_4-benzoyl), 4.36 (2H, s, *meta* on η^5-C_5H_4-benzoyl), 4.35 - 4.27 {1H, m, -CH($CH_2CH(CH_3)_2$)}, 4.15 (2H, q, *J* = 7.2 Hz, -OCH_2CH_3) , 3.92 - 3.86 {6H, m, (η^5-C_5H_4-alkyl), (-NHCH_2CO-)}, 1.69 - 1.45 {6H, m, (-CH_3), (-CH($CH_2CH(CH_3)_2$)}, 1.15 (3H, t, *J* = 7.2 Hz, -OCH_2CH_3), 0.90 - 0.85 {6H, m, -CH($CH_2CH(CH_3)_2$};

^{13}C NMR (100 MHz) δ (DMSO- *d_6*): 171.7 (C=O), 169.2 (C=O), 166.8 (C=O), 136.5 (C_q), 135.8 (C_q), 129.4, 128.2, 127.3, 126.1, 86.4 (C_{ipso} η^5-C_5H_4-alkyl), 82.1 (C_{ipso} η^5-C_5H_4-benzoyl), 71.4 (C_{meta} η^5-C_5H_4-benzoyl), 70.1 (C_{meta} η^5-C_5H_4-alkyl), 68.1 (C_{ortho} η^5-C_5H_4-alkyl), 66.5 (C_{ortho} η^5-C_5H_4-benzoyl), 61.0 (-OCH_2CH_3, -ve DEPT), 51.0 {-CH($CH_2CH(CH_3)_2$)}, 42.7 (-NHCH_2CHO-, -ve DEPT), 39.5 {-CH($CH_2CH(CH_3)_2$), -ve DEPT}, 25.0{-CH($CH_2CH(CH_3)_2$)}, 22.7 {-CH($CH_2CH(CH_3)_2$)}, 21.4 {-CH($CH_2CH(CH_3)_2$)}, 14.9 (-OCH_2CH_3), 13.0 (-CH_3).

1-methyl-1'-*N*-{*meta*-(ferrocenyl) benzoyl} glycine L-phenylalanine ethyl ester (71)

Glycine L-phenyalanine ethyl ester hydrochloride (0.20 g, 0.78 mmol) was used as a starting material. The crude product was purified by column chromatography {eluent 1:1 hexane: ethyl acetate} yielding the titled product as a red oil (0.06 g, 14 %),

$[\alpha]_D^{20}$ = +8 ^{o} (*c* 0.1, EtOH);

Mass spectrum: $[M+Na]^+$ found: 575.1774

$C_{31}H_{32}N_2O_4FeNa$ requires: 575.1766

I.R. υ_{max} (KBr): 3273 (NH), 1729 (C=O_{ester}), 1653 (C=O_{amide}), 1599 (C=O_{amide}) cm^{-1};

UV-Vis λ_{max} EtOH: 333, 449 nm;

^{1}H NMR (400 MHz) δ (DMSO- *d_6*): 8.68 (1H, t, *J* = 6.0 Hz, -CONH-), 8.32 (1H, d, *J* = 7.6 Hz, -CONH-), 7.99 (1H, s, ArH), 7.71 - 7.69 (2H, m, ArH), 7.40 (1H, t, *J* = 7.0 Hz, ArH), 7.20 - 7.17 {5H, m, -CH(CH_2Ph)}, 4.83 (2H, s, *ortho* on η^5-C_5H_4-benzoyl), 4.45 - 4.40 {1H, m, -CH(CH_2Ph)}, 4.35 (2H, s, *meta* on η^5-C_5H_4-benzoyl), 4.04 (2H, q,

J = 7.2 Hz, -O<u>CH$_2$</u>CH$_3$) , 3.95 - 3.87 {6H, m, (η^5-C$_5$<u>H$_4$</u>-alkyl), (-NH<u>CH$_2$</u>CO-)}, 3.06 - 2.93 {2H, m, -CH(<u>CH$_2$</u>Ph)}, 1.55 (3H, s, -<u>CH$_3$</u>), 1.12 (3H, t, *J* = 7.2 Hz, -OCH$_2$<u>CH$_3$</u>);
^{13}C NMR (100 MHz) δ (DMSO- *d$_6$*): 170.4 (C=O), 169.2 (C=O), 166.3 (C=O), 137.2 (C$_q$), 134.9 (C$_q$), 130.3 (C$_q$), 129.1, 128.4, 127.3, 126.1, 125.5, 124.1, 122.7, 91.2 (C$_{ipso}$ η^5-<u>C$_5$</u>H$_4$-alkyl), 80.0 (C$_{ipso}$ η^5-<u>C$_5$</u>H$_4$-benzoyl), 70.4 (C$_{meta}$ η^5-<u>C$_5$</u>H$_4$-benzoyl), 70.0 (C$_{meta}$ η^5-<u>C$_5$</u>H$_4$-alkyl), 68.4 (C$_{ortho}$ η^5-<u>C$_5$</u>H$_4$-alkyl), 67.9 (C$_{ortho}$ η^5-<u>C$_5$</u>H$_4$-benzoyl), 60.8 (-O<u>CH$_2$</u>CH$_3$, -ve DEPT), 53.0 {-<u>CH</u>(CH$_2$Ph)}, 42.7 (-NH<u>CH$_2$</u>CHO-, -ve DEPT), 37.7 {-CH(<u>CH$_2$</u>Ph), -ve DEPT}, 14.1 (-OCH$_2$<u>CH$_3$</u>), 13.0 (-<u>CH$_3$</u>).

1-methyl-1'-*N*-{*ortho*-(ferrocenyl) benzoyl} glycine glycine ethyl ester (72)

Glycine glycine ethyl ester hydrochloride (0.13 g, 0.78 mmol) was used as a starting material. The crude product was purified by column chromatography {eluent 1:1 hexane: ethyl acetate} yielding the titled product as a red oil (0.08 g, 22%),
Mass spectrum: $[M+Na]^+$ found: 485.1289
$C_{24}H_{26}N_2O_4FeNa$ requires: 499.1291
I.R. υ_{max} (KBr): 3310 (NH), 1741 (C=O$_{ester}$), 1627 (C=O$_{amide}$), 1618 (C=O$_{amide}$) cm^{-1};
UV-Vis λ_{max} EtOH: 330, 445 nm;
^{1}H NMR (400 MHz) δ (*d$_6$* DMSO): 8.74 (1H, t, *J* = 6.0 Hz, -CON<u>H</u>-), 8.33 (1H, t, *J* = 6 Hz, -CON<u>H</u>-), 7.99 (1H, d, *J* = 7.0 Hz, Ar<u>H</u>), 7.80 (1H, t, *J* = 7.2 Hz, Ar<u>H</u>), 7.69 (1H, t, *J* = 6.4 Hz, Ar<u>H</u>), 7.40 (1H, d, *J* = 7.6 Hz, Ar<u>H</u>), 4.83 (2H, s, *ortho* on η^5-C$_5$<u>H$_4$</u>-benzoyl), 4.36 (2H, s, *meta* on η^5-C$_5$<u>H$_4$</u>-benzoyl), 4.11 (2H, q, *J* = 7.2 Hz, -O<u>CH$_2$</u>CH$_3$), 3.96 - 3.85 {8H, m, (η^5-C$_5$<u>H$_4$</u>-alkyl), (-NH<u>CH$_2$</u>CHO-), (-NH<u>CH$_2$</u>CHO-)}, 1.60 (3H, s, -<u>CH$_3$</u>), 1.19 (3H, t, *J* = 7.2 Hz, -OCH$_2$<u>CH$_3$</u>);
^{13}C NMR (100 MHz) δ (*d$_6$* DMSO): 170.5 (C=O), 169.0 (C=O), 168.3 (C=O), 137.5 (C$_q$), 135.8 (C$_q$), 130.4, 128.2, 127.3, 126.1, 93.3 (C$_{ipso}$ η^5-<u>C$_5$</u>H$_4$-alkyl), 83.6 (C$_{ipso}$ η^5-<u>C$_5$</u>H$_4$-benzoyl), 71.7 (C$_{meta}$ η^5-<u>C$_5$</u>H$_4$-benzoyl), 70.5 (C$_{meta}$ η^5-<u>C$_5$</u>H$_4$-alkyl), 68.9 (C$_{ortho}$ η^5-<u>C$_5$</u>H$_4$-alkyl), 66.2 (C$_{ortho}$ η^5-<u>C$_5$</u>H$_4$-benzoyl), 61.5 (-O<u>CH$_2$</u>CH$_3$, -ve DEPT), 43.5 (-NH<u>CH$_2$</u>CHO-, -ve DEPT), 40.7 (-NH<u>CH$_2$</u>CHO-, -ve DEPT), 14.6 (-OCH$_2$<u>CH$_3$</u>), 14.0 (-<u>CH$_3$</u>).

1-methyl-1'-*N*-{*ortho*-(ferrocenyl) benzoyl} glycine L-alanine ethyl ester (73)

Glycine L-alanine ethyl ester hydrochloride (0.14 g, 0.78 mmol) was used as a starting material. The crude product was purified by column chromatography {eluent 1:1 hexane: ethyl acetate} yielding the titled product as a red oil (0.07 g, 19%),

$[\alpha]_D^{20} = -15^o$ (*c* 0.1, EtOH);

Mass spectrum: $[M+Na]^+$ found: 499.1395

$C_{25}H_{28}N_2O_4FeNa$ requires: 499.1396

I.R. υ_{max} (KBr): 3300 (NH), 1743 ($C=O_{ester}$), 1630 ($C=O_{amide}$), 1600 ($C=O_{amide}$) cm^{-1};

UV-Vis λ_{max} EtOH: 324, 448 nm;

^{1}H NMR (400 MHz) δ (DMSO- *d_6*): 8.74 (1H, t, *J* = 6.0 Hz, -CONH-), 8.33 (1H, d, *J* = 6 Hz, -CONH-), 7.99 (1H, d, *J* = 7.2 Hz, ArH), 7.81 (1H, t, *J* = 7.0 Hz, ArH), 7.69 (1H, t, *J* = 6.4 Hz, ArH), 7.40 (1H, d, *J* = 7.6 Hz, ArH), 4.80 (2H, s, *ortho* on η^5-C_5H_4-benzoyl), 4.35 (2H, s, *meta* on η^5-C_5H_4-benzoyl), 4.31- 4.24 (1H, m, -$CHCH_3$), 4.11 (2H, q, *J* = 6.8 Hz, -OCH_2CH_3), 3.93 - 3.84 {6H, m, (η^5-C_5H_4-alkyl), (-$NHCH_2CO$-)}, 1.58 (3H, s, -CH_3), 1.30 (3H, t, *J* = 6.2 Hz, -$CHCH_3$), 1.17 (3H, t, *J* = 6.8 Hz, -OCH_2CH_3);

^{13}C NMR (100 MHz) δ (DMSO- *d_6*): 171.9 (C=O), 169.0 (C=O), 168.2 (C=O), 137.5 (C_q), 136.8 (C_q), 130.4, 128.2, 127.3, 126.1, 92.6 (C_{ipso} η^5-C_5H_4-alkyl), 84.0 (C_{ipso} η^5-C_5H_4-benzoyl), 71.0 (C_{meta} η^5-C_5H_4-benzoyl), 68.3 (C_{meta} η^5-C_5H_4-alkyl), 68.0 (C_{ortho} η^5-C_5H_4-alkyl), 66.1 (C_{ortho} η^5-C_5H_4-benzoyl), 62.4 (-OCH_2CH_3, -ve DEPT), 47.3 (-$CHCH_3$), 42.0 (-$NHCH_2CHO$-, -ve DEPT), 17.1 (-$CHCH_3$), 14.9 (-OCH_2CH_3), 13.4 (-CH_3).

1-methyl-1'-*N*-{*ortho*-(ferrocenyl) benzoyl} glycine L-leucine ethyl ester (74)

Glycine L-leucine ethyl ester hydrochloride (0.17 g, 0.78 mmol) was used as a starting material. The crude product was purified by column chromatography {eluent 1:1 hexane: ethyl acetate} yielding the titled product as a red oil (0.06 g, 15%),

$[\alpha]_D^{20} = -21^o$ (*c* 0.1, EtOH);

I.R. υ_{max} (KBr): 3260 (NH), 1742 ($C=O_{ester}$), 1639 ($C=O_{amide}$), 1611 ($C=O_{amide}$) cm^{-1};

UV-Vis λ_{max} EtOH: 322, 449 nm;

^{1}H NMR (400 MHz) δ (DMSO- d_6): 8.43 (1H, t, J = 7.6 Hz, -CONH-), 8.23 (1H, d, J = 7.6 Hz, -CONH-), 7.83 (1H, d, J = 7.2 Hz, ArH), 7.50 (1H, t, J = 6.8 Hz, ArH), 7.27 (1H, t, J = 6.8 Hz, ArH), 7.15 (1H, d, J = 7.2 Hz, ArH), 4.82 (2H, s, *ortho* on η^5-C_5H_4-benzoyl), 4.37 - 4.20 {3H, m, (*meta* on η^5-C_5H_4-benzoyl), (-CH($CH_2CH(CH_3)_2$)}, 4.07 (2H, q, J = 7.0 Hz, -OCH_2CH_3), 3.96 - 3.85 {6H, m, (η^5-C_5H_4-alkyl), (-NHCH_2CO-)}, 1.63 - 1.49 {6H, m, (-CH_3), (-CH($CH_2CH(CH_3)_2$)}, 1.18 (3H, t, J = 7.0 Hz, -OCH$_2CH_3$), 0.91 - 0.89 {6H, m, -CH($CH_2CH(CH_3)_2$)};

^{13}C NMR (100 MHz) δ (DMSO- d_6): 172.9 (C=O), 169.4 (C=O), 167.8 (C=O), 136.2 (C_q), 134.8 (C_q), 133.1, 128.8, 127.4, 126.8, 90.1 (C_{ipso} η^5-C_5H_4-alkyl), 85.6 (C_{ipso} η^5-C_5H_4-benzoyl), 71.1 (C_{meta} η^5-C_5H_4-benzoyl), 70.0 (C_{meta} η^5-C_5H_4-alkyl), 69.8 (C_{ortho} η^5-C_5H_4-alkyl), 67.3 (C_{ortho} η^5-C_5H_4-benzoyl), 61.4 (-OCH_2CH_3, -ve DEPT), 51.2 {-CH($CH_2CH(CH_3)_2$)}, 43.8 (-NHCH_2CHO-, -ve DEPT), 41.2 {-CH($CH_2CH(CH_3)_2$), -ve DEPT}, 24.9 {-CH($CH_2CH(CH_3)_2$)}, 22.9 {-CH($CH_2CH(CH_3)_2$)}, 21.9 {-CH($CH_2CH(CH_3)_2$)}, 14.2 (-OCH$_2CH_3$), 13.1 (-CH_3).

1-methyl-1'-*N*-{*ortho*-(ferrocenyl) benzoyl} glycine L-phenylalanine ethyl ester (75)

Glycine L-phenylalanine ethyl ester hydrochloride (0.20 g, 0.78 mmol) was used as a starting material. The crude product was purified by column chromatography {eluent 1:1 hexane: ethyl acetate} yielding the titled product as a red oil (0.05 g, 12%),

$[\alpha]_D^{20}$ = +10^o (*c* 0.1, EtOH);

I.R. υ_{max} (KBr): 3253 (NH), 1755 (C=O$_{ester}$), 1663 (C=O$_{amide}$), 1601 (C=O$_{amide}$) cm^{-1};

UV-Vis λ_{max} EtOH: 323, 449 nm;

^{1}H NMR (400 MHz) δ (DMSO- d_6): 8.58 (1H, t, J = 6.0 Hz, -CONH-), 8.32 (1H, d, J = 7.6 Hz, -CONH-), 8.07 (1H, d, J = 7.0 Hz, ArH), 7.81 (1H, t, J = 7.2 Hz, ArH), 7.35 (1H, t, J = 7.0 Hz, ArH), 7.21 - 7.18 {5H, m, -CH(CH_2Ph)}, 4.83 (2H, s, *ortho* on η^5-C_5H_4-benzoyl), 4.45 - 4.43 {1H, m, -CH(CH_2Ph)}, 4.35 (2H, s, *meta* on η^5-C_5H_4-benzoyl), 4.00 (2H, q, J = 7.2 Hz, -OCH_2CH_3), 3.97 - 3.85 {6H, m, (η^5-C_5H_4-alkyl), (-NHCH_2CO-) }, 3.01 - 2.93 {2H, m, -CH(CH_2Ph)}, 1.54 (3H, s, -CH_3), 1.10 (3H, t, J = 7.2 Hz, -OCH$_2CH_3$);

^{13}C NMR (100 MHz) δ (DMSO- d_6): 172.1 (C=O), 169.2 (C=O), 167.3 (C=O), 137.0 (C_q), 131.0 (C_q), 129.7 (C_q), 128.7, 128.0, 127.4, 126.4, 125.9, 124.7, 123.7, 93.2 (C_{ipso}

η^5-$\underline{C}_5H_4$-alkyl), 83.9 (C_{ipso} η^5-$\underline{C}_5H_4$-benzoyl), 70.4 (C_{meta} η^5-$\underline{C}_5H_4$-benzoyl), 70.0 (C_{meta} η^5-$\underline{C}_5H_4$-alkyl), 68.3 (C_{ortho} η^5-$\underline{C}_5H_4$-benzoyl), 67.9 (C_{ortho} η^5-$\underline{C}_5H_4$-alkyl), 62.4 (-O$\underline{CH_2}CH_3$, -ve DEPT), 51.6 {-$\underline{CH}(CH_2Ph)$}, 42.7 (-NH$\underline{CH_2}$CHO-, -ve DEPT), 35.7 {-CH($\underline{CH_2}$Ph), -ve DEPT}, 13.9 (-OCH$_2\underline{CH_3}$), 13.0 (-$\underline{CH_3}$).

General procedure for the synthesis of 1-ethyl-1'-*N-ferrocenyl* benzoyl dipeptide ethyl esters

1-ethyl-1'-*N*-{*para*-(ferrocenyl) benzoyl} glycine glycine ethyl ester (76)

Glycine glycine ethyl ester hydrochloride (0.12 g, 0.75 mmol) was used as a starting material. The crude product was purified by column chromatography {eluent 1:1 hexane: ethyl acetate} yielding the titled product as an orange solid (0.12 g, 34%), m.p 108 - 110 ^oC;

Mass spectrum: $[M+Na]^+$ found: 499.1290

$C_{25}H_{28}N_2O_4FeNa$ requires: 499.1296

I.R. υ_{max} (KBr): 3301 (NH), 1740 (C=O$_{ester}$), 1622 (C=O$_{amide}$), 1602 (C=O$_{amide}$) cm^{-1};

UV-Vis λ_{max} EtOH: 360, 450 nm;

^{1}H NMR (400 MHz) δ (DMSO- d_6): 8.80 (1H, t, J = 6.4 Hz, -CON$\underline{H}$-), 8.38 (1H, t, J = 6.4 Hz, -CON$\underline{H}$-), 7.87 (2H, d, J = 5.6 Hz, Ar$\underline{H}$), 7.65 (2H, d, J = 5.6 Hz, Ar$\underline{H}$), 4.89 (2H, t, J = 1.2 Hz, *ortho* on η^5-$C_5\underline{H}_4$-benzoyl), 4.42 (2H, t, J = 1.2 Hz, *meta* on η^5-$C_5\underline{H}_4$-benzoyl), 4.15 (2H, q, J = 6.8 Hz, -O$\underline{CH_2}CH_3$), 4.05 - 3.90 {8H, m, (η^5-$C_5\underline{H}_4$-alkyl), (-NH$\underline{CH_2}$CO-), (-NH$\underline{CH_2}$CO-)}, 2.12 (2H, q, J = 7.6 Hz, -$\underline{CH_2}CH_3$), 1.23 (3H, t, J = 6.8 Hz, -OCH$_2\underline{CH_3}$), 1.02 (3H, t, J = 7.6 Hz, -CH$_2\underline{CH_3}$);

^{13}C NMR (100 MHz) δ (DMSO- d_6): 169.8 (C=O), 169.7 (C=O), 166.3 (C=O), 142.6 (C_q), 130.8 (C_q), 127.5, 125.2, 91.3 (C_{ipso} η^5-$\underline{C}_5H_4$-alkyl), 83.0 (C_{ipso} η^5-$\underline{C}_5H_4$-benzoyl), 69.9 (C_{meta} η^5-$\underline{C}_5H_4$-benzoyl), 68.8 (C_{meta} η^5-$\underline{C}_5H_4$-alkyl), 68.5 (C_{ortho} η^5-$\underline{C}_5H_4$-alkyl), 66.9 (C_{ortho} η^5-$\underline{C}_5H_4$-benzoyl), 60.4 (-O$\underline{CH_2}CH_3$, -ve DEPT), 42.4 (-NH$\underline{CH_2}$CHO-, -ve DEPT), 40.7 (-NH$\underline{CH_2}$CHO-, -ve DEPT), 20.8 (-$\underline{CH_2}CH_3$, -ve DEPT), 14.5 (-OCH$_2\underline{CH_3}$), 14.0 (-CH$_2\underline{CH_3}$).

1-ethyl-1'-*N*- {*para*-(ferrocenyl) benzoyl} glycine L-alanine ethyl ester (77)

Glycine L-alanine ethyl ester hydrochloride (0.13 g, 0.75 mmol) was used as a starting material. The crude product was purified by column chromatography {eluent 1:1 hexane: ethyl acetate} yielding the titled product as a red oil (0.09 g, 25%),

$[\alpha]_D^{20} = -16^o$ (*c* 0.1, EtOH);

Mass spectrum: $[M+Na]^+$ found: 513.1454

$C_{26}H_{30}N_2O_4FeNa$ requires: 513.1453

I.R. υ_{max} (KBr): 3290 (NH), 1753 ($C=O_{ester}$), 1626 ($C=O_{amide}$), 1608 ($C=O_{amide}$) cm^{-1};

UV-Vis λ_{max} EtOH: 359, 449 nm;

^{1}H NMR (400 MHz) δ (DMSO- d_6): 8.68 (1H, t, *J* = 6.0 Hz, -CONH-), 8.40 (1H, t, *J* = 7.2 Hz, -CONH-), 7.81 (2H, d, *J* = 7.8 Hz, ArH), 7.60 (2H, d, *J* = 7.8 Hz, ArH), 4.82 (2H, t, *J* = 1.6 Hz, *ortho* on η^5-C_5H_4-benzoyl), 4.37 (2H, t, *J* = 1.6 Hz, *meta* on η^5-C_5H_4-benzoyl), 4.28 - 4.25 (1H, m, -CHCH$_3$), 4.15 (2H, q, *J* = 6.8 Hz, -OCH$_2$CH$_3$), 3.90 - 3.85 {6H, m, (η^5-C_5H_4-alkyl), (-NHCH$_2$CO-)}, 2.10 (2H, q, *J* = 7.6 Hz, -CH$_2$CH$_3$), 1.31 (3H, t, *J* = 6.4 Hz, -CHCH$_3$), 1.18 (3H, t, *J* = 6.8 Hz, -OCH$_2$CH$_3$), 0.98 (3H, t, *J* = 7.6 Hz, -CH$_2$CH$_3$);

^{13}C NMR (100 MHz) δ (DMSO- d_6): 171.7 (C=O), 168.7 (C=O), 167.2 (C=O), 142.5 (C_q), 130.8 (C_q), 127.4, 125.2, 92.3 (C_{ipso} η^5-C_5H_4-alkyl), 82.0 (C_{ipso} η^5-C_5H_4-benzoyl), 71.0 (C_{meta} η^5-C_5H_4-benzoyl), 69.8 (C_{meta} η^5-C_5H_4-alkyl), 68.7 (C_{ortho} η^5-C_5H_4-alkyl), 66.0 (C_{ortho} η^5-C_5H_4-benzoyl), 61.4 (-OCH$_2$CH$_3$, -ve DEPT), 48.0 (-CHCH$_3$), 43.0 (-NHCH$_2$CHO-, -ve DEPT), 22.8 (-CH$_2$CH$_3$, -ve DEPT), 18.0 (-CHCH$_3$), 14.5 (-OCH$_2$CH$_3$), 13.9 (-CH$_2$CH$_3$).

1-ethyl-1'-*N*-{*para*-(ferrocenyl) benzoyl} glycine L-leucine ethyl ester (78)

Glycine L-leucine ethyl ester hydrochloride (0.16 g, 0.75 mmol) was used as a starting material. The crude product was purified by column chromatography {eluent 1:1 hexane: ethyl acetate} and recrystallisation from hexane: ethyl acetate yield the desired product as an orange solid (0.07 g, 18%), m.p 97 - 99 ^{o}C;

$[\alpha]_D^{20} = -12^o$ (*c* 0.1, EtOH);

Mass spectrum: $[M+Na]^+$ found: 555.1919

$C_{29}H_{36}N_2O_4FeNa$ requires: 555.1922

I.R. υ_{max} (KBr): 3280 (NH), 1740 (C=O_{ester}), 1641 (C=O_{amide}), 1615 (C=O_{amide}) cm^{-1};
UV-Vis λ_{max} EtOH: 357, 446 nm;
^{1}H NMR (400 MHz) δ (DMSO- *d_6*): 8.68 (1H, t, *J* = 6.0 Hz, -CONH-), 8.34 (1H, d, *J* = 7.6 Hz, -CONH-), 7.82 (2H, d, *J* = 8.2 Hz, ArH), 7.61 (2H, d, *J* = 8.2 Hz, ArH), 4.81 (2H, t, *J* = 1.6 Hz, *ortho* on η^5-C_5H_4-benzoyl), 4.36 (2H, t, *J* = 1.6 Hz, *meta* on η^5-C_5H_4-benzoyl), 4.30 - 4.25 {1H, m, -$CH(CH_2CH(CH_3)_2)$}, 4.15 (2H, q, *J* = 7.2 Hz, -OCH_2CH_3) , 3.97 - 3.87 {6H, m, (η^5-C_5H_4-alkyl), (-$NHCH_2CO$-)}, 2.00 (2H, q, *J* = 7.2 Hz, -CH_2CH_3), 1.69 - 1.50 {3H, m, -$CH(CH_2CH(CH_3)_2)$}, 1.15 (3H, t, *J* = 7.2 Hz, -OCH_2CH_3), 0.90 - 0.85 {6H, m, -$CH(CH_2CH(CH_3)_2)$}, 0.76 (3H, t, *J* = 7.2 Hz, -CH_2CH_3);
^{13}C NMR (100 MHz) δ (DMSO- *d_6*): 173.4 (C=O), 170.0 (C=O), 166.9 (C=O), 140.1 (C_q), 130.8 (C_q), 127.4, 125.2, 92.1 (C_{ipso} η^5-C_5H_4-alkyl), 83.1 (C_{ipso} η^5-C_5H_4-benzoyl), 71.0 (C_{meta} η^5-C_5H_4-benzoyl), 69.9 (C_{meta} η^5-C_5H_4-alkyl), 68.1 (C_{ortho} η^5-C_5H_4-alkyl), 67.2 (C_{ortho} η^5-C_5H_4-benzoyl), 61.4 (-OCH_2CH_3, -ve DEPT), 51.3 {-$CH(CH_2CH(CH_3)_2)$}, 42.6 (-$NHCH_2CHO$-, -ve DEPT), 39.3 {-$CH(CH_2CH(CH_3)_2)$, -ve DEPT}, 28.1 {-$CH(CH_2CH(CH_3)_2)$}, 23.4 (-CH_2CH_3, -ve DEPT), 22.9 {-$CH(CH_2CH(CH_3)_2)$}, 21.0 {-$CH(CH_2CH(CH_3)_2)$}, 15.1 (-OCH_2CH_3), 13.0 (-CH_2CH_3).

1-ethyl-1'-*N*- {*para*-(ferrocenyl) benzoyl} glycine L-phenylalanine ethyl ester (79)

Glycine L-phenylalanine ethyl ester hydrochloride (0.19 g, 0.75 mmol) was used as a starting material. The crude product was purified by column chromatography {eluent 1:1 hexane: ethyl acetate} and recrystallisation from hexane: ethyl acetate yield the desired product as an orange solid (0.07 g, 17%), m.p 92 - 94 ^{o}C;
$[\alpha]_D^{20}$ = +12^{o} (*c* 0.1, EtOH);
Mass spectrum: $[M+Na]^+$ found: 589.1770
$C_{32}H_{34}N_2O_4FeNa$ requires: 589.1769
I.R. υ_{max} (KBr): 3303 (NH), 1742 (C=O_{ester}), 1629 (C=O_{amide}), 1608 (C=O_{amide}) cm^{-1};
UV-Vis λ_{max} EtOH: 356, 450 nm;
^{1}H NMR (400 MHz) δ (DMSO- *d_6*): 8.60 (1H, t, *J* = 6.0 Hz, -CONH-), 8.37 (1H, d, *J* = 7.6 Hz, -CONH-), 7.85 (2H, d, *J* = 7.4 Hz, ArH), 7.63 (2H, d, *J* = 7.4 Hz, ArH), 7.27 - 7.21 {5H, m, -$CH(CH_2Ph)$}, 4.83 (2H, t, *J* = 1.6 Hz, *ortho* on η^5-C_5H_4-benzoyl),

4.48 - 4.46 {1H, m, -CH(CH_2Ph)}, 4.37 (2H, t, *J* = 1.6 Hz, *meta* on η^5-C_5H_4-benzoyl), 4.00 (2H, q, *J* = 6.8 Hz, - OCH_2CH_3), 3.90 - 3.83 {6H, m, (η^5-C_5H_4-alkyl), (-NHCH_2CO-)}, 3.06 - 2.93 {2H, m, -CH(CH_2Ph)}, 2.08 (2H, q, *J* = 7.6 Hz, -CH_2CH_3), 1.12 (3H, t, *J* = 6.8 Hz, -OCH$_2$$CH_3$), 0.98 (3H, t, *J* = 7.6 Hz, -CH_2CH_3);

^{13}C NMR (100 MHz) δ (DMSO- d_6): 170.8 (C=O), 168.2 (C=O), 166.7 (C=O), 137.0 (C_q), 132.7 (C_q), 130.1 (C_q), 128.9, 127.2, 126.9, 124.0, 120.2, 93.1 (C_{ipso} η^5-C_5H_4-alkyl), 84.0 (C_{ipso} η^5-C_5H_4-benzoyl), 71.4 (C_{meta} η^5-C_5H_4-benzoyl), 68.4 (C_{meta} η^5-C_5H_4-alkyl), 67.5 (C_{ortho} η^5-C_5H_4-alkyl), 66.4 (C_{ortho} η^5-C_5H_4-benzoyl), 61.2 (-O$CH_2$$CH_3$, -ve DEPT), 51.6 (-CH($CH_2$Ph)), 43.0 (-NH$CH_2$CHO-, -ve DEPT), 38.0 {-CH(CH_2Ph), -ve DEPT}, 24.5 (-$CH_2$$CH_3$, -ve DEPT), 13.3 (-OCH$_2$$CH_3$), 13.0 (-$CH_2$$CH_3$).

1-ethyl-1'-*N*- {*meta*-(ferrocenyl)-benzoyl}-glycine-glycine ethyl ester (80)

Glycine glycine ethyl ester hydrochloride (0.12 g, 0.75 mmol) was used as a starting material. The crude product was purified by column chromatography {eluent 1:1 hexane: ethyl acetate} yielding the titled product as a red oil (0.09 g, 25%),

Mass spectrum: $[M+Na]^+$ found: 499.1287

$C_{25}H_{28}N_2O_4FeNa$ requires: 499.1296

I.R. υ_{max} (KBr): 3311 (NH), 1741 (C=O_{ester}), 1622 (C=O_{amide}), 1601 (C=O_{amide}) cm^{-1};

UV-Vis λ_{max} EtOH: 332, 440 nm;

^{1}H NMR (400 MHz) δ (DMSO- d_6): 8.49 (1H, t, *J* = 6.0 Hz, -CONH-), 8.23 (1H, t, *J* = 6 Hz, -CONH-), 7.87 (1H, s, ArH), 7.67 - 7.63 (2H, m, ArH), 7.36 (1H, t, *J* = 7.2 Hz, ArH), 4.58 (2H, t, *J* = 1.6 Hz, *ortho* on η^5-C_5H_4-benzoyl), 4.20 (2H, t, *J* = 1.6 Hz, *meta* on η^5-C_5H_4-benzoyl), 4.11 (2H, q, *J* = 7.2 Hz, - OCH_2CH_3), 3.98 - 3.87 {8H, m, (η^5-C_5H_4-alkyl), (-NHCH_2CO-), (-NHCH_2CO-)}, 1.96 (2H, q, *J* = 7.6 Hz, -CH_2CH_3), 1.26 (3H, t, *J* = 7.2 Hz, -OCH$_2$$CH_3$), 1.03 (3H, t, *J* = 7.6 Hz, -CH_2CH_3);

^{13}C NMR (100 MHz) δ (DMSO- d_6): 169.8 (C=O), 168.7 (C=O), 166.3 (C=O), 139.6 (C_q), 134.1 (C_q), 128.8, 128.5, 124.2, 124.1, 91.2 (C_{ipso} η^5-C_5H_4-alkyl), 83.1 (C_{ipso} η^5-C_5H_4-benzoyl), 70.0 (C_{meta} η^5-C_5H_4-benzoyl), 68.8 (C_{meta} η^5-C_5H_4-alkyl), 68.5 (C_{ortho} η^5-C_5H_4-alkyl), 66.2 (C_{ortho} η^5-C_5H_4-benzoyl), 60.3 (-O$CH_2$$CH_3$, -ve DEPT), 42.4 (-NH$CH_2$CHO-, -ve DEPT), 40.6 (-NHCH_2CHO-, -ve DEPT), 20.8 (-$CH_2$$CH_3$, -ve DEPT), 14.4 (-OCH$_2$$CH_3$), 14.0 (-$CH_2$$CH_3$).

1-ethyl-1'-*N*-{*meta*-(ferrocenyl) benzoyl} glycine L-alanine ethyl ester (81)

Glycine L-alanine ethyl ester hydrochloride (0.13 g, 0.75 mmol) was used as a starting material. The crude product was purified by column chromatography {eluent 1:1 hexane: ethyl acetate} yielding the titled product as a red oil (0.08 g, 22%),

$[\alpha]_D^{20} = -18^o$ (*c* 0.1, EtOH);

Mass spectrum: $[M+Na]^+$ found: 513.1458

$C_{25}H_{28}N_2O_4FeNa$ requires: 513.1453

I.R. υ_{max} (KBr): 3290 (NH), 1739 ($C=O_{ester}$), 1635 ($C=O_{amide}$), 1605 ($C=O_{amide}$) cm^{-1};

UV-Vis λ_{max} EtOH: 333, 444 nm;

^{1}H NMR (400 MHz) δ (DMSO- d_6): 8.60 (1H, t, *J* = 6.0 Hz, -CONH-), 8.40 (1H, d, *J* = 7.0 Hz, -CONH-), 8.00 (1H, s, ArH), 7.68 - 7.64 (2H, m, ArH), 7.40 (1H, t, *J* = 7.2 Hz, ArH), 4.68 (2H, t, *J* = 1.6 Hz, *ortho* on η^5-C_5H_4-benzoyl), 4.34 (2H, t, *J* = 1.6 Hz, *meta* on η^5-C_5H_4-benzoyl), 4.30 - 4.24 (1H, m, -CHCH$_3$), 4.00 (2H, q, *J* = 6.8 Hz, -OCH$_2$CH$_3$), 3.96 - 3.82 {6H, m, (η^5-C_5H_4-alkyl), (-NHCH$_2$CO-)}, 2.05 (2H, q, *J* = 7.6 Hz, -CH$_2$CH$_3$), 1.28 (3H, t, *J* = 6.4 Hz, -CHCH$_3$), 1.20 (3H, t, *J* = 6.8 Hz, -OCH$_2$CH$_3$), 0.96 (3H, t, *J* = 7.6 Hz, -CH$_2$CH$_3$);

^{13}C NMR (100 MHz) δ (DMSO- d_6): 172.5 (C=O), 169.0 (C=O), 166.2 (C=O), 137.5 (C_q), 135.8 (C_q), 130.4, 129.2, 127.0, 125.2, 91.0 (C_{ipso} η^5-C_5H_4-alkyl), 84.0 (C_{ipso} η^5-C_5H_4-benzoyl), 71.5 (C_{meta} η^5-C_5H_4-benzoyl), 69.3 (C_{meta} η^5-C_5H_4-alkyl), 68.1 (C_{ortho} η^5-C_5H_4-alkyl), 66.5 (C_{ortho} η^5-C_5H_4-benzoyl), 62.4 (-OCH$_2$CH$_3$, -ve DEPT), 47.6 (CHCH$_3$), 42.8 (-NHCH$_2$CHO-, -ve DEPT), 21.8 (-CH$_2$CH$_3$, -ve DEPT), 19.0 (-CHCH$_3$), 14.1 (-OCH$_2$CH$_3$), 13.5 (-CH$_2$CH$_3$).

1-ethyl-1'-*N*-{*meta*-(ferrocenyl) benzoyl} glycine L-leucine ethyl ester (82)

Glycine L-leucine ethyl ester hydrochloride (0.16 g, 0.75 mmol) was used as a starting material. The crude product was purified by column chromatography {eluent 1:1 hexane: ethyl acetate} yielding the titled product as a red oil (0.07 g, 18%),

$[\alpha]_D^{20} = -13^o$ (*c* 0.1, EtOH);

Mass spectrum: $[M+Na]^+$ found: 555.1933

$C_{29}H_{36}N_2O_4FeNa$ requires: 555.1922

I.R. υ_{max} (KBr): 3260 (NH), 1737 ($C=O_{ester}$), 1643 ($C=O_{amide}$), 1615 ($C=O_{amide}$) cm^{-1};

UV-Vis λ_{max} EtOH: 333, 445 nm;

^{1}H NMR (400 MHz) δ (DMSO- *d_6*): 8.68 (1H, t, *J* = 6.0 Hz, -CONH-), 8.34 (1H, d, *J* = 6.8 Hz, -CONH-), 8.01 (1H, s, ArH), 7.65 - 7.62 (2H, m, ArH), 7.45 (1H, t, *J* = 7.0 Hz, ArH), 4.78 (2H, t, *J* = 1.6 Hz, *ortho* on η^5-C_5H_4-benzoyl), 4.30 (2H, t, *J* = 1.6 Hz, *meta* on η^5-C_5H_4-benzoyl), 4.34 - 4.26 {1H, m, -CH($CH_2CH(CH_3)_2$)}, 4.09 (2H, q, *J* = 7.0 Hz, -OCH_2CH_3), 3.97 - 3.86 {6H, m, (η^5-C_5H_4-alkyl), (-NHCH_2CO-)}, 2.04 (2H, q, *J* = 7.2 Hz, -CH_2CH_3), 1.60 - 1.40 {3H, m, -CH($CH_2CH(CH_3)_2$)}, 1.10 (3H, t, *J* = 7.0 Hz, -OCH_2CH_3), 0.88 - 0.84 {6H, m, -CH($CH_2CH(CH_3)_2$)}, 0.74 (3H, t, *J* = 7.2 Hz, -CH_2CH_3);

^{13}C NMR (100 MHz) δ (DMSO- *d_6*): 170.9 (C=O), 168.9 (C=O), 166.4 (C=O), 138.5 (C_q), 135.8 (C_q), 130.1, 128.2, 127.3, 125.1, 89.9 (C_{ipso} η^5-C_5H_4-alkyl), 83.1 (C_{ipso} η^5-C_5H_4-benzoyl), 71.9 (C_{meta} η^5-C_5H_4-benzoyl), 69.3 (C_{meta} η^5-C_5H_4-alkyl), 68.0 (C_{ortho} η^5-C_5H_4-alkyl), 66.5 (C_{ortho} η^5-C_5H_4-benzoyl), 62.5 (-OCH_2CH_3, -ve DEPT), 50.3 {-CH($CH_2CH(CH_3)_2$)}, 43.0 (-NHCH_2CHO-, -ve DEPT), 39.9 {-CH($CH_2CH(CH_3)_2$), -ve DEPT}, 24.4 (-CH_2CH_3, -ve DEPT), 26.5 {-CH($CH_2CH(CH_3)_2$)}, 23.0 {-CH($CH_2CH(CH_3)_2$)}, 22.4 {-CH($CH_2CH(CH_3)_2$)}, 14.4 (-OCH_2CH_3), 13.7 (-CH_2CH_3).

1-ethyl-1'-*N*-{*meta*-(ferrocenyl) benzoyl} glycine L-phenylalanine ethyl ester (83)

Glycine L-phenylalanine ethyl ester hydrochloride (0.19 g, 0.75 mmol) was used as a starting material. The crude product was purified by column chromatography {eluent 1:1 hexane: ethyl acetate} yielding the titled product as a red oil (0.07 g, 18%),

$[\alpha]_D^{20}$ = +16^o (*c* 0.1, EtOH);

Mass spectrum: $[M+Na]^+$ found: 589.1768

$C_{32}H_{34}N_2O_4FeNa$ requires: 589.1769

I.R. υ_{max} (KBr): 3300 (NH), 1739 ($C=O_{ester}$), 1633 ($C=O_{amide}$), 1601 ($C=O_{amide}$) cm^{-1};

UV-Vis λ_{max} EtOH: 332, 444 nm;

^{1}H NMR (400 MHz) δ (DMSO- *d_6*): 8.54 (1H, t, *J* = 6.0 Hz, -CONH-), 8.30 (1H, d, *J* = 7.4 Hz, -CONH-), 8.07 (1H, s, ArH), 7.69 - 7.67 (2H, m, ArH), 7.35 (1H, t, *J* = 7.0 Hz, ArH), 7.22 - 7.19 {5H, m, -CH(CH_2Ph)}, 4.83 (2H, t, *J* = 1.6 Hz, *ortho* on η^5-C_5H_4-benzoyl), 4.43 - 4.40 {1H, m, -CH(CH_2Ph)}, 4.37 (2H, t, *J* = 1.6 Hz, *meta* on η^5-C_5H_4-benzoyl), 4.08 (2H, q, *J* = 7.2 Hz, - OCH_2CH_3), 3.95 - 3.88 {6H, m, (η^5-C_5H_4-

alkyl), (-NH$\underline{CH_2}$CO-)}, 3.00 - 2.90 {2H, m, -CH($\underline{CH_2}$Ph)}, 2.05 (2H, q, *J* = 7.6 Hz, -$\underline{CH_2}CH_3$), 1.10 (3H, t, *J* = 7.2 Hz, -OCH$_2\underline{CH_3}$), 0.90 (3H, t, *J* = 7.6 Hz, -CH$_2\underline{CH_3}$);
^{13}C NMR (100 MHz) δ (DMSO- d_6): 172.4 (C=O), 169.7 (C=O), 167.0 (C=O), 135.0 (C_q), 131.7 (C_q), 130.7 (C_q), 129.7, 128.2, 127.4, 126.0, 124.2, 123.2, 122.7, 89.1 (C_{ipso} η^5-$\underline{C_5}H_4$-alkyl), 83.0 (C_{ipso} η^5-$\underline{C_5}H_4$-benzoyl), 73.2 (C_{meta} η^5-$\underline{C_5}H_4$-benzoyl), 69.9 (C_{meta} η^5-$\underline{C_5}H_4$-alkyl), 67.7 (C_{ortho} η^5-$\underline{C_5}H_4$-alkyl), 66.1 (C_{ortho} η^5-$\underline{C_5}H_4$-benzoyl), 60.1 (-O$\underline{CH_2}CH_3$, -ve DEPT), 52.8 {-$\underline{CH}$(CH_2Ph)}, 42.9 (-NH$\underline{CH_2}$CHO-, -ve DEPT), 37.8 (-CH($\underline{CH_2}$Ph), -ve DEPT), 24.0 (-$\underline{CH_2}CH_3$, -ve DEPT), 14.9 (-OCH$_2\underline{CH_3}$), 14.2 (-CH$_2\underline{CH_3}$).

1-ethyl-1'-*N*-{*ortho*-(ferrocenyl) benzoyl} glycine glycine ethyl ester (84)

Glycine glycine ethyl ester hydrochloride (0.12 g, 0.75 mmol) was used as a starting material. The crude product was purified by column chromatography {eluent 1:1 hexane: ethyl acetate} yielding the titled product as a red oil (0.08 g, 22%),
Mass spectrum: $[M+Na]^+$ found: 499.1292
$C_{25}H_{28}N_2O_4FeNa$ requires: 499.1296
I.R. υ_{max} (KBr): 3310 (NH), 1739 (C=O$_{ester}$), 1631 (C=O$_{amide}$), 1617 (C=O$_{amide}$) cm^{-1};
UV-Vis λ_{max} EtOH: 325, 444 nm;
^{1}H NMR (400 MHz) δ (DMSO- d_6): 8.72 (1H, t, *J* = 6.0 Hz, -CON$\underline{H}$-), 8.34 (1H, t, *J* = 6 Hz, -CON$\underline{H}$-), 8.00 (1H, d, *J* = 7.4 Hz, Ar$\underline{H}$), 7.81 (1H, t, *J* = 7.2 Hz, Ar$\underline{H}$), 7.70 (1H, t, *J* = 6.4 Hz, Ar$\underline{H}$), 7.40 (1H, d, *J* = 7.6 Hz, Ar$\underline{H}$), 4.82 (2H, t, *J* = 1.6 Hz, *ortho* on η^5-$C_5\underline{H_4}$-benzoyl), 4.31 (2H, t, *J* = 2 Hz, *meta* on η^5-$C_5\underline{H_4}$-benzoyl), 4.10 (2H, q, *J* = 6.8 Hz, - O$\underline{CH_2}CH_3$), 3.97 - 3.85 {8H, m, (η^5-$C_5\underline{H_4}$-alkyl), (-NH$\underline{CH_2}$CO-), (-NH$\underline{CH_2}$CO-)}, 2.07 (2H, q, *J* = 7.6 Hz, -$\underline{CH_2}CH_3$), 1.18 (3H, t, *J* = 6.8 Hz, -OCH$_2\underline{CH_3}$), 0.98 (3H, t, *J* = 7.6 Hz, -CH$_2\underline{CH_3}$);
^{13}C NMR (100 MHz) δ (DMSO- d_6): 169.8 (C=O), 168.3 (C=O), 165.2 (C=O), 135.6 (C_q), 133.8 (C_q), 128.5, 127.2, 126.0, 124.0, 92.3 (C_{ipso} η^5-$\underline{C_5}H_4$-alkyl), 81.0 (C_{ipso} η^5-$\underline{C_5}H_4$-benzoyl), 71.0 (C_{meta} η^5-$\underline{C_5}H_4$-benzoyl), 68.7 (C_{meta} η^5-$\underline{C_5}H_4$-alkyl), 68.0 (C_{ortho} η^5-$\underline{C_5}H_4$-alkyl), 66.1 (C_{ortho} η^5-$\underline{C_5}H_4$-benzoyl), 62.4 (-O$\underline{CH_2}CH_3$, -ve DEPT), 43.4 (-NH$\underline{CH_2}$CHO-, -ve DEPT), 41.7 (-NH$\underline{CH_2}$CHO-, -ve DEPT), 22.8 (-$\underline{CH_2}CH_3$, -ve DEPT), 14.2 (-OCH$_2\underline{CH_3}$), 13.0 (-CH$_2\underline{CH_3}$).

1-ethyl- 1'-*N*-{*ortho*-(ferrocenyl) benzoyl} glycine L-alanine ethyl ester (85)

Glycine L-alanine ethyl ester hydrochloride (0.13 g, 0.75 mmol) was used as a starting material. The crude product was purified by column chromatography {eluent 1:1 hexane: ethyl acetate} yielding the titled product as a red oil (0.07 g, 19%),

$[\alpha]_D^{20} = -19^o$ (*c* 0.1, EtOH);

Mass spectrum: $[M+Na]^+$ found: 513.1447

$C_{25}H_{28}N_2O_4FeNa$ requires: 513.1453

I.R. υ_{max} (KBr): 3289 (NH), 1740 ($C=O_{ester}$), 1632 ($C=O_{amide}$), 1608 ($C=O_{amide}$) cm^{-1};

UV-Vis λ_{max} EtOH: 325, 443 nm;

^{1}H NMR (400 MHz) δ (DMSO- d_6): 8.48 (1H, t, *J* = 6.0 Hz, -CONH-), 8.34 (1H, d, *J* = 7.2 Hz, -CONH-), 8.01 (1H, d, *J* = 6.8 Hz, ArH), 7.81 (1H, t, *J* = 7.2 Hz, ArH), 7.70 (1H, t, *J* = 6.4 Hz, ArH), 7.41 (1H, d, *J* = 7.4 Hz, ArH), 4.72 (2H, t, *J* = 1.6 Hz, *ortho* on η^5-C_5H_4-benzoyl), 4.38 (2H, t, *J* = 1.6 Hz, *meta* on η^5-C_5H_4-benzoyl), 4.30 - 4.26 (1H, m, - $CHCH_3$), 4.10 (2H, q, *J* = 6.8 Hz, - OCH_2CH_3), 3.92 - 3.80 {6H, m, (η^5-C_5H_4-alkyl), (-$NHCH_2CO$-)}, 2.00 (2H, q, *J* = 7.6 Hz, -CH_2CH_3), 1.30 (3H, t, *J* = 6.4 Hz, -$CHCH_3$), 1.15 (3H, t, *J* = 6.8 Hz, -OCH_2CH_3), 0.90 (3H, t, *J* = 7.6 Hz, -CH_2CH_3);

^{13}C NMR (100 MHz) δ (DMSO- d_6): 172.5 (C=O), 168.0 (C=O), 167.2 (C=O), 138.5 (C_q), 134.0 (C_q), 129.0, 128.8, 127.5, 124.1, 92.7 (C_{ipso} η^5-C_5H_4-alkyl), 81.2 (C_{ipso} η^5-C_5H_4-benzoyl), 70.9 (C_{meta} η^5-C_5H_4-benzoyl), 69.8 (C_{meta} η^5-C_5H_4-alkyl), 68.5 (C_{ortho} η^5-C_5H_4-alkyl), 66.2 (C_{ortho} η^5-C_5H_4-benzoyl), 60.8 (-OCH_2CH_3, -ve DEPT), 49.6 (-$CHCH_3$), 42.2 (-$NHCH_2CHO$-, -ve DEPT), 25.8 (-CH_2CH_3, -ve DEPT), 17.6 (-$CHCH_3$), 14.8 (-OCH_2CH_3), 14.0 (-CH_2CH_3).

1-ethyl-1'-*N*-{*ortho*-(ferrocenyl) benzoyl} glycine leucine ethyl ester (86)

Glycine L-leucine ethyl ester hydrochloride (0.16 g, 0.75 mmol) was used as a starting material. The crude product was purified by column chromatography {eluent 1:1 hexane: ethyl acetate} yielding the titled product as a red oil (0.06 g, 15%),

$[\alpha]_D^{20} = -11^o$ (*c* 0.1, EtOH);

I.R. υ_{max} (KBr): 3275 (NH), 1747 ($C=O_{ester}$), 1649 ($C=O_{amide}$), 1614 ($C=O_{amide}$) cm^{-1};

UV-Vis λ_{max} EtOH: 360, 451 nm;

^{1}H NMR (400 MHz) δ(DMSO- d_6): 8.68 (1H, t, J = 6.0 Hz, -CONH-), 8.34 (1H, d, J = 7.6 Hz, -CONH-), 8.11 (1H, d, J = 6.6 Hz, ArH), 7.80 (1H, t, J = 7.2 Hz, ArH), 7.70 (1H, t, J = 6.4 Hz, ArH), 7.40 (1H, d, J = 7.6 Hz, ArH), 4.83 (2H, t, J = 1.6 Hz, *ortho* on η^5-C_5H_4-benzoyl), 4.33 (2H, t, J = 1.6 Hz, *meta* on η^5-C_5H_4-benzoyl), 4.32 - 4.28 {1H, m, -CH($CH_2CH(CH_3)_2$)}, 4.20 (2H, q, J = 7.0 Hz, - OCH_2CH_3), 3.96 - 3.87 {6H m, (η^5-C_5H_4-alkyl), (-NHCH_2CO-)}, 2.02 (2H, q, J = 7.2 Hz, -CH_2CH_3), 1.65 - 1.40 {3H, m, -CH($CH_2CH(CH_3)_2$)}, 1.07 (3H, t, J = 7.0 Hz, -OCH_2CH_3), 0.92 - 0.88 {6H, m, -CH($CH_2CH(CH_3)_2$)}, 0.70 (3H, t, J = 7.2 Hz, - CH_2CH_3);
^{13}C NMR (100 MHz) δ (DMSO- d_6): 170.4 (C=O), 169.6 (C=O), 166.4 (C=O), 136.6 (C_q), 135.8 (C_q), 131.4, 128.2, 127.7, 124.1, 92.4 (C_{ipso} η^5-C_5H_4-alkyl), 82.1 (C_{ipso} η^5-C_5H_4-benzoyl), 71.0 (C_{meta} η^5-C_5H_4-benzoyl), 70.4 (C_{meta} η^5-C_5H_4-alkyl), 68.5 (C_{ortho} η^5-C_5H_4-alkyl), 66.9 (C_{ortho} η^5-C_5H_4-benzoyl), 61.4 (-OCH_2CH_3, -ve DEPT), 52.3 {-CH($CH_2CH(CH_3)_2$)}, 43.1 (-NHCH_2CHO-, -ve DEPT), 40.1 {-CH($CH_2CH(CH_3)_2$), -ve DEPT}, 27.9 {-CH($CH_2CH(CH_3)_2$)}, 24.4 (-CH_2CH_3, -ve DEPT), 21.7 {-CH($CH_2CH(CH_3)_2$)}, 20.4 {-CH($CH_2CH(CH_3)_2$)}, 14.7 (-OCH_2CH_3), 13.0 (-CH_2CH_3).

1-ethyl-1'-*N*- {*ortho*-(ferrocenyl) benzoyl} glycine L-phenylalanine ethyl ester (87)

Glycine L-phenylalanine ethyl ester hydrochloride (0.19 g, 0.75 mmol) was used as a starting material. The crude product was purified by column chromatography {eluent 1:1 hexane: ethyl acetate} yielding the titled product as a red oil (0.06 g, 14%),
$[\alpha]_D^{20}$ = +14^o (c 0.1, EtOH);
I.R. υ_{max} (KBr): 3303 (NH), 1744 (C=O_{ester}), 1629 (C=O_{amide}), 1608 (C=O_{amide}) cm^{-1};
UV-Vis λ_{max} EtOH: 325, 444 nm;
^{1}H NMR (400 MHz) δ (DMSO- d_6): 8.68 (1H, t, J = 6.0 Hz, -CONH-), 8.32 (1H, d, J = 7.6 Hz, -CONH-), 8.03 (1H, d, J = 7.0 Hz, ArH), 7.81 (1H, t, J = 7.2 Hz, ArH), 7.79 (1H, t, J = 6.4 Hz, ArH), 7.38 (1H, d, J = 6.8 Hz, ArH), 7.23 - 7.19 (5H, m, -CH(CH_2Ph)), 4.83 (2H, t, J = 1.6 Hz, *ortho* on η^5-C_5H_4-benzoyl), 4.49 - 4.47 {1H, m, -CH(CH_2Ph)}, 4.37 (2H, t, J = 1.6 Hz, *meta* on η^5-C_5H_4-benzoyl), 4.04 (2H, q, J = 6.4 Hz, -OCH_2CH_3), 3.89 - 3.80 {6H, m, (η^5-C_5H_4-alkyl), (-NHCH_2CO-)}, 3.08 - 2.95

{2H, m, -CH(CH$_2$Ph)}, 2.02 {2H, q, *J* = 7.6 Hz, -CH$_2$CH$_3$), 1.16 (3H, t, *J* = 6.4 Hz, -OCH$_2$CH$_3$), 0.94 (3H, t, *J* = 7.6 Hz, -CH$_2$CH$_3$);

^{13}C NMR (100 MHz) δ (DMSO- *d*$_6$): 171.5 (C=O), 169.1 (C=O), 168.2 (C=O), 139.0 (C$_q$), 130.9 (C$_q$), 129.1 (C$_q$), 128.5, 128.4, 127.1, 126.6, 125.2, 124.2, 121.7, 92.1 (C$_{ipso}$ η^5-C$_5$H$_4$-alkyl), 81.1 (C$_{ipso}$ η^5-C$_5$H$_4$-benzoyl), 71.4 (C$_{meta}$ η^5-C$_5$H$_4$-benzoyl), 69.9 (C$_{meta}$ η^5-C$_5$H$_4$-alkyl), 68.9 (C$_{ortho}$ η^5-C$_5$H$_4$-alkyl), 67.9 (C$_{ortho}$ η^5-C$_5$H$_4$-benzoyl), 62.8 (-OCH$_2$CH$_3$, -ve DEPT), 53.6 {-CH(CH$_2$Ph)}, 42.2 (-NHCH$_2$CHO-, -ve DEPT), 39.8 {-CH(CH$_2$Ph), -ve DEPT}, 23.0 (-CH$_2$CH$_3$, -ve DEPT), 15.0 (-OCH$_2$CH$_3$), 14.1 (-CH$_2$CH$_3$).

General procedure for the synthesis of 1-propyl-1'-*N*-*ferrocenyl* benzoyl dipeptide ethyl esters

1-propyl-1'-*N*-{*para*-(ferrocenyl) benzoyl} glycine glycine ethyl ester (88)

Glycine glycine ethyl ester (0.12 g, 0.72 mmol) was used as a starting material. The crude product was purified by column chromatography {eluent 1:1 hexane: ethyl acetate} and recrystallisation from hexane: ethyl acetate yield the desired product as an orange solid (0.09 g, 26%), m.p 118 - 120 ^{o}C;

Mass spectrum: $[M+Na]^+$ found: 513.1464

$C_{26}H_{30}N_2O_4FeNa$ requires: 513.1453

I.R. υ_{max} (KBr): 3389 (NH), 1735 (C=O$_{ester}$), 1626 (C=O$_{amide}$), 1609 (C=O$_{amide}$) cm^{-1};

UV-Vis λ_{max} EtOH: 361, 450 nm;

^{1}H NMR (400 MHz) δ (DMSO- *d*$_6$): 8.76 (1H, t, *J* = 5.6 Hz, -CONH-), 8.40 (1H, t, *J* = 5.6 Hz, -CONH-), 7.82 (2H, d, *J* = 8.0 Hz, ArH), 7.60 (2H, d, *J* = 8.0 Hz, ArH), 4.85 (2H, s, *ortho* on η^5-C$_5$H$_4$-benzoyl), 4.38 (2H, s, *meta* on η^5-C$_5$H$_4$-benzoyl), 4.11 (2H, q, *J* = 6.8 Hz, -OCH$_2$CH$_3$), 3.90 - 3.80 {8H, m, (η^5-C$_5$H$_4$-alkyl), (-NHCH$_2$CO-), (-NHCH$_2$CO-)}, 2.07 (2H, t, *J* = 7.6 Hz, -CH$_2$CH$_2$CH$_3$), 1.38 - 1.28 (2H, m, -CH$_2$CH$_2$CH$_3$), 1.18 (3H, t, *J* = 6.8 Hz, -OCH$_2$CH$_3$), 0.76 (3H, t, *J* = 7.2 Hz, -CH$_2$CH$_2$CH$_3$);

^{13}C NMR (100 MHz) δ (DMSO- *d*$_6$): 169.8 (C=O), 168.3 (C=O), 166.9 (C=O), 142.5 (C$_q$), 130.8 (C$_q$), 127.5, 125.2, 90.1 (C$_{ipso}$ η^5-C$_5$H$_4$-alkyl), 83.0 (C$_{ipso}$ η^5-C$_5$H$_4$-benzoyl), 71.7 (C$_{meta}$ η^5-C$_5$H$_4$-benzoyl), 69.8 (C$_{meta}$ η^5-C$_5$H$_4$-alkyl), 68.5 (C$_{ortho}$ η^5-C$_5$H$_4$-alkyl),

66.7 (C_{ortho} η^5-$\underline{C}_5H_4$-benzoyl), 62.4 (-O$\underline{CH_2}CH_3$, -ve DEPT), 42.8 (-NH$\underline{CH_2}$CHO-, -ve DEPT), 41.9 (-NH$\underline{CH_2}$CHO-, -ve DEPT), 32.8 (-$\underline{CH_2}CH_2CH_3$, -ve DEPT), 25.0 (-$CH_2\underline{CH_2}CH_3$, -ve DEPT), 14.5 (-$OCH_2\underline{CH_3}$), 14.0 (-$CH_2CH_2\underline{CH_3}$).

1-propyl-1'-*N*- {*para*-(ferrocenyl) benzoyl} glycine L-alanine ethyl ester (89)

Glycine L-alanine ethyl ester hydrochloride (0.13 g, 0.72 mmol) was used as a starting material. The crude product was purified by column chromatography {eluent 1:1 hexane: ethyl acetate} yielding the titled product as a red oil (0.08 g, 22%),

$[\alpha]_D^{20}$ = -14° (*c* 0.1, EtOH);

Mass spectrum: $[M+Na]^+$ found: 527.1632

$C_{26}H_{30}N_2O_4FeNa$ requires: 527.1609

I.R. υ_{max} (KBr): 3295 (NH), 1743 (C=O_{ester}), 1636 (C=O_{amide}), 1608 (C=O_{amide}) cm^{-1};

UV-Vis λ_{max} EtOH: 360, 451 nm;

^{1}H NMR (400 MHz) δ (DMSO- d_6): 8.68 (1H, t, *J* = 6.0 Hz, -CON$\underline{H}$-), 8.41 (1H, d, *J* = 7.0 Hz, -CON$\underline{H}$-), 7.78 (2H, d, *J* = 7.4 Hz, Ar$\underline{H}$), 7.64 (2H, d, *J* = 7.4 Hz, Ar$\underline{H}$), 4.82 (2H, s, *ortho* on η^5-$C_5\underline{H}_4$-benzoyl), 4.37 (2H, s, *meta* on η^5-$C_5\underline{H}_4$-benzoyl), 4.30 - 4.25 (1H, m, -$\underline{CH}CH_3$), 4.08 (2H, q, *J* = 6.8 Hz, -O$\underline{CH_2}CH_3$), 3.95 - 3.88 {6H, m, (η^5-$C_5\underline{H}_4$-alkyl), (-NH$\underline{CH_2}$CO-)}, 2.07 (2H, t, *J* = 7.6 Hz, -$\underline{CH_2}CH_2CH_3$), 1.40 - 1.27 {5H, m, (-$CH_2\underline{CH_2}CH_3$), (-$CH\underline{CH_3}$)}, 1.18 (3H, t, *J* = 6.8 Hz, -$OCH_2\underline{CH_3}$), 0.74 (3H, t, *J* = 7.2 Hz, -$CH_2CH_2\underline{CH_3}$);

^{13}C NMR (100 MHz) δ (DMSO- d_6): 171.0 (C=O), 169.2 (C=O), 168.6 (C=O), 141.5 (C_q), 132.8 (C_q), 128.4, 124.2, 90.3 (C_{ipso} η^5-$\underline{C}_5H_4$-alkyl), 83.0 (C_{ipso} η^5-$\underline{C}_5H_4$-benzoyl), 71.5 (C_{meta} η^5-$\underline{C}_5H_4$-benzoyl), 68.7 (C_{meta} η^5-$\underline{C}_5H_4$-alkyl), 68.2 (C_{ortho} η^5-$\underline{C}_5H_4$-alkyl), 67.9 (C_{ortho} η^5-$\underline{C}_5H_4$-benzoyl), 62.4 (-O$\underline{CH_2}CH_3$, -ve DEPT), 49.6 (-$\underline{CH}CH_3$), 43.0 (-NH$\underline{CH_2}$CHO-, -ve DEPT), 32.0 (-$\underline{CH_2}CH_2CH_3$, -ve DEPT), 22.8 (-$CH_2\underline{CH_2}CH_3$, -ve DEPT), 17.6 (-$\underline{CH}CH_3$), 14.8 (-$OCH_2\underline{CH_3}$), 13.9 (-$CH_2CH_2\underline{CH_3}$).

1-propyl-1'-*N*-{*para*-(ferrocenyl) benzoyl} glycine L-leucine ethyl ester (90)

Glycine L-leucine ethyl ester hydrochloride (0.16 g, 0.72 mmol) was used as a starting material. The crude product was purified by column chromatography {eluent 1:1 hexane: ethyl acetate} and recrystallisation from hexane: ethyl acetate yield the desired product as an orange solid (0.06 g, 15%), m.p 76 - 78 ^{o}C;

$[\alpha]_D^{20}$ = -15^{o} (*c* 0.1, EtOH);

Mass spectrum: $[M+Na]^+$ found: 569.2197

$C_{30}H_{38}N_2O_4FeNa$ requires: 569.2181

I.R. υ_{max} (KBr): 3275 (NH), 1749 (C=O_{ester}), 1629 (C=O_{amide}), 1613 (C=O_{amide}) cm^{-1};

UV-Vis λ_{max} EtOH: 360, 451 nm;

^{1}H NMR (400 MHz) δ (DMSO- d_6): 8.67 (1H, t, *J* = 6.0 Hz, -CON<u>H</u>-), 8.33 (1H, d, *J* = 7.6 Hz, -CON<u>H</u>-), 7.85 (2H, d, *J* = 7.6 Hz, Ar<u>H</u>), 7.66 (2H, d, *J* = 7.6 Hz, Ar<u>H</u>), 4.88 (2H, s, *ortho* on η^5-$C_5\underline{H}_4$-benzoyl), 4.37 (2H, s, *meta* on η^5-$C_5\underline{H}_4$-benzoyl), 4.33 - 4.27 {1H, m, -<u>CH</u>($CH_2CH(CH_3)_2$)}, 4.14 (2H, q, *J* = 7.2 Hz, - O<u>CH_2</u>CH_3), 3.97 - 3.86 {6H m, (η^5-$C_5\underline{H}_4$-alkyl), (-NH<u>CH_2</u>CO-)}, 2.00 (2H, t, *J* = 7.6 Hz, -<u>CH_2</u>CH_2CH_3), 1.69 - 1.45 {3H, m, -CH(<u>CH_2</u><u>CH</u>$(CH_3)_2$)}, 1.40 - 1.27 (2H, m, -CH_2<u>CH_2</u>CH_3), 1.15 (3H, t, *J* = 7.2 Hz, -OCH_2<u>CH_3</u>), 0.91 - 0.83 {6H, m, -CH(CH_2CH(<u>CH_3</u>)$_2$)}, 0.72 (3H, t, *J* = 7.2 Hz, - CH_2CH_2<u>CH_3</u>);

^{13}C NMR (100 MHz) δ (DMSO- d_6): 171.4 (C=O), 169.4 (C=O), 168.1 (C=O), 140.1 (C_q), 131.8 (C_q), 129.4, 126.2, 89.8 (C_{ipso} η^5-<u>C_5</u>H_4-alkyl), 84.1 (C_{ipso} η^5-<u>C_5</u>H_4-benzoyl), 71.2 (C_{meta} η^5-<u>C_5</u>H_4-benzoyl), 69.9 (C_{meta} η^5-<u>C_5</u>H_4-alkyl), 68.5 (C_{ortho} η^5-<u>C_5</u>H_4-alkyl), 67.9 (C_{ortho} η^5-<u>C_5</u>H_4-benzoyl), 62.8 (-O<u>CH_2</u>CH_3, -ve DEPT), 52.1 {-<u>CH</u>($CH_2CH(CH_3)_2$)}, 42.5 (-NH<u>CH_2</u>CHO-, -ve DEPT), 40.0 {-CH(<u>CH_2</u>$CH(CH_3)_2$), -ve DEPT}, 32.0 (-<u>CH_2</u>CH_2CH_3, -ve DEPT), 26.4 {-CH(CH_2<u>CH</u>$(CH_3)_2$)}, 23.5 (-CH_2<u>CH_2</u>CH_3, -ve DEPT), 23.7 {-CH(CH_2CH(<u>CH_3</u>)$_2$)}, 22.4 {-CH(CH_2CH(<u>CH_3</u>)$_2$)}, 14.9 (-OCH_2<u>CH_3</u>), 14.0 (-CH_2CH_2<u>CH_3</u>).

1-propyl-1'-*N*-{*para*-(ferrocenyl) benzoyl} glycine L-phenylalanine ethyl ester (91)

Glycine L-phenyalanine ethyl ester hydrochloride (0.18 g, 0.72 mmol) was used as a starting material. The crude product was purified by column chromatography {eluent

1:1 hexane: ethyl acetate} and recrystallisation from hexane: ethyl acetate yield the desired product as an orange solid (0.06 g, 14%), m.p 74 - 75 ^{o}C;

$[\alpha]_D^{20}$ = +11^{o} (*c* 0.1, EtOH);

Mass spectrum: $[M+Na]^+$ found: 603.2046

$C_{33}H_{36}N_2O_4FeNa$ requires: 603.2034

I.R. υ_{max} (KBr): 3292 (NH), 1737 (C=O_{ester}), 1630 (C=O_{amide}), 1609 (C=O_{amide}) cm^{-1};

UV-Vis λ_{max} EtOH: 360, 452 nm;

^{1}H NMR (400 MHz) δ (DMSO- *d_6*): 8.56 (1H, t, *J* = 6.0 Hz, -CONH-), 8.27 (1H, d, *J* = 7.6 Hz, -CONH-), 7.71 (2H, d, *J* = 8.0 Hz, ArH), 7.51 (2H, d, *J* = 8.0 Hz, ArH), 7.18 - 7.12 {5H, m, -CH(CH_2Ph)}, 4.74 (2H, s, *ortho* on η^5-C_5H_4-benzoyl), 4.40 - 4.38 {1H, m, -CH(CH_2Ph)}, 4.27 (2H, s, *meta* on η^5-C_5H_4-benzoyl), 3.96 (2H, q, *J* = 7.2 Hz, -OCH_2CH_3), 3.84 - 3.79 {6H, m, (η^5-C_5H_4-alkyl), (-NHCH_2CO-)}, 2.92 - 2.85 {2H, m, -CH(CH_2Ph)}, 1.90 (2H, t, *J* = 7.6 Hz, -$CH_2CH_2CH_3$), 1.30 - 1.29 (2H, m, -$CH_2CH_2CH_3$), 1.04 (3H, t, *J* = 7.2 Hz, -OCH_2CH_3), 0.66 (3H, t, *J* = 7.2 Hz, -$CH_2CH_2CH_3$);

^{13}C NMR (100 MHz) δ (DMSO- *d_6*): 169.8 (C=O), 168.7 (C=O), 166.3 (C=O), 140.6 (C_q), 137.0 (C_q), 134.1 (C_q), 128.8, 128.5, 126.2, 124.2, 124.1, 91.5 (C_{ipso} η^5-C_5H_4-alkyl), 83.1 (C_{ipso} η^5-C_5H_4-benzoyl), 70.0 (C_{meta} η^5-C_5H_4-benzoyl), 68.8 (C_{meta} η^5-C_5H_4-alkyl), 68.0 (C_{ortho} η^5-C_5H_4-alkyl), 66.2 (C_{ortho} η^5-C_5H_4-benzoyl), 60.1 (-OCH_2CH_3, -ve DEPT), 52.8 (-CH(CH_2Ph), 42.8 (-NHCH_2CHO-, -ve DEPT), 36.4 {-CH(CH_2Ph), -ve DEPT}, 31.0 (-$CH_2CH_2CH_3$, -ve DEPT), 20.6 (-$CH_2CH_2CH_3$, -ve DEPT), 14.4 (-OCH_2CH_3), 14.0 (-$CH_2CH_2CH_3$).

1-propyl-1'-*N*-{*meta*-(ferrocenyl) benzoyl} glycine glycine ethyl ester (92)

Glycine glycine ethyl ester hydrochloride (0.12 g, 0.72 mmol) was used as a starting material. The crude product was purified by column chromatography {eluent 1:1 hexane: ethyl acetate} yielding the titled product as a red oil (0.08 g, 23 %),

Mass spectrum: $[M+Na]^+$ found: 513.1454

$C_{26}H_{30}N_2O_4FeNa$ requires: 513.1453

I.R. υ_{max} (KBr): 3295 (NH), 1737 (C=O_{ester}), 1631 (C=O_{amide}), 1609 (C=O_{amide}) cm^{-1};

UV-Vis λ_{max} EtOH: 334, 445 nm;

^{1}H NMR (400 MHz) δ (DMSO- d_6): 8.74 (1H, t, *J* = 6.0 Hz, -CONH-), 8.30 (1H, t, *J* = 6 Hz, -CONH-), 8.08 (1H, s, ArH), 7.69 - 7.66 (2H, m, ArH), 7.40 (1H, t, *J* = 7.0 Hz, ArH), 4.80 (2H, s, *ortho* on η^5-C_5H_4-benzoyl), 4.34 (2H, s, *meta* on η^5-C_5H_4-benzoyl), 4.01 (2H, q, *J* = 6.8 Hz, -O$CH_2$$CH_3$), 3.95 - 3.85 {8H, m, ($\eta^5$-$C_5H_4$-alkyl), (-NH$CH_2$CO-), (-NH$CH_2$CO-)}, 2.00 (2H, t, *J* = 7.6 Hz, -$CH_2$$CH_2CH_3$), 1.40 - 1.30 (2H, m, -$CH_2CH_2CH_3$), 1.12 (3H, t, *J* = 7.2 Hz, -OCH_2CH_3), 0.70 (3H, t, *J* = 7.2 Hz, -$CH_2CH_2CH_3$);

^{13}C NMR (100 MHz) δ (DMSO- d_6): 170.8 (C=O), 169.1 (C=O), 165.5 (C=O), 138.5 (C_q), 135.8 (C_q), 128.2, 127.9, 127.0, 123.2, 92.5 (C_{ipso} η^5-C_5H_4-alkyl), 83.0 (C_{ipso} η^5-C_5H_4-benzoyl), 71.7 (C_{meta} η^5-C_5H_4-benzoyl), 69.8 (C_{meta} η^5-C_5H_4-alkyl), 68.4 (C_{ortho} η^5-C_5H_4-alkyl), 66.7 (C_{ortho} η^5-C_5H_4-benzoyl), 62.4 (-O$CH_2$$CH_3$, -ve DEPT), 42.8 (-NH$CH_2$CHO-, -ve DEPT), 41.9 (-NHCH_2CHO-, -ve DEPT), 32.8 (-$CH_2$$CH_2CH_3$, -ve DEPT), 25.0 (-$CH_2$$CH_2CH_3$, -ve DEPT), 14.5 (-O$CH_2$$CH_3$), 14.0 (-$CH_2CH_2$$CH_3$).

1-propyl-1'-*N*-{*meta*-(ferrocenyl) benzoyl} glycine L-alanine ethyl ester (93)

Glycine L-alanine ethyl ester hydrochloride (0.13 g, 0.72 mmol) was used as a starting material. The crude product was purified by column chromatography {eluent 1:1 hexane: ethyl acetate} yielding the titled product as a red oil (0.08 g, 22%),

$[\alpha]_D^{20}$ = -16^o (*c* 0.1, EtOH);

Mass spectrum: $[M+Na]^+$ found: 527.1621

$C_{27}H_{32}N_2O_4FeNa$ requires: 527.1609

I.R. υ_{max} (KBr): 3290 (NH), 1739 (C=O_{ester}), 1635 (C=O_{amide}), 1605 (C=O_{amide}) cm^{-1};

UV-Vis λ_{max} EtOH: 330, 449 nm;

^{1}H NMR (400 MHz) δ (DMSO- d_6): 8.65 (1H, t, *J* = 6.0 Hz, -CONH-), 8.41 (1H, d, *J* = 7.2 Hz, -CONH-), 8.10 (1H, s, ArH), 7.71 - 7.69 (2H, m, ArH), 7.42 (1H, t, *J* = 7.0 Hz, ArH), 4.80 (2H, s, *ortho* on η^5-C_5H_4-benzoyl), 4.35 (2H, s, *meta* on η^5-C_5H_4-benzoyl), 4.30 - 4.25 (1H, m, -$CH$$CH_3$), 4.10 (2H, q, *J* = 6.8 Hz, -O$CH_2$$CH_3$), 3.97 - 3.85 {6H, m, ($\eta^5$-$C_5H_4$-alkyl), (-NH$CH_2$CO-)}, 2.00 (2H, t, *J* = 7.6 Hz, -$CH_2$$CH_2CH_3$), 1.35 - 1.25 {5H, m, (-$CH_2$$CH_2CH_3$), (-$CH$$CH_3$)}, 1.10 (3H, t, *J* = 6.8 Hz, -O$CH_2$$CH_3$), 0.72 (3H, t, *J* = 7.2 Hz, -$CH_2CH_2$$CH_3$);

^{13}C NMR (100 MHz) δ (DMSO- d_6): 170.0 (C=O), 169.5 (C=O), 168.2 (C=O), 135.5 (C_q), 132.8 (C_q), 130.4, 129.2, 126.4, 123.9, 92.3 (C_{ipso} η^5-$\underline{C}_5H_4$-alkyl), 82.6 (C_{ipso} η^5-$\underline{C}_5H_4$-benzoyl), 71.6 (C_{meta} η^5-$\underline{C}_5H_4$-benzoyl), 68.9 (C_{meta} η^5-$\underline{C}_5H_4$-alkyl), 68.4 (C_{ortho} η^5-$\underline{C}_5H_4$-alkyl), 67.9 (C_{ortho} η^5-$\underline{C}_5H_4$-benzoyl), 61.4 (-O$\underline{CH_2}$$CH_3$, -ve DEPT), 48.6 (-$\underline{CH}$$CH_3$), 41.0 (-NH$\underline{CH_2}$CHO-, -ve DEPT), 31.9 (-$\underline{CH_2}$$CH_2CH_3$, -ve DEPT), 21.0 (-$CH_2\underline{CH_2}CH_3$, -ve DEPT), 18.0 (-CH$\underline{CH_3}$), 14.2 (-OCH$_2\underline{CH_3}$), 13.9 (-$CH_2CH_2\underline{CH_3}$).

1-propyl- 1'-*N*-{*meta*-(ferrocenyl) benzoyl} glycine L-leucine ethyl ester (94)

Glycine L-leucine ethyl ester hydrochloride (0.16 g, 0.72 mmol) was used as a starting material. The crude product was purified by column chromatography {eluent 1:1 hexane: ethyl acetate} yielding the titled product as a red oil (0.07 g, 18%),

$[\alpha]_D^{20}$ = -18^o (*c* 0.1, EtOH);

Mass spectrum: $[M+Na]^+$ found: 569.2193

$C_{30}H_{38}N_2O_4FeNa$ requires: 569.2181

I.R. υ_{max} (KBr): 3260 (NH), 1736 ($C=O_{ester}$), 1643 ($C=O_{amide}$), 1612 ($C=O_{amide}$) cm^{-1};

UV-Vis λ_{max} EtOH: 331, 448 nm;

^{1}H NMR (400 MHz) δ (DMSO- d_6): 8.65 (1H, t, *J* = 6.0 Hz, -CON$\underline{H}$-), 8.30 (1H, d, *J* = 7.6 Hz, -CON$\underline{H}$-), 8.00 (1H, s, Ar$\underline{H}$), 7.72 - 7.70 (2H, m, Ar$\underline{H}$), 7.39 (1H, t, *J* = 7.0 Hz, Ar$\underline{H}$), 4.83 (2H, s, *ortho* on η^5-$C_5\underline{H}_4$-benzoyl), 4.35 (2H, t, *J* = 1.6 Hz, *meta* on η^5-$C_5\underline{H}_4$-benzoyl), 4.30 - 4.28 {1H, m, -$\underline{CH}$($CH_2CH(CH_3)_2$)}, 4.19 (2H, q, *J* = 7.2 Hz, -O$\underline{CH_2}$$CH_3$) , 3.95 - 3.88 {6H, m, (η^5-$C_5\underline{H}_4$-alkyl), (-NH$\underline{CH_2}$CO-)}, 2.08 (2H, t, *J* = 7.6 Hz, -$\underline{CH_2}$$CH_2CH_3$), 1.69 - 1.45 {3H, m, -CH($\underline{CH_2}$$\underline{CH}$$(CH_3)_2$)}, 1.35 - 1.25 (2H, m, -$CH_2\underline{CH_2}CH_3$), 1.19 (3H, t, *J* = 7.2 Hz, -OCH$_2\underline{CH_3}$), 0.89 - 0.83 {6H, m, -CH(CH_2CH($\underline{CH_3}$)$_2$)}, 0.70 (3H, t, *J* = 7.2 Hz, - $CH_2CH_2\underline{CH_3}$);

^{13}C NMR (100 MHz) δ (DMSO- d_6): 171.9 (C=O), 169.6 (C=O), 166.1 (C=O), 139.1 (C_q), 137.8 (C_q), 132.4, 129.7, 127.2, 125.7, 89.4 (C_{ipso} η^5-$\underline{C}_5H_4$-alkyl), 83.3 (C_{ipso} η^5-$\underline{C}_5H_4$-benzoyl), 71.0 (C_{meta} η^5-$\underline{C}_5H_4$-benzoyl), 70.4 (C_{meta} η^5-$\underline{C}_5H_4$-alkyl), 68.4 (C_{ortho} η^5-$\underline{C}_5H_4$-alkyl), 66.1 (C_{ortho} η^5-$\underline{C}_5H_4$-benzoyl), 61.4 (-O$\underline{CH_2}$$CH_3$, -ve DEPT), 51.3 (-$\underline{CH}$($CH_2CH(CH_3)_2$), 42.9 (-NH$\underline{CH_2}$CHO-, -ve DEPT), 40.0 {-CH($\underline{CH_2}$$CH(CH_3)_2$), -ve DEPT}, 31.0 (-$\underline{CH_2}$$CH_2CH_3$, -ve DEPT), 27.4 (-CH($CH_2\underline{CH}(CH_3)_2$) 24.7 (-$CH_2\underline{CH_2}CH_3$, -ve DEPT), 23.2 {-CH($CH_2$CH($\underline{CH_3}$)$_2$)}, 22.4 -CH($CH_2$CH($\underline{CH_3}$)$_2$), 14.6 (-OCH$_2\underline{CH_3}$), 13.6 (-$CH_2CH_2\underline{CH_3}$).

1-propyl-1'-*N*-{*meta*-(ferrocenyl) benzoyl} glycine L-phenylalanine ethyl ester (95)

Glycine L-phenylalanine ethyl ester hydrochloride (0.18 g, 0.72 mmol) was used as a starting material. The crude product was purified by column chromatography {eluent 1:1 hexane: ethyl acetate} yielding the titled product as a red oil (0.07 g, 17%),

$[\alpha]_D^{20} = -13^o$ (*c* 0.1, EtOH);

Mass spectrum: $[M+Na]^+$ found: 603.2032

$C_{33}H_{36}N_2O_4FeNa$ requires: 603.2034

I.R. υ_{max} (KBr): 3300 (NH), 1745 ($C=O_{ester}$), 1633 ($C=O_{amide}$), 1612 ($C=O_{amide}$) cm^{-1};

UV-Vis λ_{max} EtOH: 330, 447 nm;

^{1}H NMR (400 MHz) δ (DMSO- d_6): 8.68 (1H, t, *J* = 6.0 Hz, -CONH-), 8.30 (1H, d, *J* = 7.6 Hz, -CONH-), 8.00 (1H, s, ArH), 7.69 - 7.68 (2H, m, ArH), 7.40 (1H, t, *J* = 7.6 Hz, ArH), 7.25 - 7.21 (5H, m, -CH(CH_2Ph)}, 4.80 (2H, s, *ortho* on η^5-C_5H_4-benzoyl), 4.49 - 4.47 {1H, m, -CH(CH_2Ph)}, 4.29 (2H, s, *meta* on η^5-C_5H_4-benzoyl), 4.00 (2H, q, *J* = 7.2 Hz, -OCH_2CH_3), 3.95 - 3.83 {6H, m, (η^5-C_5H_4-alkyl), (-NHCH_2CO-)}, 3.06 - 2.90 {2H, m, -CH(CH_2Ph)}, 1.99 (2H, t, *J* = 7.6 Hz, -$CH_2CH_2CH_3$), 1.40 - 1.27 (2H, m, -$CH_2CH_2CH_3$), 1.11 (3H, t, *J* = 7.2 Hz, -OCH_2CH_3), 0.70 (3H, t, *J* = 7.2 Hz, -$CH_2CH_2CH_3$);

^{13}C NMR (100 MHz) δ (DMSO- d_6): 171.9 (C=O), 169.2 (C=O), 166.9 (C=O), 137.0 (C_q), 132.7 (C_q), 130.1 (C_q), 128.7, 127.2, 126.8, 126.1, 125.2, 124.9, 123.7, 89.1 (C_{ipso} η^5-C_5H_4-alkyl), 84.0 (C_{ipso} η^5-C_5H_4-benzoyl), 71.4 (C_{meta} η^5-C_5H_4-benzoyl), 69.4 (C_{meta} η^5-C_5H_4-alkyl), 67.5 (C_{ortho} η^5-C_5H_4-alkyl), 66.3 (C_{ortho} η^5-C_5H_4-benzoyl), 62.4 (-OCH_2CH_3, -ve DEPT), 53.7 (-CH(CH_2Ph)), 43.2 (-NHCH_2CHO-, -ve DEPT), 39.2 {-CH(CH_2Ph), -ve DEPT}, 33.8 (-$CH_2CH_2CH_3$, -ve DEPT), 20.6 (-$CH_2CH_2CH_3$, -ve DEPT), 14.9 (-OCH_2CH_3), 13.1 (-$CH_2CH_2CH_3$).

1-propyl- 1'-*N*- {*ortho*-(ferrocenyl) benzoyl} glycine glycine ethyl ester (96)

Glycine-glycine ethyl ester hydrochloride (0.12 g, 0.72 mmol) was used as a starting material. The crude product was purified by column chromatography {eluent 1:1 hexane: ethyl acetate} yielding the titled product as a red oil (0.08 g, 23%),

Mass spectrum: $[M+Na]^+$ found: 513.1464

$C_{26}H_{30}N_2O_4FeNa$ requires: 513.1453

I.R. υ_{max} (KBr): 3387 (NH), 1735 (C=O_{ester}), 1629 (C=O_{amide}), 1609 (C=O_{amide}) cm^{-1};

UV-Vis λ_{max} EtOH: 325, 443 nm;

^{1}H NMR (400 MHz) δ(DMSO- d_6): 8.76 (1H, t, *J* = 5.6 Hz, -CONH-), 8.34 (1H, t, *J* = 5.6 Hz, -CONH-), 7.98 (1H, d, *J* = 7.4 Hz, ArH), 7.86 (1H, t, *J* = 7.2 Hz, ArH), 7.70 (1H, t, *J* = 6.8 Hz, ArH), 7.39 (1H, d, *J* = 7.6 Hz, ArH), 4.83 (2H, s, *ortho* on η^5-C_5H_4-benzoyl), 4.36 (2H, s, *meta* on η^5-C_5H_4-benzoyl), 4.12 (2H, q, *J* = 6.8 Hz, - OCH_2CH_3) , 3.96 - 3.85 {8H, m, (η^5-C_5H_4-alkyl), (-$NHCH_2CO$-), (-$NHCH_2CO$-)}, 2.05 (2H, t, *J* = 7.6 Hz, -$CH_2CH_2CH_3$), 1.35 - 1.27 (2H, m, -$CH_2CH_2CH_3$), 1.10 (3H, t, *J* = 6.8 Hz, -OCH_2CH_3), 0.72 (3H, t, *J* = 7.2 Hz, - $CH_2CH_2CH_3$);

^{13}C NMR (100 MHz) δ (DMSO- d_6): 168.8 (C=O), 168.3 (C=O), 167.9 (C=O), 142.5 (C_q), 137.8 (C_q), 130.2, 129.5, 128.9, 126.7, 91.8 (C_{ipso} η^5-C_5H_4-alkyl), 81.9 (C_{ipso} η^5-C_5H_4-benzoyl), 71.7 (C_{meta} η^5-C_5H_4-benzoyl), 69.1 (C_{meta} η^5-C_5H_4-alkyl), 67.0 (C_{ortho} η^5-C_5H_4-alkyl), 66.2 (C_{ortho} η^5-C_5H_4-benzoyl), 61.9 (-OCH_2CH_3, -ve DEPT), 44.4 (-$NHCH_2CHO$-, -ve DEPT), 42.8 (-$NHCH_2CHO$-, -ve DEPT), 32.8 (-$CH_2CH_2CH_3$, -ve DEPT), 24.5 (-$CH_2CH_2CH_3$, -ve DEPT), 14.3 (-OCH_2CH_3), 13.1 (-$CH_2CH_2CH_3$).

1-propyl- 1'-*N*-{*ortho*-(ferrocenyl) benzoyl} glycine L-alanine ethyl ester (97)

Glycine L-alanine ethyl ester hydrochloride (0.13 g, 0.72 mmol) was used as a starting material. The crude product was purified by column chromatography {eluent 1:1 hexane: ethyl acetate} yielding the titled product as a red oil (0.07 g, 19%),

$[\alpha]_D^{20}$ = -19^o (*c* 0.1, EtOH);

Mass spectrum: $[M+Na]^+$ found: 527.1617

$C_{27}H_{32}N_2O_4FeNa$ requires: 527.1609

I.R. υ_{max} (KBr): 3291 (NH), 1740 (C=O_{ester}), 1639 (C=O_{amide}), 1618 (C=O_{amide}) cm^{-1};

UV-Vis λ_{max} EtOH: 325, 446 nm;

^{1}H NMR (400 MHz) δ (DMSO- d_6): 8.68 (1H, t, *J* = 6.0 Hz, -CONH-), 8.41 (1H, d, *J* = 7.0 Hz, -CONH-), 8.01 (1H, d, *J* = 7.6 Hz, ArH), 7.80 (1H, t, *J* = 7.2 Hz, ArH), 7.79 (1H, t, *J* = 6.0 Hz, ArH), 7.38 (1H, d, *J* = 7.6 Hz, ArH), 4.85 (2H, s, *ortho* on η^5-C_5H_4-benzoyl), 4.37 (2H, s, *meta* on η^5-C_5H_4-benzoyl), 4.33 - 4.28 (1H, m, - $CHCH_3$), 4.11 (2H, q, *J* = 6.4 Hz, - OCH_2CH_3) , 3.92 - 3.85 {6H, m, (η^5-C_5H_4-alkyl), (-$NHCH_2CO$-)},

2.05 (2H, t, *J* = 7.6 Hz, -$\underline{CH_2}CH_2CH_3$), 1.38 - 1.29 {5H, m, (-$CH_2\underline{CH_2}CH_3$), (-$CH\underline{CH_3}$)}, 1.14 (3H, t, *J* = 6.4 Hz, -$OCH_2\underline{CH_3}$), 0.70 (3H, t, *J* = 7.2 Hz, -$CH_2CH_2\underline{CH_3}$);

^{13}C NMR (100 MHz) δ (DMSO- d_6): 172.9 (C=O), 169.0 (C=O), 166.2 (C=O), 137.2 (C_q), 135.8 (C_q), 130.4, 128.6, 127.4, 124.8, 91.3 (C_{ipso} η^5-$\underline{C}_5H_4$-alkyl), 81.2 (C_{ipso} η^5-$\underline{C}_5H_4$-benzoyl), 72.0 (C_{meta} η^5-$\underline{C}_5H_4$-benzoyl), 68.8 (C_{meta} η^5-$\underline{C}_5H_4$-alkyl), 68.5 (C_{ortho} η^5-$\underline{C}_5H_4$-alkyl), 67.9 (C_{ortho} η^5-$\underline{C}_5H_4$-benzoyl), 60.4 (-O$\underline{CH_2}CH_3$, -ve DEPT), 47.6 (-$\underline{CH}CH_3$), 42.0 (-NH$\underline{CH_2}$CHO-, -ve DEPT), 31.0 (-$\underline{CH_2}CH_2CH_3$, -ve DEPT), 22.8 (-$CH_2\underline{CH_2}CH_3$, -ve DEPT), 17.4 (-CH$\underline{CH_3}$), 15.0 (-$OCH_2\underline{CH_3}$), 14.0 (-$CH_2CH_2\underline{CH_3}$).

1-propyl- 1'-*N*-{*ortho*-(ferrocenyl) benzoyl} glycine L-leucine ethyl ester (98)

Glycine L-leucine ethyl ester hydrochloride (0.12 g, 0.72 mmol) was used as a starting material. The crude product was purified by column chromatography {eluent 1:1 hexane: ethyl acetate} yielding the titled product as a red oil (0.05 g, 14%),

$[\alpha]_D^{20}$ = -17^o (*c* 0.1, EtOH);

I.R. υ_{max} (KBr): 3272 (NH), 1751 (C=O_{ester}), 1633 (C=O_{amide}), 1610 (C=O_{amide}) cm^{-1};

UV-Vis λ_{max} EtOH: 324, 446 nm;

^{1}H NMR (400 MHz) δ(DMSO- d_6): 8.67 (1H, t, *J* = 6.0 Hz, -CON$\underline{H}$-), 8.33 (1H, d, *J* = 7.6 Hz, -CON$\underline{H}$-), 8.03 (1H, d, *J* = 7.2 Hz, Ar$\underline{H}$), 7.81 (1H, t, *J* = 7.0 Hz, Ar$\underline{H}$), 7.79 (1H, t, *J* = 6.4 Hz, Ar$\underline{H}$), 7.31 (1H, d, *J* = 7.6 Hz, Ar$\underline{H}$), 4.79 (2H, s, *ortho* on η^5-$C_5\underline{H}_4$-benzoyl), 4.35 (2H, s, *meta* on η^5-$C_5\underline{H}_4$-benzoyl), 4.30 - 4.27 {1H, m, -$\underline{CH}(CH_2CH(CH_3)_2)$}, 4.17 (2H, q, *J* = 7.2 Hz, - O$\underline{CH_2}CH_3$), 3.95 - 3.84 {6H, m, (η^5-$C_5\underline{H}_4$-alkyl), (-NH$\underline{CH_2}$CO-)}, 2.07 (2H, t, *J* = 7.6 Hz, -$\underline{CH_2}CH_2CH_3$), 1.69 - 1.45 {3H, m, -CH($\underline{CH_2}\underline{CH}(CH_3)_2$)}, 1.38 - 1.23 (2H, m, -$CH_2\underline{CH_2}CH_3$), 1.17 (3H, t, *J* = 7.2 Hz, -$OCH_2\underline{CH_3}$), 0.90 - 0.85 {6H, m, -CH($CH_2CH(\underline{CH_3})_2$)}, 0.74 (3H, t, *J* = 7.2 Hz, -$CH_2CH_2\underline{CH_3}$);

^{13}C NMR (100 MHz) δ (DMSO- d_6): 170.9 (C=O), 168.5 (C=O), 167.1 (C=O), 139.5 (C_q), 135.8 (C_q), 129.4, 127.9, 125.2, 124.9, 91.4 (C_{ipso} η^5-$\underline{C}_5H_4$-alkyl), 82.9 (C_{ipso} η^5-$\underline{C}_5H_4$-benzoyl), 71.0 (C_{meta} η^5-$\underline{C}_5H_4$-benzoyl), 70.4 (C_{meta} η^5-$\underline{C}_5H_4$-alkyl), 69.2 (C_{ortho} η^5-$\underline{C}_5H_4$-alkyl), 66.8 (C_{ortho} η^5-$\underline{C}_5H_4$-benzoyl), 61.4 (-O$\underline{CH_2}CH_3$, -ve DEPT), 51.3 {-$\underline{CH}(CH_2CH(CH_3)_2)$}, 43.9 (-NH$\underline{CH_2}$CHO-, -ve DEPT), 41.0 {-CH($\underline{CH_2}CH(CH_3)_2$), -ve DEPT}, 31.0 (-$\underline{CH_2}CH_2CH_3$, -ve DEPT), 27.7 {-CH($CH_2\underline{CH}(CH_3)_2$)}, 24.4 (-

$CH_2\underline{CH_2}CH_3$, -ve DEPT), 22.7 {-CH($CH_2CH(\underline{CH_3})_2$)}, 21.4 {-CH($CH_2CH(\underline{CH_3})_2$)}, 14.6 (-$OCH_2\underline{CH_3}$), 13.6 (-$CH_2CH_2\underline{CH_3}$).

1-propyl-1'-*N*-{*ortho*-(ferrocenyl) benzoyl} glycine L-phenylalanine ethyl ester (99)

Glycine L-phenylalanine ethyl ester hydrochloride (0.18 g, 0.72 mmol) was used as a starting material. The crude product was purified by column chromatography {eluent 1:1 hexane: ethyl acetate} yielding the titled product as a red oil (0.06 g, 13%),

$[\alpha]_D^{20} = +17^o$ (*c* 0.1, EtOH);

I.R. υ_{max} (KBr): 3288 (NH), 1730 ($C=O_{ester}$), 1629 ($C=O_{amide}$), 1615 ($C=O_{amide}$) cm^{-1};

UV-Vis λ_{max} EtOH: 324, 445 nm;

^{1}H NMR (400 MHz) δ(DMSO- d_6): 8.50 (1H, t, *J* = 6.0 Hz, -CON<u>H</u>-), 8.26 (1H, d, *J* = 7.0 Hz, -CON<u>H</u>-), 7.91 (1H, d, *J* = 7.0 Hz, Ar<u>H</u>), 7.78 (3H, t, *J* = 7.2 Hz, Ar<u>H</u>), 7.49 (1H, t, *J* = 7.2 Hz, Ar<u>H</u>), 7.30 (1H, d, *J* = 7.0 Hz, Ar<u>H</u>) 7.16 - 7.10 {5H, m, -CH($CH_2\underline{Ph}$)}, 4.73 (2H, s, *ortho* on η^5-$C_5\underline{H}_4$-benzoyl), 4.40 - 4.38 {1H, m, -<u>CH</u>(CH_2Ph)}, 4.27 (2H, s, *meta* on η^5-$C_5\underline{H}_4$-benzoyl), 3.96 (2H, q, *J* = 7.2 Hz, -O$\underline{CH_2}CH_3$), 3.83 - 3.79 {6H, m, (η^5-$C_5\underline{H}_4$-alkyl), (-NH$\underline{CH_2}$CO-)}, 2.84 - 2.80 {3H, m, -CH($\underline{CH_2}$Ph)}, 1.88 (2H, t, *J* = 7.6 Hz, -$\underline{CH_2}CH_2CH_3$), 1.39 - 1.33 (2H, m, -$CH_2\underline{CH_2}CH_3$), 1.14 (3H, t, *J* = 7.2 Hz, -$OCH_2\underline{CH_3}$), 0.76 (3H, t, *J* = 7.2 Hz, -$CH_2CH_2\underline{CH_3}$);

^{13}C NMR (100 MHz) δ (DMSO- d_6): 169.6 (C=O), 168.6 (C=O), 166.3 (C=O), 136.0 (C_q), 134.1 (C_q), 128.8 (C_q), 128.5, 126.2, 125.1, 124.2, 123.1, 122.2, 120.8, 91.2 (C_{ipso} η^5-$\underline{C}_5H_4$-alkyl), 83.1 (C_{ipso} η^5-$\underline{C}_5H_4$-benzoyl), 69.9 (C_{meta} η^5-$\underline{C}_5H_4$-benzoyl), 68.8 (C_{meta} η^5-$\underline{C}_5H_4$-alkyl), 68.5 (C_{ortho} η^5-$\underline{C}_5H_4$-alkyl), 66.2 (C_{ortho} η^5-$\underline{C}_5H_4$-benzoyl), 60.3 (-O$\underline{CH_2}CH_3$, -ve DEPT), 50.0 {-<u>CH</u>(CH_2Ph)}, 42.4 (-NH$\underline{CH_2}$CHO-, -ve DEPT), 36.2 (-CH($\underline{CH_2}$Ph), -ve DEPT), 31.1 (-$\underline{CH_2}CH_2CH_3$, -ve DEPT), 20.8 (-$CH_2\underline{CH_2}CH_3$, -ve DEPT), 14.3 (-$OCH_2\underline{CH_3}$), 14.1 (-$CH_2CH_2\underline{CH_3}$).

General procedure for the preparation of starting materials for ethynyl ferrocenyl dipeptide derivatives

(2-Formyl-1-chlorovinyl) ferrocene (100) [3]

Acetylferrocene (22.8 g, 99.96 mmol) was dissolved in *N, N*-dimethylformamide (25 ml) at 0 °C under nitrogen. Phosphorus oxychloride (25 ml) was added to dimethylformamide (25 ml) at 0 °C under nitrogen and stirred for 25 min resulting in a viscous red complex. The viscous complex was added to the acetylferrocene mixture over 2 hr and further stirred for 3 hr at 0 °C. Diethyl ether (80 ml), sodium acetate (116 g, mmol) and deionised water (20 ml) were added to reaction mixture. The reaction mixture was stirred at room temperature for 12 hr and then conc. sodium bicarbonate solution was added. The resulting solution was extracted with ethyl acetate. The solvent was evaporated to yield the crude product which was purified by column chromatography (eluent 9:1 hexane: diethyl ether) yielding the title compound as deep purple crystals. (17 g, 62%), mp. 76 - 77 °C (lit. [3] 76 - 77 °C);

^{1}H NMR (400 MHz) δ (DMSO- d_6): 10.03 (1H, d, J = 7.2 Hz, -C<u>H</u>O), 6.32 {1H, d, J = 7.2 Hz, η^5-C_5H_4-C=C<u>H</u>(Cl)-}. 4.68 {2H, t, J = 2.0 Hz, *ortho* on η^5-C_5<u>H_4</u>-C=CH(Cl)-}, 4.49 {2H, t, J = 2.0 Hz, *meta* on η^5-C_5<u>H_4</u>-C=CH(Cl)-}, 4.17 (5H, s, η^5-C_5<u>H_5</u>);

^{13}C NMR (100 MHz) δ (DMSO- d_6): 190.8 (C=O), 155.4 (η^5-C_5H_4-C=<u>C</u>H(Cl)-), 120.4 (η^5-C_5H_4-<u>C</u>=CH(Cl)-), 80.1 (C_{ortho} η^5-<u>C_5</u>H_4-C=CH(Cl)-), 72.3 (η^5-<u>C_5</u>H_5), 70.1 (C_{meta} η^5-<u>C_5</u>H_4-C=CH(Cl)-), 68.9 (C_{ipso} η^5-<u>C_5</u>H_4-C=CH(Cl)-).

Ethynyl ferrocene (101) [4]

Potassium *tert*-butoxide (10.24 g, 91.25 mmol) was added to dry tetrahydrofuran (100 ml) at 0 °C under nitrogen and stirred for 25 min. (2-Formyl-1-chlorovinyl) ferrocene (5 g, 18.25 mmol) was added slowly over 10 min and the reaction mixture was stirred at 0°C for 30 min and refluxed at 80 °C for 4 hr. The reaction mixture was poured into ice then neutralised with conc. hydrochloric acid. The resulting solution was extracted with hexane and the solvent was evaporated to yield the crude product which was purified by column chromatography (eluent 9:1 hexane: diethyl ether) yielding the title compound as a red solid. (1.87 g, 49%) m.p 52 -53 °C, (lit. [4] 52 - 53 °C);

^{1}H NMR (400 MHz) δ (DMSO- d_6): 4.68 (2H, t, J = 2.0 Hz, *ortho* on η^5-C$_5$H$_4$-C≡CH), 4.25 - 4.15 {7H, m, (*meta* on η^5-C$_5$H$_4$-C≡CH), (η^5-C$_5$H$_5$)}, 2.74 (1H, s, η^5-C$_5$H$_4$-C≡CH);
^{13}C NMR (100 MHz) δ (DMSO- d_6): 82.5 (η^5-C$_5$H$_4$-C≡CH), 73.5 (η^5-C$_5$H$_4$-C≡CH), 71.8 (C$_{ortho}$ η^5-C$_5$H$_4$-C≡CH), 70.1 (η^5-C$_5$H$_5$), 68.7 (C$_{meta}$ η^5-C$_5$H$_4$-C≡CH), 63.5 (C$_{ipso}$ η^5-C$_5$H$_4$-C≡CH).

para-(ferrocenyl) ethynyl benzoic acid (102)

Ethynyl ferrocene (2.00 g, 9.52 mmol) and 4-bromobenzoic acid (1.91 g, 9.52 mmol) were mixed together and dissolved in 50 ml of a 1:1 mixture of dry triethylamine and tetrahydrofuran under nitrogen for 10 min. Triphenylphosphine (0.20 g, 0.76 mmol), *bis*(triphenylphosphine)palladium(II) dichloride (0.28 g, 0.38 mmol) and copper(I) iodide (0.07 g, 0.38 mmol) were mixed together and added to the reaction mixture. The reaction mixture was stirred for 10 min and refluxed at 80 ^{o}C for 12 hr. The reaction mixture was vacuum filtered. The solvent was removed *in vacuo* to yield the crude product. The crude product was purified by column chromatography (eluent 1:1 hexane: ethyl acetate) yielding the title compound as a red solid (2.53 g, 81%), mp 147 - 149 ^{o}C;
^{1}H NMR (400 MHz) δ (DMSO- d_6): 12.83 (1H, s, -COOH), 7.90 (2H, d, J = 9.2 Hz, ArH), 7.58 (2H, d, J = 9.2 Hz, ArH), 4.61 (2H, t, J = 2.0 Hz, *ortho* on η^5-C$_5$H$_4$-C≡C-), 4.38 (2H, t, J = 2.0 Hz, *meta* on η^5-C$_5$H$_4$-C≡C-), 4.29 (5H, s, η^5-C$_5$H$_5$);
^{13}C NMR (100 MHz) δ (DMSO- d_6): 171.0 (C=O), 138.2 (C$_q$), 136.1(C$_q$), 133.0, 131.0, 96.4 (η^5-C$_5$H$_4$-C≡C-), 87.0 (η^5-C$_5$H$_4$-C≡C-), 71.4 (C$_{ortho}$ η^5-C$_5$H$_4$-C≡C-), 70.1 (η^5-C$_5$H$_5$), 69.7 (C$_{meta}$ η^5-C$_5$H$_4$-C≡C-), 64.0 (C$_{ipso}$ η^5-C$_5$H$_4$-C≡C-).

6-(Ferrocenyl) ethynyl-2-naphthoic acid (103)

Ethynyl ferrocene (2.00 g, 9.52 mmol) and 6-bromo-2-naphthoic acid (2.39 g, 9.52 mmol) were used as starting materials. The crude product was purified by column chromatography (eluent 1:1 hexane: ethyl acetate) to yield the desired product as a red solid. (2.34 g, 64%), mp 167- 169 ^{o}C;

^{1}H NMR (400 MHz) δ (DMSO- *d_6*): 12.87 (1H, s, -COOH), 8.13 (1H, s, ArH), 7.95 - 7.48 (5H, m, (ArH), 4.60 (2H, t, *J* = 2.0 Hz, *ortho* on η^5-C_5H_4-C≡C-), 4.27 (2H, t, *J* = 2.0 Hz *meta* on η^5-C_5H_4-C≡C-), 4.19 (5H, s, η^5-C_5H_5);
^{13}C NMR (100 MHz) δ (DMSO- *d_6*): 172.7 (C=O), 134.9 (C_q), 134.6 (C_q), 134.0 (C_q), 132.2 (C_q), 131.6, 130.3, 128.1, 128.0, 127.8, 120.8, 90.3 (η^5-C_5H_4-C≡C-), 85.7 (η^5-C_5H_4-C≡C-), 71.4 (C_{ortho} η^5-C_5H_4-C≡C-), 69.9 (η^5-C_5H_5), 68.7 (C_{meta} η^5-C_5H_4-C≡C-), 65.8 (C_{ipso} η^5-C_5H_4-C≡C-).

5-(Ferrocenyl) ethynyl-2-furanoic acid (104)

Ethynyl ferrocene (2.00 g, 9.52 mmol) and 5-bromo-2-furanoic acid (1.82 g, 9.52 mmol) was used as starting materials. The crude product was purified by column chromatography (eluent 1:1 hexane: ethyl acetate) to yield the desired product as a red oil (2.10 g, 69%);
^{1}H NMR (400 MHz) δ (DMSO- *d_6*): 11.5 (1H, s, COOH), 7.06 (1H, d, *J* = 3.6 Hz, ArH), 6.56 (1H, d, *J* = 3.6 Hz, ArH), 4.48 (2H, s, *ortho* on η^5-C_5H_4-C≡C-) , 4.24 (2H, s, *meta* on η^5-C_5H_4-C≡C-), 4.16 (5H, s, η^5-C_5H_5);
^{13}C NMR (100 MHz) δ (DMSO- *d_6*): 167.9 (C=O), 146.5 (C_q), 139.3 (C_q), 116.1, 116.0, 94.5 (η^5-C_5H_4-C≡C-), 75.0 (η^5-C_5H_4-C≡C-), 71.7 (C_{ortho} η^5-C_5H_4-C≡C-), 70.2 (η^5-C_5H_5), 69.5 (C_{meta} η^5-C_5H_4-C≡C-), 65.1 (C_{ipso} η^5-C_5H_4-C≡C-).

General procedure for the preparation of *N*-{*para*-(ferrocenyl) ethynyl benzoyl} amino acids and dipeptide esters

***N*-{*para*-(ferrocenyl) ethynyl benzoyl} glycine glycine methyl ester (105)**

N-para-(ferrocenyl) ethynyl benzoic acid (1.00 g, 3.03 mmol) was dissolved in dichloromethane (100 ml) at 0 ^{o}C. *N*-(3-dimethylaminopropyl)-*N*'-ethylcarbodiimide hydrochloride (0.58 g, 3.03 mmol), 1-hydroxybenzotriazole (0.35 g, 3.03 mmol), glycine glycine methyl ester hydrochloride (0.44 g, 3.03 mmol) and triethylamine (6 ml) were added and the reaction mixture was allowed to stir at 0 ^{o}C for 45 min. The reaction mixture was then allowed to stir at room temperature for 48 h, and washed with water and brine. The organic layer was dried over $MgSO_4$. The solvent was removed *in vacuo* to yield the crude product, that was purified by column chromatography (eluent 1:1 hexane: ethyl acetate) yielding the title compound as an orange solid (0.35 g, 25%), m.p 169 - 171 ^{o}C;

Mass spectrum: $[M+Na]^+$ found: 481.0814

$C_{24}H_{22}N_2O_4FeNa$ requires: 481.0827

I.R. υ_{max} (KBr): 3261 (NH), 2204 (-C≡C-), 1736 (C=O_{ester}), 1658 (C=O_{amide}), 1603 (C=O_{amide}) cm^{-1};

UV-Vis λ_{max} EtOH: 385, 490 nm;

^{1}H NMR (400 MHz) δ (DMSO- d_6): 8.91 (1H, t, *J* = 6.0 Hz, -CON<u>H</u>-), 8.40 (1H, t, *J* = 6.0 Hz, -CON<u>H</u>-), 7.90 (2H, d, *J* = 8.0 Hz, Ar<u>H</u>), 7.58 (2H, d, *J* = 8.0 Hz, Ar<u>H</u>), 4.60 (2H, s, *ortho* on η^5-C_5<u>H</u>$_4$-C≡C-), 4.37 (2H, s, *meta* on η^5-C_5<u>H</u>$_4$-C≡C-), 4.29 (5H, s, η^5-C_5<u>H</u>$_5$), 3.93 (2H, d, *J* = 5.6 Hz, -NH<u>CH$_2$</u>CO-), 3.86 (2H, d, *J* = 5.6 Hz, -NH<u>CH$_2$</u>CO-), 3.63 (3H, s, - O<u>CH$_3$</u>);

^{13}C NMR (100 MHz) δ (DMSO- d_6): 170.2 (C=O), 168.9 (C=O), 167.8 (C=O), 131.9 (C_q), 130.0 (C_q), 127.7, 126.0, 91.2 (η^5-C_5H_4-C≡<u>C</u>-), 84.1 (η^5-C_5H_4-<u>C</u>≡C-), 71.8 (C_{ortho} η^5-<u>C</u>$_5$H$_4$-C≡C-), 69.8 (η^5-<u>C</u>$_5$H$_5$), 68.2 (C_{meta} η^5-<u>C</u>$_5$H$_4$-C≡C-), 64.9 (C_{ipso} η^5-<u>C</u>$_5$H$_4$-C≡C-), 51.7 (-O<u>C</u>H$_3$), 48.7, (-NH<u>C</u>H$_2$CO-, -ve DEPT), 40.5 (-NH<u>C</u>H$_2$CO-, -ve DEPT).

***N*-{*para*-(ferrocenyl) ethynyl benzoyl} glycine glycine ethyl ester (106)**

Glycine glycine ethyl ester hydrochloride (0.48 g, 3.03 mmol) was used as a starting material. The crude product was purified by column chromatography (eluent 1:1

hexane: ethyl acetate) and recrystallisation from hexane: ethyl acetate yielded the desired product as a red solid (0.32 g, 22%), m.p 178 - 180 ^{o}C;

Mass spectrum: $[M+Na]^{+}$ found: 495.0972

$C_{25}H_{24}N_2O_4FeNa$ requires: 495.0983

I.R. υ_{max} (KBr): 3261(NH), 2204 (-C≡C-), 1736 ($C=O_{ester}$), 1658 ($C=O_{amide}$), 1603 ($C=O_{amide}$) cm^{-1};

UV-Vis λ_{max} EtOH: 385, 490 nm;

^{1}H NMR (400 MHz) δ (DMSO- d_6): 8.89 (1H, t, *J* = 6.4 Hz, -CONH-), 8.36 (1H, t, *J* = 6.4 Hz, -CONH-), 7.90 (2H, d, *J* = 9.2 Hz, ArH), 7.58 (2H, d, *J* = 9.2 Hz, ArH), 4.61 (2H, t, *J* = 2.0 Hz, *ortho* on η^5-C_5H_4-C≡C-), 4.38 (2H, t, *J* = 2.0 Hz, *meta* on η^5-C_5H_4-C≡C-), 4.29 (5H, s, η^5-C_5H_5), 4.10 (2H, q, *J* = 7.2 Hz, -O$CH_2$$CH_3$), 3.91 (2H, d, *J* = 6.0 Hz, -NHCH_2CO-), 3.84 (2H, d, *J* = 6.0 Hz, -NHCH_2CO-), 1.19 (3H, t, *J* = 7.2 Hz, -OCH_2CH_3);

^{13}C NMR (100 MHz) δ (DMSO- d_6): 170.0 (C=O), 169.3 (C=O), 168.2 (C=O), 132.2 (C_q), 130.7 (C_q), 127.7, 126.0, 90.9 (η^5-C_5H_4-C≡C-), 84.3 (η^5-C_5H_4-C≡C-), 72.0 (C_{ortho} η^5-C_5H_4-C≡C-), 70.5 (η^5-C_5H_5), 69.1 (C_{meta} η^5-C_5H_4-C≡C-), 67.6 (C_{ipso} η^5-C_5H_4-C≡C-), 62.0 (-OCH_2CH_3, -ve DEPT), 49.6 (-NHCH_2CO-, -ve DEPT), 42.3, (-NHCH_2CO-, -ve DEPT), 13.9 (-OCH_2CH_3).

N-{*para*-(ferrocenyl) ethynyl benzoyl} glycine L-alanine methyl ester (107)

Glycine L-alanine methyl ester hydrochloride (0.48 g, 3.03 mmol) was used as a starting material. The crude product was purified by column chromatography (eluent 1:1 hexane: ethyl acetate) and recrystallisation from hexane: ethyl acetate yielded the desired product as a red solid (0.25 g, 17%), m.p 112 - 114 ^{o}C;

$[\alpha]_D^{20}$ = -25 ^{o} (*c* 0.1, EtOH);

Mass spectrum: $[M+Na]^{+}$ found: 495.0965

$C_{25}H_{24}N_2O_4FeNa$ requires: 495.0983

I.R. υ_{max} (KBr): 3336 (NH), 2205 (-C≡C-), 1734 ($C=O_{ester}$), 1660 ($C=O_{amide}$), 1604 ($C=O_{amide}$) cm^{-1};

UV-Vis λ_{max} EtOH: 391, 488 nm;

^{1}H NMR (400 MHz) δ ($CDCl_3$): 7.73 (2H, d, *J* = 8.4 Hz, ArH), 7.48 (1H, t, *J* = 6.8 Hz, -CONH-), 7.45 (2H, d, *J* = 8.4 Hz, ArH), 7.33 (1H, d, *J* = 7.2 Hz, -CONH-), 4.55 (1H,

quin, J = 7.2 Hz, -CHCH$_3$), 4.44 (2H, t, J = 2 Hz, *ortho* on η^5-C$_5$H$_4$-C≡C-), 4.21 - 4.13 {9H, m, (*meta* on η^5-C$_5$H$_4$-C≡C-), (η^5-C$_5$H$_5$), (-NHCH$_2$CO-)}, 3.66 (3H, s, -OCH$_3$), 1.36 (3H, d, J = 7.2 Hz, -CHCH$_3$);

^{13}C NMR (100 MHz) δ (CDCl$_3$): 173.2 (C=O), 168.6 (C=O), 167.2 (C=O), 132.0 (C$_q$), 131.4 (C$_q$), 127.8, 127.2, 91.7 (η^5-C$_5$H$_4$-C≡C-), 85.1 (η^5-C$_5$H$_4$-C≡C-), 70.7 (C$_{ortho}$ η^5-C$_5$H$_4$-C≡C-), 69.2 (η^5-C$_5$H$_5$), 68.2 (C$_{meta}$ η^5-C$_5$H$_4$-C≡C-), 66.5 (C$_{ipso}$ η^5-C$_5$H$_4$-C≡C-), 52.4 (-OCH$_3$), 48.3 (-CHCH$_3$), 43.5 (-NHCH$_2$CO-, -ve DEPT), 18.1 (-CHCH$_3$).

_N_-{*para*-(ferrocenyl) ethynyl benzoyl} glycine L-alanine ethyl ester (108)

Glycine L-alanine ethyl ester hydrochloride (0.52 g, 3.03 mmol) was used as a starting material. The crude product was purified by column chromatography (eluent 1:1 hexane: ethyl acetate) and recrystallisation from hexane: ethyl acetate yielded the desired product as a red solid (0.30 g, 20%), m.p 115 - 117 ^{o}C;

$[\alpha]_D^{20}$ = -23 ^{o} (*c* 0.1, EtOH);

Mass spectrum: $[M+Na]^+$ found: 509.1127

$C_{26}H_{26}N_2O_4FeNa$ requires: 509.1140

I.R. υ_{max} (KBr): 3275 (NH), 2204 (-C≡C-), 1739 (C=O$_{ester}$), 1652 (C=O$_{amide}$), 1604 (C=O$_{amide}$) cm^{-1};

UV-Vis λ_{max} EtOH: 389, 489 nm;

^{1}H NMR (400 MHz) δ (CDCl$_3$): 7.81 (2H, d, J = 8.0 Hz, ArH), 7.54 - 7.51 {3H, m, (ArH), (-CONH-)} 7.33 (1H, t, J = 7.2 Hz, -CONH-), 4.54 (1H, quin, J = 6.8 Hz, -CHCH$_3$), 4.53 (2H, t, J = 1.6 Hz, *ortho* on η^5-C$_5$H$_4$-C≡C-), 4.28 (2H, t, J = 1.6 Hz, *meta* on η^5-C$_5$H$_4$-C≡C-), 4.26 (5H, s, η^5-C$_5$H$_5$), 4.23 - 4.10 {4H, m, (-OCH$_2$CH$_3$), (-NHCH$_2$CO-)}, 1.44 (3H, d, J = 7.2 Hz, -CHCH$_3$), 1.28 (3H, t, J = 7.2 Hz, -OCH$_2$CH$_3$);

^{13}C NMR (100 MHz) δ (CDCl$_3$): 172.8 (C=O), 168.9 (C=O), 165.2 (C=O), 132.0 (C$_q$), 130.4 (C$_q$), 127.5, 126.9, 91.0 (η^5-C$_5$H$_4$-C≡C-), 84.9 (η^5-C$_5$H$_4$-C≡C-), 71.6 (C$_{ortho}$ η^5-C$_5$H$_4$-C≡C-), 70.1 (η^5-C$_5$H$_5$), 69.2 (C$_{meta}$ η^5-C$_5$H$_4$-C≡C-), 66.0 (C$_{ipso}$ η^5-C$_5$H$_4$-C≡C-), 61.6 (-OCH$_2$CH$_3$, -ve DEPT), 48.4 (-CHCH$_3$), 42.0 (-NHCH$_2$CO-, -ve DEPT), 18.7 (-CHCH$_3$), 14.2 (-OCH$_2$CH$_3$).

***N*-{*para*-(ferrocenyl) ethynyl benzoyl} glycine D-alanine methyl ester (109)**

Glycine D-alanine methyl ester hydrochloride (0.48 g, 3.03 mmol) was used as a starting material. The crude product was purified by column chromatography (eluent 1:1 hexane: ethyl acetate) and recrystallisation from hexane: ethyl acetate yielded the desired product as a red solid (0.21 g, 15%), m.p 129 - 131 ^{o}C;

$[\alpha]_D^{20}$ = +25 ^{o} (*c* 0.1, EtOH);

Mass spectrum: $[M+Na]^+$ found: 495.0978

$C_{25}H_{24}N_2O_4FeNa$ requires: 495.0983

I.R. υ_{max} (KBr): 3354 (NH), 2207 (-C≡C-), 1735 ($C=O_{ester}$), 1621 ($C=O_{amide}$), 1604 ($C=O_{amide}$) cm^{-1};

UV-Vis λ_{max} EtOH: 387, 492 nm;

^{1}H NMR (400 MHz) δ ($CDCl_3$): 7.73 (2H, d, *J* = 8.4 Hz, Ar<u>H</u>), 7.45 (2H, d, *J* = 8.4 Hz, Ar<u>H</u>), 7.25 (1H, t, *J* = 5.6 Hz, -CON<u>H</u>-), 7.07 (1H, d, *J* = 6.8 Hz, -CON<u>H</u>-), 4.55 - 4.50 (1H, m, -<u>CH</u>CH_3), 4.45 (2H, t, *J* = 1.6 Hz, *ortho* on η^5-C_5<u>H</u>$_4$-C≡C-), 4.21 - 4.14 {9H, m, (*meta* on η^5-C_5<u>H</u>$_4$-C≡C-), (η^5-C_5H_5), (-NH<u>CH_2</u>CO-)}, 3.68 (3H, s, -OCH_3), 1.38 (3H, d, *J* = 7.2 Hz, -CH<u>CH_3</u>);

^{13}C NMR (100 MHz) δ ($CDCl_3$): 173.2 (C=O), 168.6 (C=O), 167.2 (C=O), 132.0 (C_q), 131.4 (C_q), 127.8, 127.2, 90.7 (η^5-C_5H_4-C≡<u>C</u>-), 84.2 (η^5-C_5H_4-<u>C</u>≡C-), 70.9 (C_{ortho} η^5-<u>C</u>$_5$H$_4$-C≡C-), 69.2 (η^5-<u>C</u>$_5$H$_5$), 68.0 (C_{meta} η^5-<u>C</u>$_5$H$_4$-C≡C-), 65.9 (C_{ipso} η^5-<u>C</u>$_5$H$_4$-C≡C-), 52.0 (-OCH_3), 47.9 (-<u>CH</u>CH_3), 42.9 (-NH<u>CH_2</u>CO-, -ve DEPT), 18.9 (-CH<u>CH_3</u>).

***N*-{*para*-(ferrocenyl) ethynyl benzoyl} glycine D-alanine ethyl ester (110)**

Glycine D-alanine ethyl ester hydrochloride (0.52 g, 3.03 mmol) was used as a starting material. The crude product was purified by column chromatography (eluent 1:1 hexane: ethyl acetate) and recrystallisation from hexane: ethyl acetate yielded the desired product as a red solid (0.27 g, 18%), m.p 69 - 71 ^{o}C;

$[\alpha]_D^{20}$ = +23 ^{o} (*c* 0.1, EtOH);

Mass spectrum: $[M+Na]^+$ found: 509.1154

$C_{26}H_{26}N_2O_4FeNa$ requires: 509.1140

I.R. υ_{max} (KBr): 3307 (NH), 2205 (-C≡C-), 1734 ($C=O_{ester}$), 1651 ($C=O_{amide}$), 1604 ($C=O_{amide}$) cm^{-1};

UV-Vis λ_{max} EtOH: 387, 494 nm;

^{1}H NMR (400 MHz) δ ($CDCl_3$): 7.72 (2H, d, *J* = 8.0 Hz, Ar<u>H</u>), 7.45 (2H, d, *J* = 8.0 Hz, Ar<u>H</u>), 7.30 (1H, t, *J* = 7.2 Hz, -CON<u>H</u>-), 7.05 (1H, d, *J* = 6.8 Hz, -CON<u>H</u>-), 4.53 (1H, quin, *J* = 6.8 Hz, -<u>CH</u>CH_3), 4.42 (2H, t, *J* = 1.6 Hz, *ortho* on η^5-C_5<u>H</u>$_4$-C≡C-), 4.20 - 4.18 {5H, m, (*meta* on η^5-C_5<u>H</u>$_4$-C≡C-), (η^5-C_5<u>H</u>$_5$)}, 4.15 - 4.10 {4H, m, (-O<u>CH_2</u>CH_3), (-NH<u>CH_2</u>CO-)}, 1.37 (3H, d, *J* = 7.2 Hz, -CH<u>CH_3</u>), 1.20 (3H, t, *J* = 7.2 Hz, -OCH_2<u>CH_3</u>);

^{13}C NMR (100 MHz) δ ($CDCl_3$): 172.7 (C=O), 168.2 (C=O), 167.9 (C=O), 132.1 (C_q), 130.4 (C_q), 127.0, 126.5, 91.0 (η^5-C_5H_4-C≡<u>C</u>-), 84.7 (η^5-C_5H_4-<u>C</u>≡C-), 71.6 (C_{ortho} η^5-<u>C</u>$_5$H$_4$-C≡C-), 70.5 (η^5-<u>C</u>$_5$H$_5$), 69.1 (C_{meta} η^5-<u>C</u>$_5$H$_4$-C≡C-), 66.7 (C_{ipso} η^5-<u>C</u>$_5$H$_4$-C≡C-), 61.6 (-OCH_2<u>CH_3</u>, -ve DEPT), 48.4 (-<u>CH</u>CH_3), 42.0 (-ve DEPT), 18.2 (-CH<u>CH_3</u>), 14.1 (-OCH_2<u>CH_3</u>).

N-{*para*-(ferrocenyl) ethynyl benzoyl} γ-aminobutyric acid methyl ester (111)

γ-Amino butyric acid methyl ester hydrochloride (0.35 g, 3.03 mmol) was used as a starting material. The crude product was purified by column chromatography (eluent 1:1 hexane: ethyl acetate) and recrystallisation from hexane: ethyl acetate yielded the desired product as a red solid (0.41 g, 32%), m.p 88 - 90 ^{o}C;

Mass spectrum: $[M+Na]^+$ found: 452.0937

$C_{24}H_{23}NO_3FeNa$ requires: 452.0925

I.R. υ_{max} (KBr): 3343 (NH), 2207 (-C≡C-), 1731 ($C=O_{ester}$), 1606 ($C=O_{amide}$) cm^{-1};

UV-Vis λ_{max} EtOH: 385, 485 nm;

^{1}H NMR (400 MHz) δ ($CDCl_3$): 7.76 (2H, d, *J* = 8.4 Hz, Ar<u>H</u>), 7.55 (2H, d, *J* = 8.4 Hz, Ar<u>H</u>), 6.65 (1H, t, *J* = 4.2 Hz, -CON<u>H</u>-), 4.53 (2H, t, *J* = 2.0 Hz, *ortho* on η^5-C_5<u>H</u>$_4$-C≡C-), 4.29 - 4.27 {7H, m, (*meta* on η^5-C_5<u>H</u>$_4$-C≡C-), (η^5-C_5<u>H</u>$_5$)}, 3.70 (3H, s, -O<u>CH_3</u>), 3.54 {2H, q, *J* = 6.4 Hz, (-NH<u>CH_2</u>CH_2CH_2-)}, 2.49 {2H, t, *J* = 6.8 Hz, (-$NHCH_2CH_2$<u>CH_2</u>-)}, 2.00 {2H, quin, *J* = 6.4 Hz, (-$NHCH_2$<u>CH_2</u>CH_2-)};

^{13}C NMR (100 MHz) δ ($CDCl_3$): 174.4 (C=O), 166.9 (C=O), 133.0 (C_q), 131.4 (C_q), 127.3, 126.9, 91.0 (η^5-C_5H_4-C≡<u>C</u>-), 85.1 (η^5-C_5H_4-<u>C</u>≡C-), 71.6 (C_{ortho} η^5-<u>C</u>$_5$H$_4$-C≡C-), 70.0 (η^5-<u>C</u>$_5$H$_5$), 69.1 (C_{meta} η^5-<u>C</u>$_5$H$_4$-C≡C-), 64.8 (C_{ipso} η^5-<u>C</u>$_5$H$_4$-C≡C-), 51.9 (-O<u>CH_3</u>), 39.8 (-NH<u>CH_2</u>CH_2CH_2-, -ve DEPT), 31.8 (-$NHCH_2CH_2$<u>CH_2</u>-, -ve DEPT), 24.3 (-$NHCH_2$<u>CH_2</u>CH_2-, -ve DEPT).

***N*-{*para*-(ferrocenyl) ethynyl benzoyl} γ-aminobutyric acid ethyl ester (112)**

γ-Amino butyric acid ethyl ester hydrochloride (0.40 g, 3.03 mmol) was used as a starting material. The crude product was purified by column chromatography (eluent 1:1 hexane: ethyl acetate) and recrystallisation from hexane: ethyl acetate yielded the desired product as a red solid (0.51 g, 38%), m.p 64 - 66 ^{o}C;

Mass spectrum: $[M+Na]^{+}$ found: 466.1101

$C_{25}H_{25}NO_3FeNa$ requires: 466.1082

I.R. υ_{max} (KBr): 3283 (NH), 2205 (-C≡C-), 1726 ($C=O_{ester}$), 1605 ($C=O_{amide}$) cm^{-1};

UV-Vis λ_{max} EtOH: 385, 490 nm;

^{1}H NMR (400 MHz) δ ($CDCl_3$): 7.73 - 7.67 (4H, m, Ar<u>H</u>), 6.65 (1H, t, *J* = 4.4 Hz, -CON<u>H</u>-), 4.55 (2H, t, *J* = 3.2 Hz, *ortho* on η^5-C_5<u>H</u>$_4$-C≡C-), 4.28 (2H, t, *J* = 3.2 Hz, *meta* on η^5-C_5<u>H</u>$_4$-C≡C-), 4.16 (5H, s, η^5-C_5<u>H</u>$_5$), 4.07 (2H, q, *J* = 7.2 Hz, -O<u>C</u>H$_2$CH$_3$), 3.45{2H, q, *J* = 6.4 Hz, -NH<u>C</u>H$_2$CH$_2$CH$_2$-), 2.38 (2H, t, *J* = 6.8 Hz, -NHCH$_2$CH$_2$<u>C</u>H$_2$-), 1.91 (2H, quin, *J* = 6.4 Hz, -NHCH$_2$<u>C</u>H$_2$CH$_2$-), 1.19 (3H, t, *J*= 7.2 Hz, -OCH$_2$<u>C</u>H$_3$);

^{13}C NMR (100 MHz) δ ($CDCl_3$): 173.0 (C=O), 167.0 (C=O), 132.7 (C_q), 131.8 (C_q), 127.2, 126.9, 90.8 (η^5-C_5H_4-C≡<u>C</u>-), 85.4 (η^5-<u>C</u>$_5$H$_4$-<u>C</u>≡C-), 70.5 (C_{ortho} η^5-<u>C</u>$_5$H$_4$-C≡C-), 68.8 (η^5-<u>C</u>$_5$H$_5$), 68.2 (C_{meta} η^5-<u>C</u>$_5$H$_4$-C≡C-), 67.1 (C_{ipso} η^5-<u>C</u>$_5$H$_4$-C≡C-), 60.7 (-O<u>C</u>H$_2$CH$_3$, -ve DEPT), 39.8 (-NH<u>C</u>H$_2$CH$_2$CH$_2$-, -ve DEPT), 32.1 (-NHCH$_2$CH$_2$<u>C</u>H$_2$-, -ve DEPT), 24.3 (-NHCH$_2$<u>C</u>H$_2$CH$_2$-, -ve DEPT), 14.8 (-OCH$_2$<u>C</u>H$_3$).

***N*-{*para*-(ferrocenyl) ethynyl benzoyl} glycine L-phenylalanine ethyl ester (113)**

Glycine L-phenylalanine ethyl ester hydrochloride (0.76 g, 3.03 mmol) was used as a starting material. The crude product was purified by column chromatography (eluent 1:1 hexane: ethyl acetate) and recrystallisation from hexane: ethyl acetate yielded the desired product as a red solid (0.20 g, 12%), m.p 118 - 120 ^{o}C;

$[\alpha]_D^{20}$ = -17 ^{o} (*c* 0.1, EtOH);

Mass spectrum: $[M+Na]^{+}$ found: 585.1442

$C_{32}H_{30}N_2O_4FeNa$ requires: 585.1453

I.R. υ_{max} (KBr): 3359 (NH), 2205 (-C≡C-), 1743 ($C=O_{ester}$), 1631 ($C=O_{amide}$), 1605 ($C=O_{amide}$) cm^{-1};

UV-Vis λ_{max} EtOH: 390, 492 nm;

^{1}H NMR (400 MHz) δ ($CDCl_3$): 7.81 (2H, d, *J* = 8.0 Hz, Ar<u>H</u>), 7.54 (2H, d, *J* = 8.0 Hz, Ar<u>H</u>), 7.25 - 7.19 {6H, m, (-CON<u>H</u>-), (-CHCH$_2$<u>Ph</u>)}, 6.87 (2H, d, *J* = 8.0 Hz, -CON<u>H</u>-), 4.86 - 4.84 (1H, m, -C<u>H</u>CH$_2$Ph), 4.54 (2H, t, *J* = 1.6 Hz, *ortho* on η^5-C$_5$<u>H</u>$_4$-C≡C-), 4.30 - 4.29 {7H, m, (*meta* on η^5-C$_5$<u>H</u>$_4$-C≡C-), (η^5-C$_5$<u>H</u>$_5$)}, 4.18 (2H, q, *J* = 7.2 Hz, -O<u>CH$_2$</u>CH$_3$), 4.23 (2H, d, *J* = 4.8 Hz, -NH<u>CH$_2$</u>CO-), 3.20 - 3.08 (2H, m, -CH<u>CH$_2$</u>Ph), 1.26 (3H, t, *J* = 7.2 Hz, -OCH$_2$<u>CH$_3$</u>);

^{13}C NMR (100 MHz) δ ($CDCl_3$):171.2 (C=O), 168.1(C=O), 167.0 (C=O), 133.7 (C_q), 132.0 (C_q), 130.1, 129.3, 128.6, 127.8, 127.2, 126.1, 91.7 (η^5-C$_5$H$_4$-C≡<u>C</u>-), 84.9 (η^5-C$_5$H$_4$-<u>C</u>≡C-), 71.1 (C_{ortho} η^5-<u>C</u>$_5$H$_4$-C≡C-), 70.4 (η^5-<u>C</u>$_5$H$_5$), 69.2 (C_{meta} η^5-<u>C</u>$_5$H$_4$-C≡C-), 67.5 (C_{ipso} η^5-<u>C</u>$_5$H$_4$-C≡C-), 62.7 (-O<u>CH$_2$</u>CH$_3$, -ve DEPT), 53.0 (-<u>CH</u>CH$_2$Ph), 42.6 (-NH<u>CH$_2$</u>CO-, -ve DEPT), 38.0 (-CH<u>CH$_2$</u>Ph, -ve DEPT), 13.7 (-OCH$_2$<u>CH$_3$</u>).

_N_-{*para*-(ferrocenyl) ethynyl benzoyl} glycine L-leucine ethyl ester (114)

Glycine L-leucine ethyl ester hydrochloride (0.65 g, 3.03 mmol) was used as a starting material. The crude product was purified by column chromatography (eluent 1:1 hexane: ethyl acetate) and recrystallisation from hexane: ethyl acetate yielded the desired product as a red solid (0.19 g, 12%), m.p 132 - 134 ^{o}C;

$[\alpha]_D^{20}$ = -18 ^{o} (*c* 0.1, EtOH);

Mass spectrum: $[M+Na]^+$ found: 551.1617

$C_{29}H_{32}N_2O_4FeNa$ requires: 551.1609

I.R. υ_{max} (KBr): 3275 (NH), 2206 (-C≡C-), 1727 (C=O$_{ester}$), 1640 (C=O$_{amide}$), 1605 (C=O$_{amide}$) cm^{-1};

UV-Vis λ_{max} EtOH: 396, 489 nm;

^{1}H NMR (400 MHz) δ ($CDCl_3$): 7.72 (2H, d, *J* = 8.4 Hz, Ar<u>H</u>), 7.45 {2H, d, *J* = 8.4 Hz, Ar<u>H</u>), 7.30 (1H, t, *J* = 5.2 Hz, -CON<u>H</u>-) 7.00 (1H, d, *J* = 8.0 Hz, -CON<u>H</u>-), 4.57 - 4.51 {1H, m, -<u>CH</u>CH$_2$CH(CH$_3$)$_2$)}, 4.45 (2H, t, *J* = 2.0 Hz, *ortho* on η^5-C$_5$<u>H</u>$_4$-C≡C-), 4.20 - 4.15 { 9H, m, (*meta* on η^5-C$_5$<u>H</u>$_4$-C≡C-), (-NH<u>CH$_2$</u>CO-), (η^5-C$_5$<u>H</u>$_5$)}, 4.13 (2H, q, *J* = 7.2 Hz, -O<u>CH$_2$</u>CH$_3$), 1.57 - 1.45 {3H, m, -CH<u>CH$_2$CH</u>(CH$_3$)$_2$)}, 1.18 (3H, t, *J* = 7.2 Hz, -OCH$_2$<u>CH$_3$</u>), 0.88 - 0.86 (6H, m, -CHCH$_2$CH(<u>CH$_3$</u>)$_2$);

^{13}C NMR (100 MHz) δ ($CDCl_3$): 171.8 (C=O), 168.9 (C=O), 167.1(C=O), 132.0 (C_q), 131.7 (C_q), 127.3, 126.8, 90.7 (η^5-C$_5$H$_4$-C≡<u>C</u>-), 84.1 (η^5-C$_5$H$_4$-<u>C</u>≡C-), 71.7 (C_{ortho} η^5-

$\underline{C}_5H_4$-C≡C-), 70.5 (η^5-$\underline{C}_5H_5$), 68.2 (C_{meta} η^5-$\underline{C}_5H_4$-C≡C-), 66.1 (C_{ipso} η^5-$\underline{C}_5H_4$-C≡C-), 61.0 (-O$\underline{C}H_2CH_3$, -ve DEPT), 50.1 (-$\underline{C}HCH_2CH(CH_3)_2$), 42.9 (-NH$\underline{C}H_2$CO-, -ve DEPT), 41.3 (-CH$\underline{C}H_2CH(CH_3)_2$, -ve DEPT), 25.8 (-CHCH$_2\underline{C}H(CH_3)_2$), 22.0 (-CHCH$_2$CH($\underline{C}H_3)_2$), 21.9 (-CHCH$_2$CH($\underline{C}H_3)_2$), 14.0 (-OCH$_2\underline{C}H_3$).

***N*-{*para*-(ferrocenyl) ethynyl benzoyl} sarcosine glycine ethyl ester (115)**

Sarcosine glycine ethyl ester hydrochloride (0.53 g, 3.03 mmol) was used as a starting material. The crude product was purified by column chromatography (eluent 1:1 hexane: ethyl acetate) and recrystallisation from hexane: ethyl acetate yielded the desired product as a red solid (0.23 g, 16%), m.p 79 - 81 ^oC;

Mass spectrum: $[M+Na]^+$ found: 509.1152

$C_{26}H_{26}N_2O_4FeNa$ requires: 509.1140

I.R. υ_{max} (KBr): 3284 (NH), 2205 (-C≡C-), 1744 (C=O$_{ester}$), 1676 (C=O$_{amide}$), 1620 (C=O$_{amide}$) cm^{-1};

UV-Vis λ_{max} EtOH: 389, 495 nm;

^{1}H NMR (400 MHz) δ ($CDCl_3$): 7.65 - 7.35 {5H, m, (-CON$\underline{H}$-), (Ar$\underline{H}$)}, 4.43 (2H, s, *ortho* on η^5-$C_5\underline{H}_4$-C≡C-), 4.30 - 3.85 {13H, m, (*meta* on η^5-$C_5\underline{H}_4$-C≡C-), (η^5-$C_5\underline{H}_5$), (-N(CH$_3$)$\underline{C}H_2$CO-), (-NH$\underline{C}H_2$CO-) (-O$\underline{C}H_2CH_3$)}, 3.15 (3H, s, -N($\underline{C}H_3$)CH$_2$CO-), 1.17 (3H, t, *J* = 7.2 Hz, -OCH$_2\underline{C}H_3$);

^{13}C NMR (100 MHz) δ ($CDCl_3$): 173.1 (C=O), 169.3 (C=O), 168.2 (C=O), 132.1 (C_q), 130.7 (C_q), 127.1, 125.9, 90.9 (η^5-C_5H_4-C≡$\underline{C}$-), 85.7 (η^5-C_5H_4-$\underline{C}$≡C-), 72.0 (C_{ortho} η^5-$\underline{C}_5H_4$-C≡C-), 70.1 (η^5-$\underline{C}_5H_5$), 69.1 (C_{meta} η^5-$\underline{C}_5H_4$-C≡C-), 67.6 (C_{ipso} η^5-$\underline{C}_5H_4$-C≡C-), 62.0 (-O$\underline{C}H_2CH_3$, -ve DEPT), 49.6 (-N(CH$_3$)$\underline{C}H_2$CO-, -ve DEPT), 42.3 (-NH$\underline{C}H_2$CO-, -ve DEPT), 38.5 (-N($\underline{C}H_3$)CH$_2$CO-), 14.3 (-OCH$_2\underline{C}H_3$).

***N*-{*para*-(ferrocenyl) ethynyl benzoyl} sarcosine glycine methyl ester (116)**

Sarcosine glycine methyl ester hydrochloride (0.49 g, 3.03 mmol) was used as a starting material. The crude product was purified by column chromatography (eluent 1:1 hexane: ethyl acetate) and recrystallisation from hexane: ethyl acetate yielded the desired product as a red solid (0.23 g, 16%), m.p 124 - 126 ^{o}C;

Mass spectrum: $[M+Na]^{+}$ found: 495.1297

$C_{25}H_{24}N_2O_4FeNa$ requires: 495.0983

I.R. υ_{max} (KBr): 3286 (NH), 2206 (-C≡C-), 1746 (C=O_{ester}), 1674 (C=O_{amide}), 1620 (C=O_{amide}) cm^{-1};

UV-Vis λ_{max} EtOH: 397, 486 nm;

^{1}H NMR (400 MHz) δ ($CDCl_3$): 7.45 - 7.35 {5H, m, (-CONH-), (ArH)}, 4.44 (2H, s, *ortho* on η^5-C_5H_4-C≡C-), 4.30 - 3.85 {11H, m, (*meta* on η^5-C_5H_4-C≡C-), (η^5-C_5H_5), (-N(CH_3)CH_2CO-), (-NHCH_2CO-)}, 3.70 (3H, s, -OCH_3), 3.04 (3H, s, -N(CH_3)CH_2CO-);

^{13}C NMR (100 MHz) δ ($CDCl_3$): 172.1 (C=O), 168.9 (C=O), 167.2 (C=O), 131.7 (C_q), 130.0 (C_q), 126.9, 125.7, 91.2 (η^5-C_5H_4-C≡C-), 84.1 (η^5-C_5H_4-C≡C-), 71.8 (C_{ortho} η^5-C_5H_4-C≡C-), 69.9 (η^5-C_5H_5), 68.2 (C_{meta} η^5-C_5H_4-C≡C-), 65.9 (C_{ipso} η^5-C_5H_4-C≡C-), 51.7 (-OCH_3), 46.2 (-N(CH_3)CH_2CO-, -ve DEPT), 41.2 (-NHCH_2CO-, -ve DEPT), 38.1 (-N(CH_3)CH_2CO-).

***N*-{*para*-(ferrocenyl) ethynyl benzoyl} sarcosine L-alanine ethyl ester (117)**

Sarcosine L-alanine ethyl ester hydrochloride (0.57 g, 3.03 mmol) was used as a starting material. The crude product was purified by column chromatography (eluent 1:1 hexane: ethyl acetate) and recrystallisation from hexane: ethyl acetate yielded the desired product as a red solid (0.21 g, 14%), m.p 99 - 101 ^{o}C;

$[\alpha]_D^{20}$ = -22 ^{o} (*c* 0.1, EtOH);

Mass spectrum: $[M+Na]^{+}$ found: 523.1292

$C_{27}H_{28}N_2O_4FeNa$ requires: 523.1296

I.R. υ_{max} (KBr): 3270 (NH), 2205 (-C≡C-), 1745 (C=O_{ester}), 1675 (C=O_{amide}), 1614 (C=O_{amide}) cm^{-1};

UV-Vis λ_{max} EtOH: 389, 486 nm;

^{1}H NMR (400 MHz) δ ($CDCl_3$): 7.60 - 7.35 {5H, m, (-CONH-), (ArH)}, 4.51- 4.40 {3H, m, (*ortho* on η^5-C_5H_4-C≡C-), (-CHCH$_3$)}, 4.19 - 3.90 {11H, m, (*meta* on η^5-C_5H_4-C≡C-), (η^5-C_5H_5), (-N(CH$_3$)CH$_2$CO-), (-OCH$_2$CH$_3$)}, 3.01 (3H, s, -N(CH$_3$)CH$_2$CO-), 1.36 (2H, d, *J* = 7.2 Hz, -CHCH$_3$), 1.21 (3H, t, *J* = 7.2 Hz, -OCH$_2$CH$_3$);

^{13}C NMR (100 MHz) δ ($CDCl_3$): 172.7 (C=O), 169.0 (C=O), 168.2 (C=O), 133.8 (C_q), 132.0 (C_q), 128.3, 127.4, 90.6 (η^5-C_5H_4-C≡C-), 85.0 (η^5-C_5H_4-C≡C-), 71.5 (C_{ortho} η^5-C_5H_4-C≡C-), 70.0 (η^5-C_5H_5), 69.1 (C_{meta} η^5-C_5H_4-C≡C-), 64.6 (C_{ipso} η^5-C_5H_4-C≡C-), 61.6 (-OCH$_2$CH$_3$, -ve DEPT), 48.2 (-CHCH$_3$), 40.1(-N(CH$_3$)CH$_2$CO-, -ve DEPT), 38.3 (-N(CH$_3$)CH$_2$CO-), 18.3 (-CHCH$_3$), 14.2 (-OCH$_2$CH$_3$).

N-{*para*-(ferrocenyl) ethynyl benzoyl} L-proline glycine ethyl ester (118)

L-Proline glycine ethyl ester hydrochloride (0.61 g, 3.03 mmol) was used as a starting material. The crude product was purified by column chromatography (eluent 1:1 hexane: ethyl acetate) and recrystallisation from hexane: ethyl acetate yielded the desired product as a red solid (0.27 g, 17%), m.p 58 - 60 ^{o}C; $[\alpha]_D^{20}$ = 17 ^{o};

Mass spectrum: $[M+Na]^+$ found: 535.1282

$C_{28}H_{28}N_2O_4FeNa$ requires: 535.1296

I.R. υ_{max} (KBr): 3313 (NH), 2205 (-C≡C-), 1735 (C=O$_{ester}$), 1652 (C=O$_{amide}$), 1604 (C=O$_{amide}$) cm^{-1};

UV-Vis λ_{max} EtOH: 395, 499 nm;

^{1}H NMR (400 MHz) δ ($CDCl_3$): 7.50 - 7.36 {5H, m, (-CONH-), (ArH)}, 4.74 (1 H, *t*, *J* = 5.2 Hz, -N(CH$_2$CH$_2$CH$_2$)CHCO-), 4.45 (2H, s, *ortho* on η^5-C_5H_4-C≡C-), 4.19 - 4.10 {9H, m, (*meta* on η^5-C_5H_4-C≡C-), (η^5-C_5H_5), (-OCH$_2$CH$_3$)}, 3.95 (2H, d, *J* = 4.0 Hz, -NHCH$_2$CO-), 3.51 - 3.40 (2H, m, -N(CH$_2$CH$_2$CH$_2$)CHCO-), 2.40 - 1.70 (4H, m, -N(CH$_2$CH$_2$CH$_2$)CHCO-), 1.20 (3H, t, *J* = 7.2 Hz, -OCH$_2$CH$_3$);

^{13}C NMR (100 MHz) δ ($CDCl_3$): 171.5 (C=O), 170.6 (C=O), 169.7 (C=O), 133.8 (C_q), 131.2 (C_q), 127.4, 126.0, 90.7 (η^5-C_5H_4-C≡C-), 84.9 (η^5-C_5H_4-C≡C-), 71.9 (C_{ortho} η^5-C_5H_4-C≡C-), 70.4 (η^5-C_5H_5), 68.1 (C_{meta} η^5-C_5H_4-C≡C-), 65.9 (C_{ipso} η^5-C_5H_4-C≡C-), 62.4 (-OCH$_2$CH$_3$, -ve DEPT), 59.8 (-N(CH$_2$CH$_2$CH$_2$)CHCO-), 50.4 (-N(CH$_2$CH$_2$CH$_2$)CHCO, -ve DEPT), 41.5 (-NHCH$_2$CO-, -ve DEPT),

27.5 (-N($CH_2CH_2\underline{CH_2}$)CHCO-, -ve DEPT), 25.4 (-N($CH_2\underline{CH_2}CH_2$)CHCO-, -ve DEPT), 13.7 (-$OCH_2\underline{CH_3}$).

_N_-{_para_-(ferrocenyl) ethynyl benzoyl} L-proline L-alanine ethyl ester (119)

L-Proline L-alanine ethyl ester hydrochloride (0.65 g, 3.03 mmol) was used as a starting material. The crude product was purified by column chromatography (eluent 1:1 hexane: ethyl acetate) and recrystallisation from hexane: ethyl acetate yielded the desired product as a red solid (0.21 g, 13%), m.p 52 - 54 ^oC;

$[\alpha]_D^{20}$ = -69 ^{o} (*c* 0.1, EtOH);

Mass spectrum: $[M+Na]^+$ found: 549.1467

$C_{29}H_{30}N_2O_4FeNa$ requires: 549.1453

I.R. υ_{max} (KBr): 3285 (NH), 2202 (-C≡C-), 1736 (C=O_{ester}), 1672 (C=O_{amide}), 1608 (C=O_{amide}) cm^{-1};

UV-Vis λ_{max} EtOH: 392, 493 nm;

^1H NMR (400 MHz) δ ($CDCl_3$): 7.69 - 7.48 {5H, m, (Ar$\underline{H}$), (-CON$\underline{H}$-)}, 4.68 (1H, t, *J* = 6.4 Hz, -N($CH_2CH_2CH_2$)C$\underline{H}$CO-), 4.57 (2H, s, *ortho* on η^5-$C_5\underline{H}_4$-C≡C-), 4.46 (1H, quin, *J* = 6.8 Hz, -C$\underline{H}CH_3$), 4.28 (2H, s, *meta* on η^5-$C_5\underline{H}_4$-C≡C-), 4.16 - 4.12 {7H, m, (η^5-$C_5\underline{H}_5$), (-O$\underline{CH_2}CH_3$)}, 3.60 - 3.40 (2H, m, (-N($\underline{CH_2}CH_2CH_2$)CHCO-), 2.40 - 1.56 (4H, m, (-N($CH_2\underline{CH_2}\underline{CH_2}$)CHCO-)}, 1.36 (3H, d, *J* = 6.4 Hz, -CH$\underline{CH_3}$), 1.21 (3H, t, *J* = 6.8 Hz, -$OCH_2\underline{CH_3}$);

^{13}C NMR (100 MHz) δ ($CDCl_3$): 173.8 (C=O), 171.9 (C=O), 169.1 (C=O), 133.0 (C_q), 131.2 (C_q), 128.9, 127.9, 90.7 (η^5-C_5H_4-C≡$\underline{C}$-), 84.4 (η^5-C_5H_4-$\underline{C}$≡C-), 72.0 (C_{ortho} η^5-$\underline{C}_5H_4$-C≡C-), 70.2 (η^5-$\underline{C}_5H_5$), 68.7 (C_{meta} η^5-$\underline{C}_5H_4$-C≡C-), 67.3 (C_{ipso} η^5-$\underline{C}_5H_4$-C≡C-), 62.4 (O$\underline{CH_2}CH_3$, -ve DEPT), 60.1 (-N($CH_2CH_2CH_2$)$\underline{CH}$CO-), 50.6 (-N($\underline{CH_2}CH_2CH_2$)CHCO-, -ve DEPT), 48.4 (-$\underline{CH}CH_3$), 27.8 (-N($CH_2CH_2\underline{CH_2}$)CHCO-, -ve DEPT), 25.6 (-N($CH_2\underline{CH_2}CH_2$)CHCO-, -ve DEPT), 18.9 (-CH$\underline{CH_3}$), 13.9 (-$OCH_2\underline{CH_3}$).

General procedure for the preparation of *N*-{6-(ferrocenyl) ethynyl-2-naphthoyl} amino acid and dipeptide ethyl esters

***N*-{6-(ferrocenyl) ethynyl-2-naphthoyl} glycine glycine ethyl ester (120)**

Glycine glycine ethyl ester hydrochloride (0.42 g, 2.63 mmol) was used as a starting material. The crude product was purified by column chromatography (eluent 1:1 hexane: ethyl acetate) and recrystallisation from hexane: ethyl acetate yielded the desired product as a red solid (0.38 g, 28%), m.p 128 - 130 ^{o}C;

Mass spectrum: $[M+Na]^{+}$ found: 545.1130

$C_{29}H_{26}N_2O_4FeNa$ requires: 545.1140

I.R. υ_{max} (KBr): 3261 (NH), 2204 (-C≡C-), 1736 ($C=O_{ester}$), 1658 ($C=O_{amide}$), 1603 ($C=O_{amide}$) cm^{-1};

UV-Vis λ_{max} EtOH: 400, 500 nm;

^{1}H NMR (400 MHz) δ ($CDCl_3$): 8.13 (1H, s, ArH), 7.95 - 7.48 {7H, m, (ArH), (-CONH-), (-CONH-)}, 4.61 (2H, t, *J* = 2.0 Hz, *ortho* on η^5-C_5H_4-C≡C-), 4.30 (2H, t, *J* = 2.0 Hz, *meta* on η^5-C_5H_4-C≡C-), 4.19 - 4.15 {11H, m, (η^5-C_5H_5), (-NHCH_2CO-), (-NHCH_2CO-), (-OCH_2CH_3)}, 1.23 (3H, t, *J* = 7.2 Hz, -OCH_2CH_3);

^{13}C NMR (100 MHz) δ ($CDCl_3$): 172.7 (C=O), 170.9 (C=O), 169.6 (C=O), 133.9 (C_q), 132.6 (C_q), 131.0 (C_q), 130.2 (C_q), 129.6, 129.3, 128.9, 128.1, 127.8, 125.8, 90.3 (η^5-C_5H_4-C≡C-), 84.7 (η^5-C_5H_4-C≡C-), 72.1 (C_{ortho} η^5-C_5H_4-C≡C-), 70.0 (η^5-C_5H_5), 69.7 (C_{meta} η^5-C_5H_4-C≡C-), 67.8 (C_{ipso} η^5-C_5H_4-C≡C-), 61.6 (-OCH_2CH_3, -ve DEPT), 42.3 (-NHCH_2CO-, -ve DEPT), 40.1 (-NHCH_2CO-, -ve DEPT), 14.8 (-OCH_2CH_3).

***N*-{6-(ferrocenyl) ethynyl-2-naphthoyl} glycine L-alanine ethyl ester (121)**

Glycine L-alanine ethyl ester hydrochloride (0.46 g, 2.63 mmol) was used as a starting material. The crude product was purified by column chromatography (eluent 1:1 hexane: ethyl acetate) and recrystallisation from hexane: ethyl acetate yielded the desired product as a red solid (0.23 g, 16%), m.p 58 - 60 ^{o}C;

$[\alpha]_D^{20}$ = -14 ^{o} (*c* 0.1, EtOH);

Mass spectrum: $[M+Na]^{+}$ found: 559.1305

$C_{30}H_{28}N_2O_4FeNa$ requires: 559.1398

I.R. υ_{max} (KBr): 3287 (NH), 2204 (-C≡C-), 1734 (C=O_{ester}), 1658 (C=O_{amide}), 1625 (C=O_{amide}) cm^{-1};

UV-Vis λ_{max} EtOH: 381, 512 nm;

^{1}H NMR (400 MHz) δ ($CDCl_3$): 8.21 (1H, s, Ar<u>H</u>), 7.87 - 7.51 {7H, m, (Ar<u>H</u>), (-CON<u>H</u>-), (-CON<u>H</u>-)}, 4.48 - 4.47 {3H, m, (-<u>CH</u>CH_3), (*ortho* on η^5-C_5<u>H</u>$_4$-C≡C-)}, 4.19 - 4.07 {11H, m, (*meta* on η^5-C_5<u>H</u>$_4$-C≡C-), (η^5-C_5<u>H</u>$_5$), (-O<u>CH_2</u>CH_3), (-NH<u>CH_2</u>CO-)}, 1.36 (3H, d, *J* = 7.2 Hz, -CH<u>CH_3</u>), 1.28 (3H, t, *J* = 6.8 Hz, -OCH_2<u>CH_3</u>);

^{13}C NMR (100 MHz) δ ($CDCl_3$): 171.8 (C=O), 169.1 (C=O), 167.9 (C=O), 134.5 (C_q), 131.5 (C_q), 130.8 (C_q), 130.4 (C_q), 129.3, 128.9, 128.0, 127.7, 124.3, 123.4, 90.4 (η^5-C_5H_4-C≡<u>C</u>-), 84.9 (η^5-C_5H_4-<u>C</u>≡C-), 71.3 (C_{ortho} η^5-<u>C</u>$_5H_4$-C≡C-), 70.1 (η^5-<u>C</u>$_5H_5$), 69.5 (C_{meta} η^5-<u>C</u>$_5H_4$-C≡C-), 65.9 (C_{ipso} η^5-<u>C</u>$_5H_4$-C≡C-), 60.3 (-O<u>CH_2</u>CH_3, -ve DEPT), 48.9 (-<u>CH</u>CH_3), 43.1 (-NH<u>CH_2</u>CO-, -ve DEPT), 17.2 (-CH<u>CH_3</u>), 13.7 (-OCH_2<u>CH_3</u>).

N-{6-(ferrocenyl) ethynyl-2-naphthoyl} sarcosine L-alanine ethyl ester (122)

Sarcosine L-alanine ethyl ester hydrochloride (0.50 g, 2.63 mmol) was used as a starting material. The crude product was purified by column chromatography (eluent 1:1 hexane: ethyl acetate) and recrystallisation from hexane: ethyl acetate yielded the desired product as a red solid (0.19 g, 13%), m.p 59 - 61 ^{o}C;

$[\alpha]_D^{20}$ = -23 ^{o} (*c* 0.1, EtOH);

Mass spectrum: $[M+Na]^+$ found: 573.1879

$C_{31}H_{30}N_2O_4FeNa$ requires: 573.1555

I.R. υ_{max} (KBr): 3308 (NH), 2206 (-C≡C-), 1732 (C=O_{ester}), 1625 (C=O_{amide}), 1538 (C=O_{amide}) cm^{-1};

UV-Vis λ_{max} EtOH: 405, 506 nm;

^{1}H NMR (400 MHz) δ ($CDCl_3$): 7.93 - 7.50 {7H, m, (-CON<u>H</u>-), (Ar<u>H</u>)}, 4.53 - 4.40 {3H, m, (*ortho* on η^5-C_5<u>H</u>$_4$-C≡C-), (-C<u>H</u>CH_3)}, 4.20 - 4.10 {11H, m, (*meta* on η^5-C_5<u>H</u>$_4$-C≡C-), (η^5-C_5<u>H</u>$_5$), (-N(CH_3)<u>CH_2</u>CO-), (-O<u>CH_2</u>CH_3)}, 3.07 (3H, s, -N(<u>CH_3</u>)CH_2CO-), 1.38 (2H, d, *J* = 7.2 Hz, -CH<u>CH_3</u>), 1.21 (3H, t, *J* = 7.2 Hz, -OCH_2<u>CH_3</u>);

^{13}C NMR (100 MHz) δ ($CDCl_3$): 172.0 (C=O), 170.2 (C=O), 169.1 (C=O), 134.4 (C_q), 132.7 (C_q), 131.6 (C_q), 130.6 (C_q), 129.4, 128.5, 128.0, 127.3, 125.0, 123.9, 91.3 (η^5-C_5H_4-C≡<u>C</u>-), 84.7 (η^5-C_5H_4-<u>C</u>≡C-), 71.1 (C_{ortho} η^5-<u>C</u>$_5H_4$-C≡C-), 69.7 (η^5-<u>C</u>$_5H_5$), 68.2 (C_{meta} η^5-<u>C</u>$_5H_4$-C≡C-), 66.2 (C_{ipso} η^5-<u>C</u>$_5H_4$-C≡C-), 61.9 (-OCH_2<u>CH_3</u>, -ve DEPT), 49.7 (-

$\underline{CH}CH_3$), 45.1 (-N(CH_3)$\underline{CH_2}$CO-, -ve DEPT), 38.2 (-N($\underline{CH_3}$)CH_2CO-), 19.0 (-CH$\underline{CH_3}$), 13.8. (-O$CH_2\underline{CH_3}$).

N-{6-(ferrocenyl) ethynyl-2-naphthoyl} L-proline glycine ethyl ester (123)

L-Proline glycine ethyl ester hydrochloride (0.53 g, 2.63 mmol) was used as a starting material. The crude product was purified by column chromatography (eluent 1:1 hexane: ethyl acetate) and recrystallisation from hexane: ethyl acetate yielded the desired product as a red solid (0.22 g, 15%), m.p 53 - 55 ^oC;

$[\alpha]_D^{20}$ = 27 ^{o} (*c* 0.1, EtOH);

Mass spectrum: $[M+Na]^+$ found: 585.1467

$C_{32}H_{30}N_2O_4FeNa$ requires: 585.1555

I.R. υ_{max} (KBr): 3313 (NH), 2205 (-C≡C-), 1735 ($C=O_{ester}$), 1652 ($C=O_{amide}$), 1604 ($C=O_{amide}$) cm^{-1};

UV-Vis λ_{max} EtOH: 400, 513 nm;

^{1}H NMR (400 MHz) δ ($CDCl_3$): 7.96 - 7.38 {7H, m, (Ar$\underline{H}$), (-CON$\underline{H}$-)}, 4.82 (1H, t, *J* = 5.2 Hz, -N($CH_2CH_2CH_2$)C$\underline{H}$CO-), 4.47 (2H, s, *ortho* on η^5-$C_5\underline{H}_4$-C≡C-), 4.21 - 4.18 { 7H, m, (*meta* on η^5-$C_5\underline{H}_4$-C≡C-), (η^5-$C_5\underline{H}_5$)}, 4.16 (2H, q, *J* = 7.2 Hz, -O$\underline{CH_2}CH_3$), 4.00 (2H, d, *J* = 5.6 Hz, -NH$\underline{CH_2}$CO-), 3.61 - 3.50 (2H, m, -N($\underline{CH_2}CH_2CH_2$)CHCO-), 2.40 - 1.70 (4H, m, -N($CH_2\underline{CH_2}\underline{CH_2}$)CHCO-), 1.21 (3H, t, *J* = 7.2 Hz, -O$CH_2\underline{CH_3}$);

^{13}C NMR (100 MHz) δ ($CDCl_3$):171.7 (C=O), 171.0 (C=O), 169.2 (C=O), 133.7 (C_q), 131.5 (C_q), 130.6 (C_q), 129.4 (C_q), 128.1, 127.9, 127.0, 127.2, 124.9, 123.0, 90.1 (η^5-C_5H_4-C≡$\underline{C}$-), 84.8 (η^5-C_5H_4-$\underline{C}$≡C-), 71.0 (C_{ortho} η^5-$\underline{C}_5H_4$-C≡C-), 70.1 (η^5-$\underline{C}_5H_5$), 69.1 (C_{meta} η^5-$\underline{C}_5H_4$-C≡C-), 64.9 (C_{ipso} η^5-$\underline{C}_5H_4$-C≡C-), 61.4 (-O$\underline{CH_2}CH_3$, -ve DEPT), 50.8 (-N($CH_2CH_2CH_2$)C$\underline{H}$CO-), 47.6 (-N($\underline{CH_2}CH_2CH_2$)CHCO-, -ve DEPT), 42.5 (-NH$\underline{CH_2}$CO-, -ve DEPT), 27.4 (-N($CH_2CH_2\underline{CH_2}$)CHCO-, -ve DEPT), 25.0 (-N($CH_2\underline{CH_2}CH_2$)CHCO -, -ve DEPT), 13.2 (-O$CH_2\underline{CH_3}$).

***N*-{6-(ferrocenyl) ethynyl-2-naphthoyl} γ-aminobutyric acid ethyl ester (124)**

γ-Amino butyric acid ethyl ester hydrochloride (0.34 g, 2.63 mmol) was used as a starting material. The crude product was purified by column chromatography (eluent 1:1 hexane: ethyl acetate) and recrystallisation from hexane: ethyl acetate yielded the desired product as a red solid (0.42 g, 32%), m.p 71 - 73 ^{o}C;

Mass spectrum: found: $[M+Na]^{+}$ 516.1255

$C_{29}H_{27}NO_3FeNa$ requires: 516.1340

I.R. υ_{max} (KBr): 3283 (NH), 2205 (-C≡C-), 1726 ($C=O_{ester}$), 1605 ($C=O_{amide}$) cm^{-1};

UV-Vis λ_{max} EtOH: 407, 504 nm;

^{1}H NMR (400 MHz) δ ($CDCl_3$): 8.18 (1H, s, Ar<u>H</u>), 7.81{1H, s, Ar<u>H</u>), 7.75 - 7.49 {5H, m, (-CON<u>H</u>-), (ArH)}, 4.47 (2H, t, *J* = 1.6 Hz, *ortho* on η^5-C_5<u>H</u>$_4$-C≡C-), 4.19 - 4.18 {7H, m, (*meta* on η^5-C_5<u>H</u>$_4$-C≡C-), (η^5-C_5<u>H</u>$_5$)}, 4.04 (2H, q, *J* = 7.2 Hz, -O<u>C</u>H$_2$CH$_3$), 3.46 (2H, q, *J* = 5.6 Hz, -NH<u>C</u>H$_2$CH$_2$CH$_2$-), 2.37 (2H, t, *J* = 6.8 Hz, -NHCH$_2$CH$_2$<u>C</u>H$_2$-), 1.87 (2H, quin, *J* = 6.4 Hz, -NHCH$_2$<u>C</u>H$_2$CH$_2$-), 1.15 (3H, t, *J* = 7.2 Hz, -OCH$_2$<u>C</u>H$_3$);

^{13}C NMR (100 MHz) δ ($CDCl_3$): 171.5 (C=O), 167.4 (C=O), 131.5 (C_q), 130.1 (C_q), 129.1 (C_q), 128.9 (C_q), 128.2, 127.6, 127.7, 126.0, 125.1, 123.0, 89.2 (η^5-C_5H_4-C≡<u>C</u>-), 85.0 (η^5-C_5H_4-<u>C</u>≡C-), 71.9 (C_{ortho} η^5-<u>C</u>$_5$H$_4$-C≡C-), 69.2 (η^5-<u>C</u>$_5$H$_5$), 68.4 (C_{meta} η^5-<u>C</u>$_5$H$_4$-C≡C-), 63.8 (C_{ipso} η^5-<u>C</u>$_5$H$_4$-C≡C-), 60.0 (-O<u>C</u>H$_2$CH$_3$, -ve DEPT), 39.0 (-NH<u>C</u>H$_2$CH$_2$CH$_2$-, -ve DEPT), 31.2 (-NHCH$_2$CH$_2$<u>C</u>H$_2$-, -ve DEPT), 23.3 (-NHCH$_2$<u>C</u>H$_2$CH$_2$-, -ve DEPT), 13.1 (-OCH$_2$<u>C</u>H$_3$).

***N*-{6-(ferrocenyl) ethynyl-2-naphthoyl} L-proline L-alanine ethyl ester (125)**

L-Proline L-alanine ethyl ester hydrochloride (0.56 g, 2.63 mmol) was used as a starting material. The crude product was purified by column chromatography (eluent 1:1 hexane: ethyl acetate) and recrystallisation from hexane: ethyl acetate yielded the desired product as a red solid (0.17 g, 11%), m.p 56 - 58 ^{o}C;

$[\alpha]_D^{20}$ = -67 ^{o} (*c* 0.1, EtOH);

Mass spectrum: found: $[M+Na]^{+}$ 599.1639

$C_{33}H_{32}N_2O_4FeNa$ requires: 599.1711

I.R. υ_{max} (KBr): 3285 (NH), 2202 (-C≡C-), 1736 ($C=O_{ester}$), 1672 ($C=O_{amide}$), 1608 ($C=O_{amide}$) cm^{-1};

UV-Vis λ_{max} EtOH: 409, 507 nm;

^{1}H NMR (400 MHz) δ ($CDCl_3$): 8.12 (1H, s, Ar<u>H</u>), 7.96 - 7.54 {6H, m, (Ar<u>H</u>), (-CON<u>H</u>-)}, 4.72 - 4.65 {3H, m, (-N($CH_2CH_2CH_2$)C<u>H</u>CO-), (*ortho* on η^5-$C_5\underline{H}_4$-C≡C-)}, 4.55 - 4.45 (1H, m, -C<u>H</u>CH_3), 4.33 (2H, s, *meta* on η^5-$C_5\underline{H}_4$-C≡C-), 4.33 - 4.12 {7H, m, (η^5-$C_5\underline{H}_5$), (-O<u>CH_2</u>CH_3)}, 3.61 - 3.49 (2H, m, -N(<u>CH_2</u>CH_2CH_2)CHCO-),
2.40 - 1.70 (4H, m, -N(CH_2<u>CH_2</u><u>CH_2</u>)CHCO-), 1.38 (3H, d, *J* = 4.4 Hz, -CH<u>CH_3</u>), 1.17 (3H, t, *J* = 7.2 Hz, -OCH_2<u>CH_3</u>);

^{13}C NMR (100 MHz) δ ($CDCl_3$): 172.1 (C=O), 169.7 (C=O), 168.2 (C=O), 134.5 (C_q), 133.5 (C_q), 132.8 (C_q), 131.6 (C_q), 130.1, 128.4, 128.0, 127.1, 124.7, 121.0, 90.1 (η^5-C_5H_4-C≡<u>C</u>-), 85.8 (η^5-C_5H_4-<u>C</u>≡C-), 71.9 (C_{ortho} η^5-$\underline{C}_5H_4$-C≡C-), 70.2 (η^5-$\underline{C}_5H_5$), 69.4 (C_{meta} η^5-$\underline{C}_5H_4$-C≡C-), 67.6 (C_{ipso} η^5-$\underline{C}_5H_4$-C≡C-), 61.9 (-O<u>CH_2</u>CH_3, -ve DEPT), 60.1 (-N($CH_2CH_2CH_2$)<u>CH</u>CO-), 50.7 (-N(CH_2CH_2<u>CH_2</u>)CHCO-, -ve DEPT), 48.5 (-<u>CH</u>CH_3), 27.2 (-N(CH_2<u>CH_2</u>CH_2)CHCO-, -ve DEPT), 25.0 (-N(<u>CH_2</u>CH_2CH_2)CHCO-, -ve DEPT), 19.2 (-CH<u>CH_3</u>), 14.0 (-OCH_2<u>CH_3</u>).

_N_-{6-(ferrocenyl) ethynyl-2-naphthoyl} glycine L-leucine ethyl ester (126)

Glycine L-leucine ethyl ester hydrochloride (0.57 g, 2.63 mmol) was used as a starting material. The crude product was purified by column chromatography (eluent 1:1 hexane: ethyl acetate) and recrystallisation from hexane: ethyl acetate yielded the desired product as a red solid (0.16 g, 11%), m.p 38 - 40 ^{o}C;

$[\alpha]_D^{20}$ = -10 ^{o} (*c* 0.1, EtOH);

Mass spectrum: found: $[M+Na]^+$ 601.1871

$C_{33}H_{34}N_2O_4FeNa$ requires: 601.1868

I.R. υ_{max} (KBr): 3275 (NH), 2206 (-C≡C-), 1727 (C=O_{ester}), 1640 (C=O_{amide}), 1605 (C=O_{amide}) cm^{-1};

UV-Vis λ_{max} EtOH: 408, 503 nm;

^{1}H NMR (400 MHz) δ ($CDCl_3$): 8.22 (1H, s, Ar<u>H</u>), 8.08 (1H, s, Ar<u>H</u>), 7.78 - 7.74 {6H, m, (Ar<u>H</u>), (-CON<u>H</u>-),(-CON<u>H</u>-)}, 4.65 - 4.50 (3H, m, -<u>CH</u>$CH_2CH(CH_3)_2$), (*ortho* on η^5-$C_5\underline{H}_4$-C≡C-)}, 4.30 - 4.00 {11H, m, (*meta* on η^5-$C_5\underline{H}_4$-C≡C-), (η^5-$C_5\underline{H}_5$), (-NH<u>CH_2</u>CO-), (-O<u>CH_2</u>CH_3)}, 1.67 - 1.55 {3H, m, -CH<u>CH_2</u><u>CH</u>$(CH_3)_2$}, 1.17 (3H, t, *J* = 7.2 Hz - OCH_2<u>CH_3</u>), 0.86 - 0.84 (6H, m, -CHCH_2CH(<u>CH_3</u>)$_2$);

^{13}C NMR (100 MHz) δ ($CDCl_3$): 172.9 (C=O), 169.4 (C=O), 167.8 (C=O), 135.0 (C_q), 133.1 (C_q), 130.7 (C_q), 130.2 (C_q), 128.8, 128.0, 127.8, 127.4, 124.0 120.8, 90.7 (η^5-C_5H_4-C≡$\underline{C}$-), 85.6 (η^5-C_5H_4-$\underline{C}$≡C-), 71.0 (C_{ortho} η^5-$\underline{C}_5H_4$-C≡C-), 69.7 (η^5-$\underline{C}_5H_5$), 68.4 (C_{meta} η^5-$\underline{C}_5H_4$-C≡C-), 67.3 (C_{ipso} η^5-$\underline{C}_5H_4$-C≡C-), 61.4 (-O$\underline{CH_2}CH_3$, -ve DEPT), 51.2 (-$\underline{CH}CH_2CH(CH_3)_2$), 43.8 (-NH$\underline{CH_2}$CO-, -ve DEPT), 41.2 (-CH$\underline{CH_2}$CH($\underline{CH_3}$)$_2$, -ve DEPT), 24.9 (-CHCH$_2$$\underline{CH}$($CH_3$)$_2$), 22.8 (-CHCH$_2$CH($\underline{CH_3}$)$_2$), 21.9 (-CHCH$_2$CH($\underline{CH_3}$)$_2$), 14.2. (-OCH$_2$$\underline{CH_3}$).

_N_-{6-(ferrocenyl) ethynyl-2-naphthoyl} sarcosine glycine ethyl ester (127)

Sarcosine glycine ethyl ester hydrochloride (0.46 g, 2.63 mmol) was used as a starting material. The crude product was purified by column chromatography (eluent 1:1 hexane: ethyl acetate) and recrystallisation from hexane: ethyl acetate yielded the desired product as a red solid (0.19 g, 13%), m.p 32 - 34 ^{o}C;

Mass spectrum: found: $[M+Na]^+$ 559.1307

$C_{30}H_{28}N_2O_4FeNa$ requires: 559.1398

I.R. υ_{max} (KBr): 3284 (NH), 2205 (-C≡C-), 1744 (C=O_{ester}), 1676 (C=O_{amide}), 1605 (C=O_{amide}) cm^{-1};

UV-Vis λ_{max} EtOH: 391, 509 nm;

^{1}H NMR (400 MHz) δ ($CDCl_3$): 7.92 - 7.49 {7H, m, (-CON$\underline{H}$-), (Ar$\underline{H}$)}, 4.48 (2H, s, *ortho* on η^5-$C_5\underline{H}_4$-C≡C-), 4.30 - 3.90 {13H, m, (*meta* on η^5-$C_5\underline{H}_4$-C≡C-), (η^5-$C_5\underline{H}_5$), (-N(CH_3)$\underline{CH_2}$CO-), (-NH$\underline{CH_2}$CO-) (-O$\underline{CH_2}CH_3$)}, 3.10 (3H, s, -N($\underline{CH_3}$)CH_2CO-), 1.19 (3H, t, *J* = 7.2 Hz, -OCH$_2$$\underline{CH_3}$);

^{13}C NMR (100 MHz) δ ($CDCl_3$): 172.7 (C=O), 170.4 (C=O), 167.2 (C=O), 133.6 (C_q), 132.7 (C_q), 131.9 (C_q), 130.8 (C_q), 129.5, 128.5, 128.1, 127.3, 125.0, 122.9, 90.1 (η^5-C_5H_4-C≡$\underline{C}$-), 85.9 (η^5-C_5H_4-$\underline{C}$≡C-), 71.8 (C_{ortho} η^5-$\underline{C}_5H_4$-C≡C-), 70.5 (η^5-$\underline{C}_5H_5$), 69.5 (C_{meta} η^5-$\underline{C}_5H_4$-C≡C-), 65.4 (C_{ipso} η^5-$\underline{C}_5H_4$-C≡C-), 61.7 (-O$\underline{CH_2}CH_3$, -ve DEPT), 48.2 (-N(CH_3)$\underline{CH_2}$CO-, -ve DEPT), 41.2 (-NH$\underline{CH_2}$CO-, -ve DEPT), 38.4 (-N($\underline{CH_3}$)CH_2CO-), 14.2 (-OCH$_2$$\underline{CH_3}$).

***N*-{6-(ferrocenyl) ethynyl-2-naphthoyl} glycine-L-phenylalanine ethyl ester (128)**

Glycine L-phenylalanine ethyl ester hydrochloride (0.66 g, 2.63 mmol) was used as a starting material. The crude product was purified by column chromatography (eluent 1:1 hexane: ethyl acetate) and recrystallisation from hexane: ethyl acetate yielded the desired product as a red solid (0.14 g, 9%), m.p 48 - 50 ^{o}C;

$[\alpha]_D^{25}$ = -15 ^{o} (*c* 0.1, EtOH);

Mass spectrum: found: $[M+Na]^+$ 635.1639

$C_{36}H_{32}N_2O_4FeNa$ requires: 635.1711

I.R. υ_{max} (KBr): 3359 (NH), 2205 (-C≡C-), 1743 ($C=O_{ester}$), 1631 ($C=O_{amide}$), 1605 ($C=O_{amide}$) cm^{-1};

UV-Vis λ_{max} EtOH: 408, 505 nm;

^{1}H NMR (400 MHz) δ ($CDCl_3$): 8.15 (1H, s, ArH), 8.00 (1H, s, ArH), 7.80 - 7.70 {6H, m, (ArH), (-CONH-),(-CONH-) },7.16 - 7.00 (5H, m, -CHCH_2Ph), 4.87 - 4.85 (1H, m, -CH(CH_2Ph)), 4.58 (2H, s, *ortho* on η^5-C_5H_4-C≡C-), 4.26 (2H, s, *meta* on η^5-C_5H_4-C≡C-), 4.20 - 3.95 {9H, m, (η^5-C_5H_5), (-OCH_2CH_3), (-NHCH_2CO-)}, 3.15 - 2.95 (2H, m, -CHCH_2Ph), 1.15 (3H, t, *J* = 7.2 Hz, -OCH_2CH_3);

^{13}C NMR (100 MHz) δ ($CDCl_3$): 171.4 (C=O), 168.0 (C=O), 167.6 (C=O), 135.8 (C_q), 134.5 (C_q), 130.9 (C_q), 130.6 (C_q), 130.2, 129.3, 128.6, 128.0, 127.8, 127.1, 126.7, 124.2, 123.4, 122.1, 91.7 (η^5-C_5H_4-C≡C-), 85.0 (η^5-C_5H_4-C≡C-), 71.6 (C_{ortho} η^5-C_5H_4-C≡C-), 70.1 (η^5-C_5H_5), 69.5 (C_{meta} η^5-C_5H_4-C≡C-), 65.8 (C_{ipso} η^5-C_5H_4-C≡C-), 61.3 (-OCH_2CH_3, -ve DEPT), 53.6 (-CHCH_2Ph), 43.0 (-NHCH_2CO-, -ve DEPT), 38.5 (-CHCH_2Ph, -ve DEPT), 14.9 (-OCH_2CH_3).

General procedure for the preparation of *N*-{5-(ferrocenyl) ethynyl-2-furanoyl} amino acid and dipeptide ethyl esters

***N*-{5-(ferrocenyl) ethynyl-2-furanoyl} glycine glycine ethyl ester (129)**

Glycine glycine ethyl ester hydrochloride (0.50 g, 3.12 mmol) was used as a starting material. The crude product was purified by column chromatography (eluent 1:1 hexane: ethyl acetate) and recrystallisation from hexane: ethyl acetate yielded the desired product as a red solid (0.55 g, 38%), m.p 94 - 96 ^{o}C;

Mass spectrum: found: $[M+Na]^+$ 485.0752

$C_{23}H_{22}N_2O_5FeNa$ requires: 485.0776

I.R. υ_{max} (KBr): 3276 (NH), 2206 (-C≡C-), 1739 ($C=O_{ester}$), 1631 ($C=O_{amide}$), 1610 ($C=O_{amide}$) cm^{-1};

UV-Vis λ_{max} EtOH: 370, 476 nm;

^1H NMR (400 MHz) δ ($CDCl_3$): 7.28 (1H, t, *J* = 4.8 Hz, -CONH-), 7.08 - 7.07 {2H, m, (-CONH-), (ArH)}, 6.53 (1H, d, *J* = 3.6 Hz, ArH), 4.47 (2H, s, *ortho* on η^5-C_5H_4-C≡C-), 4.23 - 4.12 {11H, m, (*meta* on η^5-C_5H_4-C≡C-), (η^5-C_5H_5), (-NHCH_2CO-), (-OCH_2CH_3)}, 4.00 (2H, d, *J* = 5.2 Hz, -NHCH_2CO-), 1.20 (3H, t, *J* = 7.2 Hz, -OCH_2CH_3);

^{13}C NMR (100 MHz) δ ($CDCl_3$):168.7 (C=O), 167.9 (C=O), 157.1 (C=O), 145.4 (C_q), 138.2 (C_q), 115.1, 115.0, 93.9 (η^5-C_5H_4-C≡C-), 74.0 (η^5-C_5H_4-C≡C-), 70.6 (C_{ortho} η^5-C_5H_4-C≡C-), 69.2 (η^5-C_5H_5), 68.5 (C_{meta} η^5-C_5H_4-C≡C-), 62.7 (C_{ipso} η^5-C_5H_4-C≡C-), 60.6 (-OCH_2CH_3, -ve DEPT), 41.7 (-NHCH_2CO-, -ve DEPT), 40.4 (-NHCH_2CO-, -ve DEPT), 13.1 (-OCH_2CH_3).

_N_-{5-(ferrocenyl) ethynyl-2-furanoyl} glycine L-alanine ethyl ester (130)

Glycine L-alanine ethyl ester hydrochloride (0.54 g, 3.12 mmol) was used as a starting material. The crude product was purified by column chromatography (eluent 1:1 hexane: ethyl acetate) and recrystallisation from hexane: ethyl acetate yielded the desired product as a red oil (0.28 g, 19%),

$[\alpha]_D^{20}$ = -20 ^{o} (*c* 0.1, EtOH);

Mass spectrum: found: $[M+Na]^+$ 499.0919

$C_{24}H_{24}N_2O_5FeNa$ requires: 499.0932

I.R. υ_{max} (KBr): 3287 (NH), 2206 (-C≡C-), 1734 ($C=O_{ester}$), 1646 ($C=O_{amide}$), 1612 ($C=O_{amide}$) cm^{-1}

UV-Vis λ_{max} EtOH: 374, 475 nm;

^1H NMR (400 MHz) δ ($CDCl_3$): 7.06 (1H, d, *J* = 3.6 Hz, ArH), 7.02 (1H, t, *J* = 5.6 Hz, -CONH-), 6.59 - 6.54 {2H, m, (ArH), (-CONH-)}, 4.56 - 4.47 {3H, m, (-$CHCH_3$), (*ortho* on η^5-C_5H_4-C≡C-) }, 4.24 - 4.21 {7H, m, (*meta* on η^5-C_5H_4-C≡C-), (η^5-C_5H_5)},

4.17 - 4.07 (4H, m, (-NHCH$_2$CO-), (-OCH$_2$CH$_3$)}, 1.38 (3H, d, *J* = 7.2 Hz, -CHCH$_3$), 1.21 (3H, t, *J* = 7.2 Hz, -OCH$_2$CH$_3$);

^{13}C NMR (100 MHz) δ ($CDCl_3$): 172.7 (C=O), 167.2 (C=O), 158.0 (C=O), 146.5 (C_q), 139.3 (C_q), 116.1, 116.0, 94.5 (η^5-C_5H_4-C≡C-), 75.0 (η^5-C_5H_4-C≡C-), 71.7 (C_{ortho} η^5-C_5H_4-C≡C-), 70.2 (η^5-C_5H_5), 69.5 (C_{meta} η^5-C_5H_4-C≡C-), 62.8 (C_{ipso} η^5-C_5H_4-C≡C-), 61.7 (-OCH$_2$CH$_3$, -ve DEPT), 48.4 (-CHCH$_3$), 42.8 (-NHCH$_2$CO-, -ve DEPT), 18.3 (-CHCH$_3$), 14.1 (-OCH$_2$CH$_3$).

_N_-{5-(ferrocenyl) ethynyl-2-furanoyl} glycine D-alanine ethyl ester (131)

Glycine D-alanine ethyl ester hydrochloride (0.54 g, 3.12 mmol) was used as a starting material. The crude product was purified by column chromatography (eluent 1:1 hexane: ethyl acetate) and recrystallisation from hexane: ethyl acetate yielded the desired product as a red solid (0.23 g, 16%), m.p 132 - 134 ^{o}C;

$[\alpha]_D^{20}$ = +20 ^{o} (*c* 0.1, EtOH);

Mass spectrum: found: $[M+Na]^+$ 499.0917

$C_{24}H_{24}N_2O_5FeNa$ requires: 499.0932

I.R. υ_{max} (KBr): 3287 (NH), 2208 (-C≡C-), 1739 (C=O_{ester}), 1642 (C=O_{amide}), 1617 (C=O_{amide}) cm^{-1};

UV-Vis λ_{max} EtOH: 373, 471 nm;

^{1}H NMR (400 MHz) δ ($CDCl_3$): 7.08 (1H, d, *J* = 3.6 Hz, ArH), 7.00 (1H, t, *J* = 5.6 Hz, -CONH-), 6.61 - 6.58 {2H, m, (ArH), (-CONH-)}, 4.54 - 4.45 {3H, m, (-CHCH$_3$), (*ortho* on η^5-C_5H_4-C≡C-)}, 4.27 - 4.25 {7H, m, (*meta* on η^5-C_5H_4-C≡C-), (η^5-C_5H_5)}, 4.10 -4.04 (4H, m, (-NHCH$_2$CO-), (-OCH$_2$CH$_3$)} 1.40 (3H, d, *J* = 7.2 Hz, -CHCH$_3$), 1.25 (3H, t, *J* = 7.2 Hz, -OCH$_2$CH$_3$);

^{13}C NMR (100 MHz) δ ($CDCl_3$): 173.7 (C=O), 163.9 (C=O), 158.6 (C=O), 140.5 (C_q), 137.3 (C_q), 117.1, 116.9, 94.0 (η^5-C_5H_4-C≡C-), 74.0 (η^5-C_5H_4-C≡C-), 71.2 (C_{ortho} η^5-C_5H_4-C≡C-), 70.5 (η^5-C_5H_5), 65.5 (C_{meta} η^5-C_5H_4-C≡C-), 64.0 (C_{ipso} η^5-C_5H_4-C≡C-), 61.1 (-OCH$_2$CH$_3$, -ve DEPT), 49.4 (-CHCH$_3$), 42.8 (-NHCH$_2$CO-, -ve DEPT), 19.3 (-CHCH$_3$), 15.0 (-OCH$_2$CH$_3$).

***N*-{5-(ferrocenyl) ethynyl-2-furanoyl} glycine L-phenylalanine ethyl ester (132)**

Glycine L-phenylalanine ethyl ester hydrochloride (0.78 g, 3.12 mmol) was used as a starting material. The crude product was purified by column chromatography (eluent 1:1 hexane: ethyl acetate) and recrystallisation from hexane: ethyl acetate yielded the desired product as a red solid (0.18 g, 10%), m.p 85 - 86 ^{o}C;

$[\alpha]_D^{20}$ = +16 ^{o} (*c* 0.1, EtOH);

Mass spectrum: found: $[M+Na]^+$ 575.1365

$C_{30}H_{28}N_2O_5FeNa$ requires: 575.1348

I.R. υ_{max} (KBr): 3278 (NH), 2207 (-C≡C-), 1739 ($C=O_{ester}$), 1642 ($C=O_{amide}$), 1620 ($C=O_{amide}$) cm^{-1}

UV-Vis λ_{max} EtOH: 375, 478 nm;

^{1}H NMR (400 MHz) δ ($CDCl_3$): 7.35 - 7.12 {8H, m, (ArH), (-CONH-), (-CONH-), (-$CHCH_2$Ph)}, 6.87 (1H, d, *J* = 3.6 Hz, ArH), 4.91 - 4.86 (1H, m, -CHCH_2Ph), 4.58 (2H, s, *ortho* on η^5-C_5H_4-C≡C-), 4.30 - 4.29 {7H, m, (*meta* on η^5-C_5H_4-C≡C-), (η^5-C_5H_5)}, 4.12 (2H, q, *J* = 7.0 Hz -OCH_2CH_3), 4.11 (2H, d, *J* = 6.8 Hz, -NHCH_2CO-), 3.17 - 3.10 (2H, m, -CHCH_2Ph), 1.31 (3H, t, *J* = 7.0 Hz, -OCH_2CH_3);

^{13}C NMR (100 MHz) δ ($CDCl_3$):171.2 (C=O), 168.0 (C=O), 157.9 (C=O), 146.5 (C_q), 139.3 (C_q), 135.6, 129.3, 128.6, 127.2, 116.1, 116.0, 94.9 (η^5-C_5H_4-C≡C-), 75.0 (η^5-C_5H_4-C≡C-), 71.7 (C_{ortho} η^5-C_5H_4-C≡C-), 70.2 (η^5-C_5H_5), 69.5 (C_{meta} η^5-C_5H_4-C≡C-), 62.9 (C_{ipso} η^5-C_5H_4-C≡C-), 61.7 (-OCH_2CH_3, -ve DEPT), 53.3 (-CHCH_2Ph), 42.8 (-NHCH_2CO-, -ve DEPT), 37.9 (-CHCH_2Ph, -ve DEPT), 14.2 (-OCH_2CH_3).

***N*-{5-(ferrocenyl) ethynyl-2-furanoyl} glycine L-leucine ethyl ester (133)**

Glycine L-leucine ethyl ester hydrochloride (0.68 g, 3.12 mmol) was used as a starting material. The crude product was purified by column chromatography (eluent 1:1 hexane: ethyl acetate) and recrystallisation from hexane: ethyl acetate yielded the desired product as a red oil (0.20 g, 12%);

$[\alpha]_D^{20}$ = -14 ^{o} (*c* 0.1, EtOH);

Mass spectrum: found: $[M+Na]^+$ 541.1385

$C_{27}H_{30}N_2O_5FeNa$ requires: 541.1402

I.R. υ_{max} (KBr): 3285 (NH), 2205 (-C≡C-), 1735 (C=O_{ester}), 1674 (C=O_{amide}), 1612 (C=O_{amide}) cm^{-1}

UV-Vis λ_{max} EtOH: 373, 474 nm;

^{1}H NMR (400 MHz) δ ($CDCl_3$): 7.11 - 7.05 {2H, m, (ArH), (-CONH-)}, 6.65 - 6.60 {2H, m, (ArH), (-CONH-)}, 4.60 - 4.54 {1H, m, -CHCH$_2$CH(CH$_3$)$_2$}, 4.48 (2H, t, *J* = 2.0 Hz, *ortho* on η^5-C_5H_4-C≡C-), 4.25 - 4.05 {11H, m, (*meta* on η^5-C_5H_4-C≡C-), (-NHCH$_2$CO-), (η^5-C_5H_5), (-OCH$_2$CH$_3$)}, 1.66 - 1.47 {3H, m, -CHCH$_2$CH(CH$_3$)$_2$}, 1.21 (3H, t, *J* = 7.0 Hz - OCH$_2$CH$_3$), 0.88 - 0.86 { 6H, m, -CHCH$_2$CH(CH$_3$)$_2$};

^{13}C NMR (100 MHz) δ ($CDCl_3$): 172.7 (C=O), 168.2 (C=O), 158.0 (C=O), 147.0 (C_q), 139.3 (C_q), 116.0, 115.9, 94.9 (η^5-C_5H_4-C≡C-), 75.0 (η^5-C_5H_4-C≡C-), 71.7 (C_{ortho} η^5-C_5H_4-C≡C-), 70.3 (η^5-C_5H_5), 69.5 (C_{meta} η^5-C_5H_4-C≡C-), 63.1 (C_{ipso} η^5-C_5H_4-C≡C-), 61.9 (-OCH$_2$CH$_3$, -ve DEPT), 51.3 (-CHCH$_2$CH(CH$_3$)$_2$), 42.8 (-NHCH$_2$CO-, -ve DEPT), 41.4 (-CHCH$_2$CH(CH$_3$)$_2$, -ve DEPT), 25.0 (-CHCH$_2$CH(CH$_3$)$_2$), 22.4 (-CHCH$_2$CH(CH$_3$)$_2$), 21.9 (-CHCH$_2$CH(CH$_3$)$_2$), 14.7 (-OCH$_2$CH$_3$).

_N_-{5-(ferrocenyl) ethynyl-2-furanoyl} sarcosine glycine ethyl ester (134)

Sarcosine glycine ethyl ester hydrochloride (0.54 g, 3.12 mmol) was used as a starting material. The crude product was purified by column chromatography (eluent 1:1 hexane: ethyl acetate) and recrystallisation from hexane: ethyl acetate yielded the desired product as a red solid (0.13 g, 9%), m.p 136 - 138 ^{o}C;

Mass spectrum: found: $[M+Na]^+$ 499.0918

$C_{24}H_{24}N_2O_5FeNa$ requires: 499.0932

I.R. υ_{max} (KBr): 3311 (NH), 2208 (-C≡C-), 1742 (C=O_{ester}), 1681 (C=O_{amide}), 1620 (C=O_{amide}) cm^{-1};

UV-Vis λ_{max} EtOH: 374, 478 nm;

^{1}H NMR (400 MHz) δ ($CDCl_3$): 7.05 {(1H, d, *J* = 3.2 Hz, ArH), 6.85 (1H, bs, -CONH-), 6.55 (1H, d, *J* = 3.2 Hz, ArH), 4.46 (2H, s, *ortho* on η^5-C_5H_4-C≡C-), 4.23 - 3.99 {13H, m, (*meta* on η^5-C_5H_4-C≡C-), (η^5-C_5H_5), (-N(CH$_3$)CH$_2$CO-), (-NHCH$_2$CO-), (-OCH$_2$CH$_3$)}, 3.20 (3H, s, -N(CH$_3$)CH$_2$CO-), 1.28 (3H, t, *J* = 6.8 Hz, -OCH$_2$CH$_3$);

^{13}C NMR (100 MHz) δ ($CDCl_3$): 171.9 (C=O), 169.1 (C=O), 158.0 (C=O), 147.0 (C_q), 139.6 (C_q), 118.0, 117.5, 94.2 (η^5-C_5H_4-C≡C-), 75.0 (η^5-C_5H_4-C≡C-), 71.0 (C_{ortho} η^5-C_5H_4-C≡C-), 70.4 (η^5-C_5H_5), 69.7 (C_{meta} η^5-C_5H_4-C≡C-), 63.8 (C_{ipso} η^5-C_5H_4-C≡C-),

61.0 (-O$\underline{CH_2}CH_3$, -ve DEPT), 51.7 (-N(CH_3)$\underline{CH_2}$CO-, -ve DEPT), 41.0 (-NH$\underline{CH_2}$CO-, -ve DEPT), 38.7 (-N($\underline{CH_3}$)CH_2CO-), 13.5 (-O$CH_2\underline{CH_3}$).

_N_-{5-(ferrocenyl) ethynyl-2-furanoyl} L-proline glycine ethyl ester (135)

L-Proline glycine ethyl ester hydrochloride (0.67 g, 3.12 mmol) was used as a starting material. The crude product was purified by column chromatography (eluent 1:1 hexane: ethyl acetate) and recrystallisation from hexane: ethyl acetate yielded the desired product as a red solid (0.16 g, 10%), m.p 128 - 130 ^oC;

$[\alpha]_D^{20}$ = 13 ^{o} (*c* 0.1, EtOH);

Mass spectrum: found: $[M+Na]^+$ 525.1078

$C_{26}H_{26}N_2O_5FeNa$ requires: 525.1089

I.R. υ_{max} (KBr): 3284 (NH), 2210 (-C≡C-), 1742 (C=O_{ester}), 1641 (C=O_{amide}), 1610 (C=O_{amide}) cm^{-1};

UV-Vis λ_{max} EtOH: 379, 477 nm;

^{1}H NMR (400 MHz) δ ($CDCl_3$): 7.34 (1H, t, *J* = 5.2 Hz, -CON$\underline{H}$-), 7.10 (1H, d, *J* = 3.6 Hz, Ar$\underline{H}$), 6.56 (1H, d, *J* = 3.6 Hz, Ar$\underline{H}$), 4.80 - 4.78 (1H, bs, -N($CH_2CH_2CH_2$)C$\underline{H}$CO-), 4.47 (2H, s, *ortho* on η^5-$C_5\underline{H}_4$-C≡C-), 4.14 - 3.95 {13H, m, (*meta* on η^5-$C_5\underline{H}_4$-C≡C-), (η^5-$C_5\underline{H}_5$), (-O$\underline{CH_2}CH_3$), (-N($\underline{CH_2}CH_2CH_2$)CHCO-), (-NH$\underline{CH_2}$CO-)}, 2.36 - 1.88 (4H, m, -N($CH_2\underline{CH_2}\underline{CH_2}$)CHCO-), 1.23 (3H, t, *J* = 6.8 Hz, -O$CH_2\underline{CH_3}$);

^{13}C NMR (100 MHz) δ ($CDCl_3$): 168.7 (C=O), 167.9 (C=O), 157.1 (C=O), 145.4 (C_q), 138.2 (C_q), 117.6, 115.7, 94.1 (η^5-C_5H_4-C≡$\underline{C}$-), 75.7 (η^5-C_5H_4-$\underline{C}$≡C-), 71.6 (C_{ortho} η^5-$\underline{C}_5H_4$-C≡C-), 69.9 (η^5-$\underline{C}_5H_5$), 68.5 (C_{meta} η^5-$\underline{C}_5H_4$-C≡C-), 64.8 (C_{ipso} η^5-$\underline{C}_5H_4$-C≡C-), 61.0 (-O$\underline{CH_2}CH_3$, -ve DEPT), 52.8 (-N($CH_2CH_2CH_2$)$\underline{CH}$CO-),

48.4 (-N($\underline{CH_2}CH_2CH_2$)CHCO-, -ve DEPT), 41.4 (-NH$\underline{CH_2}$CO-, -ve DEPT), 27.5 (-N($CH_2CH_2\underline{CH_2}$)CHCO-, -ve DEPT), 24.9 (-N($CH_2\underline{CH_2}CH_2$)CHCO-, -ve DEPT), 13.0 (-O$CH_2\underline{CH_3}$).

_N_-{5-(ferrocenyl) ethynyl-2-furanoyl} L-proline L-alanine ethyl ester (136)

L-Proline L-alanine ethyl ester hydrochloride (0.71 g, 3.12 mmol) was used as a starting material. The crude product was purified by column chromatography (eluent

1:1 hexane: ethyl acetate) and recrystallisation from hexane: ethyl acetate yielded the desired product as a red solid (0.14 g, 9%), m.p 34 - 36 ^{o}C;

$[\alpha]_D^{20}$ = -45 ^{o} (*c* 0.1, EtOH);

Mass spectrum: found: $[M+Na]^+$ 539.1249

$C_{27}H_{28}N_2O_5FeNa$ requires: 539.1245

I.R. υ_{max} (KBr): 3289 (NH), 2206 (-C≡C-), 1736 ($C=O_{ester}$), 1674 ($C=O_{amide}$), 1630 ($C=O_{amide}$) cm^{-1};

UV-Vis λ_{max} EtOH: 376, 479 nm;

^{1}H NMR (400 MHz) δ ($CDCl_3$): 7.30 (1H, t, *J* = 5.2 Hz, -CONH-), 7.09 (1H, d, *J* = 3.6 Hz, ArH), 6.56 (1H, d, *J* = 3.6 Hz, ArH), 4.47 (1H, t, *J* = 7.0 Hz, -N($CH_2CH_2CH_2$)CHCO-), 4.46 - 4.43 {3H, m, (*ortho* on η^5-C_5H_4-C≡C-), (-CHCH$_3$)}, 4.23 - 4.19 {7H, m, (*meta* on η^5-C_5H_4-C≡C-), (η^5-C_5H_5)}, 4.12 (2H, q, *J* = 7.2 Hz, -OCH_2CH$_3$), 3.73 - 3.56 (2H, m, -N($CH_2CH_2CH_2$)CHCO-), 2.50 - 1.80 (4H, m, -N($CH_2CH_2CH_2$)CHCO-), 1.34 (3H, d, *J* = 7.2 Hz, -CHCH$_3$) 1.20 (3H, t, *J* = 7.2 Hz, -OCH$_2$CH$_3$);

^{13}C NMR (100 MHz) δ ($CDCl_3$): 173.4 (C=O), 170.9 (C=O), 158.5 (C=O), 147.4 (C_q), 140.7 (C_q), 118.5, 115.7, 94.7 (η^5-C_5H_4-C≡C-), 75.1 (η^5-C_5H_4-C≡C-), 71.7 (C_{ortho} η^5-C_5H_4-C≡C-), 70.2 (η^5-C_5H_5), 69.5 (C_{meta} η^5-C_5H_4-C≡C-), 63.0 (C_{ipso} η^5-C_5H_4-C≡C-), 61.4 (-OCH_2CH$_3$, -ve DEPT), 49.3 (-N($CH_2CH_2CH_2$)CHCO-),

48.1 (-N($CH_2CH_2CH_2$)CHCO-, -ve DEPT), 46.8 (-CHCH$_3$),

27.0 (-N($CH_2CH_2CH_2$)CHCO-, -ve DEPT), 25.6 (-N($CH_2CH_2CH_2$)CHCO-, -ve DEPT), 18.2 (-CHCH$_3$), 14.2 (-OCH$_2$CH$_3$).

N-{5-(ferrocenyl) ethynyl-2-furanoyl} sarcosine L-alanine ethyl ester (137)

Sarcosine L-alanine ethyl ester hydrochloride (0.59 g, 3.12 mmol) was used as a starting material. The crude product was purified by column chromatography (eluent 1:1 hexane: ethyl acetate) and recrystallisation from hexane: ethyl acetate yielded the desired product as a red oil (0.12 g, 8%);

$[\alpha]_D^{20}$ = -19 ^{o} (*c* 0.1, EtOH);

Mass spectrum: found: $[M+Na]^+$ 513.1080

$C_{25}H_{26}N_2O_5FeNa$ requires: 513.1089

I.R. υ_{max} (KBr): 3317 (NH), 2206 (-C≡C-), 1745 ($C=O_{ester}$), 1671 ($C=O_{amide}$), 1640 ($C=O_{amide}$) cm^{-1};

UV-Vis λ_{max} EtOH: 375, 474 nm;

^{1}H NMR (400 MHz) δ ($CDCl_3$): 7.05 (1H, d, *J* = 3.2 Hz, ArH), 6.85 - 6.86 (1H, bs, -CONH-), 6.55 (1H, d, *J* = 3.2 Hz, ArH), 4.48 - 4.45 {3H, m, (*ortho* on η^5-C_5H_4-C≡C-), (-C<u>H</u>CH_3)}, 4.19 - 3.90 {11H, m, (*meta* on η^5-C_5H_4-C≡C-), (η^5-C_5H_5), (-N(CH_3)CH_2CO-), (-O$CH_2$$CH_3$)}, 3.00 (3H, s, -N($CH_3$)$CH_2$CO-), 1.35 (2H, d, *J* = 7.2 Hz, -CHCH_3), 1.23 (3H, t, *J* = 6.8 Hz, -O$CH_2$$CH_3$);

^{13}C NMR (100 MHz) δ ($CDCl_3$): 173.7 (C=O), 168.6 (C=O), 159.0 (C=O), 145.0 (C_q), 138.6 (C_q), 118.0, 116.5, 93.9 (η^5-C_5H_4-C≡C-), 76.0 (η^5-C_5H_4-C≡C-), 71.9 (C_{ortho} η^5-C_5H_4-C≡C-), 70.8 (η^5-C_5H_5), 67.7 (C_{meta} η^5-C_5H_4-C≡C-), 63.9 (C_{ipso} η^5-C_5H_4-C≡C-), 61.3 (-O$CH_2$$CH_3$, -ve DEPT), 47.2 (-C<u>H</u>CH_3), 40.1 (-N(CH_3)CH_2CO-, -ve DEPT), 38.5 (-N(CH_3)CH_2CO-), 18.5 (-CHCH_3), 14.2 (-O$CH_2$$CH_3$).

_N_-{5-(ferrocenyl) ethynyl-2-furanoyl} γ-aminobutyric acid ethyl ester (138)

γ-Amino butyric acid ethyl ester hydrochloride (0.41 g, 3.12 mmol) was used as a starting material. The crude product was purified by column chromatography (eluent 1:1 hexane: ethyl acetate) and recrystallisation from hexane: ethyl acetate yielded the desired product as a red oil (0.34 g, 25%);

Mass spectrum: found: $[M+Na]^+$ 456.0854

$C_{23}H_{23}NO_4FeNa$ requires: 456.0874

I.R. υ_{max} (KBr): 3287 (NH), 2206 (-C≡C-), 1735 ($C=O_{ester}$), 1640 ($C=O_{amide}$) cm^{-1}

UV-Vis λ_{max} EtOH: 372, 484 nm;

^{1}H NMR (400 MHz) δ ($CDCl_3$): 7.06 (1H, d, *J* = 3.5 Hz, ArH), 7.02 (1H, t, *J* = 5.6 Hz, -CONH-), 6.65 {1H, d, *J* = 3.5 Hz, ArH), 4.56 (2H, t, *J* = 2.0 Hz, *ortho* on η^5-C_5H_4-C≡C-), 4.27 (2H, t, *J* = 2.0 Hz, *meta* on η^5-C_5H_4-C≡C-), 4.16 (5H, s, η^5-C_5H_5), 4.04 (2H, q, *J* = 7.2 Hz, -O$CH_2$$CH_3$), 3.43 {2H, q, *J* = 6.4 Hz, (-NH$CH_2$$CH_2$$CH_2$-)}, 2.38 (2H, t, *J* = 6.8 Hz, -NH$CH_2$$CH_2$$CH_2$-), 1.90 {2H, quin, *J* = 6.4 Hz, -NH$CH_2$$CH_2$$CH_2$-), 1.17 (3H, t, *J*= 7.2 Hz, -O$CH_2$$CH_3$);

^{13}C NMR (100 MHz) δ ($CDCl_3$): 173.4 (C=O), 170.9 (C=O), 147.0 (C_q), 141.0 (C_q), 117.3, 115.7, 94.2 (η^5-C_5H_4-C≡C-), 75.7 (η^5-C_5H_4-C≡C-), 71.2 (C_{ortho} η^5-C_5H_4-C≡C-), 70.9 (η^5-C_5H_5), 69.0 (C_{meta} η^5-C_5H_4-C≡C-), 63.7 (C_{ipso} η^5-C_5H_4-C≡C-), 60.4 (-

O$\underline{CH_2}CH_3$, -ve DEPT), 39.8 (-NH$\underline{CH_2}CH_2CH_2$-, -ve DEPT), 34.0 (-NHCH$_2$CH$_2\underline{CH_2}$-, -ve DEPT), 25.3 (-NHCH$_2\underline{CH_2}$CH$_2$-, -ve DEPT), 13.5 (-OCH$_2\underline{CH_3}$).

References:

1. http://www.sigmaaldrich.com/catalog/product/aldrich/122459?lang=en&region=IE
2. http://www.sigmaaldrich.com/catalog/product/aldrich/106860?lang=en&region=IE
3. Gibson, E. S., *Transition Metals in Organic Chemistry.*, Oxford University Press., **1997.**
4. Rosenblum, M., Brawn, N., Papenmeier, J., Applebaum, M., *J. Organomet. Chem.* **1966**, *6*, 173.

Appendix 1: Abbreviations and Units

A

A	absorbance
ATR	attenuated total reflection
AR	androgen receptor

B

BF_4^-	tetrafluoroborate ion
Br	bromine
bs	broad singlet (spectroscopy)
BuLi	Butyllithium

C

C	carbon; concentration
Calc.	calculated
Cq	quaternary carbon
$CDCl_3$	deuterated chloroform
Cl	chlorine
Co	cobalt
Cu(1)	copper (1)
CO_2	carbon dioxide
Cp	cyclopentadienyl ring
COSY	correlated spectroscopy
C=O	carbonyl
CBr_4	

D

d	doublet (spectroscopy)
DCC	1,3-dicyclohexylcarbdiimide

DCM	dichloromethane
DCU	Dublin City University
dd	doublet of doubles
DEPT-135	distortionless enhancement by polarisation transfer
DMSO-d_6	deuterated dimethylsulfoxide

E

e^-	electron
EDC	*N*-(3-dimethylaminopropyl)-*N'*-ethylcarbodiimide hydrochloride
ESR	electron spin resonance
ER	estrogen receptor
ER(+)	estrogen receptor positive cells
ER(-)	estrogen receptor negative cells
EtOH	ethanol

F

Fc/Fc^+	ferrocene/ferrocenium ion
Fe	iron
Fe(II)	ferrous ion
Fe(III)	ferric ion
FT	Fourier transform

G

Ga	gallium
Gly	glycine
Gaba	gamma-amino butyric acid

H

H	hydrogen
H_2O	water
HCl	hydrochloric acid

HQMC	Heteronuclear multiple quantum coherence
HOBt	1-hydroxybenzotriazole
H_3PO_4	phosphoric acid

I

IC_{50}	half maximal inhibitory concentration
IR	infra red spectroscopy

J

J	coupling constant

K

KBr	potassium bromide

L

l	path length (cm)
L-Ala	L-alanine
L-Phe	L-phenyalanine
L-Leu	L-leucine
L-pro	L-proline
Lit	literature

M

m	*meta*; mass
m	multiplet (spectral)
M	metal; mitosis phase
MeOH	methanol
$MgSO_4$	magnesium sulphate
MLCT	metal-ligand charge transfer
mp	melting point
MS	mass spectrometry

N

NICB	National Institute for Cellular Biotechnology
NMR	nuclear magnetic resonance
NaOH	sodium hydroxide
NHS	*N*-hydroxysuccinimide
NSCLC	non-small cell lung carcinoma

O

o	*ortho*
O	oxygen
OH	hydroxy

P

p	*para*
P	phosphorous
Pt	platnium
ppm	parts per million
$POCl_3$	phosphorus oxychloride
PPh_3	triphenylphosphine
Pd	palladim

Q

q	quartet

R

Rh	rhodium
Ru	ruthenium
RNA	ribonucleic acid
RSD	relative standard deviation
ROS	reactive oxygenated species

S

s	singlet
SARS	structure activity relationship
SERM	selective estrogen receptor modulator
SCLC	small cell lung carcinoma
Sar	sarcosine

T

TEA	triethylamine
TMS	tetramethylsilane
TFA	trifluoroacetic acid
Ti	titanium
THF	tetrahydrofuran
t-BuOK	potassium *tert*-butoxide

U

UV	ultraviolet

V

V	vanadium
Vis	visible

W

WHO	World Health Organisation

Units

cm	centimetre
cm^{-1}	wavenumber / per centimetre
g	gram
hr	hour

Hz	hertz
M	molar
MHz	megahertz
ml	millilitre
mm	millimetre
mM	millimolar
mmol	millimolar
µl	microlitre
µM	micromolar
^{o}C	degree celcius
ppm	parts per million
s	second
δ	chemical shift
%	percentage

.

Appendix 11: Publication

Journal of Organometallic Chemistry xxx (2012) 1–7

Contents lists available at SciVerse ScienceDirect

Journal of Organometallic Chemistry

journal homepage: www.elsevier.com/locate/jorganchem

The synthesis, structural characterization and *in vitro* anti-cancer activity of novel *N*-{6-(ferrocenyl) ethynyl-2-naphthoyl} amino acid and dipeptide ethyl esters

Andy G. Harry [a], James Murphy [b], William E. Butler [a,b], Rachel Tiedt [b], Áine Mooney [a,b], Jennifer C. Manton [a], Mary T. Pryce [a], Norma O'Donovan [b], Naomi Walsh [b], John Crown [c], Dilip K. Rai [d], Peter T.M. Kenny [a,b,*]

[a] School of Chemical Sciences, Dublin City University, Dublin 9, Ireland
[b] National Institute for Cellular Biotechnology, Dublin City University, Dublin 9, Ireland
[c] Dept. of Medical Oncology, St. Vincent's University Hospital, Dublin 4, Ireland
[d] Dept. of Food Biosciences, Teagasc Food Research Centre, Ashtown, Dublin 15, Ireland

ARTICLE INFO

Article history:
Received 25 October 2012
Received in revised form
29 November 2012
Accepted 30 November 2012

Keywords:
Ferrocene
Bioorganometallic chemistry
Dipeptides
Cytotoxicity
Lung cancer

ABSTRACT

N-{6-(Ferrocenyl) ethynyl-2-naphthoyl} amino acid and dipeptide ethyl esters **2–8** were prepared by coupling 6-(ferrocenyl) ethynyl-2-naphthoic acid **1** to the amino acid ethyl ester GABA(OEt) and the dipeptide ethyl esters GlyGly(OEt), GlyAla(OEt), SarGly(OEt), SarAla(OEt), ProGly(OEt) and ProAla(OEt) using the standard *N*-(3-dimethylaminopropyl)-*N'*-ethylcarbodiimide hydrochloride (EDC), 1-hydroxybenzotriazole (HOBt) protocol. All the compounds were fully characterized using a combination of ^{1}H NMR, ^{13}C NMR, DEPT-135 and $^{1}H-^{13}C$ COSY (HMQC) spectroscopy, electrospray ionization mass spectrometry (ESI-MS) and cyclic voltammetry (CV). Compounds, **2–8** showed micromolar activity in the H1299 NSCLC cell line, with IC_{50} values in the range of 3.2–7.2 μM.

1. Introduction

Ferrocene is a particularly attractive candidate for incorporation into biomolecules and biologically active compounds due to its aromatic character, redox properties and low toxicity [1–3]. The redox properties of ferrocene have often been implicated in its cytotoxicity [4]. Ferricenium salts that are known to inhibit tumour growth have been shown to produce hydroxyl (HO•) radicals under physiological conditions, leading to oxidatively damaged DNA [5]. The catalytic generation of intracellular reactive oxygen species (ROS) such as the HO• radical offers an attractive and alternative method to target and kill cancer cells [6].

The medicinal application of ferrocene derivatives is currently an active area of research, with countless reports showing their activity *in vitro* and *in vivo* against several diseases including fungal and bacterial infections, human immunodeficiency virus (HIV), malaria and cancer [7]. Perhaps the most popular and well-researched application of ferrocene and its derivatives is in the area of cancer research [8]. Over the past decade Jaouen and co-workers have comprehensively investigated the *in vitro* anti-cancer activity of ferrocifen, a ferrocenyl analogue of tamoxifen, and various related derivatives [9]. Their most promising drug candidates contain a [3]-ferrocenophane motif and have a potent *in vitro* anti-proliferative effect in breast and prostate cancer cell lines [10–12]. This research group has reported the anti-proliferative effects of ferrocenyl benzoyl and ferrocenyl naphthoyl bioconjugates in the H1299 lung cancer cell line [13–19]. These *N*-(ferrocenyl)benzoyl and naphthoyl dipeptide esters consist of three components, namely: (i) an electroactive core, (ii) a conjugated linker that lowers the oxidation potential of the ferrocene moiety and (iii) an amino acid or peptide derivative that can interact with other biomolecules *via* secondary interactions such as hydrogen bonding. In an effort to improve the cytotoxicity of these derivatives, we are currently modifying the conjugated linker moiety and conducting variations of the peptide chain. The compounds prepared in this study have an ethynyl group linked to the ferrocene and the naphthoyl spacer group.

* Corresponding author. School of Chemical Sciences, Dublin City University, Dublin 9, Ireland. Tel.: +353 1 7005689; fax: +353 1 7005503.
E-mail address: peter.kenny@dcu.ie (P.T.M. Kenny).

0022-328X/$ – see front matter © 2012 Elsevier B.V. All rights reserved.
http://dx.doi.org/10.1016/j.jorganchem.2012.11.041

Herein, we report the synthesis and structural characterization of novel *N*-{6-(ferrocenyl) ethynyl-2-naphthoyl} amino acid and dipeptide ethyl esters. The dipeptide ethyl esters GlyGly(OEt), SarGly(OEt) and GlyAla(OEt) were employed in this investigation as they were shown to have IC_{50} values of 0.13, 0.14 and 1.3 μM respectively, in the H1299 lung cancer cell line. The dipeptide ethyl esters SarAla(OEt), ProGly(OEt) and ProAla(OEt) were selected as they are closely related analogues of the most active compounds.

The synthesis of the new ferrocenyl bioconjugates involved Sonogashira coupling of ethynyl ferrocene to generate 6-(ferrocenyl) ethynyl-2-naphthoic acid [20]. A series of dipeptide esters were coupled to the 6-(ferrocenyl) ethynyl-2-naphthoic acid to generate the new class of compounds which were characterized by a combination of ^{1}H NMR, ^{13}C NMR, DEPT-135, ^{1}H–^{13}C COSY spectroscopy, cyclic voltammetry and mass spectrometry. In addition, we present the *in vitro* anti-cancer activity of compounds **2–8** against the human lung carcinoma cell line H1299.

2. Results and discussion

2.1. Synthesis

2.1.1. Synthesis of N-{6-(ferrocenyl) ethynyl-2-naphthoyl} amino acid and dipeptide ethyl esters 2–8

6-(Ferrocenyl) ethynyl-2-naphthoic acid **1** was prepared by coupling ethynyl ferrocene to 6-bromo-2-naphthoic acid *via* the Sonogashira reaction [20]. The ^{1}H NMR spectrum showed signals for the aromatic ring protons at δ 8.13 (1H, s) and between δ 7.95–7.48 (5H, m) for the 2,6-disubstituted naphthalene ring system. The carboxylic acid proton was present at δ 12.87. The ferrocenyl *ortho* and *meta* protons on the (η^5-$C_5\underline{H}_4$) ring were observed at δ 4.27 and δ 4.19, respectively, and an intense signal was present at δ 4.19 for the (η^5-$C_5\underline{H}_5$) ring. The free N-terminal amino acid GABA(OEt) and the free N-terminal dipeptide ethyl esters GlyGly(OEt), GlyAla(OEt), SarGly(OEt), SarAla(OEt), ProGly(OEt) and ProAla(OEt) were coupled to 6-(ferrocenyl) ethynyl-2-naphthoic acid **1** using EDC and HOBt in the presence of excess triethylamine in dichloromethane (Scheme 1). EDC was used in preference to the less expensive coupling reagent *N,N'*-dicyclohexylcarbodiimide (DCC) as its reaction by-products are easier to remove compared to those of DCC, namely dicyclohexylurea (DCU). Purification by column chromatography furnished the pure products in yields of 11–32% and all compounds gave spectroscopic data in accordance with the proposed structures. The relatively low yields of products obtained are partly due to the coupling procedure. The first step in amide bond formation in the coupling protocol is formation of the O-acylisourea ester intermediate. This intermediate is highly reactive and thus, side-reactions can pose a serious problem and can result in extensive racemisation resulting in low yields. The addition of HOBt stabilizes the O-acylisourea ester intermediate thus suppressing side reactions, however the addition does not result in 100% suppression. As the reaction proceeds upon addition of the amino acid and dipeptide ethyl esters the HOBt is displaced resulting in the formation of compounds **2–8**. As a result of the complexity of the reaction which is associated with the competing reactions, low yields for compounds **2–8** were obtained. Also in the EDC/HOBt coupling reaction when primary amine amino acid and dipeptide ethyl esters, namely, GABA(OEt), GlyGly(OEt) and GlyAla(OEt)} are used, the yields are generally higher than that of the secondary amine dipeptide ethyl esters SarGly(OEt), SarAla(OEt), ProGly(OEt) and ProAla(OEt). For example the percentage yield of *N*-{6-(ferrocenyl) ethynyl-2-naphthoyl}-glycine-glycine ethyl ester **3** obtained was 28% whereas the percentage yield of *N*-{6-(ferrocenyl) ethynyl-2-naphthoyl}-sarcosine-glycine ethyl ester **5** was only 13%.

The *N*-{6-(ferrocenyl) ethynyl-2-naphthoyl} amino acid and dipeptide ethyl esters **2–8** were characterized by a combination of IR, UV–Vis, ^{1}H NMR, ^{13}C NMR, DEPT-135 and ^{1}H–^{13}C COSY (HMQC) spectroscopy and cyclic voltammetry (CV). Electrospray ionization (ESI) mass spectrometry in conjunction with tandem mass spectrometry (MS/MS) was also employed in the analysis.

2.2. ^{1}H and ^{13}C spectroscopic analysis

All the proton and carbon chemical shifts for compounds **2–8** were unambiguously assigned by a combination of DEPT-135 and ^{1}H–^{13}C COSY (HMQC). The ^{1}H and ^{13}C NMR spectra for compounds **2–8** showed peaks in the ferrocene region characteristic of a monosubstituted ferrocene moiety [21–25]. The *ortho* protons on the cyclopentadiene ring attached to the (–C≡C–) spacer moiety appear in the region δ 4.4 to δ 4.72, the *meta* protons occur in the range δ 4.33 to δ 3.9 and usually overlap with the unsubstituted (η^5-$C_5\underline{H}_5$) ring which also appears between δ 4.33 and δ 3.90.

The ^{13}C NMR spectra of compounds **2–8** show signals in the region δ 63.6 to δ 74.2 indicative of a monosubstituted ferrocene unit. The *ipso* carbon of the (η^5-$\underline{C}_5H_4$) ring appears in the range of δ 63.6 to δ 67.8. This signal is absent in the DEPT-135 spectra. The carbon atoms of the ethynyl group appear in the range of δ 85.0 to δ 91.4 and are also

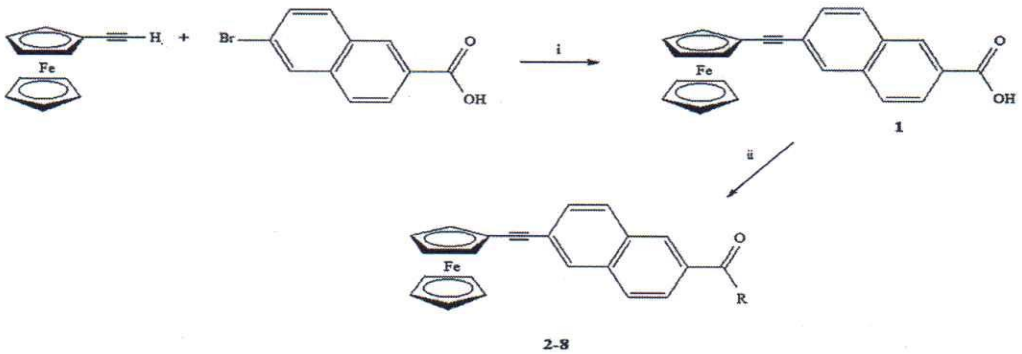

Scheme 1. Synthesis of *N*-{6-(ferrocenyl) ethynyl-2-naphthoyl} amino acid and dipeptide ethyl esters **2–8**, (i) TEA, PPh_3, Bis(triphenylphosphine)palladium(II) dichloride, THF, Cu(I) (ii) EDC, HOBt, triethylamine, amino acid and dipeptide ethyl esters, R = GABA(OEt) **2**, GlyGly(OEt) **3**, GlyAla(OEt) **4**, SarGly(OEt) **5**, SarAla(OEt) **6**, ProGly(OEt) **7** and ProAla(OEt) **8**.

Please cite this article in press as: A.G. Harry, et al., Journal of Organometallic Chemistry (2012), http://dx.doi.org/10.1016/j.jorganchem.2012.11.041

absent in the DEPT-135 spectra. The carbon atoms of the aromatic naphthalene ring are non-equivalent and therefore ten signals are visible in the region of δ 120.8 to δ 135.8 for compounds **2–8**. The quaternary carbon atoms of the aromatic ring and the methylene carbon atoms of derivatives **2–8** were identified by DEPT-135. Complete spectroscopic data for all the compounds is presented in the experimental section.

2.3. Mass spectrometry

Soft ionization techniques such as electrospray ionization (ESI) mass spectrometry permit the analysis of thermolabile and non-volatile analytes [26]. Electrospray ionization (ESI) mass spectrometry was employed in the analysis of compounds **2–8** and confirmed the correct relative molecular mass for all the compounds.

Tandem mass spectrometry was used to determine the fragmentation pattern of *N*-{6-(ferrocenyl) ethynyl-2-naphthoyl}-glycine-glycine ethyl ester **3**. In the MS/MS spectrum of *N*-{6-(ferrocenyl) ethynyl-2-naphthoyl}-glycine-glycine ethyl ester **3** the sequence specific fragment ions are present at *m/z* 335, *m/z* 363, *m/z* 391 and *m/z* 419 (Fig. 1). The product ions at *m/z* 335 and *m/z* 363 correspond to the *N*-{6-(ferrocenyl) ethynyl-2-naphthyl and *N*-{6-(ferrocenyl) ethynyl-2-naphthoyl} subunits respectively figure. However, the expected a_1 and b_1 product ions at *m/z* 392 and *m/z* 420 were not observed, instead $a_1 - 1$ and $b_1 - 1$ product ions were observed at *m/z* 391 and *m/z* 419 respectively. Obviously a hydrogen atom has also been lost during the fragmentation process. This is unusual as these a_1 and b_1 fragment ions are usually produced without loss of a hydrogen atom [27]. The formation of $a_1 - 1$ and $b_1 - 1$ ions in the mass spectra of *N*-{*para*-(ferrocenyl)benzoyl}-glycine-L-alanine ethyl ester was investigated by tandem mass spectrometry and deuterium labelling studies. The results showed that $b_1 - 1$ product ions arise from the loss of a hydrogen atom attached to the nitrogen and not to the α-carbon of the glycine residue [28].

2.4. Electrochemistry

The CV curves for compounds **2–8** exhibit quasi-reversible behaviour similar to the Fc/Fc^+ redox couple. The $E^{o\prime}$ (oxidation potential) values for the *N*-{6-(ferrocenyl) ethynyl-2-naphthoyl} amino acid and dipeptide ethyl esters **2–8** showed values in the 119–162 mV range (versus Fc/Fc^+). The values for compounds **2–8** are higher than those reported for the *N*-(6-ferrocenyl-2-naphthoyl) derivatives (42–56 mV versus Fc/Fc^+), but are lower than ferrocenyl dipeptide ester derivatives [17,19]. For example, Fc-Ala-Ala-OMe, was reported as $E^{o\prime} = 230$ mV (vs Fc/Fc^+) [29].

2.5. In vitro anti-cancer activity of 2–8

The *N*-{6-(ferrocenyl) ethynyl-2-naphthoyl} amino acid and dipeptide ethyl esters **2–8** have been prepared as part of an ongoing SAR study. The *in vitro* anti-proliferative effect of compounds **2–8** was studied in the H1299 non-small cell lung cancer (NSCLC) cell line. Proliferation was measured using the acid phosphatase assay. Thus 1×10^3 cells per well were seeded in 96 well plates. The plates were incubated overnight at 37 °C followed by addition of the compound at a concentration of 10 μM and incubated for a further 5 days. The results of this biological study are reported in Table 1 and are expressed as % cell growth inhibition relative to the untreated controls. The % cell growth inhibition was lowest for compound **2** at 68% and highest for compounds **6** and **8** at 94% cell growth inhibition. The IC_{50} values for derivatives **2–8** were then determined by the acid phosphatase assay as previously described [30]. This colorimetric end-point assay is an indirect measure of cytotoxicity which evaluates the enzyme activity of cells after a given treatment period. Acid phosphatase is an enzyme which dephosphorylates *p*-nitrophenyl phosphate substrate converting it to *p*-nitrophenol which in the presence of strong alkali can be quantified colorimetrically. The cells were treated with the *N*-{6-(ferrocenyl) ethynyl-2-naphthoyl} amino acid and dipeptide ethyl esters **2–8** at a range of concentrations (from 1 μM to 100 μM) and were incubated for 5 days until cell confluency reached 80–90%. Cell survival was established through determination of the acid phosphatase activity of surviving cells and growth inhibition calculated relative to controls (untreated cells). The results for compounds **2–8** are depicted in Fig. 2 and Table 2 displays the IC_{50} values for derivatives **2–8** and the control drug cisplatin.

It can be seen from Fig. 2 that the *N*-{6-(ferrocenyl) ethynyl-2-naphthoyl} amino acid and dipeptide ethyl esters **2–8** all exert a cytotoxic effect on the human lung carcinoma cell line H1299. All seven derivatives have an IC_{50} value that is lower than 7.2 μM. The most active compound was *N*-{6-(ferrocenyl) ethynyl-2-naphthoyl}-sarcosine-L-alanine ethyl ester which had an IC_{50} value of 3.2 μM. It is interesting to note that this compound has the lowest $E^{o\prime}$ value of 119 mV. However for compounds **2–5** the presence of the ethynyl moiety had a negative effect of anti-proliferative effect compared to analogous compounds prepared previously lacking the ethynyl group [17–19]. For

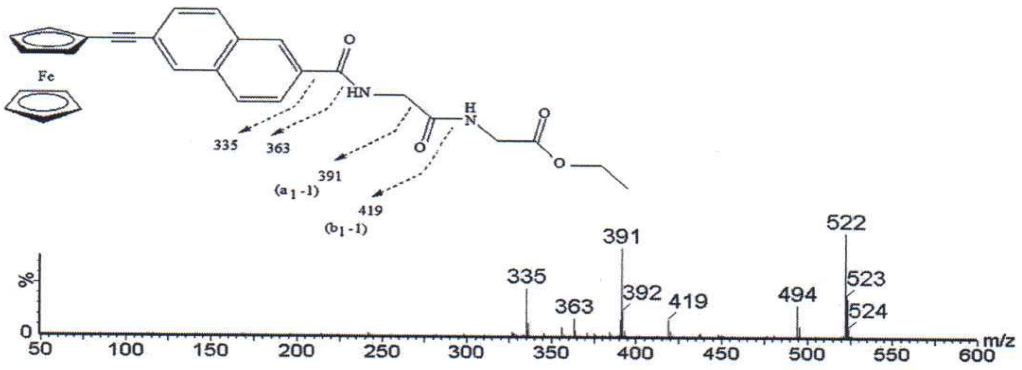

Fig. 1. MS/MS spectrum of *N*-{6-(ferrocenyl) ethynyl-2-naphthoyl}-glycine-glycine ethyl ester **3**.

Please cite this article in press as: A.G. Harry, et al., Journal of Organometallic Chemistry (2012), http://dx.doi.org/10.1016/j.jorganchem.2012.11.041

Table 1
% Growth inhibition values for compounds **2–8** against human lung carcinoma cell line H1299.

Compound name	% Growth inhibition
N-(6-(Ferrocenyl) ethynyl-2-naphthoyl)-γ-aminobutyric acid ethyl ester **2**	68
N-(6-(Ferrocenyl) ethynyl-2-naphthoyl)-glycine-glycine ethyl ester **3**	89
N-(6-(Ferrocenyl) ethynyl-2-naphthoyl)-glycine-L-alanine ethyl ester **4**	84
N-(6-(Ferrocenyl) ethynyl-2-naphthoyl)-sarcosine-glycine ethyl ester **5**	90
N-(6-(Ferrocenyl) ethynyl-2-naphthoyl)-sarcosine-L-alanine ethyl ester **6**	94
N-(6-(Ferrocenyl) ethynyl-2-naphthoyl)-L-proline-glycine ethyl ester **7**	82
N-(6-(Ferrocenyl) ethynyl-2-naphthoyl)-L-proline-L-alanine ethyl ester **8**	94

example for *N*-(6-(ferrocenyl) ethynyl-2-naphthoyl)-γ-aminobutyric acid ethyl ester the IC_{50} value is 7.2 μM whereas for *N*-(6-ferrocenyl-2-naphthoyl)-γ-aminobutyric acid ethyl ester the IC_{50} value was 0.62 μM. The *in vitro* cytotoxicity of the platinum(II)-based anti-cancer drug cisplatin was also evaluated against the H1299 cell line, and was found to have an IC_{50} value of 1.5 ± 0.1 μM (Table 2). Thus, compounds **2–8** are less cytotoxic *in vitro* than the clinically employed anti-cancer drug cisplatin.

3. Conclusions

In conclusion, the novel *N*-{6-(ferrocenyl) ethynyl-2-naphthoyl} amino acid and dipeptide ethyl esters **2–8** were synthesized and fully characterized by a range of NMR spectroscopic techniques, mass spectrometry and cyclic voltammetry. Compounds **2–8** were tested *in vitro* against the human lung carcinoma cell line H1299. Compounds **2–8** showed micromolar activity in the H1299 NSCLC cell line, with IC_{50} values in the range of 3.2–7.2 μM. However insertion of the ethynyl group had a negative effect on the anti-proliferative effect compared to analogous compounds prepared previously lacking the ethynyl group.

4. Experimental

4.1. General procedures

All chemicals were purchased from Sigma–Aldrich, Lennox Chemicals, Fluorochem Limited or Tokyo Chemical Industry UK

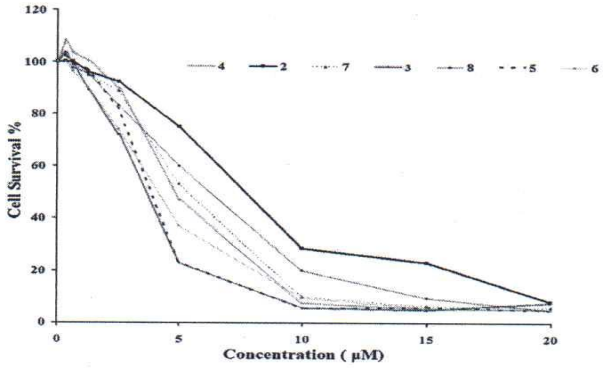

Fig. 2. Cytotoxicity of derivatives **2–8**.

Table 2
IC_{50} values for compounds **2–8** and cisplatin against human lung carcinoma cell line H1299.

Compound	IC_{50} value (μM)
Cisplatin	1.5 ± 0.1
N-(6-(Ferrocenyl) ethynyl-2-naphthoyl)-γ-aminobutyric acid ethyl ester **2**	7.2 ± 1.5
N-(6-(Ferrocenyl) ethynyl-2-naphthoyl)-glycine-glycine ethyl ester **3**	5.0 ± 4.1
N-(6-(Ferrocenyl) ethynyl-2-naphthoyl)-glycine-L-alanine ethyl ester **4**	5.0 ± 3.6
N-(6-(Ferrocenyl) ethynyl-2-naphthoyl)-sarcosine-glycine ethyl ester **5**	4.7 ± 3.7
N-(6-(Ferrocenyl) ethynyl-2-naphthoyl)-sarcosine-L-alanine ethyl ester **6**	3.2 ± 6.6
N-(6-(Ferrocenyl) ethynyl-2-naphthoyl)-L-proline-glycine ethyl ester **7**	5.1 ± 1.3
N-(6-(Ferrocenyl) ethynyl-2-naphthoyl)-L-proline-L-alanine ethyl ester **8**	3.8 ± 2.0

Limited; and used as received. Commercial grade reagents were used without further purification. When necessary, all solvents were purified and dried prior to use. Riedel-Haën silica gel was used for thin layer and column chromatography. Melting points were determined using a Stuart melting point (SMP3) apparatus and are uncorrected. Optical rotation measurements were made on a Perkin–Elmer 343 Polarimeter and are quoted in units of 10^{-1} deg cm^2 g^{-1}. Infrared spectra were recorded on a Perkin–Elmer Spectrum 100 FT-IR with ATR. UV–Vis spectra were recorded on a Hewlett Packard 8452 A diode array UV–Vis spectrophotometer. ^1H and ^{13}C NMR spectra were recorded in deuterated solvents on a Bruker Avance 400 NMR. The ^1H and ^{13}C NMR chemical shifts are reported in ppm (parts per million). Tetramethylsilane (TMS) or the residual solvent peaks were used as an internal reference. All coupling constants (*J*) are in Hertz. Electrospray ionisation mass spectra were performed on a Micromass LCT mass spectrometer. Tandem mass spectra were obtained on a Micromass Quattro *micro*™ LC–MS/MS triple quadrupole mass spectrometer.

Cyclic voltammograms were recorded in anhydrous acetonitrile (Sigma–Aldrich), with 0.1 M tetrabutylammonium hexafluorophosphate ($TBAPF_6$) as a supporting electrolyte, using a CH Instruments 600a electrochemical analyzer (Pico-Amp Booster and Faraday Cage). The experiments were carried out at room temperature. A three-electrode cell consisting of a glassy carbon working-electrode, a platinum wire counter-electrode and an Ag|AgCl reference electrode was used. The glassy carbon electrode was polished with 0.3 μm alumina followed by 0.05 μm alumina, between each experiment to remove any surface contaminants. The scan rate was 0.1 V s^{-1}. The concentration range of the ferrocene compounds was 1.0 mM in acetonitrile. The $E^{o\prime}$ values obtained for the test samples were referenced relative to the ferrocene/ferricenium redox couple.

4.2. General procedure for the synthesis of the starting materials

4.2.1. 6-Ferrocenyl ethynyl-2-naphthoic acid **1**

Ethynyl ferrocene (2.00 g, 9.52 mmol) and 6-bromo-2-naphthoic acid (2.39 g, 9.52 mmol) were mixed together and dissolved in 50 ml of a 1:1 mixture of dry triethylamine and tetrahydrofuran under nitrogen for 10 min. Triphenylphosphine (0.20 g, 0.76 mmol), bis(triphenylphosphine)palladium(II) dichloride (0.28 g, 0.38 mmol) and copper(I) iodide (0.07 g, 0.38 mmol) were mixed together and added to the reaction mixture. The reaction mixture was stirred for 10 min and refluxed at 80 °C for 12 h. The reaction mixture was vacuum

Please cite this article in press as: A.G. Harry, et al., Journal of Organometallic Chemistry (2012), http://dx.doi.org/10.1016/j.jorganchem.2012.11.041

filtered. The solvent was removed *in vacuo* to yield the crude product. The crude product was purified by column chromatography (eluant 1:1 hexane:ethyl acetate) to yield the desired product as a red solid (2.34 g, 64%), mp 167–169 °C.

^{1}H NMR (400 MHz) δ (DMSO-d_6): 12.87 (1H, s, –COOH), 8.13 (1H, s, ArH), 7.95–7.48 (5H, m, (ArH)), 4.60 (2H, t, J = 2.0 Hz, *ortho* on η^5-C_5H_4–C≡C–), 4.27 (2H, t, J = 2.0 Hz *meta* on η^5-C_5H_4–C≡C–), 4.19 (5H, s, η^5-C_5H_5).

^{13}C NMR (100 MHz) δ (DMSO-d_6): 172.7 (C=O), 134.9 (C_q), 134.6 (C_q), 134.0 (C_q), 132.2 (C_q), 131.6, 130.3, 128.1, 128.0, 127.8, 120.8, 90.3 (η^5-C_5H_4–C≡C–), 85.7 (η^5-C_5H_4–C≡C–), 71.4 (C_{ortho} η^5-C_5H_4–C≡C–), 69.9 (η^5-C_5H_5), 68.7 (C_{meta} η^5-C_5H_4–C≡C–), 65.8 (C_{ipso} η^5-C_5H_4–C≡C–).

4.3. General procedure for the synthesis of N-{6-(ferrocenyl) ethynyl-2-naphthoyl} amino acid and dipeptide ethyl esters

4.3.1. N-{6-(Ferrocenyl) ethynyl-2-naphthoyl}-γ-aminobutyric acid ethyl ester 2

6-(Ferrocenyl) ethynyl-2-naphthoic acid (1.00 g, 2.63 mmol) was dissolved in dichloromethane (100 ml) at 0 °C. *N*-(3-dimethylaminopropyl)-*N'*-ethylcarbodiimide hydrochloride (0.50 g, 2.63 mmol), 1-hydroxybenotriazole (0.36 g, 2.63 mmol), γ-aminobutyric acid ethyl ester hydrochloride (0.34 g, 2.63 mmol) and triethylamine (6 ml) were added and the reaction mixture was allowed to stir at 0 °C for 45 min. The reaction mixture was then allowed to stir at room temperature for 48 h. The reaction mixture was washed with water and brine. The organic layer was dried over $MgSO_4$. The solvent was removed *in vacuo* to yield the crude product. The crude product was purified by column chromatography (eluant 1:1 hexane:ethyl acetate) and recrystallisation from hexane:ethyl acetate yielded the desired product as a red solid (0.42 g, 32%), m.p. 71–73 °C; $E^{o\prime}$ = 131 mV (vs Fc/Fc$^+$).

Mass spectrum: found: [M + Na]$^+$ 516.1255.

$C_{29}H_{27}NO_3FeNa$ requires: 516.1340.

I.R. υ_{max} (KBr): 3283 (NH), 2205 (–C≡C–), 1726 (C=O$_{ester}$), 1605 (C=O$_{amide}$) cm^{-1}.

UV–Vis λ_{max} EtOH: 268 (ε 308) nm.

^{1}H NMR (400 MHz) δ ($CDCl_3$): 8.18 (1H, s, ArH), 7.81{1H, s, ArH}, 7.75–7.49 {5H, m, (–CONH–), (ArH)}, 4.47 (2H, t, J = 1.6 Hz, *ortho* on η^5-C_5H_4–C≡C–), 4.19–4.18 {7H, m, (*meta* on η^5-C_5H_4–C≡C–), (η^5-C_5H_5)}, 4.04 (2H, q, J = 7.2 Hz, –OCH_2CH_3), 3.46 (2H, q, J = 5.6 Hz, –$NHCH_2CH_2CH_2$–), 2.37 (2H, t, J = 6.8 Hz, –$NHCH_2CH_2CH_2$–), 1.87 (2H, quin, J = 6.4 Hz, –$NHCH_2CH_2CH_2$–), 1.15 (3H, t, J = 7.2 Hz, –OCH_2CH_3).

^{13}C NMR (100 MHz) δ ($CDCl_3$): 171.5 (C=O), 167.4 (C=O), 131.5 (C_q), 130.1 (C_q), 129.1 (C_q), 128.9 (C_q), 128.2, 127.6, 127.7, 126.0, 125.1, 123.0, 89.2 (η^5-C_5H_4–C≡C–), 85.0 (η^5-C_5H_4–C≡C–), 71.9 (C_{ortho} η^5-C_5H_4–C≡C–), 69.2 (η^5-C_5H_5), 68.4 (C_{meta} η^5-C_5H_4–C≡C–), 63.8 (C_{ipso} η^5-C_5H_4–C≡C–), 60.0 (–OCH_2CH_3, -ve DEPT), 39.0 (–$NHCH_2CH_2CH_2$–, -ve DEPT), 31.2 (–$NHCH_2CH_2CH_2$–, -ve DEPT), 23.3 (–$NHCH_2CH_2CH_2$–, -ve DEPT), 13.1 (–OCH_2CH_3).

4.3.2. N-{6-(Ferrocenyl) ethynyl-2-naphthoyl}-glycine-glycine ethyl ester 3

Glycine-glycine ethyl ester hydrochloride (0.42 g, 2.63 mmol) was used as a starting material. The crude product was purified by column chromatography (eluant 1:1 hexane:ethyl acetate) and recrystallisation from hexane:ethyl acetate yielded the desired product as a red solid (0.38 g, 28%), m.p. 128–130 °C; $E^{o\prime}$ = 141 mV (vs Fc/Fc$^+$).

Mass spectrum: [M + Na]$^+$ found: 545.1130.

$C_{29}H_{26}N_2O_4FeNa$ requires: 545.1140.

I.R. υ_{max} (KBr): 3261 (NH), 2204 (–C≡C–), 1736 (C=O$_{ester}$), 1658 (C=O$_{amide}$), 1603 (C=O$_{amide}$) cm^{-1}.

UV–Vis λ_{max} EtOH: 278 (ε 310) nm.

^{1}H NMR (400 MHz) δ ($CDCl_3$): 8.13 (1H, s, ArH), 7.95–7.48 {7H, m, (ArH), (–CONH–), (–CONH–)}, 4.61 (2H, t, J = 2.0 Hz, *ortho* on η^5-C_5H_4–C≡C–), 4.30 (2H, t, J = 2.0 Hz, *meta* on η^5-C_5H_4–C≡C–), 4.19–4.15 {11H, m, (η^5-C_5H_5), (–$NHCH_2CO$–), (–$NHCH_2CO$–), (–OCH_2CH_3)}, 1.23 (3H, t, J = 7.2 Hz, –OCH_2CH_3).

^{13}C NMR (100 MHz) δ ($CDCl_3$): 172.7 (C=O), 170.9 (C=O), 169.6 (C=O), 133.9 (C_q), 132.6 (C_q), 131.0 (C_q), 130.2 (C_q), 129.6, 129.3, 128.9, 128.1, 127.8, 125.8, 90.3 (η^5-C_5H_4–C≡C–), 84.7 (η^5-C_5H_4–C≡C–), 72.1 (C_{ortho} η^5-C_5H_4–C≡C–), 70.0 (η^5-C_5H_5), 69.7 (C_{meta} η^5-C_5H_4–C≡C–), 67.8 (C_{ipso} η^5-C_5H_4–C≡C–), 61.6 (–OCH_2CH_3, -ve DEPT), 42.3 (–$NHCH_2CO$–, -ve DEPT), 40.1 (–$NHCH_2CO$–, -ve DEPT), 14.8 (–OCH_2CH_3).

4.3.3. N-{6-(Ferrocenyl) ethynyl-2-naphthoyl}-glycine-L-alanine ethyl ester 4

Glycine-L-alanine ethyl ester hydrochloride (0.46 g, 2.63 mmol) was used as a starting material. The crude product was purified by column chromatography (eluant 1:1 hexane:ethyl acetate) and recrystallisation from hexane:ethyl acetate yielded the desired product as a red solid (0.23 g, 16%), m.p. 58–60 °C; $E^{o\prime}$ = 139 mV (vs Fc/Fc$^+$); $[\alpha]_D^{20}$ = −14° (c 0.1, EtOH).

Mass spectrum: [M + Na]$^+$ found: 559.1305.

$C_{30}H_{28}N_2O_4FeNa$ requires: 559.1398.

I.R. υ_{max} (KBr): 3287 (NH), 2204 (–C≡C–), 1734 (C=O$_{ester}$), 1658 (C=O$_{amide}$), 1625 (C=O$_{amide}$) cm^{-1}.

UV–Vis λ_{max} EtOH: 242 (ε 316) nm.

^{1}H NMR (400 MHz) δ ($CDCl_3$): 8.21 (1H, s, ArH), 7.87–7.51 {7H, m, (ArH), (–CONH–), (–CONH–)}, 4.48–4.47 {3H, m, (–$CHCH_3$), (*ortho* on η^5-C_5H_4–C≡C–)}, 4.19–4.07 {11H, m, (*meta* on η^5-C_5H_4–C≡C–), (η^5-C_5H_5), (–OCH_2CH_3), (–$NHCH_2CO$–)}, 1.36 (3H, d, J = 7.2 Hz, –$CHCH_3$), 1.28 (3H, t, J = 6.8 Hz, –OCH_2CH_3).

^{13}C NMR (100 MHz) δ ($CDCl_3$): 171.8 (C=O), 169.1 (C=O), 167.9 (C=O), 134.5 (C_q), 131.5 (C_q), 130.8 (C_q), 130.4 (C_q), 129.3, 128.9, 128.0, 127.7, 124.3, 123.4, 90.4 (η^5-C_5H_4–C≡C–), 84.9 (η^5-C_5H_4–C≡C–), 71.3 (C_{ortho} η^5-C_5H_4–C≡C–), 70.1 (η^5-C_5H_5), 69.5 (C_{meta} η^5-C_5H_4–C≡C–), 65.9 (C_{ipso} η^5-C_5H_4–C≡C–), 60.3 (–OCH_2CH_3, -ve DEPT), 48.9 (–$CHCH_3$), 43.1 (–$NHCH_2CO$–, -ve DEPT), 17.2 (–$CHCH_3$), 13.7 (–OCH_2CH_3).

4.3.4. N-{6-(Ferrocenyl) ethynyl-2-naphthoyl}-sarcosine-glycine ethyl ester 5

Sarcosine-glycine ethyl ester hydrochloride (0.46 g, 2.63 mmol) was used as a starting material. The crude product was purified by column chromatography (eluant 1:1 hexane:ethyl acetate) and recrystallisation from hexane:ethyl acetate yielded the desired product as a red solid (0.19 g, 13%), m.p. 32–34 °C; $E^{o\prime}$ = 162 mV (vs Fc/Fc$^+$).

Mass spectrum: found: [M + Na]$^+$ 559.1307.

$C_{30}H_{28}N_2O_4FeNa$ requires: 559.1398.

I.R. υ_{max} (KBr): 3284 (NH), 2205 (–C≡C–), 1744 (C=O$_{ester}$), 1676 (C=O$_{amide}$), 1605 (C=O$_{amide}$) cm^{-1}.

UV–Vis λ_{max} EtOH: 252 (ε 313) nm.

^{1}H NMR (400 MHz) δ ($CDCl_3$): 7.92–7.49 {7H, m, (–CONH–), (ArH)}, 4.48 (2H, s, *ortho* on η^5-C_5H_4–C≡C–), 4.30–3.90 {13H, m, (*meta* on η^5-C_5H_4–C≡C–), (η^5-C_5H_5), (–$N(CH_3)CH_2CO$–), (–$NHCH_2CO$–) (–OCH_2CH_3)}, 3.10 (3H, s, –$N(CH_3)CH_2CO$–), 1.19 (3H, t, J = 7.2 Hz, –OCH_2CH_3).

^{13}C NMR (100 MHz) δ ($CDCl_3$): 172.7 (C=O), 170.4 (C=O), 167.2 (C=O), 133.6 (C_q), 132.7 (C_q), 131.9 (C_q), 130.8 (C_q), 129.5, 128.5, 128.1, 127.3, 125.0, 122.9, 90.1 (η^5-C_5H_4–C≡C–), 85.9 (η^5-C_5H_4–C≡C–), 71.8 (C_{ortho} η^5-C_5H_4–C≡C–), 70.5 (η^5-C_5H_5), 69.5 (C_{meta} η^5-C_5H_4–C≡C–), 65.4 (C_{ipso} η^5-C_5H_4–C≡C–), 61.7 (–OCH_2CH_3, -ve DEPT), 48.2 (–$N(CH_3)CH_2CO$–, -ve DEPT), 41.2 (–$NHCH_2CO$–, -ve DEPT), 38.4 (–$N(CH_3)CH_2CO$–), 14.2 (–OCH_2CH_3).

Please cite this article in press as: A.G. Harry, et al., Journal of Organometallic Chemistry (2012), http://dx.doi.org/10.1016/j.jorganchem.2012.11.041

4.3.5. N-{6-(Ferrocenyl) ethynyl-2-naphthoyl}-sarcosine-L-alanine ethyl ester ***6***

Sarcosine-L-alanine ethyl ester hydrochloride (0.50 g, 2.63 mmol) was used as a starting material. The crude product was purified by column chromatography (eluant 1:1 hexane:ethyl acetate) and recrystallisation from hexane:ethyl acetate yielded the desired product as a red solid (0.19 g, 13%), m.p. 59–61 °C; $E^{o\prime}$ = 119 mV (vs Fc/Fc^+); $[\alpha]_D^{20} = -23°$ (*c* 0.1, EtOH).

Mass spectrum: $[M + Na]^+$ found: 573.1879.

$C_{31}H_{30}N_2O_4FeNa$ requires: 573.1555.

I.R. υ_{max} (KBr): 3308 (NH), 2206 (−C≡C−), 1732 (C═O_{ester}), 1625 (C═O_{amide}), 1538 (C═O_{amide}) cm^{-1}.

UV–Vis λ_{max} EtOH: 261 (ε 304) nm.

^1H NMR (400 MHz) δ ($CDCl_3$): 7.93–7.50 {7H, m, (−CONH−), (ArH)}, 4.53–4.40 {3H, m, (*ortho* on η^5-C_5H_4−C≡C−), (−CHCH$_3$)}, 4.20–4.10 {11H, m, (*meta* on η^5-C_5H_4−C≡C−), (η^5-C_5H_5), (−N(CH$_3$)CH$_2$CO−), (−OCH$_2$CH$_3$)}, 3.07 (3H, s, −N(CH$_3$)CH$_2$CO−), 1.38 (2H, d, J = 7.2 Hz, −CHCH$_3$), 1.21 (3H, t, J = 7.2 Hz, −OCH$_2$CH$_3$).

^{13}C NMR (100 MHz) δ ($CDCl_3$): 172.0 (C═O), 170.2 (C═O), 169.1 (C═O), 134.4 (C_q), 132.7 (C_q), 131.6 (C_q), 130.6 (C_q), 129.4, 128.5, 128.0, 127.3, 125.0, 123.9, 91.3 (η^5-C_5H_4−C≡C−), 84.7 (η^5-C_5H_4−C≡C−), 71.1 (C_{ortho} η^5-C_5H_4−C≡C−), 69.7 (η^5-C_5H_5), 68.2 (C_{meta} η^5-C_5H_4−C≡C−), 66.2 (C_{ipso} η^5-C_5H_4−C≡C−), 61.9 (−OCH$_2$CH$_3$, -ve DEPT), 49.7 (−CHCH$_3$), 45.1 (−N(CH$_3$)CH$_2$CO−, -ve DEPT), 38.2 (−N(CH$_3$)CH$_2$CO−), 19.0 (−CHCH$_3$), 13.8 (−OCH$_2$CH$_3$).

4.3.6. N-{6-(Ferrocenyl) ethynyl-2-naphthoyl}-L-proline-glycine ethyl ester ***7***

L-Proline-glycine ethyl ester hydrochloride (0.53 g, 2.63 mmol) was used as a starting material. The crude product was purified by column chromatography (eluant 1:1 hexane:ethyl acetate) and recrystallisation from hexane:ethyl acetate yielded the desired product as a red solid (0.22 g, 15%), m.p. 53–55 °C; $E^{o\prime}$ = 153 mV (vs Fc/Fc^+); $[\alpha]_D^{20} = +27°$ (*c* 0.1, EtOH).

Mass spectrum: $[M + Na]^+$ found: 585.1467.

$C_{32}H_{30}N_2O_4FeNa$ requires: 585.1555.

I.R. υ_{max} (KBr): 3313 (NH), 2205 (−C≡C−), 1735 (C═O_{ester}), 1652 (C═O_{amide}), 1604 (C═O_{amide}) cm^{-1}.

UV–Vis λ_{max} EtOH: 254 (ε 317) nm.

^1H NMR (400 MHz) δ ($CDCl_3$): 7.96–7.38 {7H, m, (ArH), (−CONH−)}, 4.82 (1H, t, J = 5.2 Hz, −N(CH$_2$CH$_2$CH$_2$)CHCO−), 4.47 (2H, s, *ortho* on η^5-C_5H_4−C≡C−), 4.21–4.18 {7H, m, (*meta* on η^5-C_5H_4−C≡C−), (η^5-C_5H_5)}, 4.16 (2H, q, J = 7.2 Hz, −OCH$_2$CH$_3$), 4.00 (2H, d, J = 5.6 Hz, −NHCH$_2$CO−), 3.61–3.50 (2H, m, −N(CH$_2$CH$_2$CH$_2$)CHCO−), 2.40–1.70 (4H, m, −N(CH$_2$CH$_2$CH$_2$)CHCO−), 1.21 (3H, t, J = 7.2 Hz, −OCH$_2$CH$_3$).

^{13}C NMR (100 MHz) δ ($CDCl_3$): 171.7 (C═O), 171.0 (C═O), 169.2 (C═O), 133.7 (C_q), 131.5 (C_q), 130.6 (C_q), 129.4 (C_q), 128.1, 127.9, 127.0, 127.2, 124.9, 123.0, 90.1 (η^5-C_5H_4−C≡C−), 84.8 (η^5-C_5H_4−C≡C−), 71.0 (C_{ortho} η^5-C_5H_4−C≡C−), 70.1 (η^5-C_5H_5), 69.1 (C_{meta} η^5-C_5H_4−C≡C−), 64.9 (C_{ipso} η^5-C_5H_4−C≡C−), 61.4 (−OCH$_2$CH$_3$, -ve DEPT), 50.8 (−N(CH$_2$CH$_2$CH$_2$)CHCO−), 47.6 (−N(CH$_2$CH$_2$CH$_2$)CHCO−, -ve DEPT), 42.5 (−NHCH$_2$CO−, -ve DEPT), 27.4 (−N(CH$_2$CH$_2$CH$_2$)CHCO−, -ve DEPT), 25.0 (−N(CH$_2$CH$_2$CH$_2$)CHCO−, -ve DEPT), 13.2 (−OCH$_2$CH$_3$).

4.3.7. N-{6-(Ferrocenyl) ethynyl-2-naphthoyl}-L-proline-L-alanine ethyl ester ***8***

L-Proline-L-alanine ethyl ester hydrochloride (0.56 g, 2.63 mmol) was used as a starting material. The crude product was purified by column chromatography (eluant 1:1 hexane:ethyl acetate) and recrystallisation from hexane:ethyl acetate yielded the desired product as a red solid (0.17 g, 11%), m.p. 56–58 °C; $E^{o\prime}$ = 133 mV (vs Fc/Fc^+); $[\alpha]_D^{20} = -67°$ (*c* 0.1, EtOH).

Mass spectrum: found: $[M + Na]^+$ 599.1639.

$C_{33}H_{32}N_2O_4FeNa$ requires: 599.1711.

I.R. υ_{max} (KBr): 3285 (NH), 2202 (−C≡C−), 1736 (C═O_{ester}), 1672 (C═O_{amide}), 1608 (C═O_{amide}) cm^{-1}.

UV–Vis λ_{max} EtOH: 270 (ε 311) nm.

^1H NMR (400 MHz) δ ($CDCl_3$): 8.12 (1H, s, ArH), 7.96–7.54 {6H, m, (ArH), (−CONH−)}, 4.72–4.65 {3H, m, (−N(CH$_2$CH$_2$CH$_2$)CHCO−), (*ortho* on η^5-C_5H_4−C≡C−)}, 4.55–4.45 (1H, m, −CHCH$_3$), 4.33 (2H, s, *meta* on η^5-C_5H_4−C≡C−), 4.33–4.12 {7H, m, (η^5-C_5H_5), (−OCH$_2$CH$_3$)}, 3.61–3.49 (2H, m, −N(CH$_2$CH$_2$CH$_2$)CHCO−),2.40–1.70 (4H, m, −N(CH$_2$CH$_2$CH$_2$)CHCO−), 1.38 (3H, d, J = 4.4 Hz, −CHCH$_3$), 1.17 (3H, t, J = 7.2 Hz, −OCH$_2$CH$_3$).

^{13}C NMR (100 MHz) δ ($CDCl_3$): 172.1 (C═O), 169.7 (C═O), 168.2 (C═O), 134.5 (C_q), 133.5 (C_q), 132.8 (C_q), 131.6 (C_q), 130.1, 128.4, 128.0, 127.1, 124.7, 121.0, 90.1 (η^5-C_5H_4−C≡C−), 85.8 (η^5-C_5H_4−C≡C−), 71.9 (C_{ortho} η^5-C_5H_4−C≡C−), 70.2 (η^5-C_5H_5), 69.4 (C_{meta} η^5-C_5H_4−C≡C−), 67.6 (C_{ipso} η^5-C_5H_4−C≡C−), 61.9 (−OCH$_2$CH$_3$, -ve DEPT), 60.1 (−N(CH$_2$CH$_2$CH$_2$)CHCO−), 50.7 (−N(CH$_2$CH$_2$CH$_2$)CHCO−, -ve DEPT), 48.5 (−CHCH$_3$), 27.2 (−N(CH$_2$CH$_2$CH$_2$)CHCO−, -ve DEPT), 25.0 (−N(CH$_2$CH$_2$CH$_2$)CHCO−, -ve DEPT), 19.2 (−CHCH$_3$), 14.0 (−OCH$_2$CH$_3$).

4.4. General procedure for in vitro cytotoxicity assays

4.4.1. Biological assays. Cell line

H1299 was obtained from the American Tissue Culture Centre (ATCC). The cell line was grown in RPMI-1640 supplemented with 10% foetal calf serum (FCS) and 1% Sodium Pyruvate at 37 °C in a 5% CO_2 humidified chamber.

4.4.2. In vitro proliferation assays

Cells in the exponential phase of growth were harvested by trypsinisation and a cell suspension of 1×10^3 cells per ml was prepared in fresh culture medium. The cell suspension (100 μL) was added to a flat bottom 96-well plate (Costar, 3599), the plates were agitated gently in order to ensure even dispersion of cells over the surface of the wells, and then the cells were incubated for an initial 24 h in a 37 °C, 5% CO_2 incubator, to allow cell attachment to the wells. A 10 mM stock solution of a test sample was prepared in dimethyl sulfoxide; dilute solutions of the test sample were prepared at 2× final concentration by spiking the cell culture medium with a calculated amount of the stock solution.

100 μL aliquots of each dilute solution was added to each well of the plate, the plate was gently agitated, and then incubated at 37 °C, 5% CO_2 for 5 days, until cell confluency reached 80–90%. Assessment of cell survival in the presence of the compounds **2–8** was determined by the acid phosphatase assay [30]. The acid phosphatase assay is highly sensitive and is easier to perform than the neutral red assay as it involves fewer steps and fewer reagents. It is also more convenient than the MTT assay because of the inherent problem of removal of the medium from the insoluble crystals. The reproducibility between replicate wells is excellent in the acid phosphatase assay and in many cases it has been shown to be better than the neutral red assay and the MTT assay.

The percentage cell growth in the presence of each compound was determined relative to the control cells. The concentration of compounds causing a 50% growth inhibition (IC_{50} of the compound) was determined using Calcusyn (Biosoft, UK).

Acknowledgements

This research was partly supported by the Health Research Board, Grant Reference Number HRA/09/86.

References

[1] T. Gianferrara, I. Bratsos, E. Alessio, Dalton Trans. 37 (2009) 7588.

Please cite this article in press as: A.G. Harry, et al., Journal of Organometallic Chemistry (2012), http://dx.doi.org/10.1016/j.jorganchem.2012.11.041

[2] C.G. Hartinger, P.J. Dyson, Chem. Soc. Rev. 38 (2009) 391.
[3] G. Gasser, I. Ott, N. Metzler-Nolte, J. Med. Chem. 54 (2011) 3.
[4] E.W. Neuse, J. Inorg. Organomet. Poly. Mater. 15 (2005) 3.
[5] G. Tabbi, C. Cassino, G. Cavigiolio, D. Colangelo, A. Ghiglia, I. Viano, D. Osella, J. Med. Chem. 45 (2002) 5786.
[6] D. Trachootham, J. Alexandre, P. Huang, Nat. Rev. Drug Dis. 8 (2009) 579.
[7] M.F.R. Fouda, M.M. Abd-Elzaher, R.A. Abdelsamaia, A.A. Labib, Appl. Organomet. Chem. 21 (2007) 613.
[8] C. Ornelas, New J. Chem. 35 (2011) 1973.
[9] A. Nguyen, A. Vessieres, E.A. Hillard, S. Top, P. Pigeon, G. Jaouen, Chimia 61 (2007) 716.
[10] D. Plazuk, A. Vessieres, E.A. Hillard, O. Buriez, E. Labbe, P. Pigeon, M.-A. Plamont, C. Amatore, J. Zakrzewski, G. Jaouen, J. Med. Chem. 52 (2009) 4964.
[11] M. Gormen, D. Plazuk, P. Pigeon, E.A. Hillard, M.-A. Plamont, S. Top, A. Vessières, G. Jaouen, Tetrahedron Lett. 51 (2010) 118.
[12] M. Gormen, P. Pigeon, S. Top, A. Vessieres, M.-A. Plamont, E.A. Hillard, G. Jaouen, MedChemComm 1 (2010) 149.
[13] A. Goel, D. Savage, S.R. Alley, P.N. Kelly, D. O'Sullivan, H. Mueller-Bunz, P.T.M. Kenny, J. Organomet. Chem. 692 (2007) 1292.
[14] A.J. Corry, A. Goel, S.R. Alley, P.N. Kelly, D. O'Sullivan, D. Savage, P.T.M. Kenny, J. Organomet. Chem. 692 (2007) 1405.
[15] A.J. Corry, N. O'Donovan, Á. Mooney, D. O'Sullivan, D.K. Rai, P.T.M. Kenny, J. Organomet. Chem. 694 (2009) 880.
[16] A.J. Corry, A. Mooney, D. O'Sullivan, P.T.M. Kenny, Inorg. Chim. Acta 362 (2009) 2957.
[17] Á. Mooney, A.J. Corry, D. O'Sullivan, D.K. Rai, P.T.M. Kenny, J. Organomet. Chem. 694 (2009) 886.
[18] Á. Mooney, A.J. Corry, C. Ní Ruairc, T. Maghoub, D. O'Sullivan, N. O'Donovan, J. Crown, S. Varughese, S.M. Draper, D.K. Rai, P.T.M. Kenny, Dalton Trans. 39 (2010) 8228.
[19] Á. Mooney, R. Tiedt, T. Maghoub, N. O'Donovan, J. Crown, B. White, P.T.M. Kenny, J. Med. Chem. 55 (2012) 5455.
[20] K. Sonogashira, J. Organomet. Chem. 653 (2002) 46–49.
[21] M.J. Sheehy, J.F. Gallagher, M. Yamashita, Y. Ida, J. White-Colangelo, J. Johnson, R. Orlando, P.T.M. Kenny, J. Organomet. Chem. 689 (2004) 1511.
[22] D. Savage, G. Malone, J.F. Gallagher, Y. Ida, P.T.M. Kenny, J. Organomet. Chem. 690 (2005) 383.
[23] D. Savage, N. Neary, G. Malone, S.R. Alley, J.F. Gallagher, P.T.M. Kenny, Inorg. Chem. Commun. 8 (2005) 429.
[24] D. Savage, G. Malone, S.R. Alley, J.F. Gallagher, A. Goel, P.N. Kelly, H. Mueller-Bunz, P.T.M. Kenny, J. Organomet. Chem. 691 (2006) 463.
[25] D. Savage, S.R. Alley, A. Goel, T. Hogan, Y. Ida, P.N. Kelly, L. Lehmann, P.T.M. Kenny, Inorg. Chem. Commun. 9 (2006) 1267.
[26] J.B. Fenn, J. Am. Soc. Mass. Spectrom. 4 (1993) 524.
[27] K. Biemann, Biomed. Environ. Mass. Spectrom. 16 (1988) 99.
[28] A. Goel, P.T.M. Kenny, Rapid Commun. Mass. Spectrom. 22 (2008) 2398.
[29] W. Bauer, K. Polborn, W. Beck, J. Organomet. Chem. 579 (1999) 269.
[30] A. Martin, M. Clynes, In Vitro Cell. Dev. Biol. 27A (1991) 183.

Please cite this article in press as: A.G. Harry, et al., Journal of Organometallic Chemistry (2012), http://dx.doi.org/10.1016/j.jorganchem.2012.11.041